Acta Universitatis Szegediensis

Acta Biologica Szegediensis

Volume 52, Number 2, 2008

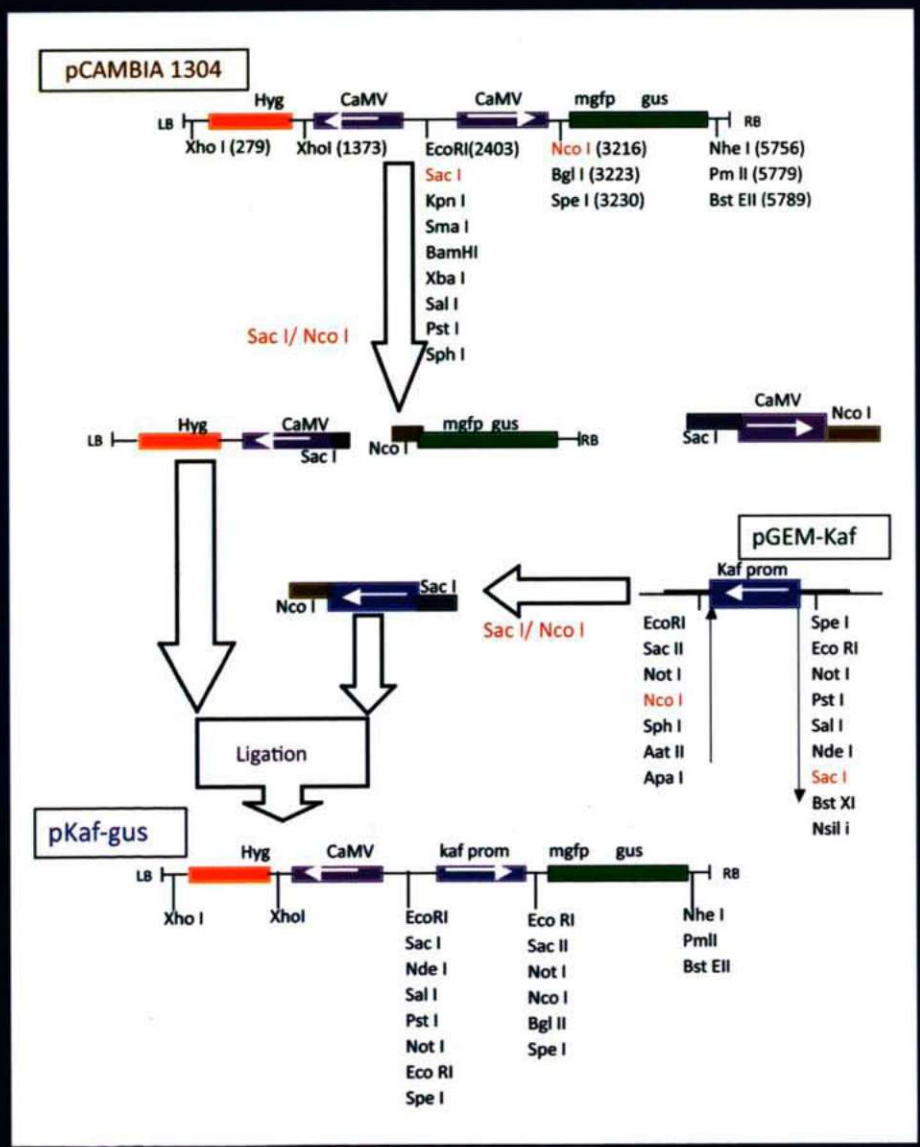

University of Szeged, Szeged, Hungary

Acta Biologica Szegediensis

Acta Biologica Szegediensis (ISSN 1588-385X print form; ISSN 1588-4082 online form), a member of the Acta Universitatis Szegediensis family of scientific journals (ISSN 0563-0592), is published yearly by the University of Szeged. Acta Biologica Szegediensis covers the growth areas of modern biology and publishes original research articles and reviews, involving, but not restricted to, the fields of anatomy, embryology and histology, anthropology, biochemistry, biophysics, biotechnology, botany and plant physiology, all areas of clinical sciences, conservation biology, ecology, genetics, microbiology, molecular biology, neurosciences, paleontology, pharmacology, physiology and pathophysiology, and zoology. Occasionally, Acta Biologica Szegediensis will publish symposium materials. Acta Biologica Szegediensis particularly encourages young investigators and clinicians to submit novel results of interest.

Submission of manuscripts

Manuscripts should be prepared in accordance with the Instructions to Authors published in each issue, also available at http://www.sci.u-szeged.hu/ABS, and submitted to:

Károly Gulya
Acta Biologica Szegediensis, Editorial Office
Department of Cell Biology and Molecular Medicine
University of Szeged
4 Somogyi u., H-6720 Szeged, Hungary
Phone: 36 (62) 544-570, fax: 36 (62) 544-569
E-mail: gulyak@bio.u-szeged.hu

Correspondence relating to the status of the manuscripts, proofs, publication, reprints and advertising should be sent to:

Tamás Mikola
Acta Biologica Szegediensis, Editorial Office
Department of Cell Biology and Molecular Medicine
University of Szeged
4 Somogyi u., H-6720 Szeged, Hungary
Phone: 36 (62) 544-569, fax: 36 (62) 544-569
E-mail: mikolat@molmed.szote.u-szeged.hu

Subscriptions

Acta Biologica Szegediensis is published yearly in two issues per volume. All subscriptions relate to the calendar year and must be pre-paid. The annual subscription rate is currently 100 USD and includes air mail delivery and handling.

Acta Biologica Szegediensis is indexed in BIOSIS Database, EMBASE, Excerpta Medica, Elsevier BIOBASE (Current Awareness in Biological Sciences) and Zoological Record.

The Table of Contents for the current issue and those for previous issues can be found at http://www.sci.u-szeged.hu/ABS.

ACTA BIOLOGICA SZEGEDIENSIS

VOLUME 52(2), 2008

Table of Contents

Articles

On the cover: Construction of a gene cassette pKaf-gus (see Mishra et al. in this issue).

Volume 52(2):257-265, 2008
Acta Biologica Szegediensis
http://www.sci.u-szeged.hu/ABS

ARTICLE

Expression and purification of the recombinant mouse tumor supressor cytochrome *b*561 protein

Alajos Bérczi[1]*, Han Asard[2]

[1]Institute of Biophysics, Biological Research Center, Hungarian Academy of Sciences, Szeged, Hungary, [2]Department of Biology, University of Antwerp, Antwerp, Belgium

ABSTRACT It has recently been recognized that ascorbate-reducible cytochrome *b*561 (Cyt-b561) proteins constitute a well-distinguished protein family amongst the two-heme containing *b*-type cytochromes, ubiquitously present in animals and plants. Of the six isoforms that have been identified in mammals, three isoformes (called CGCytb, DCytb, and LCytb) have been cloned and expressed in yeast and/or bacterial cells. The recombinant proteins have been characterized in some detail. A particular gene product of the 3p21.3 (human) and 9F1 (mouse) chromosomal region, a so-called tumor supressor protein (101F6, TSP10), was identified as a Cyt-b561 protein by sequence homology. We have cloned and expressed the mouse tumor supressor Cyt-b561 protein (TSCytb) in yeast (*Saccharomyces serevisiae*), without and with a His_6-tag on either the N- or the C-terminus. The C-terminal His_6-tagged recombinant protein was purified on Ni-NTA His•Bind resin to almost homogeneity. Using optical spectroscopy we show that TSCytb is indeed an ASC-reducible cytochrome *b*561 protein and that ASC-reducibility is not affected by the presence of a His_6-tag on the C-terminus. Minor differences in the properties of TSCytb and the other three mammalian Cyts-b561 are discussed. **Acta Biol Szeged 52(2):257-265 (2008)**

KEY WORDS

101F6
ASC
recombinant cytochrome *b*561
mouse
TSP10
tumor suppressor protein
yeast expression

b-Type cytochromes are metallo proteins containing one or more iron:protoporphyrine-IX complexes as a chromophore. A recently discovered group of *b*-type cytochromes, called cytochromes *b*561 (Cyts-b561), consists of (i) ascorbate(ASC)-reducible, (ii) *trans*-membrane proteins with six trans-membrane helices, which (iii) have two heme *b* centers (iv) coordinated in a particular way by four well-conserved histidine residues to four consecutive *trans*-membrane α-helices (Bashtovyy et al. 2003; Tsubaki et al. 2005). The two heme *b* prosthetic groups, with different redox potential values, reside on opposite sides of the *trans*-membrane proteins making them ideal for serving as *trans*-membrane electron transporters. The Cytb-561 that was discovered first is the chromaffin granule Cyt-b561 that had already been known as chromomembrin B (Flatmark and Terland 1971; Silsand and Flatmark 1974; Apps et al. 1980). This protein functions as an electron transporter providing electrons from cytosolic ASC through the chromaffin granule membrane to intravesicular dopamine β-hydroxylase (Njus and Kelley 1993; Njus et al. 2001). After resolving the full genomic sequence of a large variety of organisms, and improving *in silico* techniques for comparing gene and protein sequences, numerous proteins were identified similar to CGCytb in various organisms, including invertebrates, vertebrates, and plants (Verelst and Asard 2003; Tsubaki et al. 2005). Three mammalian and one plant Cyts-b561, namely the chromaffin granule Cyt-b561 (CGCytb), the duodenal Cyt-b561 (DCytb; [McKie et al. 2001]), the lysosomal Cyt-b561 (LCytb; [Zhang et al. 2006]), and the tonoplast Cyt-b561 (TCytb; [Griesen et al. 2004]), showed ASC-dependent *trans*-membrane ferrireductase activity when expressed in yeast cells (Su and Asard 2006; Bérczi et al. 2007). However, CGCytb is participating in ASC regeneration in chromaffin granules (Kent and Fleming 1987; Njus and Kelley 1993) while another isoform, DCytb, appears to be involved in extracellular recycling of ASC of human erythrocytes (Su et al. 2006). Only DCytb has already been shown to be involved in iron metabolism (McKie et al. 2001; Vargas et al. 2003). The biological function of LCytb and TCytb has not yet been elucidated.

At the level of genomic and predicted protein sequences, a human tumor supressor protein (the 101F6 gene product) has been identified as putative member of the Cyts-b561 (Lerman and Minna 2000; Ponting 2001). The mouse homologue was also discovered, sequenced, and shown to be 85% and 95% identical with the human sequences on the cDNA and protein sequence level, respectively (Lerman and Minna 2000). Both proteins have (i) 6 *trans*-membrane α-helices with (ii) 222 residues, (iii) the N- and C-termini in the cytoplasm, and (iv) 4 well-conserved histidine residues for binding two heme b prosthetic groups. 101F6 mRNA is widely expressed in animal tissues, and the mouse mRNA is especially abundant in liver, kidney, and lung (Mizutani et al. 2007), while the human protein is most abundant in liver, placenta, and lung

Accepted Sept 19, 2008
*Corresponding author. E-mail: berczi@brc.hu

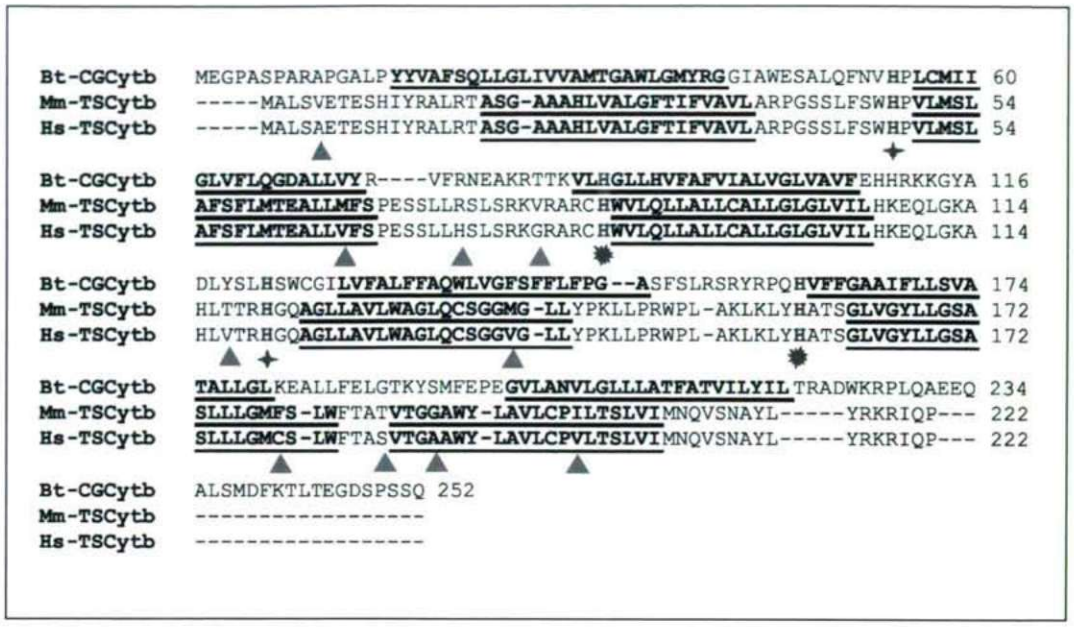

Figure 1. Multiple alignment of bovine (*Bos taurus*, Bt) CGCytb, mouse (*Mus musculus*, Mm) TSCytb, and human (*Homo sapiens*, Hs) TSCytb using Clustal W (v. 2.0.1) software (http://www.ebi.ac.uk/Tools/clustalw2/index.html). Predicted trans-membrane segments are bold faced, underlined, and obtained by using HMMTOP (http://www.enzim.hu/hmmtop/). The highly conserved His residues binding the two hemes are labelled in pairs with stars (* and +). Gray triangles (▲) show the 10 amino acid residues where the mouse and human TSCytb are different.

(Lerman and Minna 2000). Expression of wild-type101F6 in tumor cells significantly inhibited cell growth and intratumoral injection of recombinant adenovirus-101F6 gene vectors, as well as systemic administration of protamine-complexed adenovirus-101F6 gene vectors, significantly suppressed tumor xenografts growth (Ji et al. 2002). Ohtani et al. (2007) have recently found that nanoparticle-mediated 101F6 gene transfer and a subpharmacologic concentration of ASC synergistically and selectively inhibited tumor cell growth by caspase-independent apoptosis and autophagy *in vitro* and *in vivo*. C terminal *myc*-tagged mouse 101F6 protein has been expressed in Chinese hamster ovary (CHO) cells and immunofluorescence microscopy was used to localize the recombinant proteins; they were found in small vesicles, including endosomes and endoplasmic reticulum of the perinuclear region (Mizutani et al. 2007). It was also shown that CHO cells expressing the C terminal *myc*-tagged mouse 101F6 protein showed higher ferric ion and azo-dye reduction level than the control CHO cells. Mizutani et al. (2007) concluded that mouse 101F6 proteins played roles in the ferrireduction via a yet unresolved mechanism.

In this paper we report on the cloning and expression of the mouse 101F6 gene in a yeast expression system, both with and without a His_6-tag on either the C-terminus or the N-terminus. It is shown that the recombinant mouse tumor suppressor protein is indeed an ASC-reducible *b*-type cytochrome and the His_6-tag on the C-terminus does not affect ASC-reducibility.

Materials and Methods

Chemicals

The protease inhibitor cocktail tablet „cOmplete", NBT (Nitro blue tetrazolium chloride), BCIP (5-Bromo-4-chloro-3-indolyl phosphate, toluidine salt) in 67% DMSO (v/v), were from Roche (Mannheim, Germany); Sucrose monolaurate (SML) was from Dojindo (Tokyo, Japan); Ni-NTA His•Bind Resin was from Novagen (Darmstadt, Germany); Difco™ yeast nitrogen base w/o amino acids was from BD (Sparks, MD, USA); other chemicals were analytical grade and from Acros (Geel, Belgium) or Fluka (Buchs, Switzerland) or Serva (Heidelberg, Germany).

Molecular biology works

For expression of untagged proteins, the cDNA of mouse TSCytb (the sequence corresponds to GenBank protein entry, NP_062694; see Fig. 1) was amplified from mouse whole brain RNA and was cloned into a pESC-His expression vector (Stratagene, La Jolla. CA), downstream of the GAL10 galactose-inducible promoter, using EcoRI and SpeI restriction sites. Yeast cells (*Saccharomyces cerevisiae*, strain YPH499: ura3-52 lys2-801^{amber}ade2-101^{ochre} trp1-Δ63 his3-Δ200 leu2-Δ1) were transformed and grown according to the manufacturer's instructions (Stratagene).

For expression of His_6-tagged proteins, a standard PCR method was used to amplify the gene for TSCytb from mouse

whole brain RNA. Primers were designed to generate EcoRI and SpeI sites for cloning into the pESC-His expression vector (Stratagene, La Jolla, CA), downstream of the GAL10 galactose-inducible promoter, and with a His_6 tag either on the C- or the N-terminus. Four oligonucleotide primers were synthesized and used for the amplification:

C-terminus, sense: 5'-GGGGGAATTCGCCACCATG-GCCCTTTCTGTGGAGACG-3'

C-terminus, antisense:

5'-CCCCACTAGTCTAGTGATGGTGATGATGGTGT-GGCTGGATCCTCTTGCGGT-3'

N-terminus, sense:

5'-GGGGGAATTCACCATGCACCATCATCACCAT-CACGCCCTTTCTGTGGAGACGGAG-3'

N-terminus, antisense: 5'-CCCCACTAGTTCATGGCT-GGATCCTCTTGCGGT-3'

First, the PCR-amplified products were inserted into pGEM-T Easy vectors (Promega Corp., Madison, WI, USA), and the resulting vectors were transformed into *E. coli* DH5α cells using calcium chloride competent cells and the NucleoSpin Plasmid QuickPure kit (Macherey-Nagel GmbH & Co., Düren, Germany). The pGEM-T Easy vectors with the inserts were isolated with the NucleoSpin Plasmid QuickPure kit and inserted into empty pESC-His vectors by using the restriction enzymes EcoRI and SpeI. The integrity of the His_6-tagged TSCytb/pESC-His vectors was confirmed by restriction digestion and DNA sequencing. Finally, pESC-His verctors were transformed into competent yeast cells (*Saccharomyces cerevisiae*, strain YPH499, ura3-52 lys2-801^{amber}ade2-101^{ochre} trp1-Δ63 his3-Δ200 leu2-Δ1) and the transformed cells were tested on SD-dropout medium (http://www.stratagene.com/manuals/217451.pdf) where the lack of histidine was the selective factor. For induction of protein expression and production of the recombinant proteins, overnight cultures were grown in SD-dropout medium, transferred to SG-dropout medium (http://www.stratagene.com/manuals/217451.pdf) and grown for 24-28 hours.

Yeast membrane preparation

Cells grown as 2 x 350 ml cultures in SG-His medium were collected by low-speed centrifugation (at 4,000 g_{max} and 10°C for 10 min) when the OD_{600}(d=1cm) reached a value of 0.8 ± 0.05. Collected cells were washed once with ice cold phosphate buffer (20 mM KH_2PO_4, 100 mM NaCl, pH 7) and pelleted as above. Washed cells were resuspended in 15 ml of ice cold homogenization buffer (50 mM MES-KOH, pH 7.0, 5 mM EDTA, 150 mM KCl, 150 mM sucrose) supplemented with freshly added 0.1% (w/v) Na-ASC and protease inhibitors (1 mM PMSF and aprotinin, pepstatin, leupeptin, antipain, chymostatin in the form of 1 dissolved cOmplete tablet). Cells were broken in a Bead Beater (Biospec Products, Bartlesville, OK, USA) with four 30 s cycles, with 2 min cooling intervals, using 0.5 mm glass beads. Beads were rinsed with 35 ml of ice cold homogenization buffer. The homogenate (50 ml) was centrifuged at 4,000 g_{max} and 5°C for 10 min to remove unlysed cells and cell debris. A yeast microsomal membrane (YM) fraction was obtained after centrifugation of the 4,000 g_{max} supernatant at 75,000 g_{max} and 4°C for 60 min (Sorvall Discovery 90 ultracentrifuge and T-647.5 rotor; Sorvall Products, L.P., Newtown, CT, USA). After centrifugation, the pellet was resuspended in 20 mM phosphate buffer, pH 7, and the membrane vesicles were stripped as before (Bérczi et al. 2005). Stripped microsomal membrane (SYM) vesicles were resuspended in phosphate buffer (50 mM NaH_2PO_4, 10% (w/v) glycerol, pH 7), and stored at −80°C until use.

Sucrose density gradient fractionation

For membrane fractionation, after stripping and final centrifugation, SYM vesicles were resuspended in 4 ml of MES-KOH buffer (50 mM MES, 10% (w/v) sucrose, pH 7) and layered on the top of a discontinuous sucrose density gradient made of 2 ml of 70% (w/v), 10 ml of 45% (w/v), 9 ml of 32% (w/v), and 8 ml of 20% (w/v) sucrose solutions in 50 mM MES-KOH buffer, pH 7. Fractionation was by centrifugation in an AH-629 swing-out rotor (Sorvall Products, L.P., Newtown, CT, USA) in a Discovery 90 ultracentrifuge at 28,900 rpm (g_{max}=150,000g), at 5°C for 3 hours. The cloudy bands at the interfaces were collected with a Pasteur pipette, diluted ten-fold by 20 mM MES-KOH, pH 7, and pelleted by centrifugation (Sorvall T-647.5 rotor and Discovery 90 ultracentrifuge) at 75,000 g_{max} and 4°C for 90 min. After centrifugation, the pellet was resuspended in phosphate buffer (50 mM NaH_2PO_4, pH 7, containing 10% (w/v) glycerol), and stored at −80°C until use.

Protein solubilization and purification by His_6-tag affinity chromatography

Frozen membrane vesicles (about 60 mg protein) in 50 mM NaH_2PO_4, 10% (w/v) glycerol, pH 7, were thawn and proteins were solubilized by sucrose monolaurate (SML) at 1 mg ml^{-1} protein concentration and 3:1 (w/w) detergent:protein ratio. The mixture was incubated on a rocker at 5°C for 90 min. Insoluble material was pelleted by high-speed centrifugation (T-647.5 rotor and Sorvall Discovery 90 ultracentrifuge) at 75,000 g_{max} and 5°C for 60 min. The supernatant containing the detergent-solubilized proteins was supplemented with 500 mM NaCl and 10 mM imidazole, the pH was adjusted to 7.8 and then mixed with 1 ml (bed volume) of Ni-NTA His•Bind resin (Novagen, Madison, WI, USA) that had been pre-equilibrated with 50 mM NaH_2PO_4, pH 7.8, containing 10% (w/v) glycerol, 1%(w/v) SML, 500 mM NaCl and 10 mM imidazole. The affinity resin was incubated with the solubilized proteins at room temperature for 30 min. After incubation, the Ni-NTA His•Bind resin with bound proteins was collected in a 10-ml disposable column and washed 3

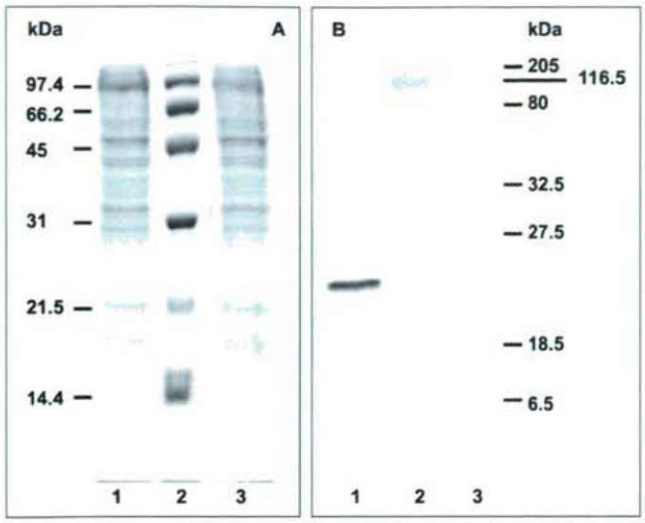

Figure 2. Coomassie Brillant Blue R-250 stained (A) and Western blotted (B) SDS-PAGE picture of YM fractions containing C-terminal (lane 1) or N-terminal (lane 3) His_6-tagged TSCytb. Molecular mass standards are on lanes 2. 25 μg (A) and 10 μg (B) of proteins were loaded.

times with 5 bed volumes of 50 mM NaH_2PO_4, pH 7.8, containing 10% (w/v) glycerol, 0.3% (w/v) SML, 500 mM NaCl and 10 mM imidazole. His_6-tagged proteins were eluted with 4 bed volumes of elution buffer (50 mM NaH_2PO_4, pH 7.0, containing 10% (w/v) glycerol, 0.3 %(w/v) SML, 150 mM NaCl and 250 mM imidazole). The affinity resin was further washed with 10 bed volumes of elution buffer while the eluate was concentrated by centrifugation using Centricon-YM100 centrifugal filter unit (Millipore, Bedford, MA, USA) and desalted by using a PD-10 desalting column (Amersham Biosciences, Uppsala, Sweden). The desalted fraction was concentrated again by centrifugation using Centricon-YM100 centrifugal filter units and the concentrated fraction was stored in 50 mM NaH_2PO_4, 10% (w/v) glycerol, 0.3 % (w/v) SML, pH 7, at –80°C until use.

Absorption spectroscopy

Absorption spectra with SYM vesicles were recorded in dual wavelength mode between 500 nm and 600 nm (with 601 nm as reference wavelength) while absorption spectra with the solubilized protein fractions were recorded in split beam mode between 350 nm and 650 nm (with buffer as reference) by using an OLIS-updated SLM-Aminco DW2000 spectrophotometer (OLIS Co., Bogart, GA, USA) with 2 nm slit-width at room temperature and under continuous stirring. First, cytochromes were oxidized by addition of ferricyanide (0.1-0.2 mM, $K_3[Fe(CN)_6]$) and the fully oxidized spectrum was recorded. Then ASC was added and the ASC-reduced spectrum was recorded. Finally Na-dithionite (DTH) was added (2-5 mM final concentration) and the DTH-reduced spectrum was obtained at room temperature. When improvement of the signal to noise ratio was needed, multiple scans were averaged. Amount of cytochromes was calculated from the reduced-minus-oxidized difference spectra by using a millimolar extinction coefficient of ε_{561nm}=30 $mM^{-1} \cdot cm^{-1}$ (Tsubaki et al. 1997; Liu et al. 2005).

Gel electrophoresis and Western blotting

Protein content of samples (both of membranes and of detergent micelles) was estimated by the modified Lowry method (Markwell et al. 1978) with deoxycholate as detergent and BSA as standard.

Proteins were resolved by SDS-PAGE (Laemmli 1970) by using 4.5% (stacking) and 12% (running) polyacrylamide gels. Samples were not heated or boiled prior to loading on gels because harsh temperature treatment is known to cause the highly hydrophobic integral membrane proteins to aggregate, preventing them from penetrating into the 12% running gel (Duong and Fleming 1982; Thomas and McNamee 1990). Low Range and Kaleidoscope Prestained molecular weight standards (BioRad, Hercules, CA, USA) were used for the Coomassie staining and for the Western blotting, respectively.

For protein visualization, gels were stained with 0.2% (w/v) Coomassie Brillant Blue R-250 in 50% (v/v) methanol, 10% (v/v) acetic acid for 2 hours and destained in 40% (v/v) methanol, 10% (v/v) acetic acid in three 30 min steps. Finally the destained gels were rinsed in 40% (v/v) methanol, 10% (v/v) acetic acid, 5% (v/v) glycerol and dried between two layers of wet cellophane sheets at room temperature.

For visualization and identification of His_6-tagged TSCytb, gels were transferred onto polyvinylidene difluoride membranes (PVDF) with a Mini Trans-Blot Electrophoretic Transfer Cell (both from BioRad, Hercules, CA, USA) in 25 mM Tris, 192 mM glycine, 20% (v/v) methanol. A mouse monoclonal antibody to the 6X-His tag (Abcam, Cambridge, UK) was used to detect the recombinant proteins. Protein-antibody complexes were visualized by alkaline phosphatase-coupled rabbit-anti-mouse secondary antibodies (Pierce, Product #: 31332, Rockford, IL, USA) after reacting with NBT/BCIP (http://www.cshprotocols.org/cgi/content/full/2007/15/pdb.rec11089).

All results shown are representative from 2 to 4 independent repetitions.

Results and Discussion

Expression and purification

The YPH499 yeast cell line and pESC-His vector has already been successfully used for cloning His_6-tagged Cytbs-561 (Griesen et al. 2004; Bérczi et al. 2005; Zhang et al. 2006) and the expression system provided recombinant CGCytb with physico-chemical properties similar to the native pro-

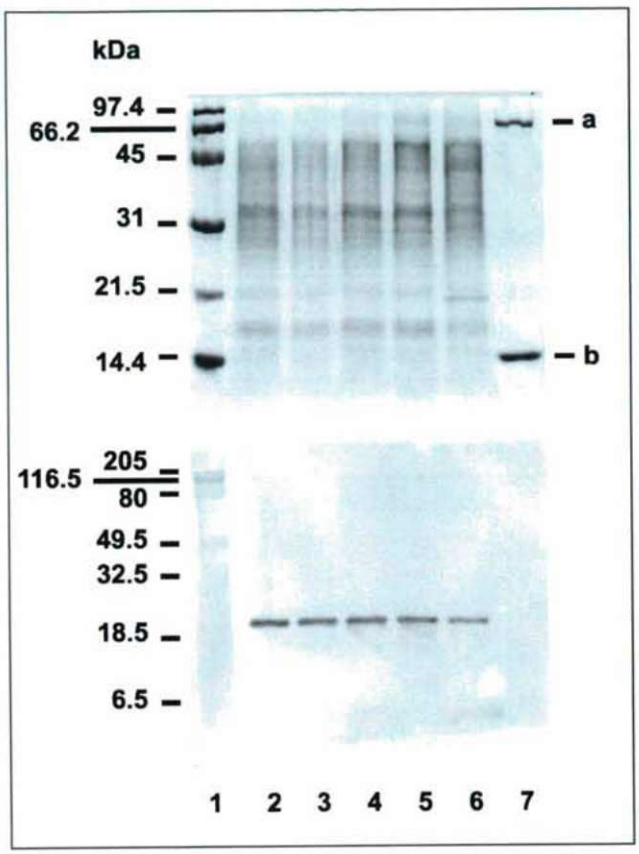

Figure 3. Coomassie Brillant Blue R-250 stained (top) and Western blotted (bottom) SDS-PAGE picture of SYM fractions containing (H_6C)TSCytb. Lanes are: 1 for molecular mass standards, 2 for SYM, 3 for SYM at the 10%/20% sucrose step interface, 4 for SYM at the 20%/32% sucrose step interface, 5 for SYM at the 32%/45% sucrose step interface, 6 for SYM at the 45%/70% sucrose step interface, and 7 for BSA and cytochrome c. 18 μg (top) and 2 μg (bottom) of protein were loaded in lanes 2 through 6. a - 66.2 kDa for BSA; b - 12.4 kDa for horse cytochrome c.

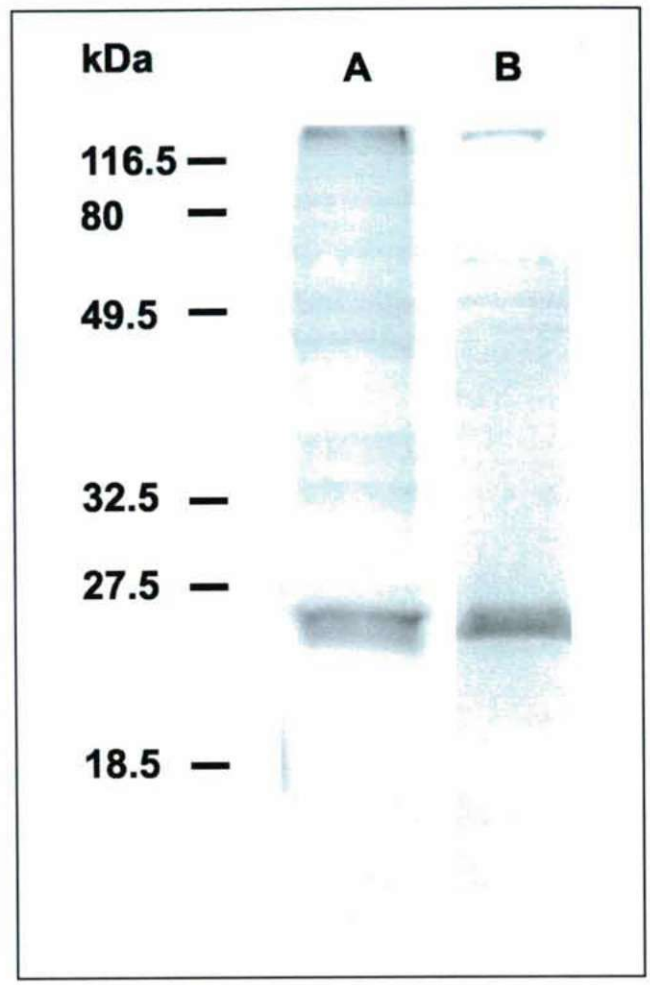

Figure 4. Coomassie Brillant Blue R-250 stained (A) and Western blotted (B) SDS-PAGE picture of highly purified (H_6C)TSCytb after PD-10 chromatography and concentration. 13 μg (A) and 3 μg (B) of proteins were loaded.

tein (Bérczi et al. 2005). Other yeast cell lines and vectors were also successfully employed in high yield expression of mammalian Cyts-b561 (Liu et al. 2005; Su and Asard 2006). It was therefore plausible to use a yeast expression system for producing appropriate amounts of a novel recombinant Cytb-561 and establishing the basic physico-chemical properties of the expressed protein. N-terminal or C-terminal His_6-tagged TSCytb was expressed and the YM fraction was used to check the expression levels. Figure 2 shows that the concentration of the N-terminal His_6-tagged TSCytb in the YM fraction was considerably lower than that of the C-terminal His_6-tagged TSCytb (hereafter (H_6C)TSCytb). This result is in agreement with former observations obtained with the His_6-tagged CGCytb and TCytb proteins (data not published), although the reason of the difference in expression levels is not yet known.

When mammalian or plant Cyts-b561 were expressed in ferrireductase-deficient yeast cells (*Δfre1Δfre2* mutant lines), the capacity of these cells to reduce extracellular ferric-compounds was restored (Su and Asard 2006; Bérczi et al. 2007). These results were indirect proof that the recombinant Cyts-b561 was at least in part, targeted to the yeast cell plasma membrane.

Continuous sucrose density gradient fractionation of YM vesicles revealed that plasma membrane vesicles assembled at position of rather high sucrose concentrations (>45% (w/v); Roberg et al. 1997). When the distribution of (H_6C) TSCytb in the SYM fraction was studied by discontinuous sucrose density gradient centrifugation and Western blotting, (H_6C)TSCytb was almost evenly distributed in membrane fractions at all sucrose density steps (Fig. 3). In fact, the lowest concentration of TSCytb appears at the highest sucrose

Table 1. Protein balance sheet. For each His_6-tag affinity chromatography step, 100S fractions from two independent experiments were used; for each solubilization step, SYM fractions from two independent membrane preparations were used; and at each membrane preparation, 700 ml of yeast cell cultures with OD_{600}(d=1 cm) of 0.8±0.05 was used. Results are the means ± s.d. from 8 independent His_6-tag affinity chromatography steps except for the last value (§) which is mean ± s.d. from 4 independent purifications. YM – yeast microsomal membranes, SYM – stripped yeast microsomal membranes, 100P – unsolubilized membranes (the 100,000 g_{max} pellet after the solubilization step), 100S – the concentrated protein fraction after solubilization, Filtrate – solubilized protein fraction which passed through the 100,000 kDa membrane filter, Unbound – solubilized proteins unbound to the Ni-NTA His•Bind Resin, (H_6C)TSCytb – concentrated His_6-tagged TSCytb proteins eluted from the Ni-NTA His•Bind Resin. n.m. is for "not measured".

Fraction	Total protein, mg	ASC-reduced TSCytb pmol·mg^{-1}
YM	198 ± 47	n.m.
SYM	143 ± 31	77± 18
100P	72 ± 15	n.m.
100S	60 ± 13	n.m.
Filtrate	5.7 ± 1.4v	n.m.
Unbound	46 ± 7	n.m.
(H_6C)TSCytb	1.2 ± 0.3	3850 ± 341 (§)

concentration step employed, *i.e.* the location at which the yeast plasma membrane is expected. Mizutani et al. (2007) showed that myc-tagged TSCytb was localized in small vesicles, including endosomes and endoplasmic reticulum of the perinuclear region, using an immunofluorescent staining technique. Therefore, the localization of (H_6C)TSCytb in the lighter SYM fractions was not a surprise. However, the rather homogeneous distribution of (H_6C)TSCytb in different and lighter populations of yeast membrane vesicles appears to be different from the mostly yeast plasma membrane localization of the other three recombinant mouse Cyts-b561 expressed in yeast. This result pointed out that enrichment of a membrane fraction containing (H_6C)TSCytb by differential and/or density gradient centrifugation before membrane solubilization could not be achieved.

As the protein balance sheet shows (Table 1), stripping of the YM vesicles resulted in the loss of about 30% of the proteins. Treatment of the SYM vesicles with the nonionic detergent SML, at a detergent:protein ratio of 3:1 (w/w) and 1 mg/ml protein concentration, resulted in solubilization of about 45% of the membrane proteins. When the solubilized fraction was concentrated by using a membrane filter with 100 kDa cut-off value, >90% of solubilized proteins were retained. About 75% of the solubilized and concentrated proteins did not bind the Ni-NTA His•Bind resin (Table 1, unbound fraction), however, only about 8% of the bound proteins were strongly associated with the resin, and eluted using the elution buffer (Table 1, (H_6C)TSCytb fraction). In order to exchange the high salt and imidazole-containing

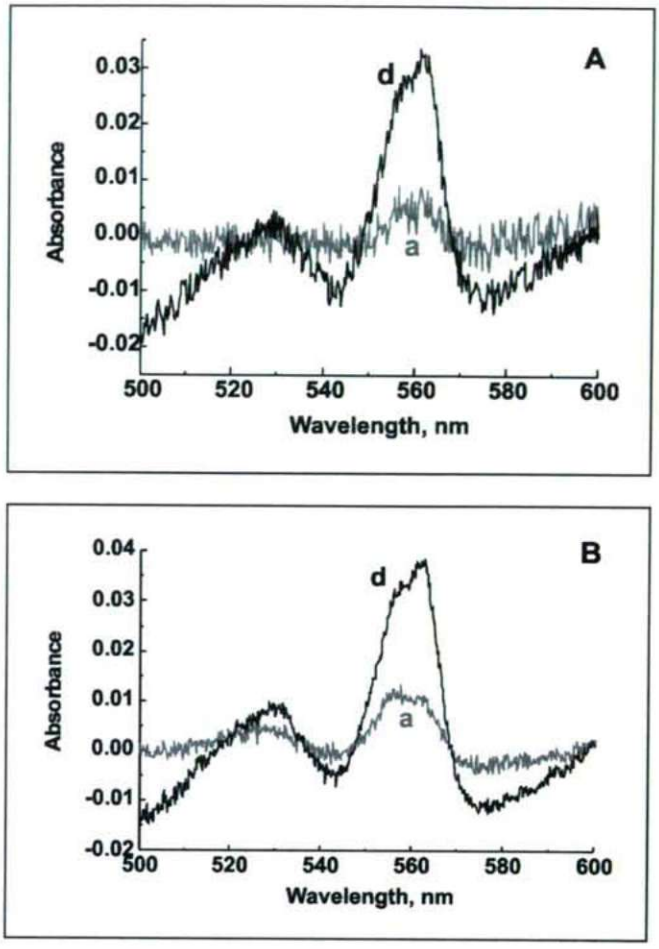

Figure 5. ASC-reduced (a) and dithionite-reduced (d) minus oxidized difference spectra of SYM fraction containing untagged (A) and His_6-tagged (B) TSCytb. 7.5 mg·ml^{-1} was the protein concentration in both cases.

elution buffer to a widely-used phosphate buffer for storage of (H_6C)TSCytb, the coral red fraction was passed through a PD-10 column and then concentrated. Figure 4 shows that the final (H_6C)TSCytb fraction contained mostly His_6-tagged TSCytb, but small amounts of contaminating proteins can be seen on the gel. Even the fraction of proteins, which did not enter the separation gel, contained (H_6C)TSCytb, according to the Western blot staining. After solubilization, protein concentration, affinity chromatography, PD-10 chromatography, and a second protein concentration step, the ASC-reducible TSCytb recovery was between 40 and 50% which is in good agreement with former results (Bérczi et al. 2007).

Spectroscopy

TSCytb was classified as member of the Cyts-b561 on the basis of its sequence homology and predicted structural similarity to bovine CGCytb (Ponting 2001; Tsubaki et al. 2005; Su and Asard 2006). Figure 5 shows that TSCytb is

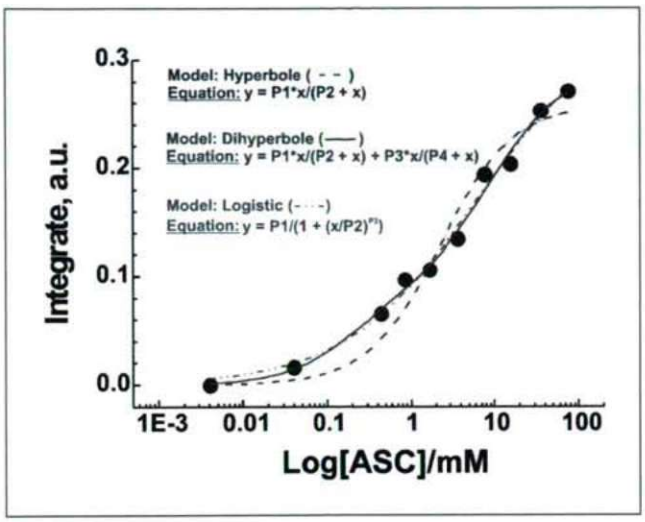

Figure 6. ASC-dependent reduction of highly purified (H_6C)TSCytb. Protein concentration was 0.4 mg·ml^{-1} Y axes are values obtained by integration between 542 and 569 nm of the (α+β)-peak in the reduced minus oxidized difference spectrum. Experimental points cannot be fitted by a single ASC-binding or -affinity site model (Hyperbole fit, dash line, r^2<0.95). However, both a two ASC-binding or -affinity site model (Dihyperbole fit, solid line) and a „logistic-type" model (Logistic fit, dash-dot-dot line) gave appropriate fits with similar r^2 values (>0.98). Mathematical analysis was with OriginPro 7.5 Data Analysis and Graphing Software.

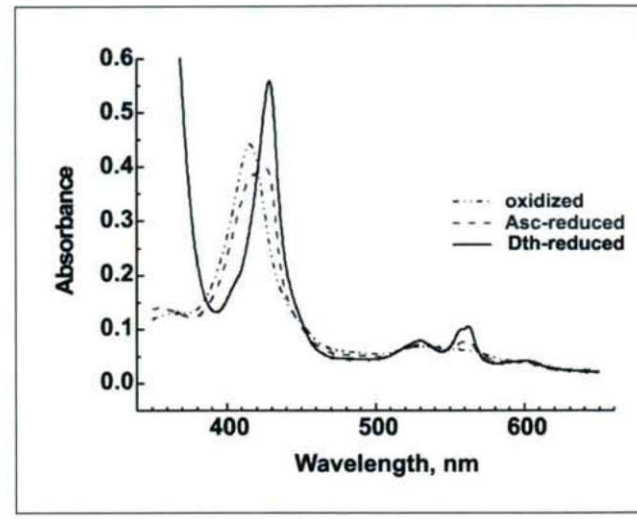

Figure 7. Oxidized, ASC-reduced and dithionite-reduced spectra of highly purified (H_6C)TSCytb. Protein concentration was 0.4 mg·ml^{-1}

indeed a membrane-associated *b*-type cytochrome, with an α-band absorbance maximum around 560 nm. TSCytb is also ASC reducible which is the basic property of Cyts-b561. It is evident that the presence of a His_6-tag on the C terminus does not affect the ASC reducibility of the protein. However, the specific ASC-reducible cytochrome *b* content of SYM vesicles (between 50 and100 pmol·mg^{-1} protein), tested with 25 mM ASC, was much lower than that obtained with other Cyts-b561 expressed in yeast (CGCytb: about 1500 pmol.mg^{-1} [Bérczi et al. 2005]; TCytb: about 400 pmol.mg^{-1} [Bérczi et al. 2007]; LCytb: about 150 pmol.mg^{-1} [Zhang et al. 2006]). It is also evident that the untagged and His_6-tagged protein in the SYM fraction had considerably lower ASC reducibility, as compared to dithionate reducibility, than either CGCytb or TCytb (see later).

Recombinant CGCytb and TCytb reached saturation in ASC-reducibility at 25 mM ASC (Lakshminarasimhan et al. 2006; Bérczi and Asard 2006). However, this was not the case with TSCytb. As seen in Figure 6, ASC-reduction continued to increase even at 75 mM ASC. It is evident that the ASC-dependent reduction of TSCytb cannot be described by a single binding or affinity site, as it was also evident with CGCytb and TCytb (Lakshminarasimhan et al. 2006; Bérczi and Asard 2006). However, the two binding or affinity site model, which could explain the ASC-dependent reduction of CGCytb and TCytb, cannot be unambiguously employed for TSCytb due to the uncertainty of experimental points; as seen in Figure 6, both a "two binding site model" and a "logistic model" provide fitted curve with r^2>0.98.

Finally, maximal reduction of *b*-type cytochromes can be obtained in the presence of 2-5 mM dithionite. The maximal ASC-reduction of CGCytb and TCytb is about 75-80% of the dithionite-reduced maximal reduction value (Bérczi et al. 2005, 2007). As Figure 7 shows, reduction of highly purified TSCytb at 50 mM ASC concentration is only about 50% of that at 5 mM dithionite concentration. This is particularly well seen in the Soret band of spectra where the disappearance of the absorption peak at 415 nm in the fully oxidized spectrum is parallel with the appearance of the γ-peak at 428 nm in the fully reduced spectrum through an isosbestic point at 421 nm.

The specific cytochrome *b* content of the highly purified (H_6C)TSCytb fraction was about 4 nmol·mg^{-1} protein (Table 1). This value is again lower than (one third of) those values obtained with highly purified recombinant mouse (H_6C) CGCytb and (H_6C)TCytb (Bérczi et al. 2005, 2007) but the difference is smaller than that observed at the level of SYM vesicles (see above). One reason for the difference between the specific TSCytb content in the SYM fraction and highly purified protein fraction could lie in different expression levels of the different recombinant proteins in yeast. However, another source for the observed differences could be that in all calculations we use the molar extinction coefficient established for the bovine CGCytb at 561 nm and with dithionite as the reducing agent. It is possible, on the basis of differences in the primary structure of Cyts-b561 (see Fig. 1), that different Cyts-b561 have different molar extinction coefficients. Furthermore, detailed reduction mechanisms with ASC and/or dithionite have not yet been established. It is well known that the presence of dithionite in solutions causes

oxygen depletion. Oxygen depletion is transient, depending on the starting concentration of dithionite and contact of the solution with air (that is mostly the case in spectrophotometer cuvettes). Since the role of oxygen as an oxidant to Cyts-b561 is not yet clear, it may affect the final reduction levels of the protein when any reducing agent is added. Taken together, we conclude that a reliable quantitative comparison between the properties of different Cyts-b561 will be possible only after establishing the proper molar extinction coefficient for each protein and the role of disolved oxygen for the reduction mechanism(s) of Cyts-b561.

Comparison of TSCytb to CGCytb and TCytb

In this paper, we have reported the expression of the His_6-tagged recombinant mouse TSCytb in the very same yeast expression system previously used for mouse CGCytb, DCytb, LCytb, and TCytb from Arabidopsis thaliana. It is shown that (i) TSCytb is an ASC-reducible *b*-type cytochrome but its sensitivity to ASC is considerably lower than that observed with CGCytb and TCytb, (ii) the specific content of TSCytb is lower than those of CGCytb and TCytb in the very same SYM fractions, (iii) the ASC-reducibility of TSCytb is lower than that of CGCytb and TCytb when compared to the maximal reduction of these Cyts-b561 by dithionite. These minor differences in the basic ASC-reducible properties might be explained by detailed sequence comparison of these proteins. Indeed, it was found that CGCytb, DCytb, LCytb, and even TCytb are evolutionary much closer to each other than to TSCytb (Tsubaki et al. 2005; Su and Asard 2006), supporting that these proteins might have little but important differences in structures which is manifested in different physico-chemical properties.

Acknowledgements

The authors thank Dr. Dan Su (Yale University, New Haven, CT, USA), Dr. Sándor Bottka (Hungarian Academy of Sciences, Hungary), Mrs Kim van Beek, Mrs Ciska Malgorzata and Mr Michiel Janssens (University of Antwerp, Antwerp, Belgium) for helpful discussions, and particularly for synthesizing the primers (Dr. Bottka), for production of pESC-His vectors containing the non-tagged (Dr. Su) and His_6-tagged (Mrs Van Beek, Mrs Malgorzata, Mr Janssens) cDNA. This work was supported by grants from the University of Antwerp (to H.A.).

References

Apps DK, Pryde JG, Phillips JH (1980) Cytochrome *b*561 is identical with chromomembrin B, a major polypeptide of chromaffin granule membranes. Neuroscience 5:2279-2287.

Asard H, Kapila J, Verelst W, Bérczi A (2001) Higher-plant plasma membrane cytochrome *b*561: a protein in search of a function. Protoplasma 217:77–93.

Bashtovyy D, Bérczi A, Asard H, Páli T (2003) Structure prediction for deheme cytochrome *b*561 protein family. Protoplasma 221:31-40.

Bérczi A, Su D, Lakshminarasimhan M, Vargas A, Asard H (2005) Heterologous expression and site-directed mutagenesis of an ASC-reducible cytochrome *b*561. Arch Biochem Biophys 443:82-92.

Bérczi A, Asard H (2006) Characterization of an ASC-reducible cytochrome *b*561 by site-directed mutagenesis. Acta Biol Szeged 50:55-59.

Bérczi A, Su D, Asard H (2007) An Arabidopsis cytochrome *b*561 with transmembrane ferrireductase capability. FEBS Lett 581:1505-1508.

Duong LT, Fleming PJ (1982) Isolation and properties of cytochrome *b*561 from bovine adrenal chromaffin granules. J Biol Chem 257:8561-8564.

Flatmark T, Terland O (1971) Cytochrome b_{561} of the bovine adrenal chromaffin granules. A high potential *b*-type cytochrome. Biochim Biophys Acta 253:487-491.

Griesen D, Su D, Bérczi A, Asard H (2004) Localization of an ASC-reducible cytochrome *b*561 in the plant tonoplast. Plant Physiol 134:726-734.

Ji L, Nizhizaki M, Gao B, Burbee D, Kondo M, Kamibayashi C, Xu K, Yen N (2002) Expression of several genes in the human chromosome 3p21.3 homozygous deletion region by an adenovirus vector results in tumor suppressor activities *in vitro* and *in vivo*. Cancer Res 62:2715-2720.

Kent UM, Fleming PJ (1987) Purified cytochrome *b*561 catalyzes transmembrane electron transfer for dopamine beta-hydroxylase and peptidyl glycine alpha-amidating monooxygenase activities in reconstituted systems. J Biol Chem 262:8174-8178.

Lakshminarasimhan M, Bérczi A, Asard H (2006) Substrate-dependent reduction of a recombinant chromaffin granule Cyt-b561 and its R72A mutant. Acta Biol Szeged 50:61-65.

Laemmli U (1970) Cleavage of structural proteins during the assembly of the head of bacteriophage T4. Nature 227:680-685.

Lerman M, Minna JD (2000) The 630-kb lung cancer homozygous deletion region on human chromosome 3p21.3: Identification and evaluation of the resident candidate tumor suppressor genes. Cancer Res 60:6116-6133.

Liu W, Kamensky Y, Kakkar R, Foley E, Kulmacz RJ, Palmer G (2005) Purification and characterization of bovine adrenal cytochrome *b*561 expressed in insect and yeast cell systems. Protein Expr Purif 40:429-439.

Markwell MAK, Haas SB, Bieber LL, Tolbert NE (1978) A modification of the Lowry procedure to simplify protein determination in membrane and lipoprotein samples. Anal Biochem 87:206-210.

McKie AT, Barrow D, Latunde-Dada GO, Rolfs A, Sager G, Mudaly E, Mudaly M, Richardson C, Barlow D, Bomford A, Peters RJ, Raja KB, Shirali S, Hediger MA, Farzaneh F, Simpson RJ (2001) An iron-regulated ferric reductase associated with the absorption of dietary iron. Science 291:1755-1759.

Mizutani A, Sanuki R, Kakimoto K, Kojo S, Taketani S (2007) Involvement of 101F6, a homologue of cytochrome b_{561}, in the reduction of ferric ions. J Biochem 142:699-705.

Njus D, Kelley PM (1993) The secretory vesicle ASC-regenerating system: a chain of concerted H^+/e^--transfer reactions. Biochim Biophys Acta 1144:235-248.

Njus D, Wigle M, Kelley PM, Kipp BH, Schlegel HB (2001) Mechanism of ascorbic acid oxidation by cytochrome *b*561. Biochemistry 40:11905-11911.

Ponting CP (2001) Domain homologues of dopamine β-hydroxylase and ferric reductase: Roles for iron metabolism in neurodegenerative disorders. Human Mol Gen 10:1853-1858.

Ohtani O, Iwamaru A, Deng W, Ueda K, Wu G, Jayachandran G, Kondo S, Atkinson EN, Minna JD, Roth JA, Ji L (2007) Tumor suppressor 101F6 and ASC synergistically and selectively inhibit non–small cell lung cancer growth by caspase-independent apoptosis and autophagy. Cancer Res 67:6293-6303.

Roberg KJ, Rowley N, Kaiser CA (1997) Physiological regulation of membrane protein sorting late in the secretory pathway of *Saccharomyces cerevisiae*. J Cell Biol 137:1469-1482.

Silsand T, Flatmark T (1974) Purification of cytochrome *b*-561. An integral heme protein of the adrenal chromaffin granule membrane. Biochim Biophys Acta 359:257-266.

Su D, Asard H (2006) Three mammalian cytochrome b_{561} are ASC dependent ferrireductases. FEBS J 273:3722-3734.

Su D, May JM, Koury MJ, Asard H (2006) Human erythrocyte membranes contain a cytochrome *b*561 that may be involved in extracellular ASC recycling. J Biol Chem 281:39852-39859.

Thomas TC, McNamee MG (1990) Purification of membrane proteins. Methods Enzymol 182:499-520.

Tsubaki M, Takeuchi F, Nakanashi N (2005) Cytochrome *b*561 protein family: Expanding roles and versatile transmembrane electron transfer abilities as predicted by a new classification system and protein sequence motif analyses. Biochim Biophys Acta 1753:174-190.

Vargas JD, Herpers B, McKie AT, Gledhill S, McDonnell J, van den Heuvel M, Davies KE, Ponting CP (2003) Stromal cell-derived receptor 2 and cytochrome *b*561 are functional ferric reductases. Biochim Biophys Acta 1651:116-123.

Verelst W, Asard H (2003) A phylogenetic study of cytochrome *b*561 proteins. Genome Biol 4:R38.

Zhang D, Su D, Bérczi A, Vargas A, Asard H (2006) An ASC-reducible cytochrome *b*561 is localized in macrophage lysosomes. Biochim Biophys Acta 1760:1903-1913.

Volume 52(2):267-270, 2008
Acta Biologica Szegediensis
http://www.sci.u-szeged.hu/ABS

ARTICLE

Effect of fruit juices and pomace extracts on the growth of Gram-positive and Gram-negative bacteria

Judit Krisch[1]*, László Galgóczy[2], Mónika Tölgyesi[1], Tamás Papp[2] and Csaba Vágvölgyi[2]

[1]Institute of Food Engineering, Faculty of Engineering, University of Szeged, Szeged, Hungary, [2]Department of Microbiology, Faculty of Science and Informatics, University of Szeged, Szeged, Hungary

ABSTRACT Extracts and juices of cultivated and wild fruits belonging to the families Rosaceae, Grossulariaceae, Moraceae, Berberidaceae, Polygonaceae, Caprifoliaceae and Cornaceae were examined for their growth reducing activity on four bacteria (*Bacillus subtilis, B. cereus* var. *mycoides, Escherichia coli* and *Serratia marcescens*). In vitro antibacterial activities were evaluated by microdilution plate assays. Black currant (*Ribes nigrum*), cornelian cherry (*Cornus mas*) and European rowan (*Sorbus aucuparia*) had the highest growth inhibition capacity.
Acta Biol Szeged 52(2):267-270 (2008)

KEY WORDS

fruit
juice
antibacterial effect
pomace extract

Fruits are rich sources of vitamins, minerals and fibres, therefore, their consumption have positive role in the maintenance of human health. Phenolic compounds present in plants (phenolic acids, flavonoids, stilbenes, lignans and complex phenolic polymers) have antioxidant activity due to their redox properties (Kahkönen et al. 1999). They can also act as metal chelators and can have antimicrobial properties. The main target of antibacterial action is usually the cell membrane where destabilization and/or permeabilisation can occur. Phenolics can also inhibit extracellular enzymes or the multidrug resistance pumps of certain bacteria. Some berry extracts exhibit bacterial antiadhesion activity, so that bacteria cannot adhere to mucosal surfaces, which is an important prerequisite for colonisation and infection (Puupponen-Pimia et al. 2004).

There has been a growing interest in plant-derived active compounds among food technologists and pharmacologists. Food industry is searching for natural preservatives and antioxidants; and medicine, for new antimicrobial agents without rapidly developing resistance. In this study, the antibacterial activity of 21 wild and cultivated fruits was investigated.

Materials and Methods

Bacteria and culture conditions

Bacillus subtilis ssp. *subtilis* BD 170, *B. cereus* var. *mycoides* ATCC 9634, *Escherichia coli* SZMC 0582, and *Serratia marcescens* SZMC 0567 were grown on T1 medium (10g glucose, 4g beef extract, 4g peptone, 1g yeast extract, 1L H_2O).

Accepted July 28, 2008
*Corresponding author. E-mail: krisch@mk.u-szeged.hu.

Fruits and extraction methods

The fruits tested are listed in Table 1. Fresh fruits were purchased on a local market (Szeged) or were harvested in the neighbourhood of Szeged or in the mountains of North-East Hungary. Fruit juices were freshly pressed and stored at -20°C. The remaining pomace was dried at 60°C in an oven for 12 h and then ground to powder. One gram of each powdered pomace was extracted 3 times with 10 ml of distilled water or methanol per cycle. The extracts were combined and evaporated to dryness at 100°C in an oven (water extracts) or at 35-40°C in a water bath (methanol extracts). The dry material was redissolved in 4 ml distilled water (water extracts) or 10% methanol-water solution (methanol extracts), and frozen in 1 ml aliquots. One sample from each extracts was dried again and weighed for dry matter content calculation. Juices and extracts were diluted in the appropriate media for the tests.

Broth microdilution method

Inocula from each bacterium (10^5 cells/ml) were prepared in LB medium (10g triptone, 10g NaCl, 2g yeast extract, 1L H_2O). 100 µl of fivefold diluted and sterile filtered juice was mixed with 100 µl cell suspension in triplicates, incubated at 37°C for 48 h, and then absorbance was measured at 620 nm. For determination of growth curves absorbance was measured repeatedly in a time span of 48-72 hours.

Results

In our tests black currant (*Ribes nigrum*), cornelian cherry (*Cornus mas*) and European rowan (*Sorbus aucuparia*) had the best inhibition capacity (Table 1). Sweet cherry cultivars, hawthorn (*Crataegus monogyna*) and elderberry (*Sambucus*

Table 1. Growth inhibition effect of fruit juices. 0 - no growth; 1 - growth ≤ 25%; 2 - growth ≤ 50%; 3 - growth ≤ 75%; 4 - growth > 75 %; 100 % is taken as the growth control. J -juice; W - water extract; M - methanol extract

	Gram positive bacteria						Gram negative bacteria					
	Bacillus subtilis			*Bacillus cereus*			*Escherichia coli*			*Serratia marcescens*		
	J	W	M	J	W	M	J	W	M	J	W	M
Rosaceae												
Prunus avium	4	4	1	4	4	4	4	4	2	4	4	4
Prunus avium Gold	4	4	4	4	3	4	4	4	2	4	4	4
Prunus cerasus	4	4	4	3	2	4	2	3	1	4	4	1
Prunus armeniaca	4	4	4	3	1	3	2	2	2	4	4	4
Crataegus monogyna	4	4	4	3	4	4	4	4	4	4	4	4
Rubus idaeus	4	4	4	1	3	4	1	4	2	0	4	1
Rubus fruticosus	4	1	1	1	1	0	1	4	1	4	4	2
Fragaria ananassa	4	4	1	1	4	1	3	4	3	4	4	4
Sorbus aucuparia	1	1	2	2	1	4	1	1	1	4	4	1
Grossulariaceae												
Ribes nigrum	1	1	1	0	4	0	0	1	1	2	1	4
Ribes rubrum	1	4	4	4	4	4	1	4	1	1	4	1
Ribes uva-crispa	1	1	4	4	1	4	1	1	1	4	1	1
Ribes x nidigrolaria	1	4	4	0	2	4	0	3	1	0	4	4
Moraceae												
Morus alba	4	4	2	4	4	0	4	4	3	4	4	4
Morus nigra	4	4	1	4	4	0	3	4	4	4	4	4
Berberidaceae												
Berberis thunbergii	4	4	1	2	4	1	1	4	2	1	4	4
Mahonia aquifolium	1	4	2	2	2	4	1	4	1	1	4	4
Caprifoliaceae												
Sambucus nigra	4	4	1	4	4	0	4	4	4	4	4	4
Sambucus alba	4	4	4	4	3	4	4	4	3	4	4	4
Polygonacea												
Rheum rhabarbarum	4	0	4	4	0	4	2	4	1	4	4	1
Cornaceae												
Cornus mas	1	1	1	2	1	0	2	3	1	4	4	0

nigra) had no or weak inhibitory effect on the tested bacteria; in some cases they even facilitated bacterial growth. Members of the *Ribes* and *Rubus* genus were generally efficient inhibitors while other members of the Rosaceae family showed a poor growth reducing effect. When inhibition was observed, best results were obtained with methanolic extracts of the pomace, followed by the juices and finally by the water extracts. In general, Gram-positive bacteria showed moderate sensitivity. The Gram-negative *E. coli* was the most sensitive strain, especially to the juices and methanolic extracts. The other Gram-negative bacterium, *S. marcescens*, turned out to be the most insensitive one (for details, see Table 1).

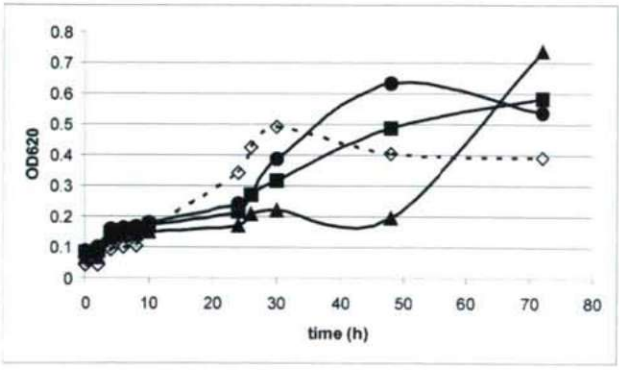

Figure 1. Effect of raspberry juice, water and methanol extract on the growth of *B. subtilis*. Empty diamond: control; filled triangle: juice; filled square: water extract of pomace, filled circle: methanolic extract of pomace.

To have a more detailed picture of the effect of fruit juices and extracts on bacterial growth, growth curves were obtain with *B. subtilis* and *E. coli* using raspberry. As seen in Figure 2, raspberry juice totally inhibited the growth of *E. coli* while the extracts had a moderate inhibitory effect. *B. subtilis* treated with raspberry juice reached, however, after a 48 hours adaptation period, a higher cell number than the untreated control. With the extracts, the adaptation period was shorter, only 24 hours, and the cell number was also higher than in the control (Fig. 1).

Raspberry juice had a two-face action on the growth of *B. subtilis* as shown by Figure 3. In ten- and twenty-fold dilutions, there was an adaptation phase of 48 and 24 hours, respectively, but then the maximal cell number considerably surpassed that of the control. With the higher dilutions, there was no adaptation phase but the second facilitatory effect was

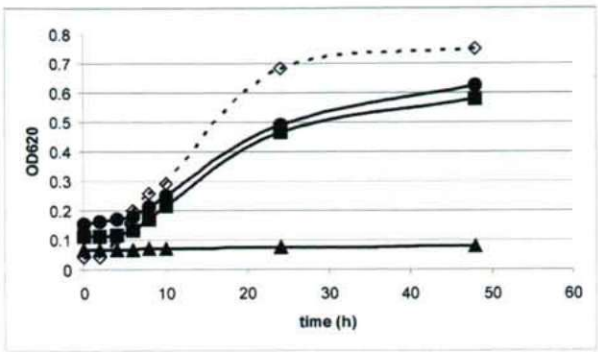

Figure 2. Effect of raspberry juice, water and methanol extract on the growth of *E. coli*. Empty diamond: control; filled triangle: juice; filled square: water extract of pomace, filled circle: methanolic extract of pomace.

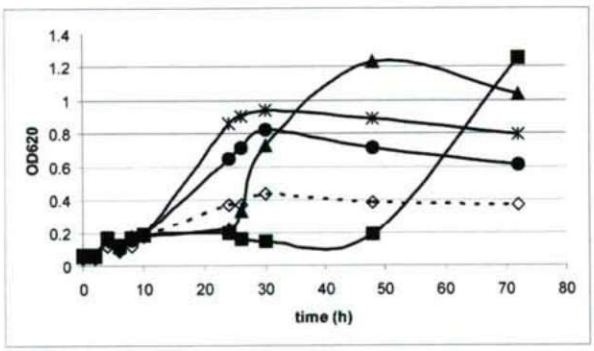

Figure 3. Effect of raspberry juice dilutions on the growth of *B. subtilis*. Empty diamond: control; filled square:10x; filled triangle:20x;, asterisk: 40x; filled circle: 80x dilution.

also less intense. In case of *E. coli*, all dilutions had more or less the same inhibitory effect (Fig. 4).

Discussion

Each juice and extract had an acidic pH ranging from 2.8 (*Ribes* spp.) to 5.5 (*Morus nigra*). The low pH of fruit juices is caused by weak organic and phenolic acids: in their undissociated forms (mainly on pH 3-5) these can interact with cell membranes and penetrate into the cells causing acidification of the cytoplasm. However, in our experiments there was only a weak correlation between acidity of the samples and their antibacterial effect.

Consumption of various berries has an important role in human health maintenance. Raspberry (*R. idaeus*) has a long tradition of use in curing diarrhoea (Ryan et al. 2001). Antibacterial activity of raspberry juice was demonstrated against *E. coli*, *S. typhimurium* and *S. epidermidis* (Ryan et al. 2001; Lee et al. 2003). In the study of Cavanagh et al. (2003), blackberry (*R. fruticosus*) juice had no growth inhibitory effect on *Salmonella* species but strongly inhibited *Klebsiella pneumoniae*. In our experiments raspberry and blackberry juice decreased the growth of *B. cereus* and *E. coli*.

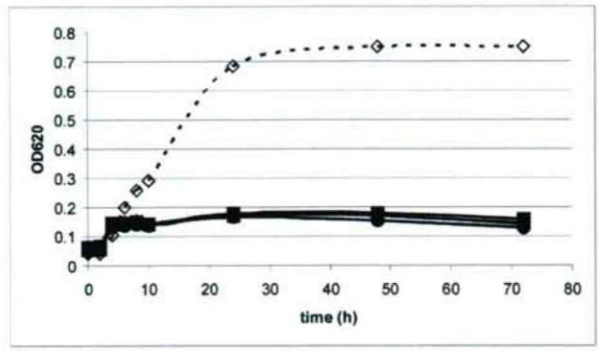

Figure 4. Effect of raspberry juice dilutions on the growth of *E. coli*. Empty diamond: control; filled square:10x; filled triangle:20x;, asterisk: 40x; filled circle: 80x dilution.

In European folk medicine, *R. nigrum* (blackcurrant) fruits have been used to support the immune and digestive systems. In previous studies (Puupponen-Pimiä et al. 2001; Cavanagh et al. 2003), blackcurrant juices and extracts were more efficient against Gram-positive bacteria than against Gram-negative ones. In our study, the blackcurrant juice caused growth inhibition on all the investigated species except of *S. marcescens*. Other investigated *Ribes* species (*R.* x *nidigrolaria*, *R. uva-crispa* and *R. rubrum*) were also among the most efficient inhibitors in our study.

Gram-negative and Gram-positive organisms show different sensitivity to several antibacterial agents because the former possess an outer membrane as part of their cell wall (Ratledge and Wilkinson 1988) restricting the diffusion of hydrophobic compounds, e.g.: essential oils (Burt 2004), and other oily substances such as guava and neem extracts (Mahfuzul Hoque et al. 2007) showed higher antimicrobial activity against Gram-positive than Gram-negative bacteria. At the same time, certain small hydrophobic compounds are known to penetrate easily to the cells generating pores in the outer membranes. The efficiency of methanolic extracts (and juices) on *E. coli* in our study suggest the presence of such non-polar molecules. Previous studies demonstrated that purple and red fruits and vegetables, with high content of anthocyanins, had substantial antibacterial effect (Harborne and Williams 2000; Lee et al. 2003). Our results with closely related coloured and non-coloured fruit species and varieties (*Sambucus nigra* and *S. alba*, *Morus nigra* and *M. alba*, *Prunus avium* Germersdorfi and *P. avium* Gold) showed, however, no real difference in their inhibitory effect. On the other hand, the dark coloured *Ribes* and *Rubus* species had excellent antibacterial action. The role of anthocyans in the growth inhibition of bacteria needs further investigation.

Acknowledgements

This work was financially supported by the grant ETT 214/2006. Tamás Papp is a grantee of the János Bolyai Research Scholarship of the Hungarian Academy of Sciences.

References

Burt S (2004) Essential oils: their antibacterial properties and potential applications in foods-a review. Int J Food Microbiol 94:223-253.

Cavanagh HMA, Hipwell M, Wilkinson JM (2003) Antibacterial activity of berry fruits used for culinary purposes. J Med Food 6:57-61.

Harborne JB, Williams CA (2000) Advances in flavonoid research since 1992. Phytochemistry 6:481.

Kahkönen MP, Hopia AI, Vuorela HJ, Rauha J-P, Pihlaja K, Kujala TS, Heinonen M (1999) Antioxidant activity of plant extracts containing phenolic compounds. J Agric Chem 47:3954-3962.

Lee YL, Cesario T, Wang Y, Shanbrom E, Thrupp L (2003) Antibacterial activity of vegetables and juices. Nutrition 19:994-996.

Mahfuzul Hoque MD, Bari ML, Inatsu Y, Juneja VK, Kawamoto S (2007) Antibacterial activity of guava (Psidium guajava L.) and neem (Azadirachta indica A. Juss.) extracts against foodborne pathogens and spoilage bacteria. Foodborn Pathogens and Disease 4:481-488.

Puupponen-Pimiä R, Nohynek L, Meier C, Kahkonen M, Heinonen M, Hopia A, Oksman-Caldentey K-M (2001) Antimicrobial properties of phenolic compounds from berries. J Appl Microbiol 90:494-507.

Puupponen-Pimia R, Nohynek L, Alakomi, HL, Oksman-Caldentey KM (2004) Bioactive berry compounds-novel tools against human pathogens. Appl Microbiol Biotechnol 67:8-18.

Ratledge C, Wilkinson SG (1988) An overview of microbial lipids. In Ratledge C, Wilkinson SG eds., Microbial Lipids vol. 1. Academic Press, London, pp. 3-22.

Ryan T, Wilkinson JM, Cavanagh HMA (2001) Antibacterial activity of raspberry cordial in vitro. Res Vet Sci 71:155-159.

Volume 52(2):271-275, 2008
Acta Biologica Szegediensis
http://www.sci.u-szeged.hu/ABS

ARTICLE

Application of *Saccharomyces cerevisiae* as a biocontrol agent against *Fusarium* infection of sugar beet plants

Moustafa El-Sayed Shalaby[1]*, Mohamed Fathi El-Nady[2]

[1]Department of Agricultural Microbiology, Faculty of Agriculture, Kafrelsheikh University, Egypt, [2]Department of Agricultural Botany, Faculty of Agriculture, Kafrelsheikh University, Egypt

ABSTRACT Applicability of *Saccharomyces cerevisiae* as a biocontrol agent of *Fusarium oxysporum* and as plant growth promoter was investigated. At 5 g L^{-1}concentration, germination rate of the soaked seeds reached 85.83% in comparison with 54.00% for the untreated ones. Plant growth parameters, chlorophyll contents, TSS and sucrose percentages were also tested. Application of 5 g L^{-1} of yeast resulted in a reduction of the pre- and post-emergence damping-off 6.67 and 11.67%, respectively. Survival of treated plants increased to 83.33% in comparison with 30.00% for the pots inoculated with the pathogen containing untreated seeds. Linear growth of *F. oxysporum* was inhibited with 39.52% and 50% by using 5 g L^{-1} and 6.35 g L^{-1} of the yeast, respectively.
Acta Biol Szeged 52(2):271-275 (2008)

KEY WORDS

sugar beet
Saccharomyces cerevisiae
growth promotion
damping-off
biological control

Nowadays, a great attention has been focused on the possibility of using natural and safe agents for promoting growth of sugar beet and for inducing its resistance against different diseases. *Saccharomyces cerevisiae* is considered a new promising plant growth promoting yeast for different crops. It became in the last few decade a positive alternative to chemical fertilizers safely used for human, animal and environment (Omran 2000). Due to its cytokinin content, yeast treatments were suggested to play a beneficial role in cell division and cell enlargement (Natio et al. 1981). Yeast as a natural stimulator is also characterized by its richness in protein 47%, carbohydrates 33%, nucleic acid 8%, lipids 4%, and different minerals 8% such as Na, Fe, Mg, K, P, S, Zn, Mn, Cu, Si, Cr, Ni, Va and Li in addition to thiamin, riboflavin, pyridoxine, hormones and other growth regulating substances, biotin, B12 and folic acid (Nagodawithana 1991). Earlier reports explained the effect of yeast application on vegetative and fruit growth due to its richness in tryptophan which consider precursor of IAA (indole acetic acid) and on flower ignition due to its effect on carbohydrate accumulation (Warring and Philips 1973).

Biological control of different plant diseases was focused primarily using bacteria or filamentous fungi (Whipps 2001). So, application of yeasts as biocontrol agents acts as a new trend against different pathogens. Potential use of yeasts as biocontrol agents of soil-borne fungal plant pathogens and as plant growth promoters were recent investigated by El-Tarabily and Sivasithamparam (2006). El-Tarabily (2004) reported that the fungal activities of *Rhizoctonia solani* diseased sugar beet plants were well suppressed by using different yeasts. Wide variety of yeasts have been used extensively for the biological control of post-harvest diseases of fruits and vegetables (Punja 1997 and Zheng et al. 2003)), against moulds of stored grains (Petrsson et al. 1999) and to control powdery mildews (Urquhart and Punja 1997).

The aim of this study was to suppress the soil-borne pathogenic fungus *Fusarium oxysporum* by using *S. cerevisiae* as biocontrol agent and as a plant growth promoter of sugar beet plants.

Materials and Methods

This investigation was carried out in experimental pots for sowing sugar beet (*Beta vulgaris* L.) during two successive seasons of 2006/2007 and 2007/2008 at Kafrelsheikh University, Egypt. The bio-compound used in this study is active dry yeast of *S. cerevisiae*. Yeast application was conducted as seed soaking, foliar spraying and as soil inoculation using three concentrations of 1, 2 and 5 g L^{-1}.

Test for plant growth promotion

Dry yeasts were well dissolved firstly in slight sugar solutions and cultivated for 12 h. Before application, the solutions were diluted to the required concentrations using sterile distilled water.

Seeds were soaked in defined yeast concentrations at overnight before sowing. Soaked seeds in pure water were acted as control. For foliar spraying or soil inoculation treatments, seeds were sown without soaking. Each treatment was represented by five replicates. Thinning was done after complete germination, leaving one plant per pot. After

Accepted Nov 26, 2008
*Corresponding author. E-mail: moustafashalaby@yahoo.com

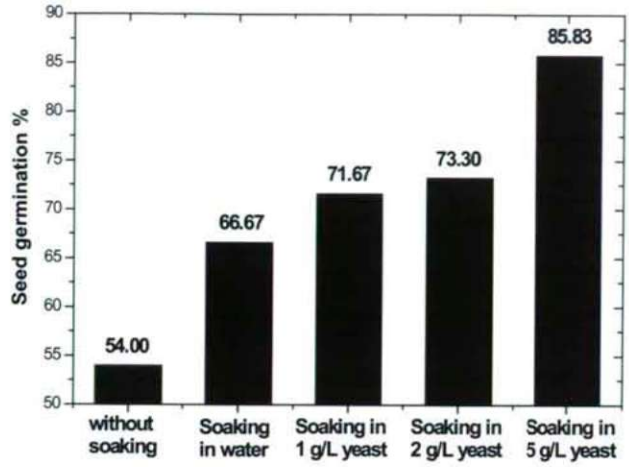

Figure 1. Effect of yeast application on germination rate of sugar beet seeds.

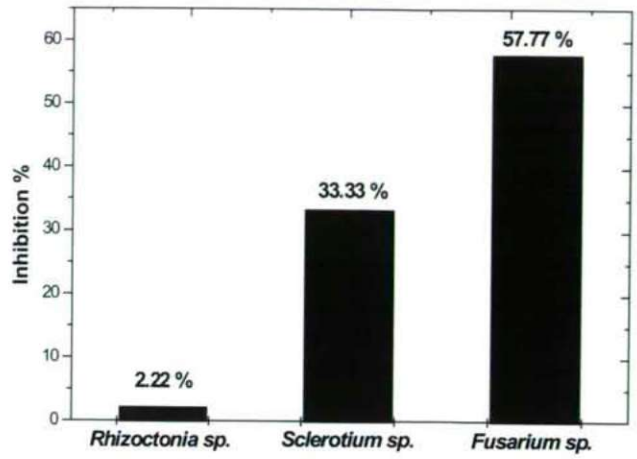

Figure 2. Antifungal activity of *S. cerevisiae* against *R. solani, S. rolfsii* and *F. oxysporum* F4.

30 days from planting, shoots were sprayed and soils were dressed with yeast solutions for both application methods. This was regularly repeated about four week's intervals during the season.

Germination rate of the seeds was calculated at seedling stage. After 90 days from planting, photosynthetic pigments (chlorophyll a, b and total) were determined according to Moran (1982).Vegetative growth parameters like leaf area, root length, root diameter, fresh and dry weigh of roots and shoots were estimated at the season end. Using root juices, total soluble solids (TSS %) were measured via a hand refractometer. For sucrose content, 26 g of root samples were treated with 176 ml of basic lead acetate and filtered through filter papers according to the procedures of Supernova et al. (1979). Sucrose content was measured in the filtrate using a saccharometer.

Biocontrol tests

Isolation of a Fusarium pathogen strain

Damping-off root samples were collected from different locations of Kafr El-sheikh governorate. After removing adhering soil particles with water, samples were cut into small pieces, surface sterilized (0.25% sodium hypochlorite, 4 min), washed several times with sterile distilled water, blotted between two sterilized filter papers and finally placed onto potato dextrose agar plates (PDA). Inoculated plates were incubated at 28°C for 3-7 days. Fungal isolates were microscopically examined and purified using the hyphal tip technique. Purified isolates were identified as *Fusarium oxysporum*. Isolates (identified as *Fusarium oxysporum*) were maintained on PDA slants at 4°C. Cultural, morphological, microscopic and pathological properties were considered to identify the fungal isolates according to Ellis (1976) and Booth (1977). Among them F4 was the most virulent isolate.

Antagonism

Growth of *F.oxysporum* F4 (FOF4) was estimated in presence of 0, 1, 2 and 5 g L^{-1} yeast on PDA medium. Plates were inoculated centrally with mycelial disks (0.5 cm in diameter) taken from 7 days old cultures. Diameters of the colonies (incubated at 28°C) were measured in every 24 hours. When growth of the fungal isolate had just covered the untreated plates, percentages of inhibition (I %) were calculated according to the formula of Topps and Wain (1957):

$$I\ \% = [(A - B)/A] \times 100$$

where, I % = percentage of inhibition, A = mean diameter growth in the control, B = mean diameter growth in a given treatment. Growth inhibition data were linear fitted and IC_{50} value was calculated.

Efficiency of yeast application against damping-off disease in sugar beet seedlings was also evaluated. Pots of 30 cm diameter were filled with autoclaved clay soil mixed with the FOF4 inoculum one week before planting. FOF4 inoculum was prepared by growing on corn meal medium at 28°C for 15 days. Inoculum was added to the plotted soil at rate of 5% w/w (Hussein 1973). Infected soil was mixed thoroughly and moistens every day. Yeast concentrations of 1, 2 and 5 g L^{-1}, adjusted at 0.70, 1.23 and 2.78 x 10^8 cell/ml, respectively, were applied at the time of planting as seed treatment. Each treatment was represented by 3 replicates. Pots were kept in greenhouse and watered when needed. Percentages of pre- and post-emergence damping off as well as survival plants were calculated up to 45 days from planting as follows:

% of pre-emergence damping-off = (No. of non emerged seeds/No. of sown seeds) x 100

Table 1. Effect of yeast on vegetative growth of sugar beet plants during two successive seasons.

Treatments	Con g/L	Leaf area Cm²	Root parameters [1,2]Cm & [3]Kg [1]Length	[2]Diameter	[3]Fresh w.	Dry weight % Shoot	Root
				2006/2007			
Control	0	103.0 a	17.33 ab	6.00 cde	0.23 bc	20.75 a	25.54 ab
Seed soaking	1	139.52 ab	17.33 ab	6.08 cde	0.23 bc	21.02 a	26.51 b
	2	145.16 b	18.33 ab	6.42 de	0.27 cd	28.55 c	26.74 b
	5	210.05 d	19.00 b	6.75 e	0.32 cd	28.79 c	28.41 c
Foliar spraying	1	137.32 ab	15.33 ab	5.83 cd	0.23 bc	28.57 c	24.65 a
	2	146.54 b	18.67 ab	5.50 bc	0.24 c	35.79 d	24.64 a
	5	162.56 bc	19.00 b	5.83 cd	0.26 c	29.43 c	33.05 d
Soil inoculation	1	192.99 cd	14.33 a	4.58 a	0.15 a	21.47 a	25.65 ab
	2	208.87 d	15.33 ab	5.00 ab	0.17 ab	22.75 ab	26.92 bc
	5	250.28 e	16.67 ab	5.92 cd	0.22 bc	26.57 bc	36.98 e
LSD at 5%		38.27	4.09	0.73	0.06	3.82	1.58
				2007/2008			
Control	0	139.42 ab	24.00 a	12.50 a	0.68abc	30.59 a	32.48 a
Seed soaking	1	117.74 a	23.00 a	12.00 a	0.41 a	44.34 d	34.77 a-d
	2	126.11 a	23.00 a	12.25 a	0.61 ab	43.15 d	33.48 ab
	5	212.17 cd	24.50 ab	20.00 c	1.21 b-e	51.17 e	36.57 cd
Foliar spraying	1	181.16bcd	25.17 ab	12.50 a	0.68 abc	37.91 c	34.30 abc
	2	184.90bcd	26.00 ab	16.50 bc	1.33 de	36.51 c	35.74 bcd
	5	208.52 cd	28.00 b	19.00 c	1.30 cde	45.54 d	43.13 e
Soil inoculation	1	163.47abc	25.50 ab	14.50 ab	0.82 a-d	31.10 ab	32.60 a
	2	227.14 d	28.00 b	18.00 bc	1.58 e	34.88 bc	37.02 d
	5	294.32 e	34.00 c	19.00 c	1.67 e	38.61 c	46.88 f
LSD at 5%		49.00	3.19	3.71	0.58	3.80	2.34

% of post-emergence damping-off = (No. of killed seedlings/total No. of emerged seedlings) x 100

% of survival plants = (No. of un-infected plants/total No. of plants) x 100.

Statistical analysis

Data were statistically tested for one-way analysis of variance (ANOVA) using SPSS computer software program and Duncan's multiple range tests were applied for comparing means (Duncan 1955).

Results and Discussion

Effect of yeast application on seed germination

The effect of *S. cerevisiae* application can be seen in Figure 1. The most effective was the highest concentration (5 g L^{-1}), where the seed germination reached to 85.83% after nine days from planting. This was in agreement with the data obtained by El-Emery (2004), who reported that germination rate of different seeds of barley, maize, pea and bean was great enhanced by using different yeast dilutions and

Table 2. Effect of yeast application on chlorophyll content of sugar beet leaves during two successive seasons.

Treatments	Con g/L	2006/2007 Chl a	Chl b	Chl a + b	2007/2008 Chl a	Chl b	Chl a + b
Control	0	16.37 a	5.40 a	21.77 a	12.72 a	3.28 a	16.00 a
Seed soaking	1	21.14 c	7.06 bc	28.20 c	12.60 a	3.12 a	15.72 a
	2	22.24 cd	7.68 bc	29.92 cde	13.40 a	3.39 a	16.79 a
	5	24.80 e	7.49 bc	32.29 f	14.11 a	4.31 a	18.42 a
Foliar spraying	1	19.40 b	6.55 abc	25.95 b	12.35 a	3.63 a	15.98 a
	2	22.71 cd	8.19 c	30.90 def	14.45 a	3.60 a	18.05 a
	5	23.67 de	8.16 c	31.83 ef	16.69 b	4.70 a	21.39 b
Soil inoculation	1	16.70 a	6.40 ab	23.10 a	13.95 a	3.38 a	17.34 a
	2	17.32 a	6.14 ab	23.46 a	17.81bc	4.57 a	22.38 bc
	5	22.07 cd	7.42 bc	29.49 cd	19.49 c	4.60 a	24.09 c
LSD at 5%		1.50	1.49	1.86	2.20	1.71	2.48

Table 3. Effect of yeast on yield quality of sugar beet plants.

Treatments	Conc. g/L	% of yield quality TSS	Sucrose
Control	0	22.20 d	20.50 bc
Seed soaking	1	18.73 b	22.15 cd
	2	21.87 d	22.63 d
	5	22.63 d	25.10 e
Foliar spraying	1	18.83 bc	19.45 ab
	2	24.47 e	20.54 bc
	5	26.47 f	23.24 d
Soil inoculation	1	15.13 a	17.78 a
	2	19.80 c	20.16 b
	5	22.80 d	25.54 e
LSD at 5%		0.99	1.70

Table 4. Effect of different concentrations of *S. cerevisiae* against *F. oxysporum* causing damping-off in sugar beet seedlings.

Treatments	% Disease expressions pre emergence damping-off	post emergence damping-off	plants survival
Un-infected (control)	5.00 a	6.08 a	92.50 d
Infected	40.00 c	50.00 b	30.00 a
Infected + 1 g L^{-1}	20.00 b	12.50 a	70.00 bc
Infected + 2 g L^{-1}	30.00 bc	13.10 a	60.00 b
Infected + 5 g L^{-1}	6.67 a	11.67 a	83.33 cd
L. S. D. at 5 %	12.51	22.31	20.59

growth of plumules, rootlets and cotyledon enlargement was also stimulated.

Effect of yeast on the vegetative growth

Table 1 shows the effect of yeast on the morphological characteristics investigated: changes were more pronounced with increasing yeast concentrations.

Due to the use of 5 g L^{-1} yeast in the soil, leaf area was more than twofold increased in both seasons, indicating enhanced cell division rate and cell enlargement. Regarding root parameters, their length, diameter and fresh weight were significantly enhanced during the second season compared to the first one, indicating a quite establishment with the experimental conditions. The highest percentage of shoot dry weight of 51.17% was achieved in the second season due to seed treatment with 5 g L^{-1} of yeast solution. Results indicate that soil application was the most suitable technique enhancing leaf area, root length, root diameter and root fresh and dry weight clearly, while the best dry weight of shoots were achieved via seed soaking in the used biofertilizer before planting. These are in agreement with data obtained by Muller and Leopold (1966), who demonstrated that enhancing effect of yeast application might be due to yeast cytokinins enhancing the accumulation of soluble metabolites. The enhancing effect of yeast on germination rate and on the vegetative growth parameters was strongly supported by Entian and Fröhlich (1984). They stated increased enzyme activity regulating catabolic productions in eukaryotic cells treated with *S. cerevisiae*.

Effect of yeast application on chlorophyll content

Table 2 shows that yeast application resulted in higher leaf pigment content in compared to the control. Irrespective the application technique, increasing in pigments formation of Chlorophyll a, b and their total was obtained via increasing yeast concentration during the tested seasons. Such increase in photosynthetic pigments formation could be attributed to the role of yeast cytokinins delaying the aging of leaves by reducing the degradation of chlorophyll and enhancing the protein and RNA synthesis (Castelfranco and Beale 1983).

Effect of yeast application on the yield quality

Effect of yeast treatment on the total soluble solids (TSS) and sucrose content are presented in Table 3. The highest TSS values were achieved via foliar spraying using 5 and 2 g L^{-1} of yeast concentrations. The greatest sucrose values were 25.54% and 25.10% obtained via soil inoculation and seed treatment.

Evaluation of *S. cerevisiae* as biocontrol agents

As a biological control agent, S. *cerevisiae* was tested *in vitro* against various soil-borne fungi of *Rhizoctonia solani*, *Sclerotium rolfsii* and *F. oxysporum* F4, causing severe symptoms in sugar beet seedlings. Data presented in Figure 2 show various inhibitory effect against these fungi. *F. oxysporum* F4 proved to be the most sensitive (57.77% growth inhibition), in comparison with *Rhizoctonia solani* and *Sclerotium rolfsii*, growth inhibition of 33.33% and 2.22%, respectively. These results are similar as of El-Tarabily (2004) and Madi et al. (1997): they reported that *R. solani* and *S. rolfsii* were effectively suppressed by some plant growth-promoting yeasts, respectively.

So, sensitivity of *F. oxysporum* F4 was also tested against 0, 1, 2, and 5 g L^{-1} of yeast concentrations. Linear growth of *F. oxysporum* F4 was inhibited with 39.52% by using 5 g L^{-1} of *S. cerevisiae*. To achieve 50% inhibition (IC_{50}), data were fitted ($R^2 = 0.999$) and 6.35 g L^{-1} of yeast are required. These results were supported by Attyia and Youssry (2001). They stated suppressed radial growth of *Macrophomina phaseolina* and *Fusarium solani* by using the local isolate of *S. cerevisiae*.

Based on these results, the potential of *S. cerevisiae* as biocontrol agent against *Fusarium oxysporum* F4 causing sever damping-off symptoms of sugar beet was evaluated in Table 4.

The lowest percentages of pre- and post-emergence damping-off were recorded by 5 g L^{-1} yeast concentration with the higher survival rate of plants of 83.33%. It indicates that *F. oxysporum* F4 was suppressed strongly by 5 g L^{-1} of *S. cerevisiae*. A similar behavior was observed by Hassan and Abd El-Rehim (2002) for controlling onion neck rot disease. They observed that, increasing yeast concentration (0.05 to 0.1%) leads to increasing reduction of the disease incidence. *Fusarium spp* was also inhibited and seed germination of watermelon was induced by using several taxa included yeast genera as plant growth promoters and as biocontrol agents (Lokesh et al. 2007). Antagonistic activity of the ascomycetous yeast strain *Pichia anomala* against *Fusarium spp* contaminated barley grains was also reported by Laitila et al. (2007) under industry conditions. So, this study is considered one of the first successful attempts using *S. cerevisiae* as promising biocontrol agents.

The results of our study indicate that *S. cerevisiae* have strong potential as plant growth promoters and as biocontrol agents of the soil-borne fungal plant pathogen *F. oxysporum* causing damping-off symptoms in sugar beet seedlings.

References

Attyia SH, Youssry AA (2001) Application of *Saccharomyces cerevisiae* as a biocontrol agent against some diseases of Solanaceae caused by *Macrophomina phaseolina* and *Fusarium solani*. Egyptian Journal of Biology 3:79-87

Booth C (1977) Fusarium: Laboratory guide to the identification of the major species. Commonwealth Mycological Institute, Kew, Surry, England.

Castelfranco PA, Beale S I (1983) Chlorophyll biosynthesis recent advances and areas of current interest. Ann Rev Plant Physiol 34:241-278.

Duncan DB (1955) Multiple range and multiple F-test Biometrics, II: 1-42

El-Emery GAE (2004) Effect of growth regulators of yeast autolysate, RNA and adenine on some seeds during germination. Arab Uni J of Agric Sci 12(1):51-67.

Ellis MB (1976) More Dematiaceous Hyphomycetes. Commonwealth Mycological Institute, Kew, Surry, England.

El-Tarabily KA (2004) Suppression of *Rhizoctonia solani* diseases of sugar beet by antagonistic and plant growth-promoting yeasts. J Appl Microbiol 96:69-75.

El-Tarabily KA, Sivasithamparam K (2006) Potential of yeasts as biocontrol agents of soil-borne fungal plant pathogens and as plant growth promoters. Mycoscience 47:25-35.

Entian K-D, Fröhlich K-U (1984) *Saccharomyces cerevisiae* mutants provide evidence of hexokinase PII as a bifunctional enzyme with catalytic and regulatory domains for triggering carbon catabolite repression. J Bacteriol 158(1):29-35.

Hassan MHA, Abd El-Rehim GH (2002) Yeast application as a biofertilizer and biocontrol agent for onion neck rot disease in relation to bulb productivity and quality. Assiut J Agric Sci 33(1):241- 251.

Hussein MS (1973) Pathological studies on root rot disease of peas (*Pisum sativum*). M. Sc. Thesis. Fac Agric Al-Azhar Univ.

Laitila A, Sarlin T, Kotaviita E, Huttunen T, Home S, Wilhelmson A (2007) Yeasts isolated from industrial maltings can suppress Fusarium growth and formation of gushing factors. J Ind Microbiol Biotechnol 34(11):701-13.

Lokesh S, Bharath BG, Raghavendra VB, Govindappa M (2007) Importance of plant growth-promoting rhizobacteria in enhancing the seed germination and growth of watermelon attacked by fungal pathogens. Acta Agronomica Hungarica 55(2):243-249.

Madi L, Katan T, Katan J, Heins Y (1997) Biological control of *Sclerotium rolfsii* and *Verticillium dahaliae* by *Talaromyces flavus* is mediated by different nichanisms. Phytopathol 87(10):1054-1060.

Moran R (1982) Formulae for determination of chlorophyllous pigments extracted with N, N-Dimethylformamide. Plant Physiol 69:1376-1381.

Muller K, Leopold AC (1966) Correlative aging and transport of p32 in corn leaves under the influence of kinetin plant 68:167-185.

Nagodawithana WT (1991) Yeast technology. Universal foods cooperation Milwauke, Wisconsin. Published by Van Nostrand, New York.

Natio K, Nagamo S, Fury K, Suzki H (1981) Effect of benzyladenine on RNA and protein synthesis in intact bean leaves at various stages of ageing. Plant Physiol 52:342-348.

Omran YA (2000) Studies on histophysiological effect of hydrogen cyanamide (Dormex) and yeast application on bud fertility, vegetative growth and yield of „Roumi Red" grape cultivar. Ph. D. Thesis, Fac of Agric Assiut Univ Egypt.

Punja ZK (1997) Comparative efficacy of bacteria, fungi and yeasts as biological control agents for disease of vegetable crops. Can J Plant Pathol 19:315-323.

Petersson S, Jonsson N, Schnürer J (1999) *Pichia anomala* as a biocontrol agent during storage of high-moisture feed grain under airtight conditions. Postharvest Biol Technol 15:175-184.

Supernova A R, Joshman A E, Loseava V A (1979) General technology of sugar and sugar substances. Pischevayapromyshlennost pub Moscow, p. 464.

Topps JH, Wain RL (1957) Investigation on fungicides. III. The fungi toxicity of 3-and 5- alkyl salicylanilide and P-chloronilines. Ann Appl Biol 45(3):506-511.

Urquhart EJ, Punja ZK (1997) Epiphytic growth and survival of *Tilletiopsis pallescens*, a potential biological control agent of *Sphaerotheca fuliginea*, on cucumber leaves. Can J Bot 75:892-901.

Warring PE, Phillips IDG (1973) The control of growth and differentiation in plants. E L B S ed., Pub by Pergamon Press Ltd. VK.

Whipps JM (2001) Microbial interactions and biocontrol in the rhizosphere. J Exp Bot 52:487-511.

Zheng DX, Sun YP, Zhang HY (2003) Yeast application for controlling apple postharvest diseases associated with *Penicillium expansum*. Bot Bull Acad Sin 44:211-216.

Volume 52(2):277-282, 2008
Acta Biologica Szegediensis
http://www.sci.u-szeged.hu/ABS

ARTICLE

Construction of gene cassette harboring HMW glutenin gene of wheat driven by γ-kafirin promoter of sorghum

Avinash Mishra[1,3]*, Ruchi Pandey[1], Sangita Bansal[1], Akash Tomar[1], V. K. Khanna[2], G. K. Garg[1]

[1]Department of Molecular Biology and Genetic Engineering, G. B. Pant University of Agriculture and Technology, Uttarakhand, Pantnagar, India, [2]Department of Genetics and Plant Breeding, G. B. Pant University of Agriculture and Technology, Uttarakhand, Pantnagar, India, [3]Discipline of Marine Biotechnology and Ecology, Central Salt and Marine Chemicals Research Institute, G. B. Marg, Bhavnagar, Gujarat, India

ABSTRACT Modern biological tools of genetic engineering and biotechnology can allow transfer of gene(s) across crop species. The r-DNA technology has tremendous potential to transfer bread making character of bread wheat into sorghum by transferring glutenin gene(s), which can improve the visico-elastic property of the sorghum flour/dough. These genes in addition to improving quality can significantly contribute to improve the nutritional status by the addition of more protein fractions also. In the simplest approach, new HMW gluten loci may be created via transformation to bioengineer sorghum quality. For this, amplified γ-kafirin promoter (574 bp) was subcloned in pCAMBIA1304 by replacing CaMV35S promoter (ca. 800 bp) of the *gus* reporter gene resulting in vector pkaf-gus, where the expression of *gus* reporter gene is under the control of γ-kafirin promoter. In order to construct a gene cassette where HMW glu gene(s) will be under the control of γ-kafirin gene promoter, kafirin promoter was first cloned in pUC19 and then HMW gene(s) were excised from their respective vectors and cloned under the control of promoter. Finally, two gene cassettes were developed as pKaf-Dx5 and pKaf-Dy10 where expression of the HMW glu gene Dx5 (8.7 kb) and Dy10 (6.4 kb) was driven by the γ-kafirin gene promoter. Both gene cassettes are ready to clone in any vector to bioengineer sorghum by genetic transformation

Acta Biol Szeged 52(2):277-282 (2008)

KEY WORDS

glutenin
kafirin
gene construct
cloning
sorghum
wheat

Sorghum improvement can be a multidirectional program. There could be different strategies for the enhancement of economic value of the sorghum. However, lysine content enhancement and dough making quality improvement are the major areas that need urgent attention. The scope to improve the nutritional and dough quality of sorghum grain protein by employing classical plant breeding seems to be limited as only low level of variations are available in sorghum gene pool for crossing. Only two mutant high lysine genes are currently available. These are spontaneous mutant gene *h1*, which was initially identified in an Ethiopian line (Singh and Axtell 1973) and *P 721 opaque* gene which was induced with ethyl methane sulphonate (EMS) (Axtell et al. 1979). Both of these lines can be defined as "low prolamin" mutants with pleiotropic effects on other grain characteristics. Hence, it has proved difficult to incorporate the high lysine phenotype into varieties with high yield and acceptable agronomic performance and processing properties.

Of all cereal grains, wheat is unique because wheat flour has the ability to form dough that exhibits the rheological properties required for the production of bread and for the wider diversity of foods. The unique properties of the wheat grain reside primarily in the gluten forming storage proteins of its endosperm. Glutenin are among the largest protein molecules in nature (Wrigley 1996) and classified as prolamins (Shewry and Halford 2002). Wheat prolamins are characterized as HMW prolamins (High molecular weight glutenin subunits, HMW-GS), S-rich prolamins (γ-gliadin, α-gliadin and B & C type of LMW-GS) and S-poor prolamins (D type of LMW glutenin). HMW-GS have been closely associated with bread making quality. After very long investigation, it was found that the *glu* D1 encoded HMW glutenin subunit pair 5+10 and *glu* 1Ax1 is associated with greater dough strength of the wheat (Shewry and Halford 2002; Altpeter et al. 2004). D'Ovidio and Anderson (1994) confirmed the role of *glu* D1 (Dx5+Dy10) in bread making quality of wheat. They analyzed that the y-type subunits are the main components responsible for dough making quality of the flour while x-type subunit have only minor effect. Two hypotheses have been proposed to explain the superior bread/ dough-making quality of wheat cultivars possessing subunits Dx5+Dy10 compared with those possessing subunits Dx2+Dy12. The first hypothesis considers that the additional cysteine residue present in the N-terminal domain of the Dx5 subunit plays an important role in influencing the disulphide cross-linked

Accepted Nov 4, 2008
*Corresponding author. E-mail: avinash@csmcri.org

glutenin network necessary for dough properties (Greene et al. 1988). The second hypothesis proposes that the higher proportion of consensus-type repeats in the Dy10 subunit gives rise to a more regular pattern of β-turns in the central repetitive domain, which is responsible for conferring better elastic properties on this subunit and consequently on the dough (Flavell et al. 1989).

Genetic engineering offers an opportunity to overcome the limitations of plant breeding and has opened up new avenues to improve the physical and nutritional quality of grain sorghum. Gene manipulation includes two major approaches. First is a gene alteration in which expression of existing seed storage protein gene(s) is enhanced by addition, deletion or substitution of certain sequences by site directed mutagenesis (Mutational breeding). Second approach is the addition of a foreign gene with novel or improved characters (Transgenic technology). Transgenic technology is worldwide used technique to enhance economic value of the crops.

Proper regulation of the expression of introgressed seed storage proteins gene is necessary for the success of a transgenic. Seed protein gene expression is not only developmentally but also metabolically regulated. Promoters including several upstream sequences are crucial and required to regulate gene expression both quantitatively and qualitatively. The regulatory sequences of promoters that define the qualitative specificity of gene expression in plants have been studied and much information has accumulated in recent years (Mishra et al. 2008). Attempts were made to express different genes in sorghum by using either constitutive promoters or gamma zein promoter however expression level was not reported (Grootboom and O'Kennedy 2003). It was therefore concluded that if the dough making quality of sorghum is to be improved by introgressing a glutenin gene, a seed specific promoter from sorghum will be better.

Alpha kafirin promoter of sorghum expresses α- kafirin proteins in abundant and it is located in the core of the protein body. β-kafirin promoter expresses protein in the interior of the protein body (Shull et al. 1992). These two promoters will be poor choice for the expression of the HMW glu gene of the wheat as the basic protein body of the sorghum gets disrupted and resultant is the alteration of basic property of the sorghum proteins. γ-kafirin proteins are found periphery of the protein body and it is expected that γ-kafirin gene promoter will allow expression of desired HMW glu gene at periphery of the protein body by replacing the γ-kafirin protein or as the floating protein bodies so that we will get better dough making quality without alteration of the basic property of the sorghum flour (Mishra et al. 2008; Bansal et al. 2008). Therefore γ-kafirin gene promoter with minimum regulatory essential motifs was isolated and its temporal and spatial expression was studied previously (Mishra et al. 2008). Proper regulation of transformed seed storage protein gene is necessary for the success of transgenic plants. Endospermal expression of native γ-kafirin gene is prerequisite for development of bioengineered grain sorghum, hence it has also been studied previously (Bansal et al. 2008). In the present study a suitable ready to use gene construct, harboring HMW glutenin gene driven by γ-kafirin promoter, was prepared for transformation, using previously isolated and characterized γ-kafirin gene promoter of sorghum (Mishra et al. 2008) and HMW glutenin gene of wheat (Pandey et al. 2008).

Materials and Methods

Cloning and sequencing of the amplified gamma kafirin gene promoter

PCR based amplified γ-kafirin gene promoter (574bp) (gene accession AJ 629151; Mishra et al. 2008) was purified using MinElute PCR Purification kit (Qiagen, Germany), according to manufacturer's instructions, cloned in pGEM *T*-easy vector (Promega, USA) and sequenced using T-7 and SP-6 primers. Sequence was analyzed using bioinformatics tools and submitted to NCBI (www.ncbi.nlm.nih.gov) data bank.

Construction of vector pKaf-gus

pCAMBIA 1304 and pGEM-kaf were isolated and subjected to restriction digestion by *Nco I* and *Sac I* (MBI fermentas, Canada) to release kafirin promoter (574 bp) from pGEM *T*-easy and CaMV35S promoter (size 800 bp) from pCAMBIA 1304. *Gamma* kafirin promoter and pCAMBIA lacking CaMV35S promoter (pCAMBIA1304△CaMV35S) were purified from gel using SNAP Gel purification kit (Invitrogen, Life Tech, USA). *Gamma* kafirin promoter was cloned in pCAMBIA1304△ CaMV35S, in place of CaMV35S promoter, the resultant plasmid was named pKaf-gus and positional cloning was confirmed by restriction digestions and PCR.

Construction of vector pKaf

Plasmid pUC 19 and gene construct pkaf-gus were isolated and digested with enzyme *Pst I* (MBI fermentas, Canada). After purification of digested plasmids, linearized pUC 19 was again digested with enzyme *BamH I* while pkaf-gus was digested with *Bgl II*. Double digested pUC 19 and γ-kafirin promoter were eluted from the agarose gel using MinElute Gel extraction kit (Qiagen, Germany) following manufacturer's instructions and *gamma*-Kafirin promoter was sub-cloned in pUC 19 vector. Subcloned kafirin promoter was transformed to *E. coli* DH 5 α strain and positive recombinants were selected and named as p*kaf*. Ligation was confirmed by restriction digestion analysis.

Construction of vector pKaf-Dx5 and pKaf-Dy10

Both glutenin genes, Dx 5 and Dy 10, cloned in pBLUSCRIPT SK$^-$, and vector pKaf were excised by double digestion us-

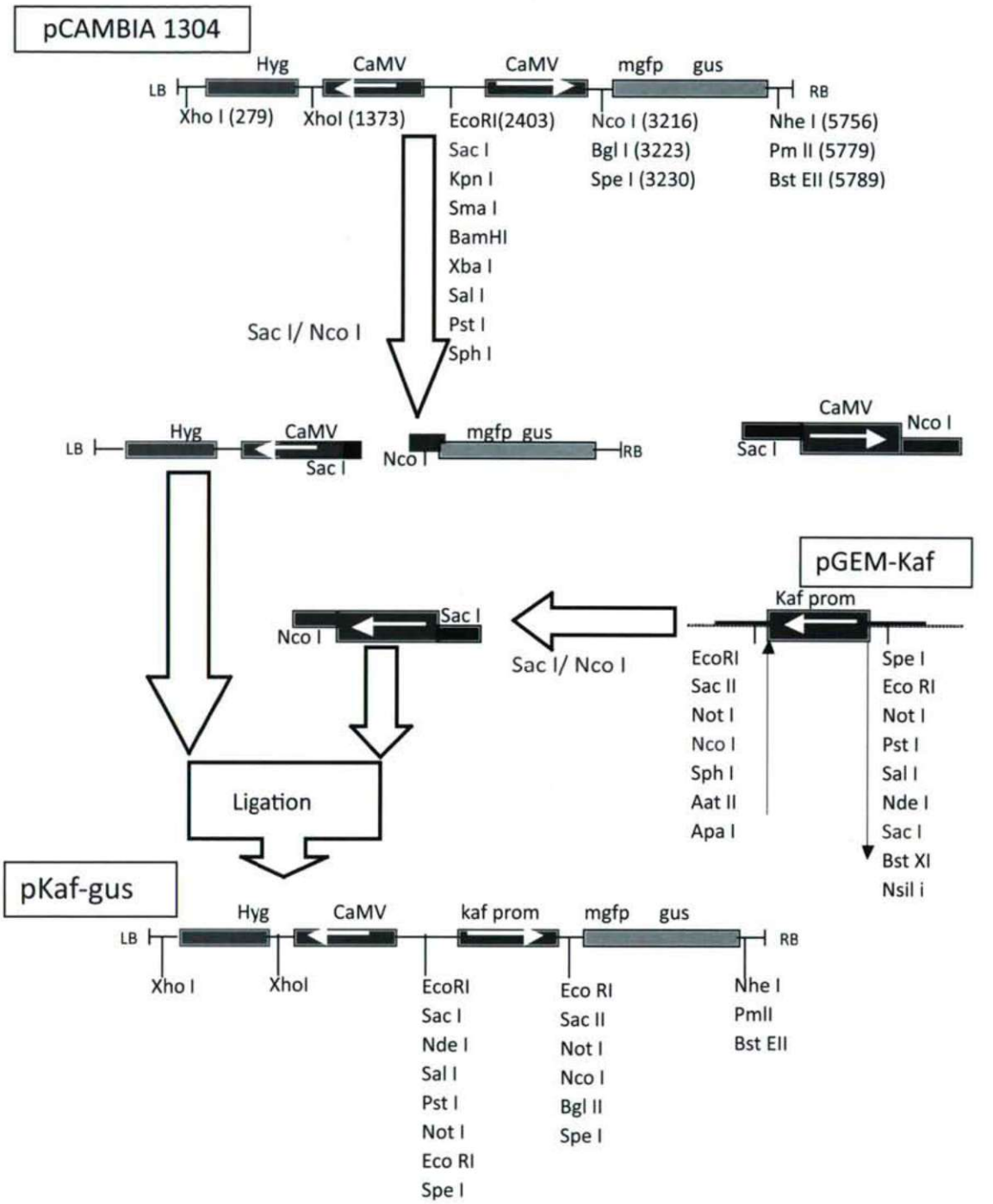

Figure 1. Strategy for construction of gene cassette pKaf-gus.

ing enzymes *Kpn I* and *Sac I* and purified using MinElute Gel extraction kit (Qiagen, Germany). HMW glu genes Dx 5 and Dy 10 were cloned at *Kpn I* and *Sac I* restriction site. Ligated product was transformed to *E. coli* DH 5 α strain and all transformed colonies were picked and recombinant clones/ plasmids were named as pKaf-Dx5 and pKaf-Dy10. Randomly selected putative colonies were inoculated in 3 ml Luria- Bertani (LB) media (1% Tryptone, 0.5% Yeast extract and 0.5% NaCl; pH 7.0) and plasmids were isolated, electrophoresed and then cloning was confirmed by restriction digestion analysis.

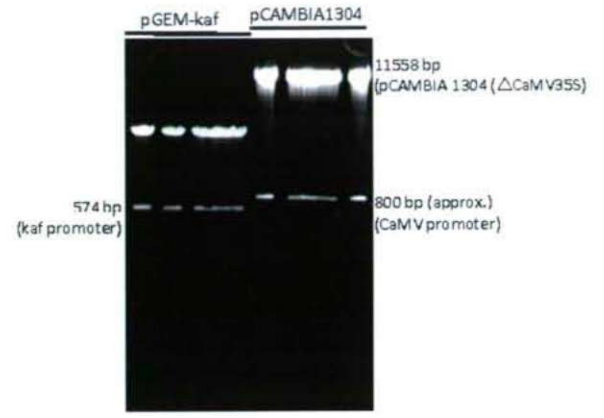

Figure 2. Excision of kafirin promoter from pGEM-kaf and CaMV promoter from pCAMBIA1304 by using restrction enzymes *Nco 1* and *Sac 1*.

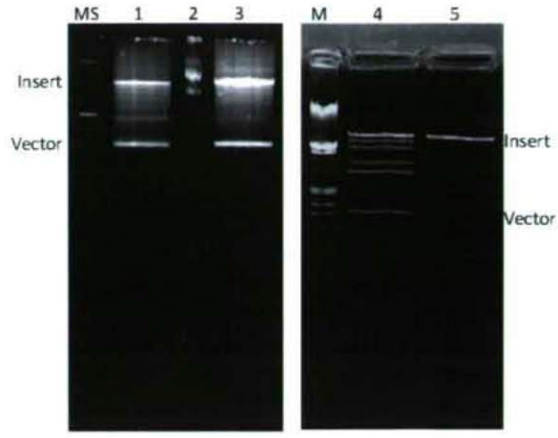

Figure 3. Excision of HMW glutenin Dx5 gene from pK+Dx 5 and Dy10 gene from pK-Dy 10 by restriction digestion with *Kpn I* and *Sac I*.
Lane MS: Marker super mix DNA ladder
Lane 1 : Partialy digested pK+Dx 5
Lane 2 : Undigested pK+Dx 5
Lane 3 : Complete digested pK+Dx 5 (to be eluted)
Lane M : Marker lambda *Hind IIII Eco RI* double digested
Lane 4 : Partial digested pK-Dy 10
Lane 5 : Complete digested pK-Dy 10 (to be eluted)

Result and Discussion

Construction of gene cassette pkaf-gus

Plasmid pCAMBIA 1304 and pCAMBIA 2301, both were available in the laboratory for the sub- cloning of the kafirin promoter(s). Both plasmids were isolated and analyzed for the suitability of sub- cloning by a series of restriction digestions. In pCAMBIA 1304, CaMV 35 S promoter of the reporter gene *gus/gfp* is flanked between *Sac I* and *Nco I* restriction enzyme while in pCAMBIA 2301, an extra *Nco I* site is present with the second CaMV 35S promoter of the selection marker gene which limits its selection for subcloning. Thus, pCAMBIA 1304 was selected for the construction of gene cassette on the basis of restriction digestion analysis and compatibility with pGEM-kaf vector. Kafirin promoter, cloned in pGEM- *T* easy vector, has expression direction from *Sac I* to *Nco I* restriction sites. In, pCAMBIA 1304, CaMV 35S promoter is also flanked with these two restriction sites and also has same expression direction (Fig. 1).

pCAMBIA 1304 and pGEM-kaf were digested with *Nco I* and after purification, again digested with *Sac I* enzyme. Digested plasmids were electrophoresed on preparative agarose gel for elution. Desired kafirin promoter of size 574 bp (gene accession AJ629151; Mishra et al. 2008) as well as pCAMBIA 1304 (△ CaMV 35 S) of size 11558 bp were eluted from the gel (Fig. 2) and a ligation reaction was set up in different molar ratios of the insert and vector. A measure of 5 µl of the ligation mix was transformed to competent cells of *E. coli* DH 5α and incubated overnight at 37°C and the best result was observed in 1:2 molar ratio. There is a possibility to grow only recombinants as neither pCAMBIA (non- recombinants) nor γ- kafirin promoters could recircularize (as double digested). All colonies were recombinants and 15 representative colonies were picked up and inoculated to LB media containing kanamycin. Plasmid of all representative colonies were isolated and ligation of kafirin promoter to pCAMBIA was confirmed by *Eco RI* restriction digestion. There is only one *Eco RI* site on pCAMBIA whereas in recombinant pCAMBIA 1304, promoter to be cloned on the behalf of CaMV promoter will bring an extra *Eco RI* site, as promoter is flanked with this enzyme site (Fig. 1). Thus, on restriction digestion with *Eco RI* enzyme, insert (cloned kaf promoter) will excise out having the expected size. These recombinant gene cassettes were named as pkaf gus and its efficacy (temporal and spatial expression) was previously checked by transforming to different sorghum tissues (Mishra et al. 2008).

Construction of gene cassettes pKaf 'glu'

The main goal of the research is to develop transgenic sorghum having good rotibread making quality and for this HMW glu gene(s) (viz. Dx5 and Dy10) of wheat were isolated and characterized (Pandey et al. 2008). A fusion of promoter and HMW glu gene(s) in a specific orientation is required.

Subcloning of kaf promoter to pUC 19

Plasmid pUC 19 and gene construct pkaf-gus were isolated in bulk and digested with enzyme *Pst I*, resulting in linearization of the plasmids. After purification of digested plasmids, linearized pUC 19 was again digested with enzyme *Bam HI* while pkaf-gus was digested with *Bgl II*. As a result of the double digestion, pUC 19 plasmid was linearized with *Pst I* and *Bam HI* protruding ends, while kafirin promoter was excised from pkaf-gus vector with *Pst I* and *Bgl II* protruding

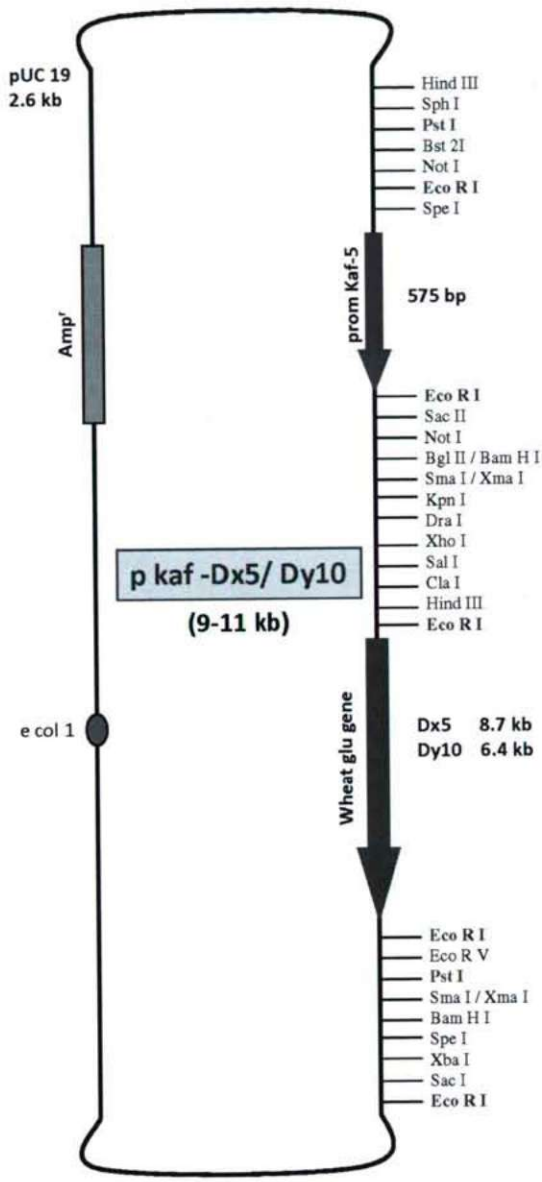

Figure 4. Restriction digestion map of gene construct pKaf -Dx5/ Dy 10.

ends. Double digested pUC 19 and kafirin promoter were eluted from the agarose gel. Kafirin promoter was ligated in pUC 19 as both insert and vector having compatible ends (*Bam HI* and *Bgl II* both leaving same protruding ends *GATC*). Subcloned kafirin promoter was transformed to *E. coli* DH 5 α strain and recombinant was selected by blue white color selection and named as pKaf. White colonies were selected, plasmid pKaf was isolated and ligation was confirmed by restriction digestion as in pUC 19 there is only one site of the *Eco RI* while in pKaf, inserted kafirin promoter was flanking within *Eco RI* site and after restriction digestion with *Eco RI*, kafirin promoter of approximate size 574 bp was excised and thus giving positive confirmation of the cloning.

Subcloning of HMW glu gene to pKaf vector

Kafirin promoter was cloned in pUC 19 in such orientation that it's expression direction is *Pst I* to *Bam HI / Bgl II*. Both glu genes Dx 5 and Dy 10 were isolated in bulk and both genes were excised by double digestion using enzyme *Kpn I* and *Sac I* (Fig 3). Excised genes were eluted from the agarose gel and purified. These eluted glu gene(s) have expression direction from *Kpn I* to *Sac I*. Vector pkaf was also double digested with same *Kpn I* and *Sac I* restriction enzymes and purified. HMW glu genes Dx 5 and Dy 10 were cloned at *Kpn I* and *Sac I* restriction sites, which is present just down-stream to kafirin promoter in same expression orientation. Ligated product was transformed to *E. coli* DH 5 α strain and all transformed colonies were picked. All grown colonies were putative recombinant as pKaf and glu gene(s) were double digested and eluted so there is no possibility of any type of self ligation. Randomly selected putative colonies were inoculated in 3 ml LB media for the plasmid isolation. There is no color selection and all colonies were found white as glu gene(s) were cloned in pKaf, which was a recombinant (kaf promoter was cloned at lac z site of the pUC 19). Recombinant clones/ plasmids were named as pKaf-Dx 5 and pKaf-Dy 10. All plasmids were electrophoresed and then digested with *Eco R I* to confirm cloning of the glu gene(s) as pKaf containing *Eco RI* site with kafirin promoter (~600 bp) while pKaf-Dx 5/ Dy 10 containing an extra *Eco RI* site with glu gene(s) (8.7 kb Dx 5 and 6.5 kb Dy 10). The map of the gene construct pKaf prom Dx 5/ Dy 10 is shown in Figure 4.

Finally, two gene cassettes were developed as pKaf-Dx5 and pKaf-Dy10 where, expression of HMW glu gene Dx5 and Dy10 was driven by the kafirin gene promoter. Both gene cassettes are ready to clone in any transformation vector by excising at *Pst I* restriction sites. Like other prolamin genes, kafirins are also subjected to tissue-specific and developmental regulation, being expressed exclusively in the starchy endosperm during mid- and late-development. This control of gene expression is exerted primarily at the transcriptional level (Bartels and Thompson 1986; Sorensen et al. 1989; Mutisya et al. 2006). Freitas et al. (1994) reported a *gus* gene expression driven by γ-kafirin gene promoter while similar type of expression was also observed by Mishra et al. (2008). DeRose et al. (1996) observed *gus* gene expression in transgenic tobacco seeds, developed by *Agrobacterium* mediated transformation, using an α-kafirin gene promoter and *uidA* gene construct. The HMW glutenin protein 1Ax1, Dx5 and Dy10 are successfully expressed in several other plants and also in *E. coli*. In these studies, HMW glutenin gene was expressed in either homologous system (*i.e.* Plant system) with plant promoter (CaMV, HMW or LMW glutenin promoter) or heterologous system (*i.e. E. coli*; Bartels et al. 1985; Galili

1989; Altpeter et al. 2004; Pandey et al. 2008). With the best of our knowledge there is no report on the expression of wheat glutenin gene(s) driven by the kafirin gene promoter and present study may be the first report on the availability of a gene construct (Fig. 4) where HMW glutenin gene is driven by kafirin gene promoter.

References

Altpeter F, Popelka JC, Wieser, H (2004) Stable expression of 1Dx5 and 1Dy10 high-molecular-weight glutenin subunit genes in transgenic rye drastically increases the polymeric glutelin fraction in rye flour. Plant Mol Biol 54:783-792.

Axtell JD, Van-Scoyoc SW, Christensen PJ, Ejeta G (1979) Current status of protein quality improvement in grain sorghum. In Seed Protein Improvement in Cereals and Grain Legumes, Vol. 1, IAEA, Vienna, pp. 357-365.

Bansal S, Mishra A, Sharma S, Khanna VK, Tomar A, Garg GK (2008) Isolation and temporal endospermal expression of *gamma* -kafirin gene of grain sorghum (Sorghum bicolor L. moench) var. M 35-1 for introgression analysis of transgene. J Cereal Sci 48:808-815.

Bartels D, Thompson RD (1986) Synthesis of messenger-RNAs coding for abundant endosperm proteins during wheat grain development. Plant Sci 46:117-125.

Bartels D, Thompson RD, Rothstein S (1985) Synthesis of a wheat storage protein subunit in Escherichia coli using novel expression vectors. Gene 35:159-167.

D'Ovidio R, Anderson OD (1994) PCR analysis to distinguish between alleles of a member of a multigene family correlated with wheat bread making quality. Theor Appl Genet 88:759-763.

De Rose RT, Begum D, Hall TC (1996) Analysis of kafirin promoter activity in transgenic tobacco seeds. Plant Mol Biol 32:1029-1035.

Flavell RB, Goldsborough AP, Robert LS, Schnick D, Thompson RD (1989) Genetic variation in wheat HMW glutenin subunits and their molecular basis of bread making quality. Biotechnology 7:1281-1285.

Freitas F, Yunes JA, Silvia MJda, Arruda P, Leite A (1994) Structural characterization and promoter activity analysis of *gamma* kafirin gene from sorghum. Mol Gen Genet 245:177-186.

Galili G (1989) Heterologous expression of a wheat high molecular weight glutenin gene in *Escherichia coli*. Proc Natl Acad Sci USA 86:7756-7760.

Greene FC, Anderson OD, Yip RE, Halford NG, Malpica-Romero JM, Shewry PR (1988) Analysis of possible quality-related sequence variations in the 1D glutenin high molecular weight subunit genes of wheat. In Miller TE, Koebner RMD, eds., Proceedings of the 7th International Wheat Genetic Symposium, IPSR, Cambridge, 735-740.

Grootboom A, O'Kennedy MM (2003) Genetic enhancement of nutritional quality of grain sorghum In Belton PS, Taylor JRN, eds., Workshop on the proteins of sorghum and millets: Enhancing nutritional and functional properties for Africa, Pretoria, South Africa.

Mishra A, Tomar A, Bansal S, Khanna VK, Garg GK (2008) Temporal and spatial expression analysis of *gamma* kafirin promoter from Sorghum (*Sorghum bicolor* L. moench) var. M 35-1. Mol Biol Rep 35:81-88.

Mutisya J, Sun C, Palmqvist S, Baguma Y, Odhiambo B, Jansson C (2006) Transcriptional regulation of the sbeIIb genes in sorghum (*Sorghum bicolor*) and barley (*Hordeum vulgare*): importance of the barley sbeIIb second intron. J Plant Physiol 163:770-780.

Pandey R, Mishra A, Garg GK, (2008) Plant promoter driven heterologous expression of HMW glutenin gene(s) subunit in *E. coli*. Mol Biol Rep 35:153-162.

Shewry PR, Halford NG (2002) Cereal seed storage proteins: structures, properties and role in grain utilization. J Exp Bot 53:947-958.

Shull JM, Watterson JJ, Kirleis AW (1992) Purification and Immunocytochemical localization of kafirins in *Sorghum bicolor* (L. Moench) endosperm. Protoplasma 171:64-74.

Singh R, Axtell JD (1973) High lysine mutant gene *(h1)* that improves protein quality and biological value of grain sorghum. Crop Sci 13:535-539.

Sorensen MB, Cameron-Mills V, Brandt A (1989) Transcriptional and post-transcriptional regulation of gene expression in developing barley endosperm. Mol Gen Genet 217:195-201

Wrigley CW (1996) Giant proteins with flour power. Nature 381:738.

Volume 52(2):283-294, 2008
Acta Biologica Szegediensis
http://www.sci.u-szeged.hu/ABS

ARTICLE

Growth, gas exchange and function of antioxidant defense system in two contrasting rice genotypes under Zn and Fe deficiency and hypoxia

Roghieh Hajiboland*, Naiere Beiramzadeh

Plant Science Department, University of Tabriz, Tabriz, Iran

ABSTRACT For study of underlying physiological mechanisms for genotypic differences in tolerance to Zn and Fe deficiency and hypoxia, two contrasting rice genotypes (*Oryza sativa* L. cv. Amol and Dashti) were studied in nutrient solution with or without aeration. Growth of the lowland genotype (Amol) was significantly improved in nutrient solution without aeration, the opposite was observed for upland genotype (Dashti). Tolerance of Amol to low Zn was higher than Dashti, in contrast the former genotype was more susceptible to Fe deficiency. Photochemistry of leaves was affected strongly by Fe but not Zn deficiency. Low supply of Zn and Fe impaired photosynthetic capacity of plants mainly via stomatal limitation and the amount of reduction in net assimilation rate correlated well with differential growth reduction under Zn and Fe deficiency stress. Under hypoxia, plants had lower stomatal conductance and transpiration rate leading to improved photosynthetic water use efficiency. Activity of ascorbate peroxidase (APX) and guaiacol peroxidase (POD) induced by low Zn supply, but low Fe caused reduction of APX, CAT and POD. Activity of SOD decreased in low Zn plants, but increased in plants suffered from Fe deficiency. Increased APX activity in response to hypoxic conditions in Amol was associated with higher tolerance in this genotype, in contrast POD activity only monitored stress conditions without any protecting role. A close correlation was observed between accumulation of $O_2^{\cdot-}$ and differential sensitivity of genotypes to hypoxia. **Acta Biol Szeged 52(2):283-294 (2008)**

KEY WORDS

chlorophyll fluorescence
lowland rice
photosynthesis
reactive oxygen species (ROS)
upland rice

Rice culture is divided into two broad groups, upland and lowland culture. Upland rice refers to rice grown on both flat and sloping fields that are prepared and seeded under dryland conditions and relies entirely on rainfall or irrigation depending on the amount of precipitation. Flooded rice, known also as lowland or waterlogged rice, is grown on flatland in flooded soils (Fageria et al. 1997).

In submerged or flooded soils, limited oxygen availability and altered chemical reactions that involve in the nutrients availability e.g. Zn and Fe for plants, creates conditions markedly different from those of drained soils. Because of water constraints, rice production is now in transition from the traditional high water consuming lowland rice cultivation on flooded fields to a new cultivation system of aerobic rice (Gao et al. 2005). Aerobic rice is grown as a dry field crop in irrigated but non-flooded soils (Bouman et al. 2005). Zinc deficiency was reported for both upland (Fageria et al. 1997; Fageria and Baligar 2005) and lowland rice (Yang et al. 1994a; Hajiboland et al. 2003), however, Fe deficiency is a common disorder of rice growing on well drained (aerobic) soils (Nerkar et al. 1984), whether these are neutral, calcareous or alkaline.

Accepted Nov 17, 2008
*Corresponding author. E-mail: ehsan@tabrizu.ac.ir

Hypoxic and anoxic conditions maintain transition metal ions in a more or less reduced state and induce formation of reactive oxygen species (ROS). The same conditions can arise within submerged plants (Hendry and Brocklebank 1985). Therefore, hypoxia survival may depend on the capacity of plant tissues to counterattack reactive oxygen species and limit damages.

One of the primary effects of these molecular species in cells is the peroxidation of membranes forming toxic products such as malondialdehyde (MDA; Kappus 1985). Plants have evolved various protective mechanisms to eliminate or reduce ROS. Enzymatic antioxidant system, which is one of the protective mechanisms including superoxide dismutase (SOD) are located in various cell compartments and catalyse the disproportion of two $O_2^{\cdot-}$ radicals to H_2O_2 and O_2 (Salin 1987). H_2O_2 is eliminated by various antioxidant enzymes such as catalase (CAT) and peroxidases (POD) converting H_2O_2 to water (Salin 1987). Ascorbate peroxidase (APX) eliminates peroxides by converting ascorbic acid to dehydroascorbate (Asada 1992). Ascorbate peroxidase and glutathione reductase (GR) are important components of the ascorbate-glutathione cycle responsible for the removal of H_2O_2 in different cellular compartments (Jiménez et al. 1997).

Activity of enzymes containing Zn or Fe as a catalytic or structural component is expected to be changed substantially in plants supplied with inadequate amounts of these nutrients. Among enzymes of antioxidant defense system, SOD contains Zn (Cu/Zn SOD isozyme) or iron (Fe-SOD isozyme in chloroplasts); iron contributes also as heme group in the structure of H_2O_2 scavenging enzymes including APX, POD and CAT (Marschner 1995). Therefore, plant growth under inadequate nutrients supply may be influenced *per se* by reduction in the capacity of antioxidant defense system.

Changes in chlorophyll fluorescence emissions are indications of changes in photosynthetic activity and the state of Photosystem II (Maxwell and Johnson 2000). The flow of electrons through PSII is indicative of the overall rate of photosynthesis and is an estimation of photosynthetic performance. It is plausible that not only low supply of Fe because of its involvement in electron transport and chlorophyll synthesis but also of Zn concerning its role for maintenance of integrity of membranes and protection of lipids and proteins against oxidative damage (Marschner 1995), may affect the photochemistry of leaves and inhibit biophysical processes of photosynthesis. Due to predominance of polyunsaturated fatty acids in thylakoid lipids (Gounaries et al. 1986), photosynthetic membranes in chloroplasts could be considered the most susceptible structures in plants grown under conditions of oxidative stresses.

Water availability differs greatly under flooded compared with non-flooded conditions. Therefore, plant strategies for water economy may be changed in transition from flooded to aerobic conditions, and every change via modification of stomatal conductance affects in turn photosynthetic CO_2 fixation. Recent studies showed that the water productivity (crop yield/water consumptively used in evapotranspiration) of rice under aerobic conditions is 32-88% higher than that under flooded conditions (Bouman et al. 2005).

In Iran, rice is the second important food crop after wheat and is cultivated mainly under flooded conditions in the north of the country. In south and central Iran, however, increasing water scarcity problem causes relatively long term non-submerged conditions during irrigation intervals in the field. Genotypes selected for higher tolerance to alternate submerged and non-submerged conditions, are now being used for upland cultivation. It is expected that, genotypes adapted and bred for one of these cultivation systems, have different tolerance to Zn and Fe deficiency and particularly hypoxia. Currently, aerobic rice varieties are developed by crossing lowland with upland varieties (Bouman et al. 2005).

Physiological basis of differences between traditional lowland genotypes with new genotypes with lower susceptibility to non-flooded conditions and its consequences for nutrients deficiency tolerance is not known. Understanding the physiological mechanisms may facilitate future breeding programs. One objective of the present work was to evaluate the functional significance of antioxidant defense capacity of plants in adaptation to Zn and Fe deficiency in combination with flooded conditions. Two contrasting rice genotypes used in this work, differed in tolerance to Zn and Fe deficiency and hypoxia. An attempt was also made to determine that up to what extent photosynthesis and related characteristics are associated with the tolerance to Zn and Fe deficiency and hypoxia.

Materials and Methods

Two genotypes of rice (*Oryza sativa* L.) were used in this work, one genotype (Amol) was chosen from north of Iran and another (Gasrol-Dashti) from south of the country because of their adaptation to their own local culture conditions. Seeds were provided by Rice Research Center (Rasht, Guilan Province, Iran) and Agricultural Research Center (Shiraz, Fars Province, Iran) for Amol and Dashti genotypes respectively.

Plants culture and treatments

The experiments were conducted in a growth chamber with a temperature regime of 25°/18°C day/night, 14/10 h light/dark period and relative humidity of 70/80% under photon flux density of 350-400 μmol m^{-2} s^{-1}. Germination of seeds and plants pre-culture were performed as described previously (Hajiboland and Salehi 2006a).

Zinc experiments

Conventional nutrient solution (Yoshida et al. 1972) was used for pre-culture of plants with Zn concentration of 0.5 μM (adequate Zn, control) and <0.08 μM (low). In the following growth period, it was necessary to use chelator-buffered nutrient solution technique (Yang et al. 1994b) for elimination of Zn contaminations and production of Zn deficient plants. Thus, sixteen-day-old plants were transferred to chelator-buffered nutrient solution consisted of two levels of added $ZnSO_4$ at 2.0 μM which equals 12 pM free Zn^{2+} activity (–Zn) or 20 μM equals 130 pM free Zn^{2+} activity (+Zn).

Fe experiments

Plants were grown in the conventional rice nutrient solution either in pre-culture or main experiment. Fe concentration in the pre-culture medium was 100 μM (adequate Fe) or 10 μM (low) and in the main experiment was 100 μM (adequate Fe, +Fe) or zero (–Fe).

Plants were grown for 21 days and nutrient solutions were completely changed every 7 days and pH was adjusted every day.

Hypoxia treatments

For comparison of growth of plants under hypoxic and aerobic conditions, plants were cultivated simultaneous in aerated

and non-aerated nutrient solutions during pre-culture as well as treatment.

Nutrient solutions were completely changed every 7 days and pH was adjusted every day.

Harvest

After washing using double-distilled water, plants were divided into shoots and roots, weighed and blotted dry on filter paper and dried at 70°C for 2 days to determine plant dry weight. Another group of plants was used for determination of root length (Tennant 1975) and chlorophyll (Moran 1982). The third group of plants was used for measurement of gas exchange parameters, chlorophyll fluorescence and determination of enzymes activity and concentration of metabolites.

Determination of gas exchange parameters

CO_2 assimilation and transpiration rates of attached leaves were measured with a calibrated portable gas exchange system (LCA-4, ADC Bioscientific Ltd., UK) always between 9:00 A.M. and 13:00 P.M. with the exception of PPFD (400-420 µmol m^{-2} s^{-1}), no microenvironmental variable inside the chamber was controlled. The net photosynthesis rate by unit of leaf area (*A*), transpiration rate (*E*), stomatal conductance to water vapor (g_s), atmospheric CO_2 molar fraction (*Ci/Ca*) and photosynthetic water use efficiency (*WUE=A/E*) were determined

Determination of chlorophyll fluorescence

Chlorophyll fluorescence parameters were recorded in parallel for gas exchange measurements in the same leaf, using a portable fluorometer (FIM, ADC Bioscientific Ltd., UK). Leaves were acclimated to dark for 30 min before measurements were taken. Initial (F_0), maximum (F_m), variable ($F_v=F_m-F_0$) as well as $F_v:F_m$ and $F_v:F_0$ ratios were recorded.

Gas exchange and chlorophyll fluorescence measurements were carried out using four independent replications as separate pots, in each pot four mature, fully expanded and attached leaves used for measurements. Average of data from each pot was obtained and the mean of four pots per treatment were subjected to statistical analysis.

Determination of enzyme activities and concentration of oxidants, total amino acids and protein

Fresh leaf samples were ground in the presence of liquid nitrogen using mortar and pestle. Each enzyme assay was tested for linearity between the volume of crude extract and the measured activity. All measurements were undertaken using spectrophotometer (Specord 200, Analytical Jena, Germany) according to optimized protocols described elsewhere (Hajiboland and Hasani 2007).

The activity of ascorbate peroxidase (APX, EC 1.11.1.11) was measured by determining ascorbic acid oxidation, one unit of APX oxidizes ascorbic acid at a rate of 1 µmol min^{-1} at 25°C. Catalase (CAT, EC 1.11.1.6) activity was assayed by monitoring the decrease in absorbance of H_2O_2 at 240 nm, unit activity was taken as the amount of enzyme, which decomposes 1 µmol of H_2O_2 in one min. Peroxidase (POD, EC 1.11.1.7) activity was assayed using the guaiacol test, the enzyme unit was calculated as enzyme protein required for the formation of 1 µmol tetraguaiacol for 1 min. Total superoxide dismutase (SOD, EC 1.15.1.1) activity was determined using monoformazan formation test. One unit of SOD was defined as the amount of enzyme required to induce a 50% inhibition of NBT reduction as measured at 560 nm, compared with control samples without enzyme aliquot. The activity of glutathione reductase (GR, EC 1.6.4.2) was assayed by following the oxidation of NADPH at 340 nm, one unit of enzyme activity was calculated as enzyme protein required for oxidation of one µmol NADPH in 1 min.

Soluble proteins were determined using a commercial Bradford reagent (Sigma) and BSA (Merck) as standard. Content of total free α-amino acids was assayed using ninhydrin colorimetric method at 570 nm, glycine was used for production of standard curve. The concentration of H_2O_2 was determined using potassium titanium-oxalate at 508 nm. Lipid peroxidation was estimated from the amount of malondialdehyde (MDA) formed in a reaction mixture containing thiobarbituric acid (Sigma) at 532 nm. MDA levels were calculated from a 1,1,3,3-tetraethoxypropane (Sigma) standard curve. The assay of NADPH-dependent $O_2^{\cdot-}$ generation was carried out by measuring the rate of SOD-inhibitable NBT reduction at 25°C.

Experiments were undertaken in complete randomized block design with 4 replications. Statistical analyses including one-way ANOVA (Tukey test) and Pearson Correlation Test were carried out using Sigma Stat (3.02) at $p<0.05$.

Results

Zinc deficiency caused significant reduction of shoot and root growth, however, genotypes differed markedly in tolerance to low Zn supply. Shoot growth of Amol was reduced by about 38%, while that of Dashti was inhibited up to 67%. Similar differential response of genotypes to low Zn stress was observed in root dry weight and length (Fig. 1).

In contrast to a high tolerance to low Zn supply, Amol was much more susceptible to Fe deficiency than Dashti. Growth reduction of Amol due to Fe deficiency was 69% and 67% for shoot of aerated and non-aerated plants respectively. The corresponding values for Dashti were only 52% and 55% under aerated and non-aerated conditions (Fig. 2).

Hypoxic conditions influenced plants growth depending on tested genotypes. In Zn and Fe sufficient plants, growth of Amol was stimulated up to 26% and 53% when grown

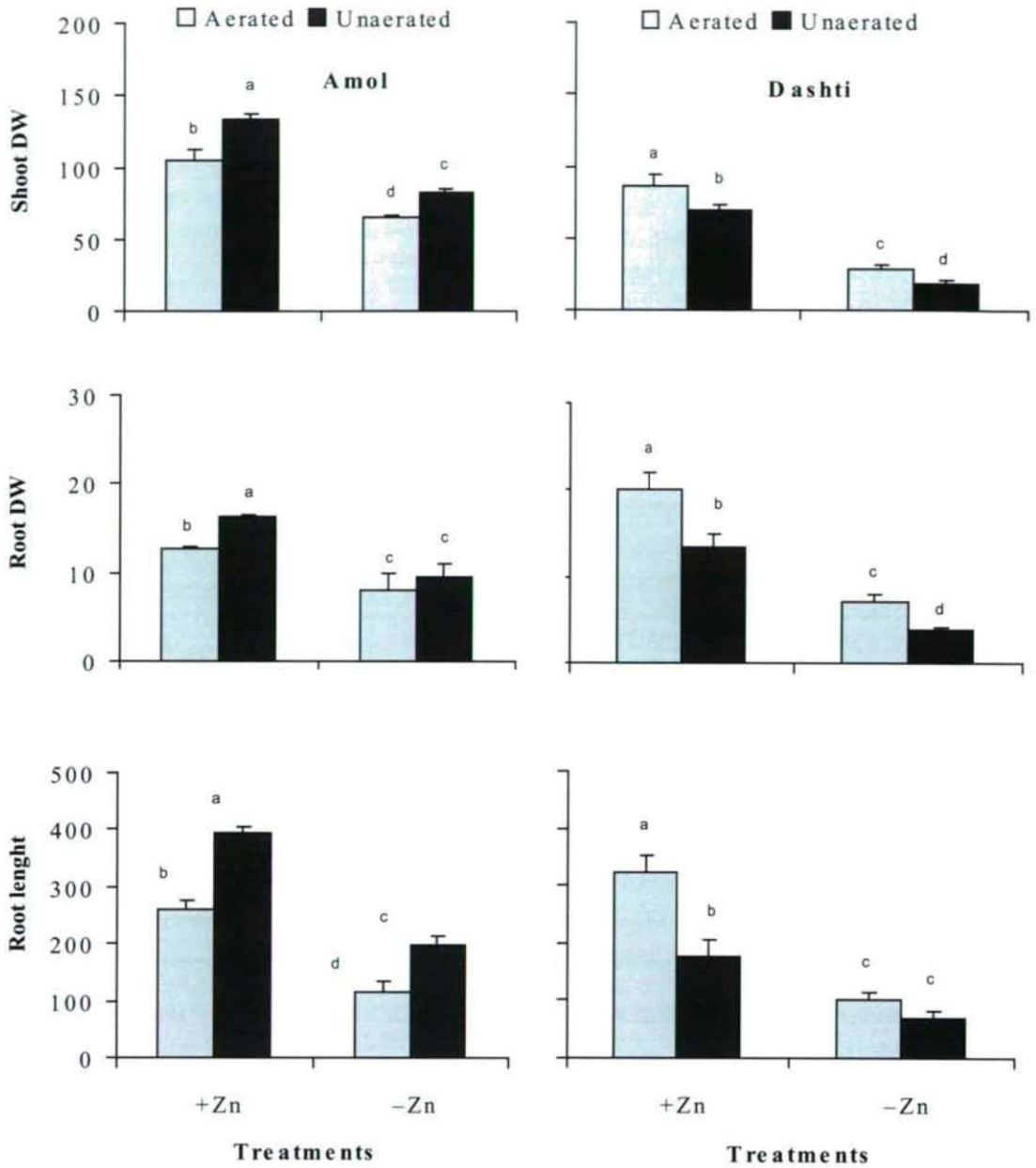

Figure 1. Effect of Zn deficiency on shoot and root dry weight (mg plant^{-1}) and root length (cm plant^{-1}) of two contrasting rice (*Oryza sativa* L. cvs. Amol and Dashti) genotypes grown under aerated or non-aerated conditions. Each value is the mean of 4 repetitions ± SD.

in non-aerated nutrient solution compared with aeration treatment in Zn and Fe experiment respectively. In contrast, Dashti showed higher root and shoot growth in aerated treatment, shoot biomass reduction due to growth in non-aerated nutrient solution was 21% and 33% in Zn and Fe experiment respectively. The same tendency was observed for Zn and Fe deficient plants (Figs. 1, 2).

Zinc deficiency did not affect the sum of chlorophyll a and b content (chlorophyll a+b) in Amol, but decreased it in Dashti particularly in non-aerated plants. Hypoxic conditions caused a slight increase of chlorophyll a+b amounts in both genotypes. F_v/F_m and F_v/F_0 ratios were not affected either by Zn deficiency or aeration treatments (Table 1).

Zinc deficient plants showed significantly lower net photosynthesis rate (A). Reduction of A was higher in Dashti (65-74%) than in Amol (47-54%). Hypoxic conditions did not affect A in both tested genotypes. Reduction of A was associated by great reduction of stomatal conductance (g_s). In addition of net photosynthesis rate, transpiration (E) was also affected negatively by low Zn supply, reduction of E by

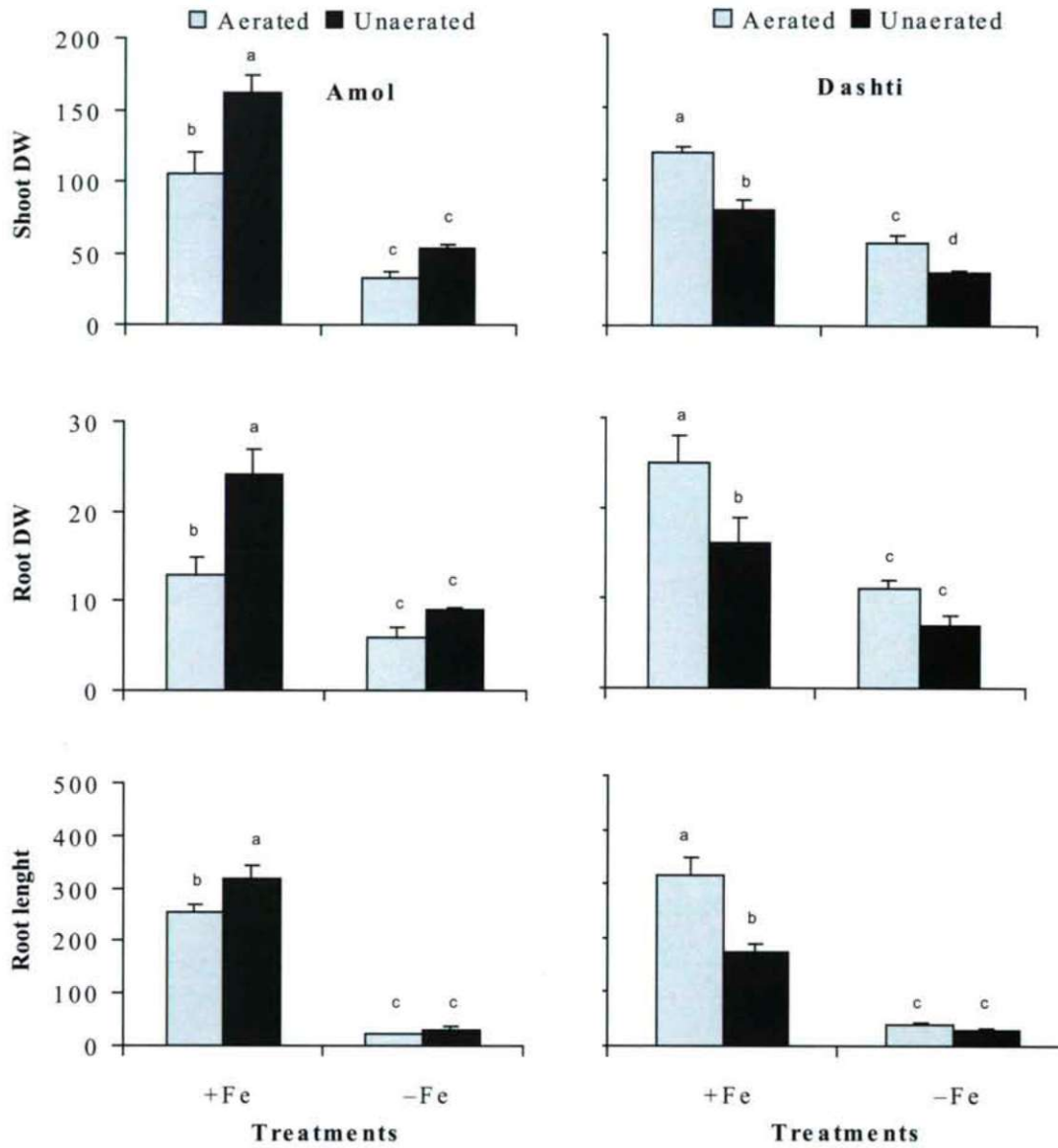

Figure 2. Effect of Fe deficiency on shoot and root dry weight (mg plant^{-1}) and root length (cm plant^{-1}) of two contrasting rice (*Oryza sativa* L. cvs. Amol and Dashti) genotypes grown under aerated or non-aerated conditions. Each value is the mean of 4 repetitions ± SD.

low Zn was higher in Dashti (67-69%) than Amol (43-52%). As the consequence of lower stomatal conductance, the *Ci/Ca* ratio increased in Zn deficient plants. Water use efficiency (*WUE*) was diminished by both low Zn supply and aeration of nutrient solution (Table 1).

As expected, the amount of chlorophyll a+b in leaves decreased dramatically in Fe deficient plants and in contrast to the effect of Zn deficiency, F_v/F_m ratio was significantly reduced by low supply of Fe. Reduction of optimal quantum efficiency of PSII in dark-adapted chloroplasts (F_v/F_m ratio) due to Fe deficiency was greater in Amol (34-17%) than Dashti (24-8%). Moreover, in Fe deficient plants, the F_v/F_m ratio was significantly affected by hypoxic conditions e.g. decreased up to 21% and 18% in Amol and Dashti respectively. The ratio of F_v/F_0 decreased with low Fe supply in both tested genotypes. The reduction was more pronounced in aerated (62-61% in Amol and Dashti respectively) than non-aerated (46-30% in Amol and Dashti respectively) plants (Table 2).

Similar with Zn deficiency, Fe deficiency conditions affected also negatively net photosynthesis rate, reduction was greater in Amol (74-81%) than Dashti (65-70%). Transpiration rate was also reduced by Fe deficiency, more in Amol (53%) than Dashti (26-33%). In accordance with the data of net photosynthesis and transpiration rate, stomatal con-

Table 1. Chlorophyll (a+b) concentration (mg g^{-1} FW), chlorophyll fluorescence and gas exchange parameters including net photosynthetic rate (*A*), transpiration (*E*), the ratio of intercellular air space and atmospheric CO_2 molar fractions (*Ci/Ca*), stomatal conductance to water vapor (*gs*) and instantaneous water use efficiency (*WUE*) in two contrasting rice genotypes (*Oryza sativa* L. cvs. Amol and Dashti) treated either with adequate or low levels of Zn under aerated or non-aerated conditions. The means refer to 4 repetitions ± SD. Data within each genotype followed by the same letter are not significantly different (P<0.05).

		Amol		Dashti	
		Aerated	Non-aerated	Aerated	Non-aerated
Chlorophyll (a+b)	+Zn	2.96±0.62 ^{a}	3.22±0.48 ^{a}	2.77±0.29 ^{ab}	3.16±0.59 ^{a}
	–Zn	1.81±0.09 ^{b}	1.93±0.16 ^{b}	2.33±0.49 ^{ab}	1.97±0.23 ^{b}
Fv/Fm	+Zn	0.788±0.002 ^{a}	0.794±0.005 ^{a}	0.800±0.004 ^{a}	0.802±0.004 ^{a}
	–Zn	0.792±0.006 ^{a}	0.797±0.001 ^{a}	0.806±0.010 ^{a}	0.807±0.004 ^{a}
Fv/F_0	+Zn	3.73±0.04 ^{b}	3.86±0.11 ^{b}	4.02±0.11 ^{a}	4.13±0.24 ^{a}
	–Zn	4.84±0.12 ^{a}	3.92±0.03 ^{b}	4.17±0.28 ^{a}	4.20±0.11 ^{a}
A	+Zn	1.12±0.14 ^{a}	1.31±0.10 ^{a}	1.58±0.11 ^{a}	1.50±0.10 ^{a}
($\mu mol\ m^{-2}\ s^{-1}$)	–Zn	0.59±0.10 ^{c}	0.60±0.06 ^{b}	0.56±0.09 ^{b}	0.39±0.09 ^{b}
E	+Zn	0.64±0.18 ^{a}	0.48±0.06 ^{abc}	0.83±0.06 ^{a}	0.73±0.12 ^{a}
($mmol\ m^{-2}\ s^{-1}$)	–Zn	0.36±0.13 ^{bc}	0.23±0.02 ^{c}	0.26±0.04 ^{b}	0.24±0.07 ^{b}
g_s	+Zn	12.67±5.03 ^{a}	8.67±4.20 ^{a}	17.33±3.05 ^{a}	15.33±4.16 ^{a}
($mol\ m^{-2}\ s^{-1}$)	–Zn	2.00±0.46 ^{b}	1.01±0.01 ^{c}	4.02±0.01 ^{b}	2.00±0.02 ^{c}
Ci/Ca	+Zn	0.548±0.034 ^{b}	0.484±0.024 ^{c}	0.493±0.033 ^{b}	0.489±0.031 ^{b}
	–Zn	0.705±0.029 ^{a}	0.648±0.027 ^{a}	0.689±0.022 ^{a}	0.737±0.039 ^{a}
WUE	+Zn	1.81±0.34 ^{b}	2.78±0.27 ^{a}	1.92±0.27 ^{ab}	2.08±0.23 ^{a}
($\mu mol\ mol^{-1}$)	–Zn	1.63±0.40 ^{b}	2.66±0.18 ^{a}	2.12±0.17 ^{a}	1.59±0.06 ^{b}

Table 2. Chlorophyll (a+b) concentration (mg g^{-1} FW), chlorophyll fluorescence and gas exchange parameters including net photosynthetic rate (*A*), transpiration (*E*), the ratio of intercellular air space and atmospheric CO_2 molar fractions (*Ci/Ca*), stomatal conductance to water vapor (*gs*) and instantaneous water use efficiency (*WUE*) in two contrasting rice genotypes (*Oryza sativa* L. cvs. Amol and Dashti) treated either with adequate or low levels of Fe under aerated or non-aerated conditions. The means refer to 4 repetitions ± SD. Data within each genotype followed by the same letter are not significantly different (P<0.05).

		Amol		Dashti	
		Aerated	Non-aerated	Aerated	Non-aerated
Chlorophyll (a+b)	+Fe	1.84±0.01 ^{b}	3.03±0.05 ^{a}	1.97±0.13 ^{b}	2.84±0.53 ^{a}
	–Fe	0.07±0.00 ^{d}	0.25±0.07 ^{c}	0.15±0.05 ^{c}	0.39±0.17 ^{c}
Fv/Fm	+Fe	0.785±0.004 ^{a}	0.791±0.001 ^{a}	0.801±0.006 ^{a}	0.805±0.003 ^{ab}
	–Fe	0.518±0.010 ^{c}	0.653±0.011 ^{b}	0.608±0.042 ^{c}	0.739±0.040 ^{b}
Fv/F_0	+Fe	3.64±0.06 ^{b}	3.80±0.02 ^{a}	3.94±0.26 ^{a}	4.15±0.07 ^{a}
	–Fe	1.38±0.07 ^{d}	2.04±0.14 ^{c}	1.52±0.20 ^{c}	2.91±0.18 ^{b}
A	+Fe	0.93±0.20 ^{a}	0.94±0.07 ^{a}	1.19±0.26 ^{a}	0.89±0.24 ^{a}
($\mu mol\ m^{-2}\ s^{-1}$)	–Fe	0.18±0.03 ^{b}	0.24±0.08 ^{b}	0.34±0.13 ^{b}	0.31±0.05 ^{b}
E	+Fe	0.51±0.09 ^{a}	0.40±0.06 ^{a}	0.61±0.10 ^{a}	0.63±0.14 ^{a}
($mmol\ m^{-2}\ s^{-1}$)	–Fe	0.24±0.11 ^{b}	0.19±0.01 ^{b}	0.45±0.13 ^{a}	0.42±0.19 ^{a}
g_s	+Fe	6.67±3.05 ^{a}	2.78±0.55 ^{b}	10.00±4.00 ^{a}	8.67±2.43 ^{a}
($mol\ m^{-2}\ s^{-1}$)	–Fe	1.00±0.01 ^{c}	1.08±0.00 ^{c}	5.33±1.16 ^{ab}	3.00±0.76 ^{b}
Ci/Ca	+Fe	0.557±0.016 ^{c}	0.622±0.018 ^{b}	0.463±0.013 ^{c}	0.504±0.014 ^{b}
	–Fe	1.089±0.031 ^{a}	1.046±0.028 ^{a}	0.836±0.023 ^{a}	0.828±0.023 ^{a}
WUE	+Fe	1.82±0.11 ^{ab}	2.39±0.35 ^{a}	2.15±0.59 ^{a}	1.48±0.64 ^{ab}
($\mu mol\ mol^{-1}$)	–Fe	0.89±0.54 ^{c}	1.26±0.44 ^{bc}	0.62±0.10 ^{c}	0.73±0.12 ^{bc}

ductance was strongly inhibited by Fe deficiency, and more reduction was observed in Amol (85-97%) compared with Dashti (48-65%). Water use efficiency (*WUE*) decreased in Fe deficient plants with no obvious genotypic difference, moreover, a slight reduction of *WUE* was observed in aerated plants (Table 2).

A significant increase in the specific activity of APX was observed in roots of non-aerated plants by low Zn supply that reached up to 46% and 65% in Amol and Dashti respectively. This increase in shoot was in tendency and observed only in Amol. On the other hand, APX activity increased in Zn deficient Amol plants by hypoxic treatment, which was significant

Table 3. Effect of Zn deficiency on the specific activity of ascorbate peroxidase (APX), catalase (CAT), peroxidase (POD), superoxide dismutase (SOD) and glutathione reductase (GR) in two genotypes of rice (*Oryza sative* L. cvs. Amol and Dashti) grown in aerated or non-aerated nutrient solution. Data in each column within each genotype followed by the same letter are not significantly different ($P<0.05$).

Genotypes	Treatments		APX	CAT	POD	SOD	GR
			nmol H_2O_2 mg^{-1} protein min^{-1}	µmol H_2O_2 mg^{-1} protein min^{-1}	µmol Guaiacol mg^{-1} protein min^{-1}	Unit mg^{-1} protein	nmol NADPH mg^{-1} protein min^{-1}
			Shoot				
	Aer.	+Zn	42.6±15.5^{a}	5.04±0.62^{a}	0.13±0.01^{b}	7.57±0.72^{a}	12.2±0.6^{a}
Amol		–Zn	51.5±1.8^{a}	5.82±0.52^{a}	0.18±0.02^{a}	4.91±0.61^{b}	10.8±2.6^{a}
	Unaer.	+Zn	45.3±9.9^{a}	6.66±0.72^{a}	0.13±0.02^{b}	8.89±0.96^{a}	9.7±0.8^{a}
		–Zn	67.8±8.7^{a}	5.49±0.64^{a}	0.19±0.01^{a}	5.54±0.23^{b}	10.4±1.7^{a}
	Aer.	+Zn	52.1±9.3^{a}	4.63±0.37^{a}	0.14±0.01^{b}	8.35±0.68^{a}	8.9±1.8^{b}
Dashti		–Zn	47.2±4.7^{a}	4.85±0.78^{a}	0.18±0.02^{b}	3.94±1.00^{b}	7.9±1.5^{b}
	Unaer.	+Zn	49.2±8.9^{a}	4.72±0.40^{a}	0.15±0.02^{b}	7.96±0.84^{a}	12.2±0.8^{a}
		–Zn	40.1±5.9^{a}	3.86±0.52^{a}	0.39±0.03^{a}	3.16±0.53^{b}	12.6±0.7^{a}
			Root				
	Aer.	+Zn	46.3±0.8^{b}	2.64±0.51^{a}	1.02±0.09^{b}	7.89±0.81^{a}	10.7±3.9^{a}
Amol		–Zn	58.2±2.6^{b}	3.97±0.84^{a}	1.73±0.08^{a}	5.34±0.42^{b}	9.8±3.9^{a}
	Unaer.	+Zn	53.3±0.8^{b}	2.37±0.18^{a}	1.03±0.15^{b}	8.77±0.95^{a}	11.9±0.7^{a}
		–Zn	88.2±10.4^{a}	3.23±0.84^{a}	1.80±0.25^{a}	5.69±0.41^{b}	10.9±1.4^{a}
	Aer.	+Zn	26.0±3.9^{b}	1.25±0.06^{a}	0.60±0.02^{b}	8.49±1.17^{a}	8.6±0.5^{a}
Dashti		–Zn	34.9±2.3^{ab}	1.20±0.06^{a}	0.54±0.01^{c}	6.56±0.55^{b}	9.1±1.4^{a}
	Unaer.	+Zn	27.9±1.4^{b}	1.42±0.17^{a}	0.64±0.04^{b}	8.48±0.67^{a}	10.2±1.4^{a}
		–Zn	40.7±9.2^{a}	1.30±0.13^{a}	1.16±0.04^{a}	5.82±0.37^{b}	9.2±1.6^{a}

in roots (52%) but in tendency in shoot. Activity of CAT did not respond either to low Zn stress or aeration treatment. In contrast, activity of POD responded to both Zn and aeration treatments in shoot and root. Zn deficiency induced activity of POD (with the exception of aerated Dashti) up to 46% and 160% for shoot and 75% and 81% for roots of non-aerated Amol and Dashti, respectively. As expected, Zn deficiency caused reduction of SOD activity in both shoot and root irrespective to aeration treatment. The most obvious response was detected in Dashti with up to 53% and 60% reduction of SOD activity under aerated and non-aerated conditions, respectively. Activity of GR did not respond to low Zn supply and hypoxia, with the exception of Dashti, in which aeration caused significant reduction of GR activity up to 48% in shoot (Table 3).

A consistent, though non significant reduction of APX activity was observed due to Fe starvation in both genotypes. As expected, activity of CAT decreased strongly by low Fe supply; considering relative amounts of reduction (% over control), inhibition of CAT activity was mainly higher in Amol than Dashti and in aerated than non-aerated plants. Similar with CAT, POD activity was also inhibited by low Fe supply. In contrast, activity of SOD increased in shoot and roots of Fe deficient plants compared with control, this effect was more prominent in Amol than Dashti. Activity of GR increased in Fe deficient plants, which was mainly in tendency and non significant (Table 4).

Concentration of H_2O_2 responded to Zn deficiency in shoot and root. In shoot, Zn deficiency caused a reduction in concentration of H_2O_2, but in roots an increase of H_2O_2 concentration was observed. Aeration caused higher accumulation of H_2O_2, significantly or in tendency. Superoxide radicals ($O_2^{\cdot-}$) accumulated in Zn deficient plants in both genotypes, however, aeration treatments had different effect on $O_2^{\cdot-}$ concentration depending on genotype. In Amol, aeration caused an increase of $O_2^{\cdot-}$ concentration in both Fe sufficient and deficient plants, in contrast, in Dashti an accumulation of $O_2^{\cdot-}$ was observed in plants grown under hypoxic conditions. Concentration of MDA increased in response to Zn deficiency. Similar with $O_2^{\cdot-}$, aeration showed a differential effect on MDA concentration, e.g. reduction in Amol and increase in Dashti under hypoxia (Table 5).

Concentration of H_2O_2 increased by low Fe supply in root, however, the opposite was observed for shoot, its concentration was lower in Fe deficient compared with control plants. Concentration of $O_2^{\cdot-}$ increased by low Fe supply, moreover, MDA concentration increased significantly or in tendency in Fe deficient plants (Table 6).

Zinc deficiency caused reduction of protein concentration in both shoot and root and in both genotypes. In this respect, two tested genotypes did not differ in their response to Zn deficiency. In accordance with the results of protein concentration, free amino acids accumulated significantly or in tendency in both shoot and root of low Zn plants (Table 5).

Table 4. Effect of Fe deficiency on the specific activity of ascorbate peroxidase (APX), catalase (CAT), peroxidase (POD), superoxide dismutase (SOD) and glutathione reductase (GR) in two genotypes of rice (*Oryza sative* L. cvs. Amol and Dashti) grown in aerated or non-aerated nutrient solution. Data in each column within each genotype followed by the same letter are not significantly different ($P<0.05$).

Genotypes	Treatments		APX nmol H_2O_2 mg^{-1} protein min^{-1}	CAT μmol H_2O_2 mg^{-1} protein min^{-1}	POD μmol Guaiacol mg^{-1} protein min^{-1}	SOD Unit mg^{-1} protein	GR nmol NADPH mg^{-1} protein min^{-1}
			Shoot				
Amol	Aer.	+Fe	46.5±17.3^{a}	4.66±0.14^{b}	0.11±0.01^{b}	9.79±0.85^{b}	14.4±2.9^{a}
		–Fe	40.9±6.9^{ab}	1.16±0.06^{c}	0.08±0.00^{c}	13.26±1.00^{a}	15.2±0.6^{a}
	Unaer.	+Fe	48.1±7.1^{a}	5.34±0.43^{a}	0.14±0.01^{a}	9.96±0.46^{b}	11.2±0.7^{a}
		–Fe	23.6±2.9^{b}	1.39±0.18^{c}	0.09±0.00^{c}	13.44±1.85^{a}	13.2±0.9^{a}
Dashti	Aer.	+Fe	46.4±2.5^{a}	4.12±0.67^{a}	0.17±0.02^{ab}	9.42±0.99^{ab}	9.2±0.9^{b}
		–Fe	30.5±8.9^{ab}	1.20±0.20^{b}	0.12±0.01^{c}	10.89±0.67^{a}	10.1±1.5^{ab}
	Unaer.	+Fe	39.2±12.4^{ab}	4.22±0.48^{a}	0.19±0.02^{a}	8.87±1.02^{b}	10.9±0.4^{ab}
		–Fe	21.6±1.7^{b}	1.48±0.05^{b}	0.15±0.01^{b}	10.47±1.00^{ab}	12.3±0.6^{a}
			Root				
Amol	Aer.	+Fe	46.9±1.3^{b}	1.57±0.27^{a}	1.02±0.04^{a}	7.11±1.11^{b}	10.9±0.7^{b}
		–Fe	45.3±5.7^{b}	0.36±0.05^{c}	0.72±0.09^{b}	12.71±1.21^{a}	13.7±0.9^{a}
	Unaer.	+Fe	60.2±7.4^{a}	0.82±0.09^{b}	1.07±0.16^{a}	7.38±0.87^{b}	14.3±1.1^{a}
		–Fe	52.7±3.8^{ab}	0.38±0.05^{c}	0.81±0.03^{b}	13.68±1.58^{a}	14.4±2.2^{ab}
Dashti	Aer.	+Fe	30.9±3.9^{a}	1.01±0.05^{b}	0.44±0.01^{a}	10.11±0.46^{b}	10.1±0.8^{a}
		–Fe	25.4±7.1^{a}	0.22±0.02^{d}	0.31±0.01^{b}	12.88±1.03^{a}	12.4±3.5^{a}
	Unaer.	+Fe	42.3±12.1^{a}	1.23±0.11^{a}	0.47±0.03^{a}	9.63±1.24^{b}	12.0±1.6^{a}
		–Fe	35.3±3.9^{a}	0.68±0.09^{c}	0.35±0.05^{b}	11.78±1.00^{ab}	13.5±0.1^{a}

Similar with Zn, Fe deficiency caused reduction of protein concentration and increase in total amino acids concentration, the latter change was mainly in tendency (Table 6).

Discussion

A distinct genotypic difference was observed in plants response to hypoxic conditions. Dry matter production of the lowland genotype (Amol) was significantly improved in nutrient solution without aeration, the opposite was observed for flooding sensitive genotype (Dashti). Root length was also affected by aeration treatments differently. Differential response of root length to hypoxia may have important consequences for nutrients acquisition of plants grown in soils with different oxygen availability.

Zinc deficiency tolerance of Amol was greater than Dashti. Amol has been characterized as an extremely Zn-efficient genotype in our previous work (Hajiboland and Salehi 2006a). Our experiment demonstrated also that, there is no direct relationship between tolerance to flooding and Zn deficiency in Iranian rice genotypes (Hajiboland and Salehi 2006b). In contrast, susceptibility to Fe deficiency was obviously related to flooding response in tested genotypes in this work as judged by biomass and chlorophyll content. Co-occurrence of flooding and high available Fe in soils is likely the cause of this relationship. Flooding causes the soil to become anaerobic with a low redox potential leading to a high and probably near toxic Fe^{2+} availability. Therefore, lowland rice genotypes have developed in an edaphic environment, in which there is no need for absorbing Fe with high efficiency that in turn has been led to higher susceptibility to Fe deficiency. In contrast, drained soils particularly calcareous ones are deficient in available Fe. Accordingly, Fe deficiency tolerance has been developed during selection and improvement of upland genotype.

Zinc deficiency did not affect strongly photochemistry of leaves, suggesting that though production of more active oxygen species in Zn deficient plants in this work, thylakoid constituents has not been damaged seriously. It was suggested that, for nutrients without direct involvement in the electron transport or chlorophyll synthesis such as Zn, a close linkage between nutritional status of leaves and spectral characteristics seems unlikely (Adams et al. 2000). However, there are reports on significant reduction of maximum quantum efficiency of PSII (Wang and Jin 2005) and severe damage to the ultrastructure of chloroplasts (Chen et al. 2007) in plants subjected to inadequate Zn supply. It is likely that, the severity and/or duration of Zn deficiency stress in our experiment were not enough for induction of serious damage to photosynthetic membranes and disturbance in the photochemistry of leaves.

In contrast, Fe deficiency depressed strongly maximal quantum efficiency of PSII (F_v/F_m). Reduction in F_v/F_m was due to both decrease in the electron transport chain (reduction of F_m) and particularly due to structural modifications of PSII mainly at the pigment level (increase in F_0). The negative effect of Fe deficiency for both rice genotypes focused mainly

Table 5. Effect of Zn deficiency on the concentration of protein (mg g^{-1} FW), total free a-amino acids (TAA), hydrogen peroxide (H_2O_2), superoxide radicals ($O_2^{\cdot-}$) and malondialdehyde (MDA) in two genotypes of rice (*Oryza sative* L. cvs. Amol and Dashti) grown in aerated or non-aerated nutrient solution. Data in each column within each genotype followed by the same letter are not significantly different (P<0.05).

Genotypes	Treatments		H_2O_2	$O_2^{\cdot-}$	MDA	Protein	TAA
			nmol g^{-1} FW	nmol g^{-1} FW	µmol g^{-1} FW	mg g^{-1} FW	mmol g^{-1} FW
			Shoot				
	Aer.	+Zn	1305±176^{a}	nd	1.49±0.29^{b}	59.5±2.1^{a}	262±33^{c}
Amol		–Zn	934±211^{a}	nd	2.74±0.69^{a}	42.7±2.7^{b}	369±23^{a}
	Unaer.	+Zn	1289±56^{a}	nd	1.05±0.91^{b}	60.2±2.3^{a}	208±20^{d}
		–Zn	1167±110^{a}	nd	1.32±0.31^{ab}	45.9±3.2^{b}	312±11^{b}
	Aer.	+Zn	1748±166^{a}	nd	3.24±0.98^{c}	65.8±4.2^{a}	183±82^{b}
Dashti		–Zn	669±36^{c}	nd	5.01±0.33^{ab}	52.7±1.6^{b}	289±31^{ab}
	Unaer.	+Zn	1077±38^{b}	nd	4.34±0.43^{bc}	68.1±1.5^{a}	276±3^{a}
		–Zn	843±116^{c}	nd	6.01±0.71^{a}	55.9±1.8^{b}	361±29^{a}
			Root				
	Aer.	+Zn	20.8±8.1^{b}	149±23^{c}	0.98±0.15^{a}	17.6±1.5^{b}	25.3±2.4^{b}
Amol		–Zn	40.5±12.7^{a}	259±30^{a}	1.04±0.15^{a}	13.3±1.5^{c}	38.3±1.9^{a}
	Unaer.	+Zn	6.5±1.7^{b}	108±19^{d}	0.52±0.09^{b}	21.3±1.4^{a}	27.4±2.2^{b}
		–Zn	18.5±5.4^{b}	191±8^{b}	0.83±0.19^{a}	17.1±1.5^{b}	36.2±2.7^{a}
	Aer.	+Zn	18.8±2.3^{c}	185±21^{c}	2.17±0.17^{b}	30.7±3.2^{a}	28.9±4.3^{b}
Dashti		–Zn	30.0±4.8^{b}	415±38^{b}	3.41±0.84^{ab}	24.7±0.7^{b}	37.3±1.3^{a}
	Unaer.	+Zn	17.6±3.8^{c}	187±29^{c}	2.54±0.26^{ab}	29.2±2.4^{a}	35.8±3.1^{ab}
		–Zn	42.2±8.1^{a}	531±82^{a}	3.95±0.89^{a}	23.8±2.3^{b}	31.3±2.5^{ab}

Table 6. Effect of Fe deficiency on the concentration of protein (mg g^{-1} FW), total free a-amino acids (TAA), hydrogen peroxide (H_2O_2), superoxide radicals ($O_2^{\cdot-}$) and malondialdehyde (MDA) in two genotypes of rice (*Oryza sative* L. cvs. Amol and Dashti) grown in aerated or non-aerated nutrient solution. Data in each column within each genotype followed by the same letter are not significantly different (P<0.05).

Genotypes	Treatments		H_2O_2	$O_2^{\cdot-}$	MDA	Protein	TAA
			nmol g^{-1} FW	nmol g^{-1} FW	µmol g^{-1} FW	mg g^{-1} FW	mmol g^{-1} FW
			Shoot				
	Aer.	+Fe	1853±429^{a}	nd	1.22±0.30^{a}	58.5±1.6^{a}	293±17^{ab}
Amol		–Fe	424±19^{c}	nd	1.35±0.12^{a}	35.8±1.2^{c}	350±46^{a}
	Unaer.	+Fe	1347±74^{b}	nd	1.06±0.20^{a}	60.1±1.9^{a}	257±7^{b}
		–Fe	344±32^{c}	nd	1.34±0.28^{a}	40.1±0.9^{b}	284±42^{ab}
	Aer.	+Fe	1367±236^{a}	nd	4.41±0.08^{b}	59.8±4.2^{a}	241±23^{a}
Dashti		–Fe	367±38^{b}	nd	5.58±1.69^{b}	44.7±1.5^{b}	293±75^{a}
	Unaer.	+Fe	1254±159^{a}	nd	5.62±1.92^{b}	59.9±1.9^{a}	249±30^{a}
		–Fe	215±69^{b}	nd	10.23±1.79^{a}	45.7±1.6^{b}	294±15^{a}
			Root				
	Aer.	+Fe	45.9±4.8^{b}	233±20^{c}	2.13±0.98^{c}	20.5±1.2^{a}	28.1±1.5^{a}
Amol		–Fe	59.5±6.2^{a}	584±55^{a}	5.75±0.00^{a}	13.2±0.4^{b}	34.2±2.6^{a}
	Unaer.	+Fe	9.2±2.9^{c}	227±24^{c}	1.52±0.37^{c}	21.1±1.0^{a}	29.4±2.6^{a}
		–Fe	36.8±2.0^{b}	464±26^{b}	4.14±0.34^{b}	13.9±0.6^{b}	33.1±3.3^{a}
	Aer.	+Fe	21.9±3.8^{c}	201±17^{b}	2.80±0.20^{c}	31.7±2.5^{a}	27.4±2.8^{a}
Dashti		–Fe	40.3±4.1^{a}	359±25^{a}	12.40±1.47^{b}	24.8±0.6^{b}	32.9±3.9^{a}
	Unaer.	+Fe	19.5±0.5^{c}	222±23^{b}	3.98±1.07^{c}	29.6±1.6^{a}	28.7±1.8^{a}
		–Fe	32.2±3.3^{b}	361±13^{a}	19.09±4.85^{a}	24.4±1.4^{b}	28.9±1.1^{a}

on the decreased proportion of active chlorophyll associated with the reaction center of PSII (decreased F_v/F_0). Increase in F_0 could be originated from increases in the dark reduction of the plastoquinone pool (Belkhodja et al. 1998) or from the inactivation of the ferredoxin, an electron transmitter, due to changes in its chemical structure. Accordingly, in Fe deficient plants a close correlation was found between the rate of net photosynthesis and photochemical properties of leaves (Table 7), suggesting that inhibited light reactions in Fe deficient leaves contributes significantly in reduction of CO_2 assimila-

Table 7. Correlation coefficient between plants dry weight and net photosynthesis rate, photochemical properties of leaves, activity of antioxidant enzymes and concentration of oxidants in two genotypes of rice (*Oryza sative* L. cvs. Amol and Dashti) grown under different nutritional status of Zn and Fe. Shoot and root dry weight data and the values for activity of enzymes in these parts were subjected to analysis of their correlation. For analysis of correlation between photosynthetic parameters and plants DW, dry weight of shoot (but not root) was regarded. Data of two studied genotypes were combined. Coefficients above the dashed line refer to the Zn experiment and those below it to the Fe experiment. ns: non significant, * significant at 0.05, ** significant at 0.01.

	Plant DW	*A*	F_v/F_m	F_v/F_0	APX	CAT	POD	SOD	GR	H_2O_2	$O_2^{\cdot-}$	MDA
Plant DW	---	0.65 ns	-0.77 *	-0.49 ns	0.08 ns	0.81 **	-0.69 **	0.30 ns	0.12 ns	0.88 **	-0.79 **	-0.15 ns
A	0.85 **	---	-0.24 ns	-0.42 ns	-0.08 ns	0.16 ns	-0.70 ns	0.94 **	-0.06 ns	0.77 **	nd	-0.31 Ns
F_v/F_m	-0.71 *	0.86 **	---	---	-0.11 ns	-0.65 ns	0.59 ns	-0.49 ns	-0.18 ns	-0.41 ns	nd	0.86 **
F_v/F_0	0.73 **	0.90 **	---	---	0.02 ns	0.00 ns	0.25 ns	-0.50 ns	0.00 ns	-0.47 ns	nd	0.36 ns
APX	0.15 ns	0.76 **	0.38 ns	0.02 ns	---	---	---	---	---	0.11 ns	-0.21 ns	-0.39 ns
CAT	0.94 **	0.92 **	0.84 **	0.00 ns	---	---	---	---	---	0.81 **	0.39 ns	-0.04 ns
POD	-0.56 **	0.65 ns	0.76 **	0.25 ns	---	---	---	---	---	-0.76 **	-0.06 ns	-0.41 ns
SOD	0.26 ns	0.82 **	-0.85 **	-0.50 ns	---	---	---	---	---	0.01 ns	-0.60 ns	-0.51 *
GR	-0.36 ns	-0.48 ns	-0.46 ns	0.00 ns	---	---	---	---	---	0.15 ns	-0.60 ns	-0.08 ns
H_2O_2	0.90 **	0.91 **	0.74 ns	-0.47 ns	0.20 ns	0.95 **	-0.55 *	-0.24 ns	-0.19 ns	---	---	0.21 Ns
$O_2^{\cdot-}$	-0.79 *	nd	nd	nd	0.06 ns	-0.75 *	-0.04 ns	0.78 *	0.60 ns	---	---	0.85 **
MDA	-0.37 ns	-0.15 ns	0.15 ns	0.08 ns	-0.44 ns	-0.35 ns	-0.11 ns	0.26 ns	0.00 ns	0.32 ns	0.30 ns	---

tion. However, even in Fe deficient plants the contribution of stomatal closure in reduction of net assimilation rate (85%) was more pronounced than that of reduction in quantum efficiency of PSII (34%). In contrast, lower assimilation rate in low Zn plants was solely attributable to the stomatal limitation. Reduction of stomatal conductance due to low supply of Zn was reported for other plants such as chickpea (Rengel et al. 2004) and maize (Wang and Jin 2005). Stomatal limitation was also observed for Fe deficient plants (Chouliaras et al. 2004; Molassiotis et al. 2006).

Aeration of nutrient solution reduced stomatal conductance in tendency or significantly and in both tested genotypes. Therefore, plants grown under aerobic conditions lost more water via transpiration, leading to lower *WUE*. Change of water management and shift from flooded to aerobic conditions in rice fields was recommended because of increasing water scarcity in the world (Bouman et al. 2005). Our results, however, showed that rice plants would have use soil water resources more inefficiently when grown in drained soils compared with flooded fields. Decrease in stomatal conductance under flooded conditions has been demonstrated in many woody species of temperate and tropical forest ecosystems (Mielke et al. 2003) and was attributed to decrease in root hydraulic conductivity under soil anaerobic conditions leading to internal water stress and reducing leaf turgor (Pezeshki 2001) or production of abscisic acid (Zhang and Zhang 1994). Very limited information is available on the effect of flooding on stomatal behavior in leaves of soil grown rice plants (Ishihara and Saito 1987). However, a field study showed that the water productivity of rice under aerobic conditions was 32-88% higher than under flooded conditions (Bouman et al. 2005). In the calculation of water productivity the amount of evapotranspiration is considered (Kassam and Smith 2001), therefore, lower values for water productivity could be the result of higher water table evaporation in the flooded soils rather higher transpiration by plants. Nevertheless, our data for nutrient solution grown plants, in which flooded conditions was simulated by only one of several factors functioning in a submerged soils, should be considered only with great cautions.

Activity of two H_2O_2 scavenging enzymes, APX and POD was induced by low Zn supply. Induction of APX and particularly POD under the effect of deficiency of macro (Tewari et al. 2007) or micronutrients (Candan and Tarhan 2003) was frequently reported. In contrast to the effect of Zn, Fe caused a reduction of APX, CAT and POD. Iron is one component of prosthetic group of peroxidases, therefore reduction of activity of peroxidases in Fe deficient plants is

expected (Marschner 1995). Activity of CAT responded more strongly to Fe deficiency than APX and POD. In addition, a close correlation observed between activity of CAT, net CO_2 assimilation and maximum quantum efficiency of PSII in Fe deficient leaves (Table 7) further confirms the relevance of using its activity as an indicator of Fe nutritional status of plants (Marschner 1995).

Activity of GR did not seem to be responsive to Fe or Zn deficiency and GR seems to be not involved in antioxidant defense system of Zn and Fe starved plants. Glutathione reductase effect on protection of plants against stresses evoked by sulfur (Hajiboland and Amjad 2007), nitrogen and K (Tewari et al. 2007) deficiency was reported, likely because of its effect on keeping reduced GSH at a given level.

Greater APX activity in Amol under hypoxic conditions, which was associated with higher tolerance (rather a growth improvement) suggests possible role for this enzyme in protection of plants against hypoxia. Change in the activity of APX was reflected in H_2O_2 concentration in plants, *i.e.* higher APX activity in non-aerated Amol was associated with lower accumulation of H_2O_2 in plants; roots were more responsive than shoot. Induction of APX activity was suggested to provide plant roots with increased tolerance to waterlogged stress (Lin et al. 2004).

Activity of POD increased in Dashti treated with hypoxia, this treatment caused stress for plants as judged by lower growth. In addition, higher POD activity in non-aerated Dashti did not result in lower H_2O_2 concentration. As it is obvious from correlation coefficient presented in Table 7, there is rather a negative relationship between POD activity and plants growth, e.g. lower growth was accompanied by higher activity of POD. It implies that, POD activity only monitored stress conditions without any protecting role. The unspecific POD activity assayed with guaiacol as a universal substrate can exhibit activity of APX (antioxidant enzyme), coniferyl alcohol peroxidase (lignifying enzyme), NADH oxidase and IAA oxidase (growth limiting peroxidases). The individual activity of these enzymes with the exception of APX, were not distinguished from the soluble pool in our extraction procedure. On the other hand, the functional significance of peroxidases measured by guaiacol test in the protection of plants against oxidative stresses has been questioned by many authors (Van Assche and Clijsters 1990; Chaoui et al. 1997; Cuypers et al. 2000).

Activity of SOD decreased in low Zn plants, which was associated with higher accumulation of $O_2^{\cdot-}$ (r=-0.60) and MDA (r=-0.51) as indicator of membrane damage. Activity of SOD was suggested to be an indicator of Zn nutritional status of plants (Cakmak et al. 1997) and is the first enzyme activity known to be reduced under low Zn stress. In contrast, SOD activity increased in plants suffered from Fe deficiency. Induction of SOD activity by low Fe supply was reported by other authors (Molassiotis et al. 2006) and is attributable to production of more reactive oxygen species in Fe deficient plants.

Increase in the $O_2^{\cdot-}$ accumulation in Fe deficient plants was observed though activity of SOD did not reduced or rather increased (r=0.78). In means that, production of $O_2^{\cdot-}$ in Fe deficient plants was much higher than the capacity of scavenging enzymes. In contrast, change in the activity of SOD in Zn deficient plants was reflected well in the concentration of $O_2^{\cdot-}$ (r=-0.60).

In this work, responses of plants to low Zn and Fe as well as hypoxia stress are mainly attributable to the accumulation of $O_2^{\cdot-}$ than that of H_2O_2 or membrane damage. Detrimental effect of $O_2^{\cdot-}$ in comparison with H_2O_2 was well demonstrated in negative correlation between concentration of $O_2^{\cdot-}$ and plants dry weight (r=-0.79). Such correlation for H_2O_2 was rather positive (r=0.88-0.90). It means that like POD activity, H_2O_2 concentration has no determinant role in plants growth response. Superoxide radical is one of the most deleterious reactive oxygen species attacks membranes and induces peroxidation of lipids (Kappus 1985). It could be assumed that, tolerance to low Zn and Fe as well as hypoxia is highly related to the activity of superoxide radical scavenging system and particularly to the concentration of $O_2^{\cdot-}$ rather to the H_2O_2 or its scavenging enzymes. The ability to maintain a balance between the formation and detoxification of superoxide radicals appeared to increase the plants tolerance to low supply of tested nutrients as well as hypoxia. The importance of the superoxide scavenging system for maintaining the structural stability of subcellular plant organelles, integrity of cell membranes and protection of proteins, DNA and chlorophyll and deleterious effects of superoxide anion in cellular metabolism (Fridovich 1995) provide a good reason for this conclusion.

References

Adams ML, Norvell WA, Philpot WD, Peverly JH (2000) Spectral detection of micronutrient deficiency in Bragg soybean. Agron J 92:261-268.

Asada K (1992) Ascorbate peroxidase-a hydrogen peroxide-scavenging enzyme in plants. Physiol Plant 85:235-241.

Belkhodja R, Morales F, Quilez R, Lopez-Millan AF, Abadia A, Abadia J (1998) Iron deficiency causes changes in chlorophyll fluorescence due to the reduction in the dark of the Photosystem II acceptor side. Photosynth Res 56:265-276.

Bouman BAM, Peng S, Castañeda AR, Visperas RM (2005) Yield and water use of tropical aerobic rice systems in the Philippines. Agric Water Manage 72:87-105.

Cakmak I, Öztürk L, Eker S, Torun B, Kalfa HI, Yilmaz A (1997) Concentration of zinc and activity of copper/zinc superoxide dismutase in leaves of rye and wheat cultivars differing in sensitivity to zinc deficiency. J Plant Physiol 151:91-95.

Candan N, Tarhan L (2003) The correlation between antioxidant enzyme activities and lipid peroxidation levels in *Mentha pulegium* organs grown in Ca^{2+}, Mg^{2+}, Cu^{2+}, Zn^{2+} and Mn^{2+} stress conditions. Plant Sci 165:769-776.

Chaoui A, Mazhoudi S, Ghorbal MH, El Ferjeni E (1997) Cadmium and zinc induction of lipid peroxidation and effects on antioxidant enzyme activities in bean (*Phaseoulus vulgaris* L.). Plant Sci 127:139-147.

Chen W, Yang X, He Z, Feng Y, Hu F (2007) Differential changes in pho-

tosynthetic capacity, 77K chlorophyll fluorescence and chloroplast ultrastructure between Zn-efficienct and Zn-inefficient rice genotypes (*Oryza sativa* L.) under low Zn stress. Physiol Plant 132:89-101.

Chouliaras V, Therios I, Molassitis A, Patakas A, Diamantidis G (2004) Effect of iron deficiency on gas exchange and catalase and peroxidase activity in citrus. J Plant Nutr 27:2085-2099.

Cuypers A, Vangronsveld J, Clijsters H (2000) Biphasic effect of copper on the ascorbate-glutathione pathway in primary leaves of *Phaseolus vulgaris* L. seedlings during the early stages of metal assimilation. Physiol Plant 110:512-517.

Fageria NK, Baligar VC, Jones CA (1997) Growth and Mineral Nutrition of Field Crops. 2nd ed. Marcel Dekker, New York, USA.

Fageria NK, Baligar VC (2005) Growth components and zinc recovery efficiency of upland rice genotypes. Pesq Agropec Bras 40:1211-1215.

Fridovich I (1995) Superoxide radical and superoxide dismutases. Ann Rev Biochem 64:97-112.

Gao X, Zou C, Zhang F, Van der Zee EATM, Hoffland E (2005) Tolerance to zinc deficiency in rice correlates with zinc uptake and translocation. Plant Soil 278:253-261.

Gounaries K, Barber J, Harwood JL (1986) The yhylakoid membranes of higher plant chloroplasts. Biochem J 237:313-326.

Hajiboland R, Amjad L (2007) Does antioxidant capacity of leaves play a role in growth response to selenium at different sulfur nutritional status? Plant Soil Environ 53:207-215.

Hajiboland R Hasani BD (2007) Responses of antioxidant defense capacity and photosynthesis of bean (*Phaseolus vulgaris* L.) plants to copper and manganese toxicity under different light intensities. Acta Biol Szeged 51:93-106.

Hajiboland R, Salehi SY (2006a) Characterization of Zn efficiency in Iranian rice genotypes I. Uptake efficiency. Gen Appl Plant Physiol (GAPP) 32(3-4):191-206.

Hajiboland R, Salehi SY (2006b) Characterization of Zn efficiency in Iranian rice genotypes II. Internal use efficiency. Gen Appl Plant Physiol (GAPP) 32 (3-4):207-222.

Hajiboland R, Yang XE, Römheld V (2003) Effects of bicarbonate and high pH on growth of Zn-efficient and Zn-inefficient genotypes of rice, wheat and rye. Plant Soil 250:349-357.

Hendry GAF, Brocklebank KJ (1985) Iron-induced oxygen radical metabolism in waterlogged plants. New Phytol. 101:199-206.

Ishihara K, Saito K (1987) Diurnal courses of photosynthesis transpiration and diffusive conductance in the single-leaf of the rice plants grown in the paddy field under submerged condition. Jpn. J. Crop Sci. 56:8–17.

Jiménez A, Hernández JA, del Río LA, Sevilla F (1997) Evidence for the presence of the ascorbate-glutathione cycle in mitochondria and peroxisomes of pea leaves. Plant Physiol. 114:275-284

Kappus H (1985) Lipid peroxidation: mechanisms, analysis, enzymology and biological relevance. In Sies H, ed., Oxidative Stress. Academic Press, London, 273-310.

Kassam A, Smith M (2001) FAO methodologies on crop water use and crop water productivity. In Proceedings of Expert Meeting on Crop Water Productivity. Rome, Italia, 1-18.

Lin K-HR, Weng C-C, Lo H-F, Chen J-T (2004) Study of the root antioxidative system of tomatoes and eggplants under waterlogged conditions. Plant Sci. 167:355-365.

Marschner H (1995) Mineral Nutrition of Higher Plants. 2nd ed. Academic Press, UK.

Maxwell K, Johnson GN (2000) Chlorophyll Fluorescence- A Practical Guide. J Exp Bot 51:659-668.

Mielke MS, de Almeida A-AF, Gomes FP, Aguilar MAG, Mangabeira PAO (2003) Leaf gas exchange, chlorophyll fluorescence and growth responses of *Genipa Americana* seedlings to soil flooding. Environ Exp Bot 50:221-231.

Molassiotis A, Tanou G, Diamantidis G, Patakas A, Therios I (2006) Effects of 4-month Fe deficiency exposure on Fe reduction mechanism, photosynthetic gas exchange, chlorophyll fluorescence and antioxidant defense in two peach rootstocks differing in Fe deficiency tolerance. J Plant Physiol 163:176-185.

Moran R (1982) Formulae for determination of chlorophyllous pigments extracted with *N,N*-Dimethylforamide. Plant Physiol. 69:1376-1381.

Nerkar YS, Misal MB, Marekar RV (1984) PBN1, a semidwarf upland rice cultivar tolerant of iron deficiency. Int Rice Res Newsl 9:15-16.

Pezeshki SR (2001) Wetland plant responses to soil flooding. Environ Exp Bot 46:299-312.

Rengel Z, McDonald GK, Jkan HR (2004) Zinc fertilization and water stress affects plant water relation, stomatal conductance and osmotic adjustment in chickpea (*Cicer arientinum* L.). Plant Soil 267:271-284.

Salin ML (1987) Toxic oxygen species and protective systems of the chloroplast. Physiol Plant 72:681-689

Tennant D (1975) A test of modified line intersect method of estimating root length. J Ecol 63:995-1001.

Tewari RK, Kumar P, Sharma PN (2007) Oxidative stress and antioxidant responses in young leaves of mulberry plants grown under nitrogen, phosphorus or potassium deficiency. J Integrative Plant Biol 49:313-322.

Van Assche F, Clijsters H (1990) Effects of metals on enzyme activity in plants. Cell and Environ 13:195-206.

Wang H, Jin JY (2005) Photosyntheric rate, chlorophyll fluorescence parameters, and lipid peroxidation of maize leaves as affected by zinc deficiency. Photosynthetica 43:591-596.

Yang X, Römheld V, Marschner H (1994a) Effect of bicarbonate on root growth and accumulation of organic acids in Zn-inefficient and Zn-efficient rice cultivars (*Oryza sativa* L.). Plant Soil 164:1-7.

Yang X, Römheld V, Marschner H, Chaney RL (1994b) Application of chelator-buffered nutrient solution technique in studies on zinc nutrition in rice (*Oryza sativa* L.) plant. Plant Soil 163:85-94.

Yoshida S, Forno DA, Cock JH, Gomez K (1972) Routine methods of solution culture for rice. In: Laboratory Manual for Physiological Studies of Rice. (2nd ed.), pp. 53-57. The International Rice Research Institute, Philippines.

Zhang J, Zhang X (1994) Can early wilting of old leaves account for much of the ABA accumulation in flooded pea plants? J Exp Bot 45:1335-1342.

Volume 52(2):295-299, 2008
Acta Biologica Szegediensis
http://www.sci.u-szeged.hu/ABS

ARTICLE

Calcium oxalate crystals in *Conyza canadensis* (L.) Cronq. and *Conyza bonariensis* (L.) Cronq. (Asteraceae: Astereae)

Ciler Meric

Department of Biology, Faculty of Arts and Sciences, Trakya University, Edirne, Turkey

ABSTRACT Calcium oxalate crystals (CaOx) are found in most organs and tissues of many plant species. In this study the morphology and distribution of CaOx crystals in *Conyza canadensis* (L.) Cronq. and *Conyza bonariensis* (L.) Cronq. belonging to Asteraceae were investigated. CaOx crystals display a similar distribution in organs and tissues of *C. canadensis* and *C. bonariensis*. For the identification of CaOx crystals a histochemical technique (using silver nitrate and rubeanic acid) was applied to the cleared organs and tissues. Crystals in cleared organs and tissues were viewed using an Olympus photomicroscope fitted with polarizing filters. The sample tissues were also investigated with a scanning electron microscope. CaOx crystals were found in stems, leaves, petals, ovaries, and styles of two species, but no crystals were observed in filament or other tissues. Druses were observed in the stem epidermis and cortex cells and leaf epidermis cells and mesophyll layers in both species. They were also determined in corolla and style cells. The pith parenchyma cells of stem had needle-shaped and bipyramidal crystals. Styloid crystals were present in the ovary of both species. Raphides were not observed in both taxa. This study provides additional information about the presence of CaOx crystals in Asteraceae.
Acta Biol Szeged 52(2):295-299 (2008)

KEY WORDS

Asteraceae
calcium oxalate crystals
Conyza canadensis
Conyza bonariensis

The genus *Conyza* Less. belonging to tribe Astereae includes herbs, shrubs and trees and comprises over 60 species which are mainly distributed in tropical and subtropical areas. The Astereae tribe is the second largest tribe of Asteraceae, with over 170 genera and 3000 species worldwide (Bremer 1994). Most widespread two species of *Conyza* genus in Europe and Turkey are *Conyza canadensis* (L.) Cronq. and *Conyza bonariensis* (L.) Cronq. (Grierson 1975; Tutin et al. 1976). *Conyza* spp. contain alkaloids, saponins, tannins, glycosides, phenols, flavonoids, oil and sphingolipids (Kong et al. 2001; Mukhtar et al. 2002). Today no literature is found about the existence of calcium oxalate crystals in *Conyza* species.

Calcium oxalate (CaOx) crystals are formed from environmentally derived calcium and biologically synthesized oxalate and they are common for most tissues and organs of plants (Franceschi and Horner 1980; Prychid and Rudall 1999; Nakata 2003). The shape and location of these crystals within a taxon are often very specific and they are used in classification of plants (Franceschi and Horner 1980; Lersten and Horner 2000). CaOx crystals occur in different plant tissues including leaves (Horner and Zindler-Frank 1982; Lersten and Horner 2000), stems (Franceschi and Horner 1980), roots (Horner et al. 2000), and seeds (Webb and Arnott 1982; Ilarslan et al. 1997, 2001). CaOx crystals also occur in floral organs including ovaries (Dormer 1961; Tilton and Horner 1980), anthers (Horner 1977; Horner and Wagner 1980; Meric and Dane 2004) and petals (Meric and Dane 2004). The only place where crystals have not been seen is the pollen (Tilton and Horner 1980). CaOx crystals are widely distributed in plant kingdom and found in over 215 families (Franceschi and Horner 1980; Molano-Flores 2001). However, their functional significance remains unclear, although various functions have been attributed to them. CaOx crystals give protection against foraging animals (Molano-Flores 2001), bind toxic oxalate (Borchert 1984) and are involved in in-plant Ca regulation (Franceschi 1989), salt stress and homeostasis (Hurkman and Tanaka 1996), light gathering (Franceschi and Horner 1980) and detoxification of heavy metals (Nakata 2003).

Conyza Less. genus belongs to Asteraceae (about 1500-1600 genera and 23000 species) which is one of the greatest families of plant kingdom (Bremer 1994). Crystals in Asteraceae were shown by a few previous studies (Dormer 1961; Horner 1977; Meric and Dane 2004). The most comprehensive review of crystal types and distribution for a single family [Zindler-Frank 1987 (Leguminosae); Wu and Kuo-Huang 1997 (Moraceae)] lacks substantial documentation. The present study is a part of an ongoing project aiming to bring to light CaOx crystals in Asteraceae and this study aims to determine the CaOx crystals in *C. canadensis* and *C. bonariensis*. Thus additional research is needed to better determine CaOx crystals in other taxa belonging to Asteraceae.

Accepted Nov 13, 2008
*Corresponding author. E-mail: cilermeric@trakya.edu.tr

Table 1. Morphologies and locations within the tissues of calcium oxalate crystals in *Conyza canadensis* and *Conyza bonariensis*.

Location	*Conyza canadensis*	*Conyza bonariensis*
stem – epidermis	druse (3.61 ± 0.33 µm)	druse (3.55 ± 0.33 µm)
stem – cortex	druse (1.89 ± 0.17 µm)	druse (2.20 ± 0.22 µm)
stem – pith parenchyma	needle-shaped, bipyramid (6.15 ± 1.94 µm, 4.44 ± 1.16 µm)	needle-shaped, bipyramid (7.79 ± 3.02 µm, 4.58 ± 1.20 µm)
leaf – epidermis	druse (4.36 ± 0.46 µm)	druse 4.03 ± 0.48 µm
leaf – mesophyll	druse (2.24 ± 0.20 µm)	druse (3.07 ± 0.29 µm)
corolla	druse (3.16 ± 0.43 µm)	druse (4.92 ± 0.83 µm)
anther	---	---
filament	---	---
ovary	styloid (6.48 ± 1.83 µm)	styloid (6.93 ± 1.33 µm)
style	druse (3.45 ± 0.53 µm)	druse (4.76 ± 0.62 µm)

Materials and Methods

Vegetative and generative organs of *Conyza canadensis* (L.) Cronq. and *Conyza bonariensis* (L.) Cronq. were used as materials. Plants were grown in the Botanical Garden of Biology Department (Trakya University).

For light microscopy, materials were fixed in the mixture of ethyl alcohol and glacial acetic acid (3:1 v/v) at room temperature overnight and then the mixture was changed to 70% ethyl alcohol. The hand-sections of fixed stems and leaves were carried out. Corollas, anthers, filaments, ovaries and styles were dissected out of florets under a stereo microscope. The samples were treated with 2.5% Clorox (sodium hypochlorite) for 4 h. After graded ethyl alcohol series, the samples were infiltrated with xylene, mounted in entellan on slides, and covered with cover slips (Ilarslan et al. 1997). Crystals were observed under bright-field optics with or without polarizers on an Olympus Photomicroscope and images were captured with an Olympus digital camera. The histochemical determination of CaOx crystals was carried out according to the procedure of Yasue (1969) on the tissue clearings. Cleared samples were immersed in 5% aqueous $AgNO_3$ for 15 min, then thoroughly rinsed in distilled water. The samples were stained with saturated rubeanic acid (dithio oxamide) (Fluka, Germany) in 70% ethanol for 1 min. All examinations were made on ten plants at the anthesis stage.

For scanning electron microscopy (SEM), samples fixed in the mixture of ethyl alcohol and glacial acetic acid were dehydrated in a graded ethyl alcohol series to absolute ethyl alcohol and dried at the critical point (Bio-Rad E 3000, Hertfordshire, UK). Dried specimens were coated with gold (Bio-Rad SC 502, Hertfordshire, UK), and examined using a Jeol JSM SEM (Jeol, Tokyo, Japan). Control samples were treated with 5% acetic acid, 10% hydrochloric acid, 3% nitric acid and 4% sulfuric acid (Molano-Flores 2001). All these tests confirmed that the crystals were calcium oxalate.

Measurements of crystals were performed using Image-Pro Plus, version 5.1 (Media Cybernetics, Silver Spring, MD). For analysis, the diameters of druses, the lengths of styloids and needle-shaped crystals, and the side lengths of bipyramidal crystals were measured. A hundred of crystals for each tissue and each crystal type were measured from randomly chosen 10 regions. Averages and standard deviations of data were calculated.

Results

Calcium oxalate crystals displayed a similar distribution in the tissues and organs of *Conyza canadensis* and *Conyza bonariensis*. Table 1 shows the distributions and types of CaOx crystals in both species.

The clearing technique removed all the cytoplasm except for cell walls and CaOx crystals and the crystals were observed easily under light microscope with bright and polarized light. Druses were present in the stem epidermis cells of *C. canadensis* and *C. bonariensis* (Fig. 1A). Almost each stem epidermis cell had a single druse crystal. The diameters of these crystals were almost similar in both species (3.61 ± 0.33 µm for *C. canadensis* and 3.55 ± 0.33 µm *C. bonariensis*). Druses were also observed in parenchyma cells of the stem cortex (Fig. 1B). The diameters of these crystals were smaller than those of stem epidermis cells (1.89 ± 0.17 µm for *C.*

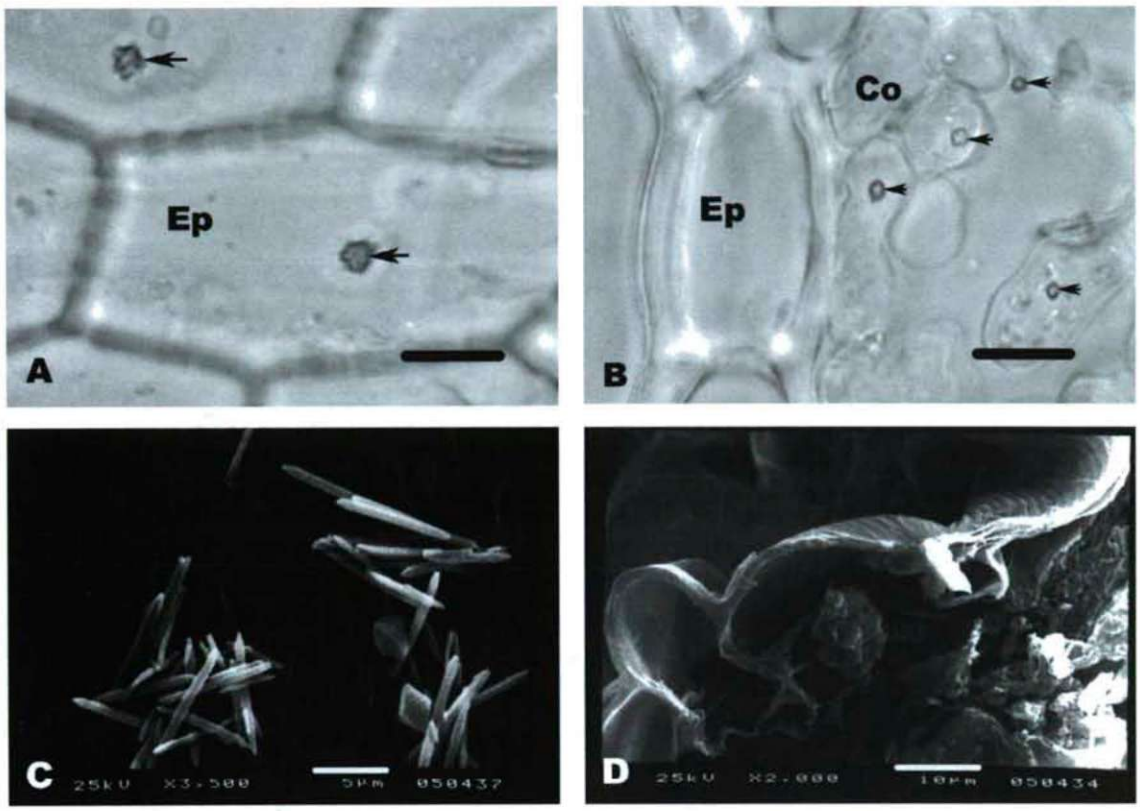

Figure 1. Calcium oxalate crystals in the tissues of *Conyza canadensis*. (A) Druse crystals in the stem epidermis cells of *C. canadensis* (arrows). (B) Druses in the stem cortex cells of *C. canadensis* (arrows) (in cleared tissues with bright light). (C) SEM photograph of needle-shaped and bipyramidal crystals in the pith parenchyma cells of stem of *C. canadensis*. (D) SEM photograph of druse crystal in the leaf epidermis cell of *C. canadensis*. Scale bar= 10 µm (A, B, D), scale bar= 5 µm (C). Ep, epidermis; Co, cortex.

canadensis and 2.20 ± 0.22 µm for *C. bonariensis*). The stem pith parenchyma cells had bipyramidal and needle-shaped crystals (Fig. 1C). The lengths of needle-shaped crystals were measured as 6.15 ± 1.94 µm for *C. canadensis* and 7.79 ± 3.02 µm for *C. bonariensis*. The side lengths of bipyramidal crystals were determined as 4.44 ± 1.16 µm and 4.58 ± 1.20 µm for *C. canadensis* and *C. bonariensis* respectively.

In leaves, druse crystals were observed in both epidermis and mesophyll cells of *C. canadensis* and *C. bonariensis*. Druses were present in both adaxial and abaxial epidermis cells of the leaves (Fig. 1D). The diameters of these crystals were measured as 4.36 ± 0.46 µm for *C. canadensis* and 4.03 ± 0.48 µm for *C. bonariensis*. They were also observed in the leaf mesophyll layers (Fig. 2A). The diameters of the druses within these cells were determined as 2.24 ± 0.20 µm and 3.07 ± 0.29 µm for *C. canadensis* and *C. bonariensis* respectively. Each leaf epidermis and mesophyll cell contained a single druse crystal.

A single druse crystal was determined in almost each cell of corollas in both species (Fig. 2B). The diameters of these crystals were measured as 3.16 ± 0.43 µm for *C. canadensis* and 4.92 ± 0.83 µm for *C. bonariensis*. Druses in corollas of *C. bonariensis* were bigger than of *C. canadensis*. Styloids were observed in each cell of ovaries in both species (Fig. 2C). The lengths of them were determined as 6.48 ± 1.83 µm and 6.93 ± 1.33 µm for *C. canadensis* and *C. bonariensis* respectively. The cells had single or a cluster of styloid crystals formed of a few of them. Druses were also observed in the style cells of the species (Fig. 2D). The diameters of these crystals were measured as 3.45 ± 0.53 µm for *C. canadensis* and 4.76 ± 0.62 µm for *C. bonariensis*. No crystals were found in the filament or other tissues. Localizations of CaOx crystals were also demonstrated by the Yasue (1969) procedure (Fig. 2B). The crystals stained brownish-black with this technique.

Discussion

CaOx crystals are present in almost every part of both vegetative and reproductive organs in plants and they are found in over 215 plant families (Franceschi and Horner 1980; Prychid and Rudall 1999; Molano-Flores 2001). Unfortunately, there are only a few studies related to the existence of them in Asteraceae (Dormer 1961; Horner 1977; Meric and Dane

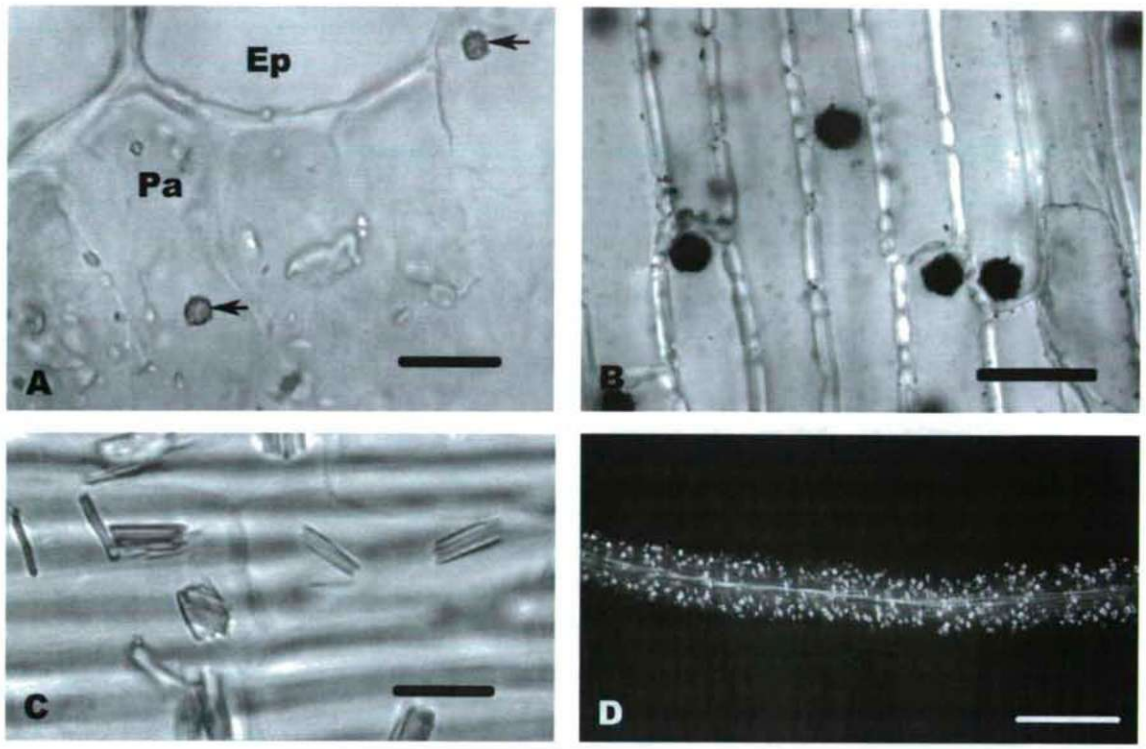

Figure 2. Calcium oxalate crystals in the tissues of *Conyza bonariensis*. (A) Druses in the leaf palisade cells of *C. bonariensis* (arrows) (in cleared tissues with bright light). (B) Druses in the corolla cells of *C. bonariensis* (stained with Yassue procedure). (C) Styloids in the ovary cells of *C. bonariensis*. (D) Druses in the style cells of *C. bonariensis* (with polarized light). Scale bar= 10 μm (A, B, C), scale bar= 100 μm (D). Ep, epidermis; Pa, parenchyma.

2004). In the present study, CaOx crystals were observed in *Conyza canadensis* and *Conyza bonariensis*. Druses were common in the tissues and organs of both taxa. They occurred in corollas, styles, leaves (epidermis and mesophyll) and stems (epidermis and cortex) of the two species investigated. The needle-shaped and bipyramidal crystals were present in the pith parenchyma cells of stems in both species. Styloids were only present in the ovaries of the specimens. No raphides were observed in the investigated tissues. Prychid and Rudall (1999) reported that druses are common in dicotyledons while raphides are widely found throughout monocotyledons.

Druses were observed in stem epidermis and cortex cells of *C. canadensis* and *C. bonariensis*. Franceschi and Horner (1980) reported that various crystals were present in the wood and parenchyma cells of some species belonging to Boraginaceae, Burseraceae, Combretaceae, Geraniaceae, Haloragaceae, Lauraceae, Leguminosae, Myrtaceae, Pinaceae, Polygonaceae, Rosaceae and Verbenaceae. Trockenbrodt (1995) determined CaOx crystals in the bark of *Quercus robur* (Fagaceae), *Ulmus glabra* (Ulmaceae), *Populus tremula* Salicaceae) and *Betula pendula* (Betulaceae).

The presence of CaOx crystals in leaves is common. In previous studies, crystals were determined in the epidermal cells of *Gleditsia triacanthos* (Leguminosae) (Borchert 1984) and *Stylosanthes guianensis* (Leguminosae) leaflets (Brubaker and Horner 1989). In addition Wu and Kuo-Huang (1997) observed druses in the epidermis of *Artocarpus altilis* (Moraceae) leaves and needles in the epidermis of *Ficus virgata* (Moraceae) leaves. Druses were determined in the mesophyll layers of *Actocarpus altilis, Cudrania cochinchinensis, Ficus virgata* and *Morus australis* (Moraceae) by Wu and Kuo-Huang (1997). Lersten and Horner (2000) reported that druses were the most common crystals in most *Prunus* species and calcium oxalate crystals in the leaves of this genus can be useful for the solution of the still unsettled systematics problems of *Prunus*. Kuo-Huang et al. (2007) suggested that druses crystals in the palisade cells of *Peperomia glabella* were utilized in the photosynthetic process and the diameters of these druses were related with light intensity.

Druse crystals were also found in corolla and style cells. Formation of this type of crystals was found to be related with changes in calcium levels within the plant (Nakata 2003). When calcium levels increased, druse crystal number and size also rapidly increased. When calcium levels decreased, number and size of druse crystals also decreased (Nakata 2003). Probably calcium is released from crystals for utilization in plant. Ca is an important component for cell wall synthesis and maintenance in higher plants and is essential

for the formation of the middle lamella. It is also related with the activation and/or stabilization of certain enzymes (Franceshi and Horner 1980). Serious abnormalities result from Ca deficiency in plants. The lack of Ca causes damage in membrane and organelle, changes in the cell wall and mitotic abnormalities (Franceshi and Horner 1980).

The presence of CaOx crystals in gynoecia was displayed in Dilleniaceae, Liliaceae, Palmae, Malvaceae, Cunoniaceae and Euphorbiaceae (Tilton and Horner 1980). Raphides are the most common type in gynoecia. But other crystal forms occur as crystal sand in carpels of *Bakeridesea* (Malvaceae) and also druses appear in several Cunoniaceae (Tilton and Horner 1980). In the ovaries of Asteraceae, CaOx crystals have been investigated in detail for the first time by Dormer (1961). Dormer (1961) determined prismatic crystals in the ovaries of *Centaurea scabiosa* (about 12 µm in length), *Silybum marianum* (about 45 µm in length), *Onopordon acanthium* (about 17x12 µm in sizes), *Carthamus tinctorius* and *Cirsium vulgare* (about 40 µm in length in both species). Also Dormer (1961) observed isodiametric crystals in the ovaries of *Arctium* sp. It appears that ovaries of Asteraceae contain crystals varying enormously in size. The investigated *Conyza* species include relatively smaller crystals (6.48 and 6.93 µm) than of previous studies (Dormer 1961). The present study aimed to determine CaOx crystals in *Conyza canadensis* and *C. bonariensis* belonging to the Asteraceae. It is probable that other members of Asteraceae might also contain crystals. Thus, further studies are necessary on the CaOx crystals in Asteraceae in order to determine the general value of crystals as a diagnostic feature for anatomical descriptions.

Acknowledgements

This study was supported by The Scientific Research Fund of Trakya University (Project No: TUBAP-624). I would like to thank in advance to TUBAP for financial support and Bilge Atay for carefully correcting the English of the manuscript.

References

Bremer K (1994) Asteraceae: cladistics and classification. Timber Press, Portland OR

Borchert R (1984) Functional anatomy of the calcium-excreting system of *Gleditsia triacanthos* L. Bot Gaz 145:474-482.

Brubaker CL, Horner HT (1989) Development of epidermal crystals in leaflets of *Stylosanthes guianensis* (Leguminosae; Papilionoideae). Can J Bot 67:1664-1670.

Dormer KJ (1961) The crystals in the ovaries of certain Compositae. Ann Bot 25:241-254.

Franceschi VR (1989) Calcium oxalate formation is a rapid and reversible process in *Lemna minor*. Protoplasma 148:130-137.

Franceschi VR, Horner HT (1980) Calcium oxalate crystals in plants. Bot Rev 46:361-427.

Grierson AJC (1975) *Conyza* Less. In Davis PH, ed., Flora of Turkey and the East Aegean Island, Vol 5, Edinburgh University Press, Edinburgh, pp. 132-133.

Horner HT (1977) A comparative light and electron microscopic study of microsporogenesis in male-fertile and cytoplasmic male-sterile sunflower (*Helianthus annuus*). Amer J Bot 64:745-759.

Horner HT, Kausch AP, Wagner BL (2000) Ascorbic acid: a precursor of oxalate in crystal idioblasts of *Yucca torreyi* in liquid root culture. Int J Plant Sci 161:861-868.

Horner HT, Wagner BL (1980) The association of druse crystals with the developing stomium of *Capsicum annuum* (Solanaceae) anthers. Amer J Bot 67:1347-1360.

Horner HT, Zindler-Frank E (1982) Histochemical, spectroscopic, and x-ray diffraction identifications of the two hydration form of calcium oxalate crystals in three legumes and *Begonia*. Can J Bot 60:1021-1027.

Hurkman WJ, Tanaka CK (1996) Effect of salt stress on germin gene expression in barley roots. Plant Physiol 110:971-977.

Ilarslan H, Palmer RG, Horner HT (2001) Calcium oxalate crystals in developing seeds of soybean. Ann Bot 88:243-257.

Ilarslan H, Palmer RG, Imsande J, Horner HT (1997) Quantitative determination of calcium oxalate and oxalate in developing seeds of soybean (Leguminosae). Amer J Bot 84:1042-1046.

Kong LD, Abliz Z, Zhou CX, Li LJ, Cheng CHK, Tan RX (2001) Glycosides and xanthine oxidase inhibitors from *Conyza bonariensis*. Phytochemistry 58:645-651.

Kuo-Huang LL, Ku MSB, Franceschi VR (2007) Correlations between calcium oxalate crystals and photosynthetic activities in palisade cells of shade-adapted *Peperomia glabella*. Bot Stud 48:155-164.

Lersten NR, Horner HT (2000) Calcium oxalate crystals types and trends in their distribution patterns in leaves of *Prunus* (Rosaceae: Prunoideae). Plant Syst Evol 224:83-96.

Meric C, Dane F (2004) Calcium oxalate crystals in floral organs of *Helianthus annuus* L. and *H. tuberosus* L. (Asteraceae). Acta Biol Szeged 48:19-23.

Molano-Flores B (2001) Herbivory and calcium concentrations affect calcium oxalate crystal formation in leaves of *Sida* (Malvaceae). Ann Bot 88:387-391.

Mukhtar N, Iqbal K, Anis I, Malik A (2002) Sphingolipids from *Conyza canadensis*. Phytochemistry 61:1005-1008.

Nakata PA (2003) Advances in our understanding of calcium oxalate crystal formation and function in plants. Plant Sci 164:901-909.

Prychid CJ, Rudall PJ (1999) Calcium oxalate crystals in monocotyledons: a review of their structure and systematics. Ann Bot 84:725-739.

Tilton VR, Horner HT (1980) Calcium oxalate raphide crystals and crystalliferous idioblasts in the carpels of *Ornithogalum caudatum*. Ann Bot 46:533-539.

Trockenbrodt M (1995) Calcium oxalate crystals in the bark of *Quercus robur, Ulmus glabra, Populus tremula* and *Betula pendula*. Ann Bot 75:281-284.

Tutin TG, Heywood VH, Burges NA, Moore DM, Valentine DH, Walters SM, Webb DA (1976) *Conyza* Less., In Flora Europaea, Vol 4, Cambridge University Press, Cambridge, p. 120.

Webb MA, Arnott HJ (1982) A survey of calcium oxalate crystals and other mineral inclusions in seeds. Scan Electron Micros 3:1109-1131.

Wu CC, Kuo-Huang LL (1997) Calcium crystals in the leaves of some species of Moraceae. Bot Bull Acad Sinica 38:97-104.

Yasue T (1969) Histochemical identification of calcium oxalate. Acta Histochem Cytoc 2:83-95.

Zindler-Frank E (1987) Calcium oxalate crystals in legums. *in* CH Stirton, ed, Advances in legume systematics, Part 3. Royal Botanic Gardens, Kew, London, 279-316.

Volume 52(2):301-305, 2008
Acta Biologica Szegediensis
http://www.sci.u-szeged.hu/ABS

ARTICLE

Sodium nitroprusside affects the level of anthocyanin and flavonol glycosides in pea (*Pisum sativum* L. cv. Arkel) leaves

Deepak Ganjewala[1]*, Sunil Boba[2] and Agepati S. Raghavendra[2]

[1]School of Biotechnology, Chemical and Biomedical Engineering, Vellore Institute of Technology University, Vellore-632 014 (T.N.), India, [2]Department of Plant Sciences, School of Life Sciences University of Hyderabad, Hyderabad 500 046 (A.P.), India

ABSTRACT The effects of sodium nitroprusside (SNP), a nitric oxide (NO) donor were investigated on the levels of anthocyanin and flavonol glycoside in pea (*Pisum sativum* L.) cv. Arkel leaves. The study was conducted in leaf discs (ca. 20 mm^2) prepared from the youngest leaves. The anthocyanin and flavonol glycosides content diminish significantly (~ 21% of each) in leaf discs following 1 mM SNP (1 mM) treatment for 3 h under light (600 µmol $M^{-2}.s^{-1}$). However, a huge increase both in the levels of anthocyanin and flavonol glycosides, 72 and 53% respectively was recorded after 2 h of 1 mM SNP treatment. 0.5 mM SNP treatment of the leaf discs did not change the anthocyanin level but considerable declined (~13%) was observed in the level of flavonol glycosides as compared to the control. Surprisingly, the anthocyanin content in no SNP treated leaf discs after 3 h of incubation under light (600 µmol $M^{-2}.s^{-1}$) increased rapidly by 72% while flavonol glycosides content by 15% only. The photosynthetic capacities of SNP treated leaf discs were drastically inhibited. The study prelude that NO in combination of light influence the accumulation of anthocyanin and flavonol glycosides in pea leaves.
Acta Biol Szeged 52(2):301-305 (2008)

KEY WORDS

anthocyanin
flavonol glycoside
glucose
Pisum sativum L. (cv. Arkel)
photosynthesis
sodium nitroprusside

Sodium nitroprusside (SNP), which releases nitric oxide upon light irradiation, is widely used as nitric oxide (NO) donor in plants and animals to investigate the effects of NO. NO is an important signaling molecule in plants. NO has gained increasing interest as important intermediate and intracellular signaling molecule in plant systems which mediates various pathophysiological and developmental processes, including expression of defense-related genes and programmed cell death, stomatal closure, seed generation and root development (Lamattina et al. 2003; Neil et al. 2003; Deak et al. 2008; Kolbert et al. 2008a, b). In the past few years, a growing amount of research has provided evidence for the multiple physiological roles of this gaseous free radical in plants (Delledonne 2001; Wendehenne et al. 2004). See a recent review, nitric oxide as a potent signaling molecule in plants by Erdei and Kolbert (2008). Several previous studies showed inhibitory effects of NO on the net photosynthesis in plants such as in oat (*Avena sativa*) and alfalfa (*Medicago sativa*) leaves (Hill and Bennett 1970). In mung bean (*Phaseolus aureus*), SNP treatment of the leaves resulted in significant decrease in activities of several photosynthetic enzymes and glucose metabolism (Lum et al. 2005). SNP has also been reported to enhance the production of secondary metabolites *viz.*, catharanthine production in *Catharanthus roseus* suspension cells (Xu et al. 2004), secondary metabolism activities of *Taxus* Cells (Wang and Wu 2005). In *Artemisia annua*, NO potentiates oligosaccharide-induced artemisinin production in Hairy Roots (Zheng et al. 2008). Until now most of the studies with SNP were primarily aimed to investigate the effects of NO on photosynthesis and very little is known about the roles of NO in plant secondary metabolism. Therefore it would be interesting to know the roles of NO on secondary metabolites *viz.*, anthocyanin and flavonol glycosides while the photosynthetic activity of plant is halted by NO. Anthocyanins are a class of secondary metabolites that contribute to the red, blue, and purple colors in a range of flowers, fruits, in leaves particularly during senescence, stems, roots, and occasionally in fruit flesh and seeds (Feild et al. 2001; Regan et al. 2001; Schaefer et al. 2004). Anthocyanins and flavonols are synthesized *via* the flavonol pathway, a branch of the phenylpropanoid pathway. The pathway leads to synthesis of anthocyanins with branches for synthesis of flavonols. The anthocyanin and flavonol glycoside composition of the genus *Pisum* is described in detail in (Furuya and Galston 1965; Statham et al. 1972).

The aim of the present study is to investigate the effects of SNP *via* photosynthesis on accumulation of secondary metabolites in pea leaves. Here, we measured anthocyanins and flavonol glycosides in pea (*Pisum sativum* L. cv. Arkel) leaf discs following the SNP treatment.

Accepted Nov 17, 2008
*Corresponding author. E-mail: deepakganjawala73@yahoo.com

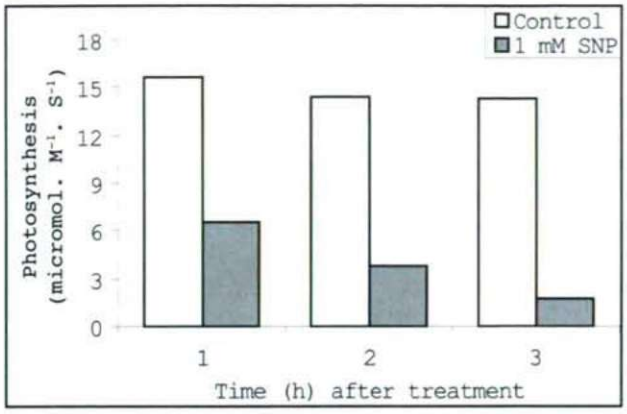

Figure 1. Changes in photosynthetic capacity of pea leaf discs following 1 mM SNP treatment. 15 leaf discs were kept in Petri dish containing 6 ml of distilled water as control, or 6 ml of different dilutions of sodium nitroprusside and incubated under light (600 $\mu mol.M^{-2}.S^{-1}$) for 3 h. Data presented in the figure are the average of the three independent experiments.

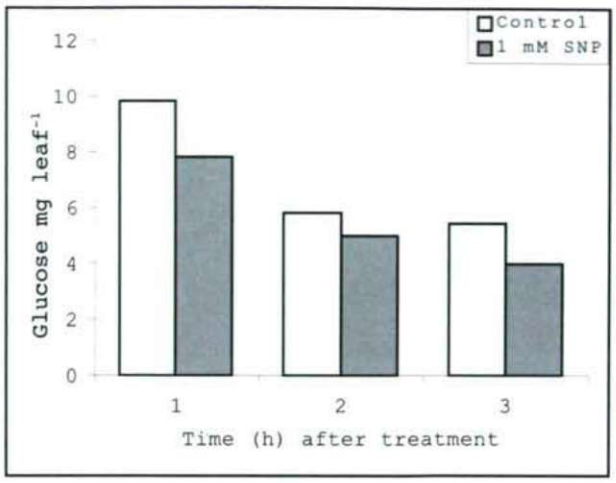

Figure 2. Changes in the glucose concentration in pea (*Pisum sativum* L.) cv. Arkel leaves after SNP treatment. Pea leaf discs were treated with 1 mM sodium nitroprusside and water (as control) under light (600 $\mu mol.M^{-2}.S^{-1}$) for 3 h. Data presented in the figure are the average of the three independent experiments.

Materials and Methods

Plant Material

Sterilized seeds of pea (*Pisum sativum* L. cv. Arkel) were grown in plastic trays filled with soil and farmyard manure (in a ratio of 1:3). Plants were grown outdoors for two weeks under 12-h-light/dark cycle and temperature of 40°/ 27°C day/ night (in summer).

Preparation of leaf discs and SNP treatment

Leaf discs (ca. 20 mm^2) of the youngest fully expanded leaves were prepared by a 15 mm diameter leaf punch and used for each measurement. To investigate the effects of SNP two sets of experiment were conducted. In the first set, 15 leaf discs were kept in Petri dish containing 6 ml of distilled water alone as control and incubated under light regime 600 $\mu mol.M^{-2}.S^{-1}$ for 3 h. In the second set, 15 leaf discs were kept in Petri dish containing 6 ml of sodium nitroprusside (0.5 to 5.0 mM) and incubated for 3 h. During the incubation, leaf discs were floating in the covered but not sealed Petri dishes. SNP solutions were prepared fresh.

Measurement of photosynthetic oxygen evolution

Photosynthetic capacity of pea leaf discs was measured in terms of O_2 evolution on illumination using Clark type oxygen electrode (Hansatech Instruments Ltd., Kings lynn, UK). After SNP treatment, the leaf discs (15 in number) were quickly blotted dry and transferred into the leaf disc oxygen electrode. The components in the chamber were arranged as per the instructions of the manufacture. The topmost capillary matting was moistened with 200 µL of 1 M bicarbonate buffer (pH 9.0). The leaf discs were arranged on this matting symmetrically. Oxygen in the chamber was calibrated for every sample as per the instructions of the manufacturer. Photosynthetic oxygen evolution was measured at a constant temperature of 25°C by a computerized leaf disc oxygen electrode system (LDp2, Hansatech Instruments Ltd. UK). Light at the required intensity was provided by an array of light emitting diodes.

Determination of anthocyanin and flavonol glycosides

Anthocyanin and flavonol glycosides were extracted according to procedure described by Hrazdina et al. (1982). 15 leaf discs were extracted with 1.0 ml methanol-0.1 N HCl for 30 min and the extract decanted. 20 µL of the extract was added to 980 µL methanol-0. 1 N HCl and the absorption spectrum recorded in a spectrophotometer. The concentration of anthocyanin was determined from the A at 530 nm using a molar extinction coefficient (ε) of 38,000 L x mol^{-1} x cm^{-1} that of the flavonol glycosides at 360 nm (ε = 20000 L x mol^{-1} x cm^{-1}, determined from a pure sample of quercetin 3-glucoside).

Pea leaf viability tests

Following the SNP treatment, viability of plant cell in epidermal strips of leaf was assessed by Evans blue (EVB). Lower epidermal layer of pea leaf was peeled of and incubated for 10 min at room temperature in EVB solution (400 mg/ml 0.65 M mannitol). After incubation, epidermal strips were viewed and photographed under bright-field transmitted light for EVB.

Table 1. Changes in the photosynthetic capacity of the pea leaf discs in response to varying concentrations of sodium nitroprusside (SNP). Data presented in the table are the average of the three independent experiments.

Treatment	Photosynthesis ($\mu mol.M^{-2}.s^{-1}$)	Photosynthesis % inhibition
Control (no SNP)	14.0	00.0
0.5 mM SNP	9.2	34.0
1 mM SNP	5.0	64.0
5 mM SNP	2.5	82.0

15 leaf discs were kept in Petri dish containing 6 ml of distilled water as control, or 6 ml of different dilutions of sodium nitroprusside and incubated under light (600 $\mu mol.M^{-2}.S^{-1}$) for 1 h.

Results

Effects of SNP on photosynthesis and glucose level

To investigate the effect of NO on photosynthesis, pea leaf discs were treated with varying sodium nitroprusside concentration (0.5 to 5 mM) under light 600 $\mu mol\ m^{-2}.\ s^{-1}$ for 3 h. Data presented in Table 1 shows that the photosynthetic capacity of the pea leaf discs rapidly diminish in accordance to the varying concentrations of the SNP. SNP affect the photosynthesis in dose dependent manner. Figure 1 depicts the changes in the net photosynthesis of the leaf discs following 1 mM SNP treatment. Photosynthesis in leaf discs was inhibited 88% as compared to the control after 3 h of 1 mM SNP treatment. Although the glucose level in non treated leaf discs after 1 h of incubation under light (600 $\mu mol\ m^{-2}.\ s^{-1}$) decreases substantially thereafter maintained at constant level, the glucose level of 1 mM SNP treated leaf discs were always found to be slightly (24-27%) lower than the glucose level of non treated leaf discs (Fig. 2). In the present study only 0.5 and 1.0 mM SNP concentrations were used because these concentrations of SNP was found to be non effective in terms of inducing cell death in leaf discs during chase period 3 h. Cell viability was tested by Evans blue staining of the pea leaf epidermis (Fig. 3).

Effects of SNP on anthocyanin and flavonol glycosides

The levels of anthocyanin and flavonol glycoside measured in non treated pea leaf discs were 13.2 and 175.0 $nmolleaf^{-1}$ respectively. As shown in Figure 4 A and B, the levels of both anthocyanin and flavonol glycosides (nmol $leaf^{-1}$) reached at peak after 2 h of 1 mM SNP treatment then immediately declined below the control (13.2 and 175.0 $nmolleaf^{-1}$) level at 3 h. During treatment period, the level of anthocyanin increased by 72% while that of flavonol glycosides by 53% from 1 to 2 h and then declined approximately by 21% after 3 h as compared to the control. The anthocyanin content (nmol $leaf^{-1}$) of the non treated leaf discs (incubated under light 600 $\mu mol\ M^{-2}.S^{-1}$ alone) used as control increases from 18.4 to 31.6 (representing 72% increase) while flavonol glycosides from 222.5 to 257 (representing only 15% increase) during the period 1 to 3 h. Therefore, light (600 $\mu mol\ M^{-2}.S^{-1}$) alone caused marked increase in the level of anthocyanin, however it adds only 15% to the level of flavonol glycosides. SNP (0.5 mM), however, not at all affected the anthocyanin content but caused a reasonable decrease (~20%) in the amount of flavonol glycoside as compared to the control during 3 h incubation period.

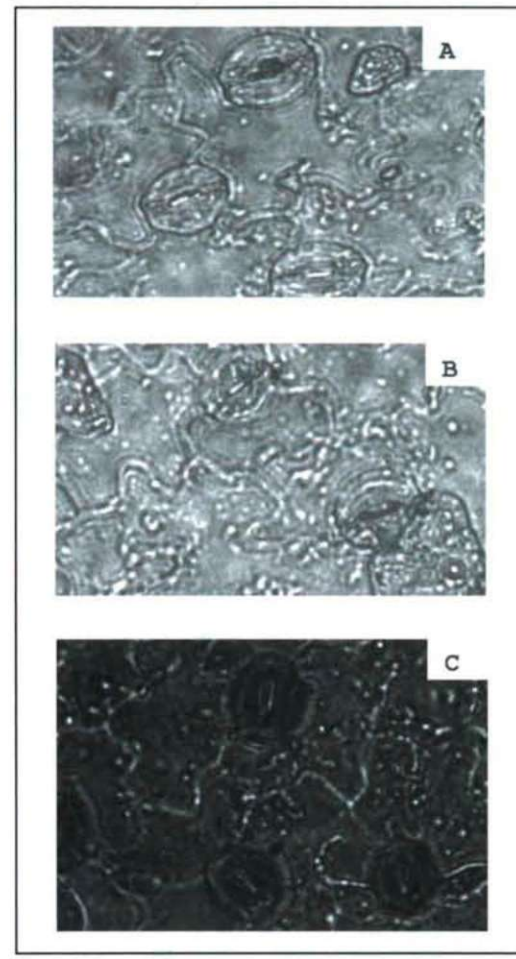

Figure 3. Cell viability Test by Evans blue (EVB) staining. None of the cell was stained when the pea epidermal strips were treated in water (as control). Also, no cell death was visible in 1 mM SNP treated leaves [A], however, the number of EVB stained cell (dead cells) significantly increased after treatment with 5 mM SNP for 3 h [C].

Discussion

Here in the present study effects SNP has been investigated on anthocyanin and flavonol glycosides accumulation in pea (*Pisum sativum* L.) cv. Arkel leaf discs to reveal the role of

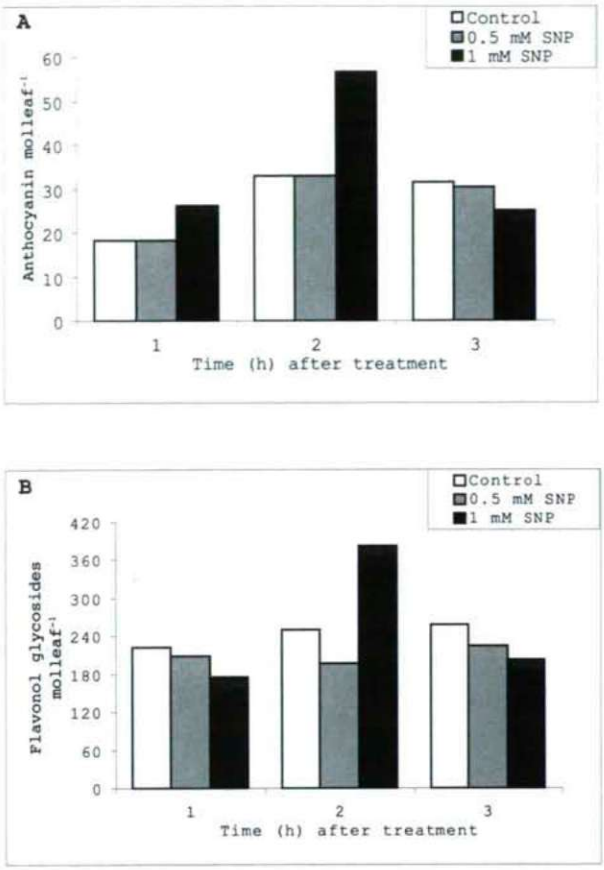

Figure 4. Changes in the anthocyanin [A] and flavonol glycosides [B] content of pea (*Pisum sativum* L.) cv. Arkel leaves after 1 mM SNP treatment. 15 leaf discs were kept in Petri dish containing 6 ml of distilled water as control (no SNP), or 6 ml of 1 mM sodium nitroprusside and incubated under light (600 µmol m^{-2}. s^{-1}) for 3 h. Data presented in the figure are the average of the three independent experiments.

NO in secondary metabolism. Pea leaves being of relatively simple construction, consisting of mono-cellular epidermal layers bounding a mono-cellular layer of tightly packed palisade cells and a 3 to 5 cell layer deep spongy mesophyll were chosen for the study (Hrazdina et al. 1982).

Several previous studies has proven the role of NO as signaling molecule in several physiological processes though could not expose exact mechanism of NO action. Although nitric oxide (NO) has crucial role in fundamental processes such as growth and development, its role in secondary metabolic processes is still poorly understood. In general, sodium nitroprusside (SNP) is used to investigate the effects of NO in plants (Delledonne et al. 2001; dePinto et al. 2002; Graziano et al. 2002; Correa-Aragunde et al. 2004). SNP releases NO in the form of nitrosonium cation (NO^+) rather than its free radical (Murgia et al. 2004) has bee described as potent inhibitors photosynthesis in different plants previously (Yamasaki, 2000; Takahashi and Yamasaki, 2002; Lum et al. 2005). Therefore, inhibition in photosynthesis observed in SNP treated pea leaf disc was expected due to release of NO from SNP. However, still the mechanism of action of NO remained poorly understood. Even if so, direct effects of NO on photosynthetic enzymes, on the photosynthetic electron transport chain and on chloroplast may result in inhibition of photosynthesis (Lum et al. 2005) or might be due to its action on photosystem-II (PSII) (Sanakis et al. 1997). Previously, Lum et al. (2005) have studied the effects of SNP on glucose metabolism in mung bean leaves. In mung bean leaves, glucose metabolism was highly affected after SNP treatment and the glucose level was almost depleted after 6 h of treatment. In the present study, no significant alteration in glucose metabolism was observed in SNP treated pea leaf discs. Hence the role of NO in glucose metabolism could not become very clear as it was reported in mung bean leaves (Lum et al. 2005).

As shown in Figure 4 (A and B), SNP treatment of pea leaf discs resulted in an overall (21%) decrease in anthocyanin and flavonol glycoside content after 3h. The depletion in amount of these two plant natural products in SNP treated leaf discs could be *via* photosynthesis which has been completely inhibited by NO released from SNP thereby stopped the energy supply for biosynthesis of anthocyanin and flavonol glycosides. However, a substantial increase in their levels at 2 h is surprising and it seems to be due to rapid metabolism of glucose providing metabolic precursor and energy for their rapid biosynthesis or may be due stimulatory effects of NO most probably via its effect on the expression phenylalanine ammonia lyase (PAL), a key enzyme in anthocyanin biosynthetic pathway.

On the other hand, anthocyanin content of pea leaf discs remarkably (73%) increased compared to a reasonable (15%) increase in flavonol glycosides following their incubation under light (600 µmol m^{-2}. s^{-1}) alone. The results suggest that in pea leaves, light would have induced the anthocyanin biosynthetic genes that resulted in higher accumulation of anthocyanins. Very recently, Takaos et al. (2006) have studied the light induced expression of *MYB* genes that regulate anthocyanin biosynthesis in red apple. Previously, Hrazdina et al. (1982) studied the distribution of biosynthetic enzymes of anthocyanins and flavonol glycosides in pea leaves. There study revealed that anthocyanins and flavonol glycosides in pea leaves are accumulated in epidermal vacuoles, while their biosynthetic enzymes are present in both epidermal and parenchyma tissues suggesting that there is close coordination between cells and tissues at the level of the precursors and end products.

In conclusion, the study revealed that SNP affects the level of anthocyanin and flavonol glycosides most probably *via* its inhibitory effects on photosynthesis in pea leaves. Also the study has revealed the role of NO in glucose metabolism in pea leaves. However, study of the effects of NO on glucose metabolism is under progress.

Acknowledgement

Author is grateful to the three prestigious academies, Indian Academy of Sciences, Bangalore, Indian National Science Academy, New Delhi, and The National Academy of Science, Allahabad for providing me Summer Research Fellowship-2008. Also I am very much thankful to the chancellor, Vellore Institute of Technology University, Vellore, for deputing me to carry out the present work.

References

Correa-Aragunde N, Graziano M, Lamattina L (2004) Nitric oxide plays a central role in determining lateral root development in tomato. Planta 218:900-906.

de Pinto MC, Tommasi F, De Gara L (2002) Changes in the antioxidant systems as part of the signaling pathway responsible for the programmed cell death activated by nitric oxide and reactive oxygen species in tobacco Bright-Yellow 2 cells. Plant Physiol 130:698-708.

Delledonne M, Zeier J, Marocco A, Lamb C (2001) Signal interactions between nitric oxide and reactive oxygen intermediates in the plant hypersensitive disease resistance response. Proc Natl Acad Sci USA 98:13454-13459.

Erdei L and Kolbert Zs (2008) Nitric oxide as a potent signalling molecule in plants. Acta Biol Szeged 52:1-5.

Feild TS, Lee DW, Holbrook NM (2001) Why leaves turn red in autumn: the role of anthocyanins in senescing leaves of red-osier dogwood. Plant Physiol 127:566-574.

Furuya M, Galston AW (1965) Flavonoid complexes in *Pisum sativum*. Nature and distribution of the major component. Phytochemistry 4:285-296.

Graziano M, Beligni MV, Lamattina L (2002) Nitric oxide improves internal iron availability in plants. Plant Physiol 130: 1852-1859.

Hill AC, Bennett JH (1970) Inhibition of apparent photosynthesis by nitrogen oxides. Atmos Environ 4:341-348.

Hrazdina G, Marx GA, Hoch HC (1982) Distribution of Secondary Plant Metabolites and Their Biosynthetic Enzymes in Pea (*Pisum sativum* L.) Leaves: Anthocyanins and Flavonol Glycosides. Plant Physiol 70:745-748.

Kolbert Zs, Bartha B, Erdei L (2008a) Exogenous auxin-induced NO synthesis is nitrate reductase-associated in *Arabidopsis thaliana* root primordial. J Plant Physiol 165:967-975.

Kolbert Zs, Bartha B, Erdei L (2008b) Osmotic stress- and indole-3-butyric acid -induced NO generations are partially distinct processes in root growth and development in *Pisum sativum* L. Physiol Plant 133:406-416.

Lamattina L, Garcia-Mata C, Graziano M, Pagnussat G (2003) Nitric oxide: the versatility of an extensive signal molecule. Annu Rev Plant Biol 54:109-136.

Lum HK, Lee CH, Butt YK, Lo SC (2005) Sodium nitroprusside affects the level of photosynthetic enzymes and glucose metabolism in *Phaseolus. aureus* (mung bean). Nitric Oxide 12:220-230.

Murgia I, de Pinto MC, Delledonne M, Soave C, De Gara L (2004) Comparative effects of various nitric oxide donors on ferritin regulation programmed cell death, and cell redox state in plant cells. J Plant Physiol 161:777-783.

Neil SJ, Desikan R, Hancock JT (2003) Nitric oxide signalling in plants. New Phytologist 159:11-35.

Regan BC, Julliot C, Simmen B, Vienot F, Charles-Dominique P, Mollon JD (2001) Fruits, foliage and the evolution of primate colour vision. Philos Trans R Soc Lond B Biol Sci 356:229-283.

Sanakis Y, Goussias C, Mason RP, Petrouleas V (1997) NO interacts with the tyrosine radical YD of photosystem II to form an iminoxyl radical. Biochemistry 36:1411-1417.

Schaefer HM, Schaefer V, Levey DJ (2004) How plant-animal interactions signal new insights in communication. Trends Ecol Evol 19:577-584.

Statham CM, Crowden RK, Harborne JB (1972) Biochemical genetics of pigmentation in *Pisum sativum*. Phytochemistry 11:1083-1088.

Takahashi S, Yamasaki H (2002) Reversible inhibition of photophosphorylation in chloroplasts by nitric oxide. FEBS Lett 512:145-148.

Takos AM, Jaffé FW, Jacob SR, Bogs J, Robinson SP, Walker AR (2006) Light-induced expression of a MYB gene regulates anthocyanin biosynthesis in red apples. Plant Physiol 142:1216-1232.

Wang JW, Wu JY (2005) Nitric Oxide is Involved in Methyl Jasmonate-induced Defense Responses and Secondary Metabolism Activities of *Taxus* Cells. Plant Cell Physiol 46:923-930.

Wendehenne D, Durner J, Klessig DF (2004) Nitric oxide: a new player in plant signalling and defense responses. Curr Opin Plant Biol 7:449-455.

Wodala B, Deák Zs, Vass I, Erdei L, Altorjay I, Horváth F (2008) In vivo target sites of nitric oxide in photosynthetic electron transport as studied by chlorophyll fluorescence in ea leaves. Plant Physiol 146:1920-1927.

Xu M, Dong J, Zhu M (2004) Effect of nitric oxide on catharanthine production and growth of *Catharanthus roseus* suspension cells. Biotech Bioengg 89:367-371.

Yamasaki H (2000) Nitrite-dependent nitric oxide production pathway: implications for involvement of active nitrogen species in photoinhibition in *vivo*. Philos Trans R Soc Lond B Biol Sci 355:1477-1488.

Zheng LP, Guo YT, Wang JW, Tan RX (2008) Nitric Oxide Potentiates Oligosaccharide-induced Artemisinin Production in *Artemisia annua* Hairy Roots. J Integrative Plant Biol 50:49-55.

Volume 52(2):307-311, 2008
Acta Biologica Szegediensis
http://www.sci.u-szeged.hu/ABS

ARTICLE

RAPD analysis of somaclonal variation in banana (*Musa acuminate* L.) cultivar Valery

Masoud Sheidai[1]*, Heywa Aminpoor[1], Zahra Noormohammadi[1], Farah Farahani[2]

[1]Shahid Beheshti University G. C., Faculty of Biological Sciences, Tehran, Iran, [2]Department of Biology, Islamic Azad University, Quem Branch, Quem, Iran

ABSTRACT Thirty decamer RAPD primers were used to study somaclonal variation among the parental plants as well as regenerated plants of the first, third, fifth, seventh and ninth sub-cultures. Eighteen out of thirty primers produced 289 bands in all the genotypes studied. Hundred and forty-two bands (48.95%) were common in the parental genotype and the regenerated plants while 147 bands were polymorph (51.40%). Among the primers used, OPI-07 produced the highest number of bands (24) while primers OPH-16 produced the lowest number (5). In total 74 specific bands were observed in the parental genotype and the regenerated plants of the sub-cultures. The presence of specific band/loci in the parental plants and loss of it in the regenerated plants of different sub-cultures indicates the loss of certain loci during tissue culture due to somaclonal variation. Such specific loci are of high importance in the genetic identification of the genotypes or somaclones from each other. Grouping of the parental cultivar and their sub-cultures regenerated plants indicate the genetic distinctness of the genotypes studied as they are placed in different clusters/groups far from each other. It also seems that the genetic variations induced in the regenerated plants increase with the time-period of the sub-culture.
Acta Biol Szeged 52(2):307-311 (2008)

KEY WORDS

banana
somaclonal variation
RAPD

Banana (*Musa acuminate* L.) with its different cultivars is cultivated in many tropical and semi-tropical countries and is considered a major staple food as well as an export commodity. Bananas are propagated vegetatively through suckers. Since most of the edible bananas are triploid and are nearly sterile and parthenocarpic, using conventional breeding methods for their improvement are difficult and cumbersome. Different approaches including mutation breeding and biotechnological methods have been applied to improve banana cultivars (Banerjee and De Langhe 1985; Wong 1986; Novak et al. 1989; Suprasanna et al. 2001, 2008).

One of the sources for inducing genetic variability in crop plants including banana is somaclonal variation. Plant tissue culture leading to somaclonal variation has been considered as a rapid and reliable approach for improvement of plants as the generated variation can be used either directly or indirectly in a breeding program aimed at crop improvement (Jain 2000) and has been used in banana cultivars to obtain superior quality banana clones (Maria and Garcia 2000; Asif and Mak 2004; Hwang and Ko 2004).

Somaclonal variation is used to describe the occurrence of genetic variants derived from *in vitro* procedures; it is also called tissue or culture-induced variation (Soniya et al. 2001). Such variation arises in tissue culture as a manifestation of epigenetic influence or a change in the genome of differentiating vegetative cells induced by tissue culture and is expected to generate stable plants carrying interesting heritable traits (Soniya et al. 2001). Four critical variables for somaclonal variation: genotype, explant origin, cultivation period and the cultural condition in which the culture is made.

The molecular markers are extensively used in germplasm characterization, fingerprinting, genetic analysis, linkage mapping, and molecular breeding. These markers are also used in identification of possible somaclonal variants at an early stage of development which is considered very useful for quality control in plant tissue culture, transgenic plant production and in the introduction of variants (Soniya et al. 2001). RAPD (Random Amplified Polymorphic DNA) analysis using PCR in association with short primers of arbitrary sequence has been demonstrated to be sensitive in detecting variation among individuals. The advantages of this technique are: a) a large number of samples can be quickly and economically analyzed using only micro-quantities of material; b) the DNA amplicons are independent from the ontogenetic expression; and c) many genomic regions can be sampled with a potentially unlimited number of markers (Soniya et al. 2001).

Among molecular markers, RAPD markers are used widely in studying the genetic diversity of somaclonal variations in various plant species (Damasco et al. 1996, 1998; Soniya et al. 2001) including banana (Hernandez et al. 2007). Damasco

Accepted Oct 8, 2008
*Corresponding author. E-mail: msheidai@yahoo.com

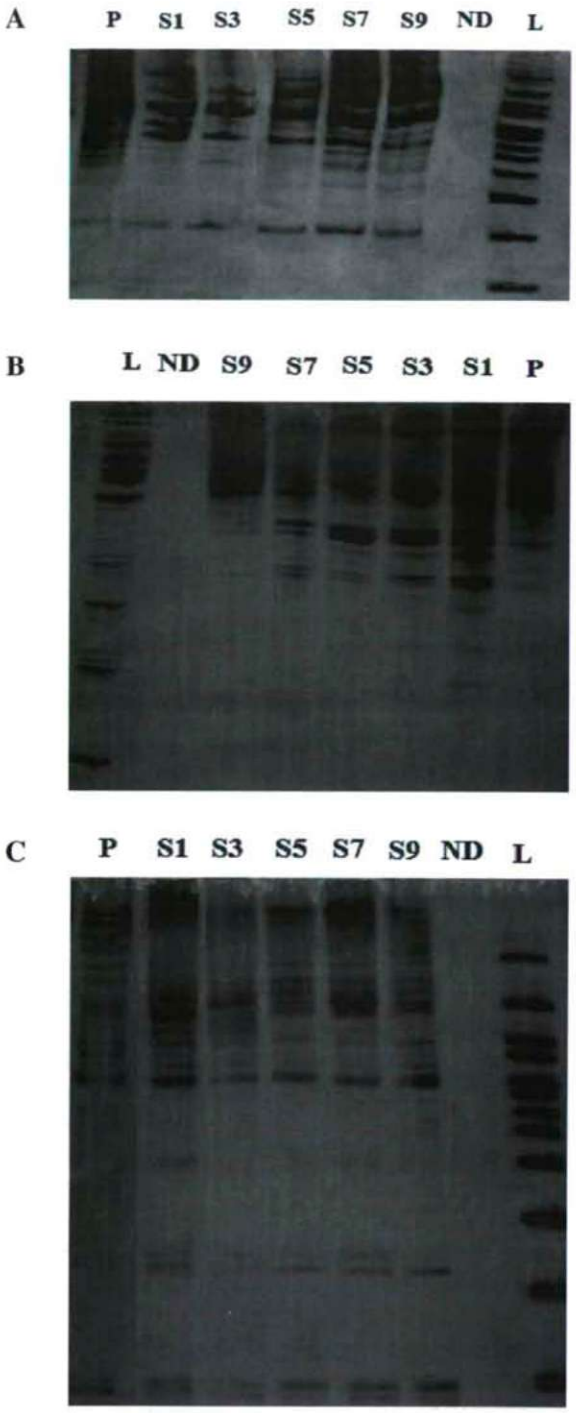

Figure 1. RAPD profile of primers OPI-07 (A), OPR-01 (B). and OPH-16 (C). Abbreviations: P = parental plants, S1, S3, S5, s7 and s9 = regenerated plants of the first, third, fifth, seventh and ninth sub-cultures respectively, ND = No DNA and L = 100 bp molecular ladder.

et al. (1996) compared normal and dwarfs banana and found a single RAPD band (OPJ-04 marker) in the normal but not in dwarf types. This was subsequently characterized into a SCAR (sequence characterized amplified region) for use as a PCR based detection system for dwarf types (Damasco et al. 1998). The present study reports the use of RAPD markers in studying the somaclonal variants obtained from tissue culture of banana cultivar Valery for the first time.

Materials and Methods

Tissue culture

Meristem-tip cultures of banana (*Musa acuminate* L.) cultivar Valery were derived from shoot apexes. Explants (ca. 10 x 10 x 6 mm) obtained from decapitated shoot apexes of suckers were surface sterilized by 70% ethanol for 20 seconds, then incubated in a 5% solution of sodium hypochloride for 20 min., followed by three rinses in sterile distilled water. The effects of cytokinins [Benzylaminopurine (BAP), kinetin (KIN) and N- phenyl – N´- 1,2,3 – thiadiazol 5-yl urea (TDZ)] combined with auxin [Indoleacetic acid (IAA)] were evaluated on basal Murashige and Skoog (MS, 11) medium. The pH was adjusted to 5.7 with 1 M NaoH before agar and charcoal was added. The cultures were maintained at 25°C with 16 h photoperiod at a photosynthetic photon flux density of 120 µmol /m ²/ s. Sub-culturing was carried out at 45-day intervals. All treatments were performed on three replications of 10 explants in experiments employing a completely randomized design. The data on shoot number, shoot length and fresh weight of shoot were analyzed by ANOVA followed by Duncan's test (15).

DNA extraction and PCR amplification

Fresh leaves of five randomly selected plants were bulked for DNA extraction. DNA was extracted from the leaves of the parental genotype and regenerated plants of the first, third, fifth, seventh and ninth sub-cultures by using acetyltrimethyl ammonium bromide (CTAB)-based procedure. For RAPD analysis, the PCR reaction mixture consisted of 1 ng template DNA, 1 x PCR buffer (10 mM Tris-HCJ pH 8.8, 250 mM KC12), 200 µM dNTPs, 0.80 µm 10-base random primers and 1 unit of Taq polymerase, in a total volume of 25 µl. DNA amplification was performed on a palm cycler GP-00 1 (Corbet, Australia). Template DNA was initially denatured at 94°C for 3 min, followed by 35 cycles of PCR amplification under the following parameters: denaturation for 1 min at 92°C, primer annealing for 1 min at 36°C and primer extension for 2 min at 72°C. A final incubation for 10 min at 72°C was performed to ensure that the primer extension reaction proceeded to completion.

Electrophoresis

The PCR amplified products were separated by electrophoresis on a 1.5% agarose gels using 0.5 X TBE buffer (44.5 mM Tris/Borate, 0.5 mM EDTA, pH 8) or 12% polyacrylamide gels. The gels were stained with ethidium bromide and visu-

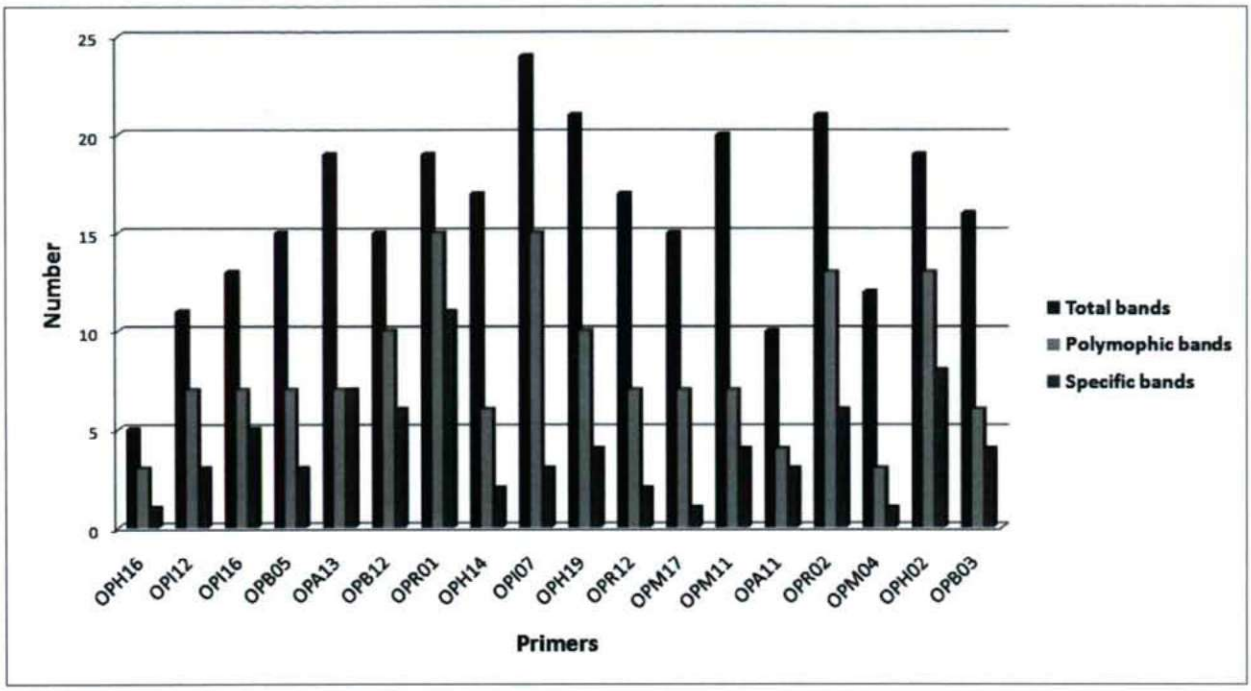

Figure 2. The number of total, polymorphic and specific bands produced by different primers in all parental and regenerated plants of different sub-cultures.

alized under UV light or silver stained for added sensitivity. RAPD markers were used named by primer origin, followed with the primer number and the size of amplified products in base pairs. Thirty random primers of Operon technology (Alameda, Canada) were used (Table 1).

The experiment was repeated for 3 times and reproducible RAPD bands were used for further analysis. The bands obtained were treated as binary characters and coded accordingly (presence =1, absence = 0). Jaccard similarity was determined among the genotypes studied to be used in clustering. The genotypes showing similarity in their RAPD characteristics were grouped by using UPGMA (Unweighted Paired Group with Arithmetic Average) and Neighbor Joining (NJ) methods as well as ordination based on principal coordinate (PCO) and principal components (PCA) analysis (Sheidai et al. 2008). NTSYS Ver. 2.02 (1998) and DARwin ver. 5 (2008) was used for statistical analyses.

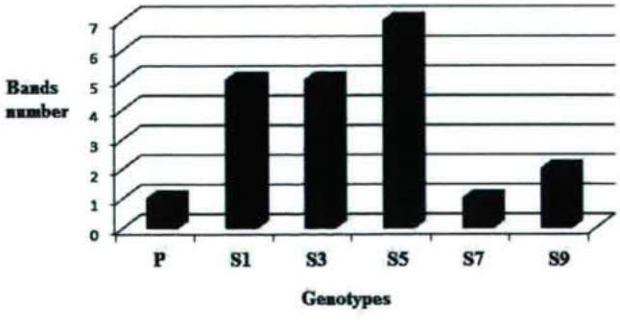

Figure 3. The number of specific bands produced by all primers in the genotypes studied.

Results

Tissue culture

TDZ promotes a higher number of shoots per explant compared to KIN, while, BAP shows intermediary results. However, the shoots developed in the presence of TDZ or KIN did not survive upon transferring. Moreover, in the absence of cytokinins, the entire shoot died within 2 weeks.

The presence of TDZ along with BAP and KIN significantly ($p< 0/05$) reduces the shoot elongation and shoots fresh weight which is in agreement with the results obtained in the order banana cultivars (Alvard et al. 1992). The number of shoots significantly increased with increasing concentration of TDZ in the media, but the elongation and fresh weight of shoots decreased significantly. The association of 0.15 mg/L TDZ and 2 mg/L IAA positively affected the multiplication of the banana cultivars, possibly due to its strong cytokinin activity (Nowak and Miczynski 2002).

At 2 mg/L concentration of BAP, the length of shoots and fresh weight of plantlets per explant was significantly increased compared to that of TDZ and KIN. The length of

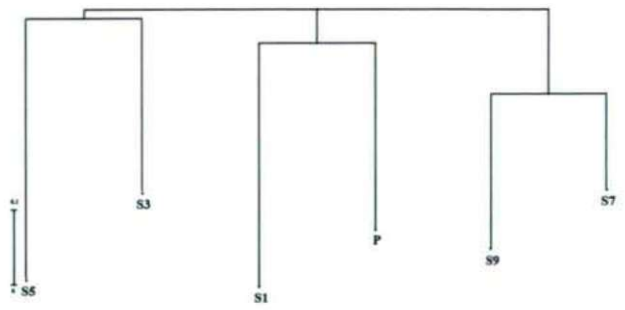

Figure 4. NJ clustering of the banana genotypes. Abbreviations: P = parental plants, S1, S, S5, S7 and S9 = regenerated plants of the first, third, fifth, seventh and ninth sub-cultures respectively.

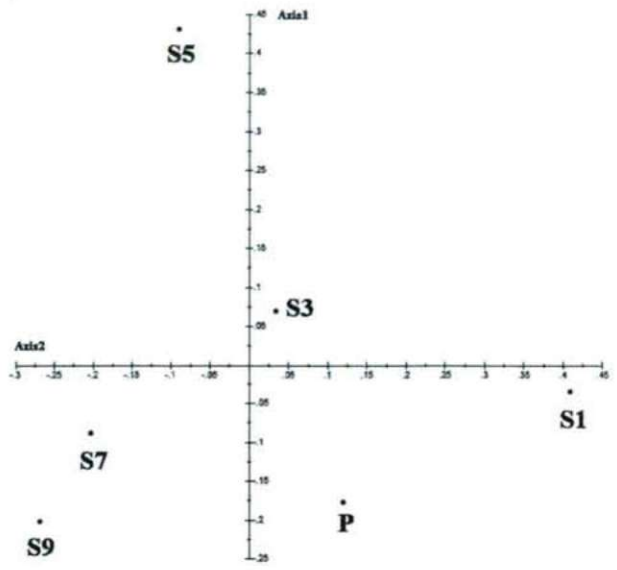

Figure 5. PCA ordination of the banana genotypes. Abbreviations: P = parental plants, S1, S, S5, S7 and S9 = regenerated plants of the first, third, fifth, seventh and ninth sub-cultures respectively.

shoots and fresh weight significantly increased with increasing concentration of BAP in the media. With 2 mg/L BAP and 1.5 mg/L KIN, a significant elongation of shoots as well as significant reduction of shoot proliferation and fresh weight occurred. At high concentration of BAP and KIN the number of shoots was significantly reduced. The final medium adopted included the salt formulation of Murashige and Skoog, 30 g/L of sucrose, N-phenyl-N–1, 2, 3- thiadiazol 5-yl Urea (0.5 mg/L) and Indoleacetic acid (2 mg/L). Under these conditions, a multiplication rate of 25 plantlets per explant was obtained in 120 days.

RAPD analysis

Eighteen RAPD primers out of 30, produced 289 bands (Figs. 1-3) in all the genotypes studied, out which, 142 bands (48.95%) were common in the parental genotypes and the regenerated plants of the sub-cultures while, 147 bands were polymorph (51.40%). Among the primers used, OPI-07 produced the highest number of bands (24) while primers OPH-16 produced the lowest number (5). The highest number of polymorphic bands (15) was observed in OPR-01 (84.20%) while the lowest number (3 bands) was observed in OPM-04 (25%).

Some of the RAPD bands/loci were present in all the genotypes except one, for example the band 1 of the primer OPH-16 was absent only in the regenerated plants of the fifth sub-culture, while bands 5, 8 and 9 of the primer OPI12 was absent only in the regenerated plants of the third sub-culture.

Some bands occurred only in one genotype and was absent in the others. The regenerated plants of the fifth sub-culture showed the highest number (7) of specific bands, while parental plants and the regenerated plants of the seventh sub-culture showed the lowest number (1) of the same. Band 1 of the primer OPI-16 occurred only in the regenerated plants of the first sub-culture, band 2 of this primer was specific for the regenerated plants of the fifth sub-culture while bands 4, 6 and 7 were specific for the regenerated plants of the first sub-culture. Similarly other primers also produced specific bands in different genotypes studied. Both clustering and ordination methods of the genotypes produced similar results separating the parental and regenerated plants in different clusters or groups (Figs. 4, 5).

Discussion

Variations observed in total number of RAPD bands as well as the number of specific bands among the parental plants and regenerated plants of different sub-cultures indicate genetic differences of the genotypes due to tissue culture and somaclonal variation induced. The presence of specific band/loci in the parental plants and loss of it in the regenerated plants of different sub-cultures indicates the loss of certain loci during tissue culture due to somaclonal variation, while the occurrence of specific bands/loci in the regenerated plants of different sub-cultures and their absence in mother plants may indicate the occurrence of genetic changes leading to formation of new binding sites in these plants. Such specific loci are of high importance in the genetic identification of the genotypes or somaclones from each other.

Since, even single base change at the primer annealing site is manifested as appearance or disappearance of RAPD bands, it could be suggested that tissue culture conditions have induced varied amount of genetic changes in different regenerated plants. Some of the molecular changes appeared identical in regenerated plants of different sub-cultures and appeared as non-parental bands. According to Soniya et al.

(2001), the reason for such commonness of genetic variation is that these plants are all derived from the same callus and the variations observed in the RAPD pattern may be due to different causes including loss/ gain of a primer annealing, due to point mutations or by the insertion or deletion of sequence or transposable elements (Peschke et al. 1991).

The occurrence of specific bands/loci in the regenerated plants of different sub-cultures shows genetic distinctness of these plants (somaclones) and the use of tissue culture in causing genetic variation in banana.

Grouping of the parental cultivar and their sub-cultures regenerated plants indicate the genetic distinctness of the genotypes studied as they are placed in different clusters/ groups far from each other (Figs. 4, 5). It also seems that the genetic variations induced in the regenerated plants increase with the time-period of the sub-culture. For example, the regenerated plants of the first sub-culture show comparatively lower degree of genetic difference from the parental plants as they are placed in the clusters much closer to each other compared to the regenerated plants of the latter sub-cultures. The findings here are in line with the earlier reports on application of RAPD in describing genetic polymorphisms among regenerated plants in several other plants including. *Apium* and *Prunus* species (Soniya et al. 2001) as well as in cotton (Sheidai et al. 2008).

Explant source is also considered as one of the critical variable for somaclonal variation. Since explants may present dissimilar regeneration rates, selection procedures can differ among different explants types. For example, plants regenerated from chrysanthemum petal epidermis-induced calli showed greater somaclonal variation than those from apex-induced calli (De Jong and Custers 1986). Therefore it may be suggested that different sources of explants may be tried in banana and compare the level of genetic variation obtained.

In conclusion, the results of present study show the occurrence of somaclonal variation due to different sub-culturing of banana cultivar Valery, and that with increase in time period of sub-culturing, possibly more genetic variation may occur. The study also shows the use of RAPD molecular markers in revealing somaclonal variation in banana and that the occurrence of specific bands/loci in the parental plants as well as in the regenerated plants of different sub-cultures may be used in the genetic identification of the genotypes or somaclones from each other.

References

Asif MJ, Mak C, Othman RY (2004) Study of resistance of *Musa acuminata* to *Fusarium oxysporum* using RAPD markers. Biol. Plants 48:93-99.

Alvard D, Cote F, Tiesson C (1992) Comparison of methods of liquid medium culture of banana micropropagation. Plant Cell Tissue Org Cul 32:55-60.

Banerjee N, De Langhe E (1985).A tissue culture technique for rapid clonal propagation and storage under minimal growth conditions of Musa (banana and plantain). Plant Cell Rep 4:351-354.

Damasco OP, Graham GC, Henry RJ, Adkins SW, Smith MK (1996) Random amplified polymorphic DNA (RAPD) detection of dwarf off types in micropropagated Cavendish bananas. Acta Hort 461:157-164.

Damasco OP, Smith MK, Adkins SW, Godwin ID (1998) Use of SCAR based marker for early detection of dwarf off-types in micropropagated 'Cavendish' bananas. Acta Hort 461:157-164.

De Jong J, Custers JBM (1986) Induced changes and flowering of Chrysanthemum after irradiation and *in vitro* culture of pedicels and petals epidermis. Euphytica 35:137-148.

Hernandez R, Rodriguez R, Ramirez T, Canal MJ, Guillen D, Noceda C, Escalona M, Corujo M, Ventura J (2007) Genetic and morphoagronomic characterization of plantain variants of *Musa* AAB clone 'CEMSA ¾ J. Food Agri Envir 5(1):220-223.

Hwang SC, Ko WH (2004) Cavendish banana cultivars resistant to Fusarium wilt acquired through somaclonal variation in Taiwan. Plant Diseases 88:580-588.

Jain SM (2000) Tissue culture induced variation in crop improvement. Euphytica 118:153-166.

Maria DCV, Garcia ED (2000) Analysis of a *Musa* spp. somaclonal variant resistant to yellow sigatoka. Plant Mol Biol Rep 18:23-31.

Murashige T, Skoog F (1962) A revised medium for rapid growth and bioassays with tobacco tissue cultures. Physi Planta 15:473-497.

Novak FJ, Afza R, Vanduren M, Perea-Dollas M, Conger BV, Xiaolang T (1989) Somatic embryogenesis and plant regeneration in suspension cultures of dessert (AA and AAA) and cooking (ABB) (*Musa* spp.). Biotech 7:154-159.

Nowak B, Miczynski K (2002) The course and efficiency of organogenesis on leaf explants of Plum Wegierka Zwykla (*Prunus domestica* L.) induced by cytokinins. Electronical Journal of Polish Agricultural Universities, Biotech 5:120-124.

Peschke VM, Philip RL, Gengenbach BG (1991) Genetic and molecular analysis of tissue-culture- derived Ac elements. Theor Appl Genet 82: 121-129.

Sheidai M, Yahyazadeh., Farahanei F., Noormohammadi Z (2008) Genetic and morphological variations induced by tissue culture in tetraploid cotton (*Gossypium hirsutum* L.) Acta Biol Szeged 52(1):33-38.

Soniya EV, Banerjee NS, Das MR (2001) Genetic analysis of somaclonal variation among callus-derived plants of tomato. Cur Sci 80:1213-1215.

Suprasanna P, Panis B, Sági L, Swennen R (2001) Establishment of embryogenic cell suspension cultures from Indian banana cultivars. 3rd and Final Research Coordination Meeting of the FAO/IAEA on Cellular biology of banana. KUL, Leuven, Belgium, September 24-26, pp. 9-10.

Suprasanna P, Sidha M, Ganapathi TR (2008) Characterization of radiation induced and tissue culture derived dwarf types in banana by using a SCAR marker. Aust J Crop Sci 1(1):47-52.

Wong WC (1986) In vitro propagation of banana (*Musa* spp.): Initiation, proliferation and development of shoot-tip cultures of defined media. Plant Cell Tissue and Org Cul 6:159-166.

Volume 52(2):313-319, 2008
Acta Biologica Szegediensis
http://www.sci.u-szeged.hu/ABS

ARTICLE

Cytogenetic variability and new chromosome number reports in *Silene* L. species (Sect. Lasiostemones, Caryophyllaceae)

Masoud Sheidai*, Mehrnoosh Nikoo, Abbaas Gholipour

Faculty of Biological Sciences, GC, Shahid Beheshti University, Tehran, Iran

ABSTRACT Karyotype and meiotic studies were performed in 19 populations of five *Silene* species of the section *Lasiostemones* Boiss., growing in Iran. The species of *S. longipetala*, *S. tenella*, *S. claviformis* and *S. Marschallii* possessed 2n = 2x = 24 chromosome number, while *S. propinqua* populations were diploid and tetraploid with two different base number of x = 10 and 12 (2n = 4x = 40). The results obtained support the earlier report on *S. Marschallii* while the chromosome number of *S. longipetala*, *S. tenella*, *S. claviformis* and *S. propinqua* are new to science. The chromosomes were mainly metacentric and sub-metacentric. The species studied differed significantly in total size of the chromosomes, size of the short arms and the long arms, indicating the role of quantitative genomic changes in the *Silene* species diversification. They also differ in their karyotypic formulae indicating the occurrence of structural changes in their chromosomes. The *Silene* species were placed in 1A, 2A and 1B classes of Stebbins karyotype symmetry which are considered relatively primitive in this system. PCA ordination of the *Silene* species indicated karyotypic distinctness of the species studied. Meiotic analysis showed that Arak population of *S. Marschalii* forms quadrivalents due to the occurrence of heterozygote translocation between two pairs of chromosomes which in turn may increase the amount of genetic variability in the next generation. Unreduced pollen grains were formed in populations of *S. Marschalii* due to multipolar cell formation, while B-chromosomes were observed in some of the species studied.

Acta Biol Szeged 52(2):313-319 (2008)

KEY WORDS

cytogenetic
Iran
Lasiostemones
Silene

The genus *Silene* L. (Caryophyllaceae) is comprised of about 700 species which are distributed throughout the world. They are mostly hermaphrodite although a few species are diocious or gynodioceious (Bari 1973; Greuter 1995). *Silene* species are mostly distributed throughout the northern hemisphere, Europe, Asia and northern Africa. They are annual, biennial, or perennial herbs with the basic chromosome number *x* = (10) 12. The genus *Silene* includes several important weedy species, some very beautiful horticultural plants and some medicinal plants (Swank 1932; Vestal 1952; Oxelman and Lidén 1995).

Several cytogenetic studies have been performed on *Silene* from different parts of the world (Heaslip 1951; Bari 1973; Melzheimer 1978; Markova et al. 2006), while such studies are not available for the *Silene* species growing in Iran. About 110 *Silene* species grow in Iran out of which about 35 species are endemic with very limited geographical distribution (Melzheimer 1980).

Most of the *Silene* species are diploid having 2n = 2x = 24, or 2n = 2x = 20 (Bari 1973), *S. fortunei* is triploid (2n = 3x = 30, Heaslip 1951), some others are tetraploid (2n = 4x = 48) and hexaploid (2n = 6x = 72) and a few species show higher polyploidy level for e.g. 2n = *c.* 96, 120 and 192 (Bari 1973). Moreover 2n = 18 is reported for *S. conica* (Sopova and Sekovski 1982) as well as *S. lacera* (Gvinianidze and Avazneli 1982), 2n = 46 for *S. firma* (Zhang 1994), which make x= 9 and x = 23 along with x= 10 and 12, the known basic chromosome numbers for the *Silene*.

Chowdhuri (1957) placed the *Silene* species in 22 sections but recent molecular studies do not support such sectional classifications particularly for the endemic North American taxa (Oxelman et al. 1997, 2000; Burleigh and Holtsford 2003).

According to Flora Iranica (Melzheimer 1980) the section *Lasiostemones* (Boiss.) is comprised of 10 species, out of which 2 species are endemic. The members of the section *Lasiostemones* are caespitose mountainous plants with perfect flowers arranged in paniculate or racemose inflorescences, possessing usually glabrous calyx and hairy or densely ciliate filaments. The present study reports the karyotypic features of 15 populations of five *Silene* species belonging to the section *Lasiostemones* as well as meiotic analysis of 4 populations of two species growing in Iran for the first time.

Accepted Oct 20, 2008
*Corresponding author. E-mail: msheidai@yahoo.com

Table 1. Karyotypic features of the Silene species and population studied.

Sp	Locality	2n	Ploidy level	TL	L	S	L/S	X	TF	KF	A1	A2	ST
1-*Silene longipetala*	Ilam	24	2x	32.18	3.22	1.99	1.62	2.68	42	11m+1sm	0.25	0.14	1A
2-*S. tenella*	Gadook	24	2x	32.18	3.29	1.99	1.65	2.68	42	11m+1sm	0.24	0.14	1B
3- *S. tenella*	Sabalan	24	2x	32.42	3.60	1.70	2.12	2.70	42	12m	0.28	0.20	2A
4- *S. tenella*	Chashm	24	2x	37.10	3.75	2.24	1.67	3.08	42	11m+1sm	0.27	0.18	1A
5- *S. tenella*	Shahdej	24	2x	32.59	3.54	2.00	1.77	2.70	43	12m	0.23	0.15	1A
6-*S. tenella*	Neor	24	2x	26.33	2.53	1.47	1.72	2.19	42	12m	0.26	0.13	1A
7- *S. claviformis*	Soodkooh	24	2x	40.90	4.68	2.70	1.73	3.40	42	11m+1sm	0.31	0.16	1A
8- *S. claviformis*	Payesib	24	2x	40.77	4.48	2.73	1.64	3.39	39	8m+4sm	0.37	0.15	2A
9- *S. Marschallii*	Gadook	24	2x	35.80	3.66	2.35	1.56	2.98	43	12m	0.24	0.24	1A
10-*S. Marschallii*	Damavand	24	2x	38.17	4.28	2.33	1.84	3.10	40	11m+1sm	0.32	0.17	1A
11- *S. Marschallii*	Lavasanat	24	2x	47.26	4.76	2.97	1.60	3.90	39	11m+1sm	0.35	0.14	1A
12- *S. Marschallii*	Bakhtiari	24	2x	36.15	3.91	2.31	1.69	2.95	42	12m	0.26	0.14	1A
13- *S. Marschallii*	Tonekabon	24	2x	37.27	3.92	2.10	1.87	3.10	41	11m+1sm	0.29	0.19	1A
14-*S. Marschallii*	Manjil	24	2x	42.92	4.63	2.16	2.14	3.57	42	12m	0.25	0.19	1B
15- *S. propinqua*	Shajoo	48	4x	--	--	--	--	--	--	--	--	--	--

Abbreviations: TL = Total chromatin length (μm), L = Size of the longest chromosome pair (μm), S = Size of the shortest chromosome pair (μm), X = Mean chromatin length (μm),, TF = Total form percentage, KF = Karyotypic formulae, A1 & A2 = Romero-Zarco indices, ST = Stebbins symmetry class.

Materials and Methods

Plant material

Karyotype and meiotic studies were performed in fifteen populations of five *Silene* species of the section *Lasiostemones* Boiss., growing in Iran. The species studied are: 1- *Silene longipetala* Vent, 2- *S. tenella* C. A. Mey. (five populations), 3- *S. claviformis* (two populations), 4- *S. Marschallii* C. A. Mey. (eight populations), 5- *S. propinqua* SCHISCHK. (two populations). Meiotic studies could be performed in four populations of *S. Marschallii* and one population of *S. propinqua*. The voucher specimens are deposited in Herbarium of Shahid Beheshti University (HSBU).

Cytological studies

For karyotypic studies freshly grown root tips were collected from the seeds of at least ten randomly selected plants in each species, pretreated with 0.002 mol 8-hydroxyquinolin (1-2 hrs.). Squash technique was used for cytological studies and karyotypic details were studied in at least 5 well-prepared metaphase plates as reported earlier (Sheidai and Rashid 2007).

The chromosomes were identified according to Levan et al. (1964), karyotype symmetry was determined according to Stebbins (1971), while other karyotypic parameters like total form percentage (TF %), coefficient of variation (CV) of the chromosome size as well as A1 and A2 indices of Romero-Zarco (1986) were determined (Sheidai and Jalilian 2008).

Meiotic studies were performed on young flower buds collected using minimum 100 metaphase/ diakinesis pollen mother cells (PMCs) and 500 anaphase and telophase cells for data collection (Sheidai and Rashid 2007). Pollen satiability as a measure of fertility was determined by staining minimum 1000 pollen grains with 2% acetocarmine: 50% glycerin (1:1) for about ½ hr. Round. Complete pollens which were stained were taken as fertile, while incomplete, shrunken pollens with no stain were considered as infertile (Sheidai and Rashid 2007).

Statistical analyses

For karyotype analyses, in order to reveal significant difference, the analysis of variance (ANOVA) followed by the least significant difference test (LSD) were performed on the size of chromosomes, size of the long arms and size of the short arms as well as arms ratio among the species and populations studied (Sheidai and Jalilian 2008). Moreover, principal components analysis (PCA) was performed to identify the most variable karyotypic characters. Karyotypic distinctness of the species studied was checked by using ordination plot of principal components analysis (PCA) (Sheidai and Jalilian 2008).

For meiotic analyses, χ^2 test was performed to detect a significant difference in chiasma frequency and chromosome pairing as well as meiotic abnormalities (Sheidai and Rashid 2007). In order to detect significant difference between poten-

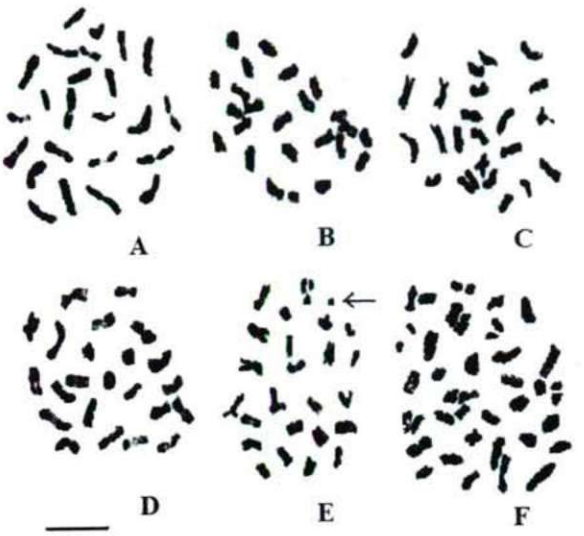

Figure 1. Representative metaphase somatic cells in the *Silene* species studied. A = *Silene Marschalii* Manjil population, B = *S. longipetala* Ilam population. C = *S. tenella* Shahdej population, D = *S. claviformis* Soodkooh population. E = *S. claviformis* Payesib population. F = *S. propinqua* Hamedan population.

tial unreduced pollen grains and the normal (reduced pollens), t-test was performed. Statistical analyses used SPSS ver. 9 (1998) and DARwin ver. 5.0.155 (2006) software.

Results and Discussion

Karyotypic features

Details of karyotypic analyses in the *Silene* species studied are presented in Table 1, Figs. 1-3. The species of *S. longipetala*, *S. tenella*, *S. claviformis* and *S. Marschallii* possessed 2n = 2x = 24 chromosome number, while *S. propinqua* was tetraploid with 2n = 4x = 48 chromosome.

The results obtained support the earlier report on *S. Marschallii* (Nersesian and Goukasian 1995), while the chromosome number of *S. longipetala*, *S. tenella*, *S. claviformis* and *S. propinqua* are new to science.

Among diploid species studied, the size of the longest chromosome varied from 2.53 µm in Neor population of *S. tenella* to 4.76 µm in Lavasanak population of *S. Marschallii* (Table 1), while the size of shortest chromosomes varied from 1.70 µm in Neor population of *S. tenella* to 2.73 µm in Payesib population of *S. claviformis*. The chromosomes were mainly metacentric (m) and sub-metacentric (sm; Table 1).

The highest haploid total chromatin length as well as mean chromosome length occurred in Lavasanat population of *S. Marschallii* (47.26 and 3.90 µm respectively), while the lowest value of the same occurred in Neor population (East Azarbayejan) of *S. tenella* (26.33 and 2.19 µm respectively).

The highest value of chromosomes size variation (CV= 24.00) occured in Gadook population of *S. Marschallii* while the lowest CV (13.00) occured in Neor population of *S. tenella*. The ANOVA and LSD tests revealed a significant differences ($p < 0.05$) for total size of the chromosomes, size of the short arms and the long arms among the species and populations studied, indicating the role of quantitative genomic changes in the *Silene* species diversification.

The *Silene* species studied differ in their karyotypic formulae indicating the occurrence of structural changes in their chromosomes (Table 1). Total form percentage (TF%) varied from 39 in Payesib population of *S. claviformis* to 43 in Shahdej population of *S. tenella* and Gadook population of *S. Marschallii* (Table 1); a higher value of TF% indicates the presence of relatively more symmetrical karyotype. The *Silene* species were placed in 1A, 2A and 1B classes of Stebbins karyotype symmetry which are considered relatively primitive in this system.

PCA analysis (data not given) shows that the first three components comprise about 79% of the total variation. In the first component with about 64% of total variance, the size of the short arms and long arms as well as total length of the chromosomes are the most variable characters and possessed the highest correlation with this component ($r > 0.80$). Moreover the ratio of long arm to short arm (L/S) of the chromosome pair number 6 possessed a high correlation ($r = 0.65$). In the second component with about 10% of total variance, L/S ratio of the chromosome pair numbers 11 and 12 possessed the highest correlation ($r > 0.50$). Therefore it seems that along with significant changes in the size of the chromosomes arms, the L/S ratio of 3 pairs of chromosomes (*i.e.* chromosome pair numbers 6, 11 and 12) have changed during the karyotype differentiation in the *Silene* species studied. Such a result supports the results of ANOVA stated earlier.

PCA ordination of the *Silene* species (Fig. 3) shows that almost the populations of each species form a distinct group. This is particularly true for *S. claviformis* as two populations of this species are placed separate from the other species. The populations of *S. Marschallii* are placed in the lower left corner of the PCA plot and the populations of *S. tenella* occupy the lower and upper part of the right side of the plot (Fig. 3), indicating karyotypic distinctness of the *Silene* species.

Chromosome pairing and segregation

Data with regard to chiasma frequency and distribution as well as chromosome pairing are provided in Table 2, Fig. 4. The populations of *S. Marschalii* showed 2n = 2x = 24 chromosome number while (Fig. 4A-D) while, Orumiyeh population of *S. propinqua* showed 2n = 40 chromosome number (Fig. 4E). Considering 2n = 4x = 48 chromosome number obtained in karyotypic study of *S. propinqua*, this species possesses two polyploidy levels of 2x and 4x and the occurrence two different basic number of x = 10 and 12. There are also other

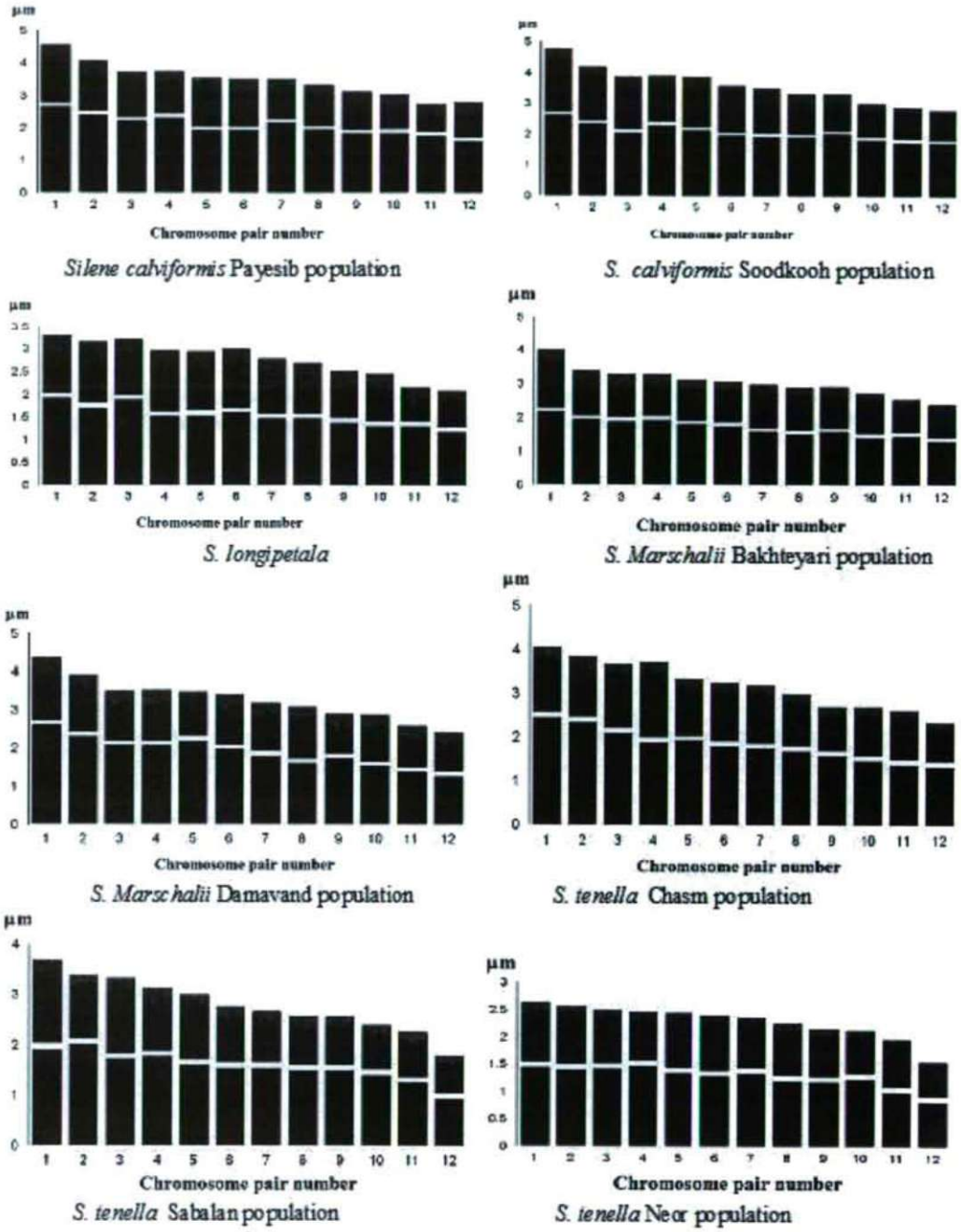

Figure 2. Representative idiograms of the *Silene* species.

Silene species with two or more different base numbers like *S. conica* with 2n = 2x = 18, 20 and 24 (Van Loon and Snelders 1979; Sopova and Sekovski 1982; Van Loon 1982) and *Silene lacera* with 2n = 2x = 18 and 24 (Gagnidze and Gviniashvili 1997; Gvinianidze and Avazneli 1982).

Among three populations of *S. Marschalii* studied, the highest value of total and intercalary chiasmata occurred in Arak population (22.50 and 3.43 respectively), while the lowest value of the same occurred in Dashtelar population (17.26 and 1.33). Arak population of *S. Marschalii* also possessed the highest mean value of ring bivalents (8.87), while Dashtelar population possessed the highest mean value of rod bivalents (5.41).

Although S. Marschalii populatins studied are diploid and are expected to form only bivalents in metaphse of meiosis-I, Arak population formed 1-2 quadrivalents (Table 2, Fig. 4D),

Table 2. Chiasma frequency and chromosomes pairing in *Silene* species studied.

Sp	Locality	2n	TX	IX	TOX	RB	ROD	I	IV
S. Marschallii	Dashtelar	24	15.83	1.33	17.26	6.00	5.41	1.16	0.00
S. Marschallii	Zanjan	24	19.33	1.33	20.66	8.33	3.20	0.93	0.00
S. Marschallii	Khansar	24	18.13	1.97	20.22	8.00	3.72	0.36	0.00
S. Marschallii	Arak	24	19.12	3.43	22.55	8.87	3.11	0.00	0.01
S. propinqua	Orumiyeh	40	26.66	4.83	31.49	13.64	6.14	0.33	0.02

Abbreviations: TX = Mean number of terminal chiasmata, IX = Mean intercalary chiasmata, TOX = Mean total chiasmata, RB = Mean number of ring bivalents, ROD = Mean number of rod bivalents, I = Mean number of univalents, IV = Mean number of quadrivalents.

Table 3. Meiotic abnormalities, pollen fertility and size of pollen grains in *Silene* species studied.

Sp	Locality	L1%	L2%	MST%	AST%	PF%	NP (μm)	2NP (μm)
S. Marschallii	Dashtelar	2.2	4.2	0.0	0.0	98.9	19.78	29.10
S. Marschallii	Khansar	5.0	6.0	0.0	4.0	98.0	27.80	48.28
S. Marschallii	Zanjan	3.0	0.0	5.0	5.0	98.0	20.10	30.75
S. propinqua	Orumiyeh	1.0	1.0	0.0	0.0	99.0	--	--

Abbreviations: L1 & L2 = Laggard chromosomes in anaphase-I & II, MST = Metaphase cells showing stickiness, AST = Anaphase cells showing stickiness, PF = Pollen fertility, NP = Mean value of the size of normal (reduced) pollen grains, 2NP = Mean value of the size of potential unreduced pollen grains.

indicating the occurrence of heterozygote translocations between two pairs of chromosomes. Such chromsomal structural changes may increase the amount of genetic variability in the gametes by forming new genetic linkage groups which may be used for adaptation to adverse environmental conditions.

Tetraploid population (Orumiyeh) of *S. propinqua* formed 1-2 quadrivalents (Table 2, Fig. 4E) as expected which may be to its autotetraploid nature. χ^2 test did not showed a significant difference for chiasma frequency and chromosome pairing among *Silene* species and poopulations studied indicating that no significant change has occurred in the number genes controlling chromosome pairing.

Variation in chiasma frequency and localization is genetically controlled (Quicke 1993) and has been reported in populations of different species (Rees and Jones 1977). Such a variation in the species and populations with the same chromosome number is considered as a means for generating new forms of recombination influencing the variability within natural populations in an adaptive way (Rees and Jones 1977).

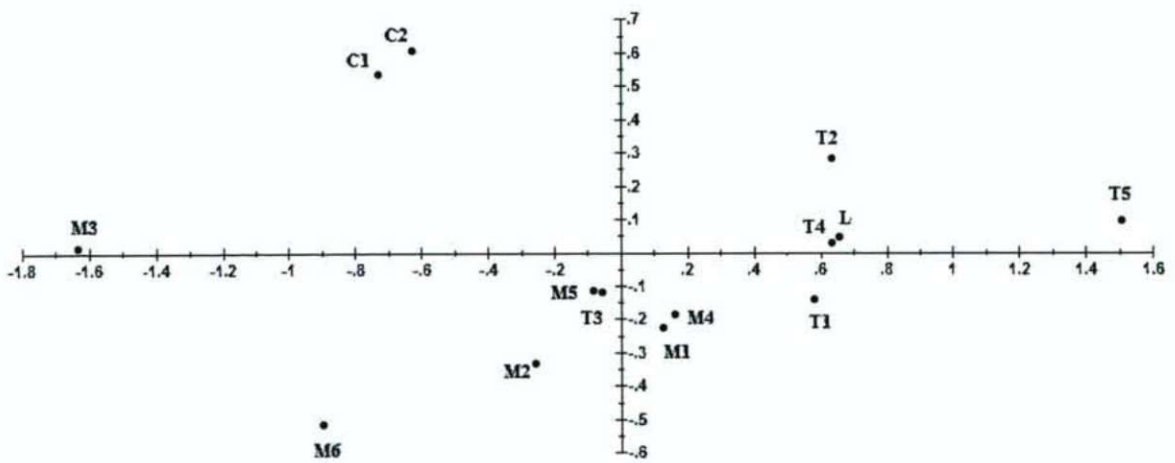

Figure 3. PCA ordination of *Silene* species based on karyotypic data. Species and populations abbreviations: C1 & C2 = Soodkooh and Payesib populations of *S. claviformis*, T1-T5 = Gadook, Sabalan, Chashm, Shahdej and Neor populations of *S. tenella*, M1-M6 = Damavand, Lavasanat, Bakhtiari, Tonekabon and Manjil populations of *S. Marschalii*, L = Ilam population of *S. longipetala*.

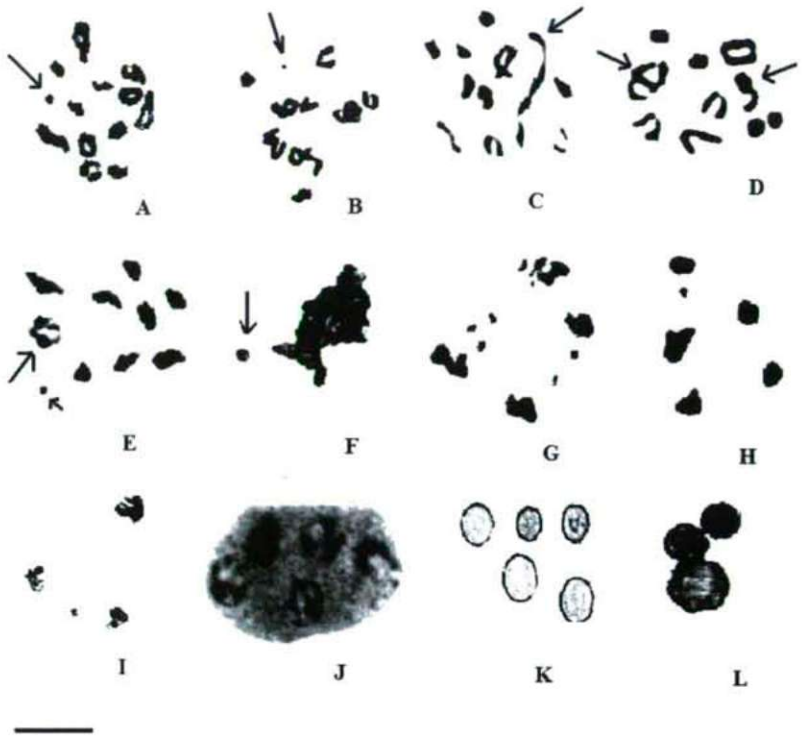

Figure 4. Representative meiotic cells in the *Silene* species studied. A & B = Meiocytes in Khansar and Arak populations of *Silene Marschalii* showing B-chromosome (arrow) respectively. C & D = Meiocyte in Arak population of *S. Marschalii* showing heterozygote translocation (arrow). E = Meiocyte in *S. Propinqua* showing quadrivalent (bigger arrow) and B-chromosome (smaller arrow). F = Meiocyte in Dashtelor population of *S. Marschalii* showing chromosomes clumping and B-chromosome (arrow). G = Telophase-II laggards in meiocyte of Khansar population of *S. Marschalii*. H = A pentaploar cell showing Laggard chromosome in Arak population of *S. Marschalii*. I = A triploar cell showing laggard chromosome in Khansar population of *S. Marschalii*. J = A pentaploar cell in Zanjan population of *S. Marschalii*. K & L = Potential unreduced (2n) pollen grain (bigger size pollen) in Zanjan and Arak populations of *S. Marschalii* respectively. Scale bar = 10 μm.

Almost in all the populations studied, laggard chromosomes and chromosomes stickiness were observed during anaphase I and II (Table 3, Fig. 4F-I). The sticky chromosomes occurred from early stages of prophase to the final stages of meiosis. The number of chromosomes involved in stickiness varied from two to many forming a complete clumping of the chromosomes (Table 3, Fig. 4F). The highest percentage of anaphase-I laggards occurred in Khansar population of *S. Marschallii* (5.00), while the highest value of the same occurred in Orumiyeh population of *S. propinqua* (1.0).

χ^2 test showed a significant difference for the percentage of chromosome stickiness and laggards among the species and populations studied. Genetic and environmental factors as well as genomic-environmental interaction have been considered as the reason for chromosome stickiness in different plant species (Nirmala and Rao 1996; Baptista-Giacomelli et al. 2000).

Multipolar cells were observed (Fig. 4, H-J) in populations of *S. Marschalii* which may be due to spindle abnormalities. Such meiotic abnormalities may lead to the formation of abnormal tetrads and pollen grains, the occurrence of aneuploidy condition as well as unreduced (2n) pollen formation (Villeux 1985; Nirmala and Rao 1996). Pollen fertility ranged from 98.00-99.00% in the populations studied (Table 3). A little reduction in pollen fertility observed may be due to meiotic abnormalities obtained.

Unreduced pollen grain formation

The occurrence of large pollen grains (possibly 2n pollen grains) was observed along with smaller (normal) pollen grains in 3 populations of *S. Marschallii* (Fig. 4K, L). The large pollen grains comprised about 1% of pollen grains in these populations.

The mean diameter of normal (reduced) pollen grains ranged from 19.78 μm to 27.80 μm while, the mean diameter of unreduced pollen grains ranged from 29.10 μm to 48.28 μm. T-test analysis revealed a significant difference ($p < 0.001$) for the size between the larger sized pollen grains and smaller sized pollen grains. The presence of giant pollen grains has been used as an indication of the production of 2n pollen (Vorsa and Bingham 1979, Bertagnolle and Thomson 1995).

Unreduced gametes are known to produce individuals with higher ploidy level through a process known as sexual polyploidization (Villeux 1985), which has been considered as the major route to the formation of naturally occurring polyploids. Different cytological mechanisms are responsible for the production of 2n gametes (Bertagnolle and Thomson 1995). The occurrence of multipolar cells and irregularities in anaphase segregation of the chromosomes might be considered as the possible mechanisms of unreduced pollen grain formation in the *S. Marschalii* populations studied. To our knowledge this is the first report on the occurrence of unreduced pollen grains in the genus *Silene*.

B-chromosomes

B-chromosomes (Bs) of 0-1 were observed in Payesib population of *S. claviformis* (Fig. 1E), Arak, Dashtelor and Khansar populations of *S. Marschallii* (Figs. 4A-B, F) as well as Orumiyeh population of *S. propinqua* (Fig. 4F). The Bs observed were much smaller than the A-chromosomes, round in shape and did not pair with the A-chromosomes. B-chromosomes are accessory chromosomes occurring in more than 1300 species of Plants and almost 500 species of animals (Camacho et al. 2000). It seems that B-chromosomes are of limitted occurrence in the *Silene* and have been reported in *Silene ciliata* (0-2, Vuillemin 1992) and *S. maritime* (0-15, Cobon 1976; Cobon and Murray 1983). The B-chromosomes when present in high number affect negatively the growth and vigor of the plants, while in low number may benefit the plant possessing them.

Acknowledgement

This project is partly supported by Iran National Scientific Foundation (INSF), with project No. 8611850.

References

Baden C (1983) Chromosome numbers in some Greek angiosperms. Willdenowia 13:335-336.

Bari EA (1973) Cytological studies in the genus *Silene* L. New Phytol 72: 833-838.

Baptista-Giacomelli FR, Pagliarini MS and Almeida JL (2000) Meiotic behavior in several Brazilian oat cultivars (*Avena sativa* L.). Cytologia 65:371-378

Bertagnolle F, Thomson JD (1995) *Gametes with the somatic chromosome number: Mechanisms of their formation and role in the evolution of autopolyploid plants.* New Phytol 129:1-22.

Burleigh JG, Holtsford TP (2003) Molecular systematics of the eastern North American *Silene* (Caryophylaceae): Evidence from nuclear ITS and chloroplast *trn*L intron sequences. Rhodora 105:76-90.

Camacho JPM, Sharbel TF, Beukeboom LW (2000) B-chromosome evolution. Phil Trans R Soc Lond, B 355:163-178.

Chowdhuri PK (1957) Studies in the genus *Silene.* Notes from the Royal Botanic Garden. Edinburgh 22:221-278.

Cobon AM, BG Murray (1983) Unstable B chromosomes in *Silene maritima* With. (Caryophyllaceae). Bot J Linn Soc 87:273-283.

Cobon AM (1976) Mitotic instability of B chromosomes in *Silene maritima* (Caryophyllaceae). In Jones K, Brandham PE editors, Current Chromosome Research. 212-213. North--Holland, Amsterdam

Gagnidze R, Gviniashvili T (1997) IOPB chromosome data 11. Newslett. Int Organ Pl Biosyst (Oslo) 26/27:20-21.

Greuter W (1995) Silene (Caryophylaceae) in Greece: A subgeneric and sectional classification. Taxon 44:543-581.

Gvinianidze ZI, Avazneli AA (1982) Khromosomnye chisla nekotorykh predstavitelej vysokogornykh floristicheskikh kompleksov Kavkaza. Soobkskc. Akademiia Nauk Gruzinskoi SSR, Institut Botaniki, Trudy, Seriia Geobtanika 106(3):577-580.

Heaslip MB (1951) Some cytological aspects in the evolution of certain species of the plant genus *Silene.* Ohio J Sci 51:62-70.

Levan A, Fredga K, Sandberg A (1964) Nomenclature for centromeric position on chromosomes. Hereditas 52:201-220.

Markova M, Martina L, Zluvova J, Janousek B, Vyskot B (2006) Karyological analysis of an interspecific hybrid between the diocious *Silene latifolia* and the hermaphroditic *Silene viscose.* Genome 42:373-379.

Melzheimer V (1978) Notes on cytology of several species of the genus *Silene* (Caryophylaceae) from central Greece and from Crete. Pl Syst Evol 130:203-207.

Melzheimer V (1980) Caryophyllaceae In: Flora Iranica, Rechinger KH ed., No.163. pp. 353-508. Akademische Druck-U. Verlagsanstalt, Graz, Austria.

Nersesian AA, Goukasian AG (1995) On the karyology of the representatives of the genus *Silene* L. s. l. (Caryophylaceae) from southern Transcaucasia. Thaiszia 5:13-19. Oxelman B, Lidén M (1995) Generic boundaries in the tribe Sileneae (Caryophylaceae) as inferred from nuclear rDNA sequences. Taxon 44:525-542.

Oxelman B, Lidén M, Berglund D (1997) Chloroplast *rps*16 intron phylogeny of the tribe Sileneae (Caryophylaceae). Pl Syst Evol 206:411-420.

Oxelman B, Lidén M, Rabeler RK, Popp M (2000) A revised generic classification of the tribe Sileneae (Caryophylaceae). Nordic J Bot 20: 743-748.

Nirmala A, Rao PN (1996) *Genetics of chromosome numerical mosaism in higher plants.* The Nucleus 39:151-175.

Quicke DLJ (1993) Principles and techniques of contemporary taxonomy. Blackie Academic & Professional, Glasgow.

Rees H, Jones RN (1977) Chromosome Genetics. London, Edward Arnold.

Romero-Zarco C (1986) A new method for estimating karyotype asymmetry. Taxon 35:526-530.

Sopova M, Sekovski Z (1982) Chromosome atlas of some Macedonian angiosperms. III. Godishen Zbornik Bioloshki Fakultet na Univerzitetot Kiril i Metodij 35:145-161.

Sheidai M, Jalilian N (2008) Karyotypic studies in some species and populations of the genus *Lotus* L. in Iran. Acta Bot Croat 67:45-52.

Sheidai M, Rashid S (2007) Cytogenetic study of some *Hordeum* L. species in Iran. Acta Biol Szeged 51:107-112.

Stebbins GL (1971) Chromosomal evolution in higher plants. Edward Arnold, London.

Swank GR (1932) The Ethnobotany of the Acoma and Laguna Indians. University of New Mexico, M.A., Thesis, p. 69.

Van Loon JC, Snelders HCM.(1979) In IOPB chromosome number reports LXV. Taxon 28:632-634.

Van Loon JC (1982) In IOPB chromosome number reports LXXVII. Taxon 31:763-764.

Vestal PA (1952) The Ethnobotany of the Ramah Navaho. Papers of the Peabody Museum of American Archaeology and Ethnology 40(4):1-94 (p. 27).

Villeux R (1985) Diploid and polyploid gametes in Crop Plants: Mechanisms of formation and utilization in plant breeding. In JANICK J ed., Plant Breed Rev Vol. 3., AVI Publishing Co. Wesport, Connecticut, p. 442.

Vuillemin F 1(992) Mediterranean chromosome number reports 2 (120). Flora Mediterranea 2:273-275.

Zhang Y-x (1994) Studies on chromosomes of some plants from Guandi Mountain, Shanxi. J Wuhan Bot Resea 12(2):201-206.

Volume 52(2):321-322, 2008
Acta Biologica Szegediensis
http://www.sci.u-szeged.hu/ABS

ARTICLE

The effect of progressive drought on water relations and photosynthetic performance of two grapevine cultivars (*Vitis vinifera* L.)

Zsolt Zsófi[1]*, Erika Tóth[1], Gyula Váradi[2], Denis Rusjan[3] and Borbála Bálo[1]

[1]KRF Research Institute for Viticulture and Enology, Eger, Hungary, [2]Research Institute for Viticulture and Enology, Corvinus University, Kecskemét, Hungary, [3]University of Ljubljana, Biotechnical Faculty, Ljubljana, Slovenia

ABSTRACT Preliminary measurements were carried out in order to asses the effect of water deficit on photosynthesis and water relations of two grapevine cultivars (*Vitis vinifera* L. cv. Kékfrankos and *Vitis vinifera* L. cv. Portugieser grafted on 5BB rootstock) tolerance and sensitive to drought, respectively. Three treatments were applied on both cultivars such as 100%, 50% and 30% field capacity under glasshouse conditions. Pre-dawn water potential and gas-exchange parameters (assimilation rate, transpiration, stomatal conductance) were consistently lower in drought stressed plants indicating moderate water stress at 50% field capacity and severe water deficit at 30% field capacity. Midday water potential indicated "close to isohydric" characteristic of both cultivars. Moderate water deficit resulted in an increase in water-use efficiency (WUE). However, Kékfrankos had a significantly higher WUE than Portugieser.
Acta Biol Szeged 52(2):321-322 (2008)

KEY WORDS

drought tolerance
grapevine cultivars
photosynthesis
water relations

Grapevine (*Vitis vinifera* L.) is a traditionally non-irrigated crop, however under arid and Mediterranean-type regions irrigation practices such as partial root-zone drying (PRD) (Dry et al. 2000) and regulated deficit irrigation (RDI; de Souza et al. 2005) have been introduced in order to improve/sustain yield and quality. Under cool climate conditions occurrence of soil water depletion is partly due to the increasing effect of climate change, (uneven and decreased precipitation accompanying with heat spells and high vapour pressure deficit) (Schultz 2000; Domokos 2003) low soil water holding capacity and steep slope exposure (van Leeuwen and Seguin 2006). Moderate water deficit has a beneficial effect on wine quality and composition, especially when grapevines are stressed during the ripening period. However, long term and severe water shortage may endanger economic yield and quality parameters of the wine. In addition, during drought periods the survival of individual plants in new plantations is also endangered without irrigation. Therefore, enhancement of water use efficiency (WUE) has become a main objective for many crops. In grapevine, moderate water stress has a positive impact on WUE (Cifre 2005), however there is evidence for variation in WUE among grapevine cultivars (Bota et al. 2001). Vineyards have high mesoclimatic variability as a result of different aspect, exposure and soil type. Under the same macroclimatic system very different water conditions can be found even within a small wine region and thus grapevines can be regularly exposed to water deficit year by year. Therefore the choice of appropriate cultivar for the given area ('terroir'- variety combination) is essential considering mesoclimatic-soil characteristics and the grapevine strategies against abiotic stresses.

The aim of our preliminary measurement was to compare two grapevine cultivars (*Vitis vinifera* L. Kékfrankos and *Vitis vinifera* L. Portugieser) under severe, moderate and non-stressed conditions to reveal possible differences in some ecophysiological responses of the varieties including WUE. Our results present some evidence for the importance of variety selection in terms of physiological background and may provide useful additional data for determining optimal 'terroir'-variety combinations.

Materials and Methods

Two grapevine cultivars *Vitis vinifera* L. Kékfrankos and *Vitis vinifera* L. Portugieser were submitted to regulated deficit irrigation under greenhouse conditions. Each grapevine were planted in 50L white container using perlite (20%), loamy soil (30%) and peat (50%) (v/v) mixture as a substrate. Three treatments were applied on varieties as 100% (non-stressed), 50% (moderately stressed) and 30% (severely stressed) field capacity. Physiological measurements were taken after 5-8 days when stressed plants reached the desired water deficit. Pre-dawn (Ψ_p) and midday water potentials (Ψ_m) were recorded with Scholander pressure-chamber (PMS, USA). Leaf gas-exchange was measured with an ADC-4 portable

Accepted July 30, 2008
*Corresponding author. E-mail: zszs@szbki-eger.hu

Table 1. Pre-dawn (Ψ_p), midday (Ψ_m) water potential, stomatal conductance (g_s), water use efficiency (WUE) of Kékfrankos (K100%, K50% and K30%) and Portugieser (P100%, P50% and P30%) grapevine (*Vitis vinifera* L.) cultivars grafted on 5BB rootstock under different water regimes (100%, 50% or 30% field capacity). Each data is the average of 3-5 records with standard deviation.

Treatments	Ψ_p (MPa)	Ψ_m (MPa)	g_s (mol m^{-2} s^{-1})	WUE (Pn/E)
K100%	-0.1 ± 0.01	-1.55 ± 0.06	0.17 ± 0.01	1.69 ± 0.2
K50%	-0.29 ± 0.01	-1.58 ± 0.1	0.09 ± 0.01	2.65 ± 0.3
K30%	-0.76 ± 0.2	-1.27 ± 0.5	0.02 ± 0.01	0.91 ± 0.7
P100%	-0.12 ± 0.02	-1.41±0.07	0.26 ± 0.04	1.68 ± 0.2
P50%	-0.26 ± 0.03	-1.62±0.07	0.12 ± 0.02	1.83 ± 0.2
P30%	-0.93 ± 0.1	-1.23±0.02	0.01 ± 0.02	0.98 ± 0.7

infrared gas analyser (ADC Bioscientific Ltd. UK.). Each measurement was taken on individual plants on leaves fully exposed to the sun at saturating light intensities.

Results and Discussion

A significant decrease was observed in pre-dawn water potential in grapevine plant under moderate and severe water deficit. Interestingly, midday water potential of severely stressed plants showed higher values in both cultivars. Non-stressed Portugieser plants exhibited a slightly higher Ψ_m than moderately stressed vines. In contrast, no differences were observed in Kékfrankos leaves Ψ_m between the treatments of 100% and 50% field capacity (Table 1). It suggests that these varieties have isohydric behaviour as it was reported by Schultz (2003) in the case of Grenache grapevine. However, Kékfrankos exhibited stronger isohydric behaviour than Portugieser.

Better water supply resulted in significantly higher stomatal conductance (g_s; Table 1), net-photosynthesis (Pn) and transpiration rate (E) (Düring 1987; de Souza 2005; data not shown). Under non-stressed and moderately stressed conditions Portugieser showed higher gs and E than Kékfrankos. However, CO_2 fixation was higher only in non-stressed Portugieser plants and no differences were found between the assimilation rates of the cultivars under moderate stress. Our results are matching with other findings (Cifre 2005) as moderate water deficit lead to an increase of water use efficiency in grapevine leaves. In addition, at this level of water stress Kékfrankos cultivar showed a higher WUE than Portugieser (Table 1). The higher WUE is partly due to the stronger stomatal regulation of Kékfrankos, however examination of metabolic processes are required to reveal the detailed physiological background of water restriction mechanisms.

In conclusion, our preliminary results presented scientific evidence for differences in water-use efficiency between grapevine cultivars. Grapevine plantation is an expensive and long time investment, therefore the choice of the appropriate cultivar is essential. The increasing frequency of heat spells and dry periods in cool climate wine regions may endanger economic yield and quality. The most endangered vineyards are on hill steep slopes and with soils with low water-holding capacity. Thus, physiological characterisation of the cultivars may provide useful additional data for the choice of the optimal terroir - variety combination.

References

Bota J, Flexas J, Medrano H (2001) Genetic variability of photosynthesis and water use in Balearic grapevine cultivars. Annals of Applied Biology 138: 353-365

Cifre J, Bota, J, Escalona, MJ, Medrano H, Flexas, J (2005) Physiological tools for irrigation scheduling in grapevine (*Vitis vinifera* L.). An open gate to improve water-use efficiency? Agriculture, Ecosystems and Environment 106: 159-170.

de Souza CR, Maroco JP, dos Santos TP, Rodrigues ML, Lopes C, Pereira JS, Chaves MM (2005) Control of stomatal aperture and carbon uptake by deficit irrigation in two grapevine cultivars. Agriculture, Ecosystems and Environment 106: 261-274.

Domonkos P (2003) Recent precipitation trends in Hungary in the context of larger scale climatic changes. Natural Hazards 26: 255-271

dos Santos TP, Lopes CM., Rodrigues ML, de Souza CR, Ricardo-da-Silva MJ, Maroco PJ, Pereira JS, Chaves MM (2007) Effects of deficit irrigation strategies on cluster microclimate for improving fruit composition of Moscatel field-grown grapevines. Scientia Horticulturae 112: 321-330.

Dry PR, Loveys BR, Düring H (2000) Partial drying of the root-zone of grape. I. Transient changes in shoot growth and gas exchange. Vitis 39: 3-7.

Düring H (1987) Stomatal responses to alterations of soil and air humidity in grapevines. Vitis 26: 9-18.

Schultz HR (2000) Climate change and viticulture: A European perspective on climatology, carbon dioxide and UV-B effects. Australian Journal of Grape and Wine Research 1: 1-12.

Schultz HR (2003) Differences in hydraulic architecture account for near-isohydric and anisohydric behaviour of two field-grown *Vitis vinifera* L. cultivars during drought. Plant, Cell and Environment 26: 1393-1405.

van Leeuwen C, Seguin G (2006) The concept of Terroir in Viticulture. Journal of Wine Research 17: No.1. 1-10.

Volume 52(2):323-327, 2008
Acta Biologica Szegediensis
http://www.sci.u-szeged.hu/ABS

ARTICLE

Tuberculosis treatment and nutritional status among the tribals of Northeast India

Mary Grace Tungdim, Satwanti Kapoor*

Department of Anthropology, University of Delhi, Delhi, India

ABSTRACT The data for the present study was collected cross-sectionally among a total sample of 247 adult tribal males between the age 20-40 years inhabiting Manipur, Northeast India. The subjects comprised of TB patients and healthy non-patients taken as control group (CG). The TB patients were categorized into three groups viz.: Before starting treatment (BST), after 2 months of treatment (2MOT), after completion of treatment(ACT). Anthropometric measurements like weight, height and mid upper arm circumference were taken for the study. The index of nutritional status like body mass index(BMI) was computed. The percentage of chronic energy deficiency (CED) based on body mass index (BMI<18.5kg/m^2) for the different groups of subjects were 64.5%(BST), 49%(2MOT), 34%(ACT) and 6.3%(CG) respectively. The CED based on mid upper arm circumference (MUAC<22.0cm) was found to be 43.5%(BST), 30.9(2MOT), 26%(ACT) respectively. Based on the World Health Organization BMI classification, the prevalence of CED (BMI<18.5kg/m^2) among tuberculosis patients in the different stages of treatment was from high to very high indicating a critical situation. The prevalence of undernutrition based on MUAC among the TB patients was also clearly evident but not so in healthy non patient subjects. Regular intake of medicine is clearly reflected in significant improvement in nutritional status indices.

Acta Biol Szeged 52(2):323-327 (2008)

KEY WORDS

tuberculosis treatment
chronic energy deficiency
tribals
Northeast India
mid upper arm circumference
body mass index

Weight loss with a concomitant loss of body fat and nutritional depletion are observed frequently in patients with pulmonary tuberculosis. Tuberculosis (TB) is one of the most globally serious health problems and is one of the most important causes of death among adults in developing countries. Worldwide, one person out of three is infected with the disease - that is, 2 billion people in total. Global estimate of the burden of tuberculosis related disease and death for 1997 indicated that 8 million people developed active tuberculosis every year and nearly 2 million died (Smith 2004). Pulmonary TB, a chronic infectious disease caused by mycobacterium tuberculosis, is characterized by prolonged cough, hemoptysis, chest pain and dyspnea. Systemic manifestations of the disease include fever, malaise, anorexia, weight loss, weakness and night sweats (Hopewell 1994).

India alone accounts for one-third of the global burden of TB and every year more than 1.8 million new cases appear in the country. Approximately 4,00,000 people die from TB every year in India, more than 1,000 die every day and 100 million work days are lost (Directorate General of Health Services 2005). The situation in the remote tribal areas is still grim. Among the tribals the prevalence of tuberculosis was found to be affected by socio-economic status, nutrition, family size, customs, beliefs and use of medical facilities (Tungdim et al. 2008).

Accepted June 19, 2008
*Corresponding author. E-mail: satwanti@yahoo.com

The use of anthropometry as an indicator of nutritional status of adults has now been well established (World Health Organization 1995). The body mass index (BMI) and high levels of undernutrition (based on BMI) is a major public health problem especially among rural underprivileged adults of developing countries (World Health Organization 1995). Although adult nutritional status can be evaluated in many ways, the BMI is the most widely used because its use is inexpensive, non-invasive and suitable for large scale surveys (Lohman et al. 1988; Ferro-Luzzi et al. 1992; James et al. 1994; Tyagi and Kapoor 2004; Tyagi et al. 2005; Sinha and Kapoor 2006; Sinha and Kapoor 2007). Thus, BMI is the most established anthropometric indicator used not only for assessment of adult nutritional status but also the socio-economic condition of a population, specially adult populations in developing countries (Shetty and James 1994; Nube et al. 1998; Khongsdier 2002; Bose et al. 2006; Bose et al. 2007). Fernald (2007) in his study among the Mexican adults found that socio-economic status is related to body mass index.

Another anthropometric measure that can be used to evaluate adult nutritional status is mid upper arm circumference (MUAC). It has been found that MUAC is particularly effective in the determination of malnutrition among adults in developing countries (James et al. 1994).

Several studies like association of body mass index and incidence of tuberculosis (Tverdal 1986), nutritional status and weight gain in patients with pulmonary tuberculosis in

Table 1. Basic data of subjects.

Subjects	n	Height(cm) Mean ± SD	Weight(kg) Mean ± SD	MUAC(cm) Mean ± SD	BMI(kg/m²) Mean ± SD
BST	62	161.6 ± 5.88	46.8 ± 6.64	22.1 ± 2.38	17.9 ± 2.18
2MOT	55	163.5 ± 5.23	50.1 ± 6.13	23.1 ± 2.39	18.7 ± 2.14
ACT	50	163.5 ± 4.93	51.8 ± 6.09	23.3 ± 2.65	19.4 ± 2.0
CG	80	163.9 ± 5.71	57.4 ± 5.82	26.0 ± 1.97	21.4 ± 2.12
F- value		2.32*	36.9*	37.4*	35.3*

*p<0.01. CG: healthy controls; BST: before starting treatment; 2MOT: after two months of treatment; ACT: after completion of treatment. MUAC: mid upper arm circumference. BMI: body mass index.

Table 2. Distribution of subjects according to nutritional status based on body mass index(BMI).

Subjects	n	CED III	CED II	CED I	Total CED	Normal	Overweight
BST	62	19.4%	16.1%	29%	64.5%	35.5%	-
2MOT	55	5.5%	20%	23.6%	49.1%	50.9%	-
ACT	50	4%	10%	20%	34%	66%	-
CG	80	-	2.5%	3.8%	6.3%	87.5%	6.3%

CG: healthy controls; BST: before starting treatment; 2MOT: after two months of treatment; ACT: after completion of treatment.

Tanzania (Kennedy et al. 1996), have been conducted. Malnutrition though observed frequently in patients with pulmonary tuberculosis(TB) but the assessment of their nutritional status during TB treatment as assessed by BMI and MUAC is non-existent on the tribals of India. In view of this, the present investigation was undertaken to study the influence of pulmonary tuberculosis treatment on the anthropometric indicators of nutritional status among the tribal adults of Manipur, Northeast India.

Materials and Methods

The present study was conducted among adult tribal males in Manipur. Manipur lies in the North-Eastern region of the Indian sub-continent, between 23° 50′ latitudes and 25° 30′ North and 93° 10′ and 94° 30′ East longitudes, bordering Myanmar in the East, Nagaland in the North, Assam and Mizoram in the West. The density of population is 82 per sq.km., the literacy rate is 59.89% and the per capita income is Rs. 3502/- (Census 1991).

According to the 1991 census report, Manipur has a population of around 1,837,149 out of which the tribal population accounts for approximately 30 percent. In the geographical classification it may be simply divided into a valley at the centre and the hills surrounding it. The hills are said to be abode of the tribals. It should be noted that all the different ethnic groups are of the same Mongoloid group and have very close similarities in their culture and traditional habits. The main occupation of the people is agriculture and rice is their staple food.

A cross sectional study among the adult pulmonary tuberculosis (TB) patients between 20-40 years of age was conducted in the four TB centers in Manipur. The TB patients selected were categorized into 3 groups in consultation with the Delhi State TB center, India as (i) Before starting treatment (BST) which includes subjects who were confirmed by the doctors as having TB and were to start their treatment (ii) The patients who had completed two months of treatment (2MOT) and this group included subjects who had been taking regular TB medicine for the last 2 months as confirmed from doctors at their respective TB centers. These subjects came to various TB centers/ hospitals for constant monitoring. The third group included subjects who were at the completion of TB treatment (ACT) as confirmed by the doctors at respective TB centers and hospitals. All these three group of subjects (BST, 2MOT & ACT) were independent of each other. None of the subjects were related to each other by birth or by marriage. Controls (CG) were healthy subjects with no history of tuberculosis, matched with cases for age, and selected from among the non-family neighbors of the patients.

Certain guidelines were laid down for selecting the subjects who had TB and were willing to co-operate in the present study, (1) only those subjects who took their medicines regularly as confirmed by the doctors and/or health workers and also followed the dietary norms as advised by doctors were taken, (2) only those subjects were retained in the sample who refrained from alcohol and smoking during the course of treatment, (3) only new cases who had pulmonary tuberculosis were taken, (4) none of the HIV +ve patients

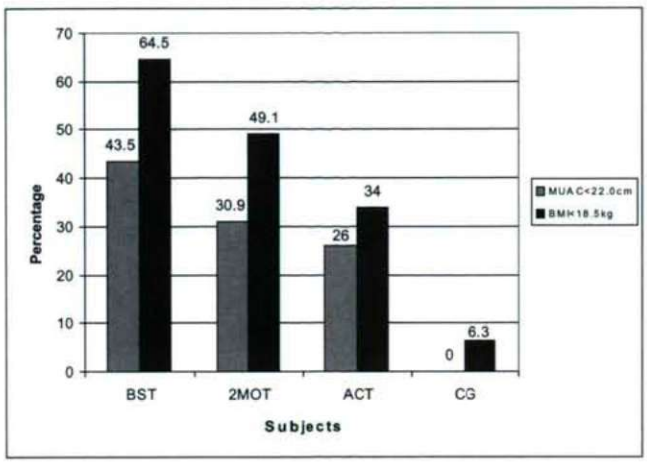

Figure 1. Prevalence of undernutrition based on body mass index and mid upper arm circumference among the subjects in different groups.

were retained in the sample. Exclusion criteria for the controls were as follows: previous anti-TB treatment, any form of disease and HIV+ve as confirmed by the doctors.

Each subject was measured for height, body weight and mid upper arm circumference. Body weight was measured to the nearest 0.1kg using a beam balance scale with subjects wearing only light clothes and no shoes. The height was measured to the nearest 0.1cm with a Harpenden anthropometer. The mid upper arm circumference was measured to the nearest 0.1 cm using a flexible steel tape. All these measurements were taken by following the techniques described by Weiner and Lourie (1981). Body mass index was calculated as body weight in kg divided by height in meter squared [BMI=wt (kg)/ height (m^2)].

The World Health Organization's classification (World Health Organization 1995) of the public health problem of low BMI, based on adult populations worldwide, was followed. This classification categorizes prevalence according to percentage of a population with BMI<18.5 as follows

Low (5-9%): warning sign, monitoring required.

Medium (10-19%): serious situation.

High (20-39%): serious situation.

Very high (≥40%): critical situation.

Nutritional status was also evaluated following the standard cut off point of MUAC (James et al. 1994). The following cut off values was used:

Under-nutrition: MUAC < 22.0cm

Normal: MUAC > 22.0cm

Descriptive statistics were performed for the anthropometric variables viz, height, body weight, MUAC and BMI for subjects in the different stages of TB treatment and healthy controls. The t-test was used for comparison between the different groups of subjects. The differences between the test groups and healthy controls in respect of each anthropometric variable were tested by one way analysis of variance(ANOVA). All data was analysed using SPSS 13.0 version.

Results

Figure 1. shows the prevalence of undernutrition based on BMI and MUAC. The subjects before starting treatment showed highest prevalence of undernutrition. The healthy control subjects also suffered from CED based on BMI only but not on MUAC.

Table 1 gives the means and standard deviations of height, weight, mid upper arm circumference (MUAC) and body mass index (BMI) according to different stages of treatment and in healthy controls. It was found that the mean values of all the measurements among subjects before starting treatment (BST) was the lowest and was highest among healthy control subjects. The ANOVA test for height ($F=2.32$, $p<0.01$), weight ($F=36.9$, $p<0.01$), MUAC($F=37.4$, $p<0.01$) and BMI($F=35.3$, $p<0.01$) showed significant differences among TB patients and healthy controls.

The percentage distribution of BMI categories is given in Table 2. Following the World Health Organization (1995) classification of CED, 64.5% of the subjects before starting treatment, 49.1% of subjects after two months of treatment, 34% of the subjects at the completion of treatment and 6.3% of the healthy controls were found to be CED.

Table 3 shows that the percentage of subjects who were undernourished based on MUAC<22.0 cm was highest among subjects before starting treatment (43.5%) followed by subjects after two months of treatment (30.9%) and then subjects at the completion of treatment. None of the healthy control subjects were found to be undernourished based on MUAC.

Table 4 displays the value of 't' with the level of significance in the anthropometric indicators of chronic energy deficiency between different groups of subjects. Both the anthropometric indicators (MUAC & BMI) of chronic energy deficiency were found to be statistically significant ($p<0.001$) between TB patients at different stages of treatment (BST, 2MOT & ACT) and the healthy controls (CG). The mid upper arm upper circumference (MUAC) was also found to be statistically significant ($p<0.05$) between subjects before starting treatment(BST) and after two months of treatment (2MOT) and after completion of treatment (ACT). The body mass index(BMI) was also found to be statistically significant ($p<0.001$) between subjects before starting treatment (BST) and after completion of treatment (ACT). The BMI also showed statistically significant difference ($p<0.05$) between patients before starting treatment (BST) and after two months of treatment(2MOT).

Discussion

Malnutrition together with socio-cultural and economic factors, poor sanitation, lack of awareness makes people

Table 3. Distribution of subjects according to nutritional status based on mid upper arm circumference (MUAC).

Subjects	n	MUAC <22.0 cm	MUAC >22.0 cm
BST	62	43.5%	56.5%
2MOT	55	30.9%	69.1%
ACT	50	26%	74%
CG	80	-	100%

CG-healthy controls; BST-before starting treatment; 2MOT-after two months of treatment; ACT-After completion of treatment. MUAC-mid upper arm circumference. BMI-body mass index.

Table 4. Value of 't' with level of significance in the anthropometric indicators of chronic energy deficiency between different groups of subjects.

Subjects	MUAC	BMI
CG & BST	10.6***	9.6***
CG & 2MOT	7.7***	7.1***
CG & ACT	6.7***	5.4***
BST & 2MOT	2.21*	2.05*
BST & ACT	2.41*	3.64***
2MOT & ACT	0.34	1.56

*p<0.05, **p<0.01, ***p<0.001. CG-healthy controls; BST-before starting treatment; 2MOT-after two months of treatment; ACT-After completion of treatment. MUAC-mid upper arm circumference. BMI-body mass index.

more susceptible to diseases. Diseases further aggravate the situation regarding the nutritional status and causes partly retardation in physical well being.

The mean value of BMI of the healthy controls in present population was higher than in many populations in Northeast India (Khongsdier 2001; Khongsdier 2002) and South Indian populations (Ferro-Luzzi et al. 1992). It was observed that weight, MUAC and BMI were significantly higher in the healthy control subjects than in the subjects who had TB and were at different stages of treatment. Tungdim et al. (2008) have found that the socio-economic status of the healthy controls was found to be comparatively higher than the TB patients at different stages of treatment which confound with the findings of Ginzburg and Dadamukhamedov (1990) and Ulijaszek (1997).

It was demonstrated that the nutritional status as assessed by body weight, body mass index and mid upper arm circumference was significantly poor in TB patients as compared with healthy controls. Similarly, Tverdal (1986) found a distinct association between an increasing risk of pulmonary TB with a decreasing body mass index which was observed for both sexes, all age groups, and at all lengths of observations. It is well established that people show a decrease in their body fat content with increasing level of physical activity or a decrease in energy intake. The decrease in energy intake might be due to less food intake, poor eating habits or anorexia. There is no doubt that one of the symptoms of TB is anorexia or loss of appetite which would cause a loss in body weight with a concomitant decrease in body fat and muscle mass.

The poor nutritional status of patients with pulmonary TB may be due to anorexia, impaired absorption of nutrients or increased catabolism (Hopewell 1994). The TB patients and healthy subjects had similar food habits and food intakes because their socio-cultural background and living conditions were similar. Thus, infectious disease such as TB may have led to impaired absorption and increased rates of metabolism (Ginzburg and Dadamukhamedov 1990; Ulijaszek 1997). TB is probably associated with more severe malnutrition than other chronic illnesses (Karyadi et al. 2000). In a study by Saha and Rao (1989) the nutritional status of the patients with TB was worse than that of those with leprosy.

The results of the present investigations have shown that there is a certain impact of treatment on the nutritional status of the TB patients. Onwubalili (1988) also found that chemotherapy was associated with progressive nutritional recovery and restoration of nutritional related indices among patients with active TB.

It was found that TB patients showed significant increase in body weight, BMI and MUAC from the time treatment started till two months of TB treatment which is supplemented by the study done by Sukumaran et al. (2002) where they found that 62% of the patients studied experienced improvement in symptoms within two months of starting treatment. Contrary to our findings, Kennedy et al. (1996) found that TB patients displayed evidence of malnutrition both before and after treatment in a longitudinal study among the Tanzanian population and thus weight gain during therapy was an unreliable indicator of overall treatment response. However, the TB patients showed no significant improvement from two months of treatment till the completion of treatment indicating the importance of regular medication in first two months of treatment and perhaps lack of proper diet even with regular treatment in later stage (2MOT to ACT) can explain the non-significant improvement in the anthropometric indices. Good diet is certainly very important during rehabilitation. The TB patients in the present study belonged to relatively low socio-economic status and had large families to feed as compared to healthy controls.

It was found that malnutrition appeared to increase the risk of developing tuberculosis which was also found by Cegielsky and McMurray (2004). It can thus be perceived that there is a strong association of tuberculosis with anthropometric indicators of CED especially BMI and MUAC. BMI<18.5kg/m^2 and MUAC<22.0 cm are found to be the likely predictors of tuberculosis in the present study and significant improvement with TB treatment in various anthropometric indices an important pointer of regular intake of medicine.

Thus, in the present study it was found that the tuberculosis patients displayed high prevalence of CED as compared to the healthy controls. A disease associated depletion of fat stores and muscle wastage was observed and with treatment, the body dimensions improved along with better fatness level, muscle strength and mass. It is quite clear that with course of treatment among patients the anthropometric indicators come closer to healthy controls.

The BMI and MUAC are significantly influenced by chronic disease like tuberculosis and that tuberculosis leads to loss of energy reserve and muscle wastage which later predisposes individuals to chronic energy deficiency.

It is evident from the present study that nutritional status as assessed by various anthropometric indices of the TB patients significantly improved with treatment. Thus, increase in weight, body mass index and mid upper arm circumference during therapy appeared to be reliable indicators of overall treatment response.

Acknowledgements

The authors are grateful to the subjects who volunteered for the study. The authors are also thankful to (L) Dr. S.P. Khanna, the then Director, Delhi TB Centre for his cooperation and guidance before the start of the fieldwork. The financial assistance to Mary Grace Tungdim from Indian Council of Medical Research is sincerely acknowledged.

References

Bose K, Bisai S, Das P, Dikshit S, Pradhan S (2007) Relationship of income with anthropometric indicators of chronic energy deficiency among adult female slum dwellers of Midnapore town. J Hum Ecol 22(2):171-176.

Bose K, Ganguly S, Mamtaz H, Mukhopadhyay A, Bhadra M (2006) High prevalence of undernutrition among Kora Mudi tribal of Bankura district, West Bengal, India. Anthropol Sci 14(1):65-68.

Cegielski JP, McMurray DN (2004) The relationship between malnutrition and tuberculosis: evidence from studies in humans and experimental animals. Int J Tuberc Lung Dis 8:286-298.

Census of India (1991) Series 20, Provisional Population Totals, paper 1, pp. 22.

Directorate of Health Services (2005) Managing the RNTCP in your area. Modules 1 to 4. New Delhi: Central TB Division, Nirman Bhawan.

Ferro-Luzzi A, Sette S, Franklin M, James WPT (1992) A simplified approach of assessing adult energy deficiency. Eur J Clin Nutr 46:173-186.

Fernald L (2007) Socio-economic status and body mass index in low income Mexican adults. Soc Sci Med 64(10):2030-2042.

Ginzberg VS, Dadamukhamedov AA (1990) Absorption of nutrients in patients with pulmonary tuberculosis. Probl Tuberk 10:44-46.

Hopewell PC (1994) Overview of clinical tuberculosis. In Bloom BR ed., Tuberculosis: Pathogenesis, Protection and Control. Washington DC: ASM Press. pp. 25-36.

James WPT, Mascie-Taylor CGN, Norgan NG, Bristrian BR, Shetty P, Ferro-Luzzi A (1994) The value of arm circumference measurements in assessing chronic energy deficiency in third world adults. Eur J Clin Nutr 48:883-894.

Karyadi E, Schultink W, Nelwan RH, Gross R, Amin Z, Dolmans WM, van der Meer JW, Hautvast JG, West CE (2000) Poor micronutrient status of active pulmonary tuberculosis patients in Indonesia. J Nutr 130:2953-2958.

Kennedy N, Ramsay A, Uiso L, Gutmann J, Ngowi FI, Gillespie SH (1996) Nutritional status and weight gain in patients with pulmonary tuberculosis in Tanzania. Trans R Soc Trop Med Hyg 90(2):162-166.

Khongsdier R (2001) Body mass index of adult males in 12 populations of Northeast India. Ann Hum Biol 28:374-383.

Khongsdier R (2002) Body mass index and morbidity in adult males of the war Khasi in Northeast India. Eur J Clin Nutr 56:484-489.

Lohman TG, Roche AF, Martorell R (1988) Anthropometric Standardization Reference Manual. Chicago: Human Kinetics Books.

Nubé M, Asenso-Okyere WK, van den Boom GJM (1998) Body mass index as indicator of standard of living in developing countries. Eur J Clin Nutr 52:136-144.

Onwubalili JK (1988) Malnutrition among tuberculosis patients in Harrow, England. Eur J Clin Nutr 42:363-366.

Saha K, Rao KN (1989) Undernutrition in lepromatous leprosy: V. Severe nutritional deficit in lepromatous patients co-infected with pulmonary tuberculosis. Eur J Clin Nutr 43:117-128.

Shetty PS, James WPT (1994) Body Mass Index: A measure of chronic energy deficiency in adults. Food and Nutrition Paper 56. Rome: Food and Agricultural Organization.

Sinha R, Kapoor R (2006) Parent-child correlation for various indices of adiposity in an endogamous Indian population. Coll Antropol 30(2): 291-296.

Sinha R, Kapoor R (2007) Sensitivity of various skinfold site to fat deposition in adolescent daughters and their mothers. Acta Biol Szeged 51(1):21-25.

Smith I (2004) What is the health, social and economic burden of tuberculosis? In Frieden T ed., Toman's tuberculosis: case detection, treatment and monitoring, Geneva: World Health Organization.

Sukumaran P, Venugopal KP, Manjooran RS (2002) A social study of compliance with DOTS. Ind J Tub 49:205-208.

Tungdim MG, Kapoor S (2008) Tungdim MG, Kapoor S, Kapoor AK (2008) Tribes, tuberculosis and treatment: A study in Northeast India. In Sinha AK, Banerjee BG, Vasishat RN, Edwin CJ eds., Bio-Social Issues in Health. New Delhi: Northern Book Centre. pp. 520-528.

Tverdal A (1986) Body mass index and incidence of tuberculosis. Eur J Respir Dis 69(5):355-362.

Tyagi R, Kapoor S (2004) Ageing in structural and functional dimensions among institutionalized and non-institutionalized senior citizens. XLII/2: 141-146.

Tyagi R, Kapoor S, Kapoor AK (2005) Body composition and fat distribution pattern of urban elderly females, Delhi, India. Coll Antropol 9(2): 493-498.

Ulijaszek S (1997) Transdisciplinarity in the study of undernutrition-infection interactions. Coll Anthropol 21:3-15.

Weiner JS, Lourie JA (1981) Practical Human Biology. London: Academic Press.

World Health Organization (1995) Physical status: the use and interpretation of Anthropometry. Technical Report Series no. 854. Geneva: World Health Organization.

Volume 52(2):329-331, 2008
Acta Biologica Szegediensis
http://www.sci.u-szeged.hu/ABS

ARTICLE

Enostosis (osteopoikylosis, bone islands) in medieval (14-15th centuries) skeletons

László G. Józsa[1]* and Gyula L. Farkas[2]

[1]Department of Morphology, National Institute of Traumatology, Budapest, Hungary, [2]Department of Anthropology, University of Szeged, Szeged, Hungary

ABSTRACT Enostosis (*i.e.* osteopoikylosis, bone islands, etc.) is a focus of mature cortical bone within cancellous bone. Bone islands are often recognized on radiographic pictures taken for other diagnostical purpose. The authors examined x-ray images of 652 long bones and 44 innominate bones of 124 adult skeletons from the 14-15th centuries AD. Six cases of enostoses were recognized (2 innominate bones, 2 fibulas, 1 femur head and 1 tibia). The biggest alteration was 22x9 mm, while most of the bone islands were 2-5 mm in size. Histological examination was performed in two cases. Microscopical view of one case showed lamellar (cortical) bone; in the other case woven bone structure was found. Enostosis of archeological bones can only be diagnosed performing routine radiographic examination.
Acta Biol Szeged 52(2):329-331 (2008)

KEY WORDS

enostosis
osteopoikylosis
archeological material

Since the earliest description by Stieda in 1905 (cit. Greenspan 1995) enostosis or bone island has been variously named and defined in literature. Stieda referred to small, dense, circumscribed shadows inside the cancellous portion of tubular bones as „kompakte Knochenkerne" (compact bone nuclei). Diverse nomenclature of this pathology includes: calcified island in medullary bone, sclerotic bone island, focal sclerosis, hamartous cortical bone, endosteoma, endosteosis, osteopoikylosis, etc. This benign lesion can be diagnosed on the basis of its characteristic radiological features. Accurate identification of the alteration is crucial in the differential diagnosis of other more significant bone lesions such as primary or metastatic tumors. Enostosis of archeological bones can only be diagnosed performing routine radiographic examination.

The aim of this study is to describe our cases recognized on x-ray images taken for other diagnostical purposes.

Materials Aand Methods

Archeological data

Bátmonostor-Pusztafalu is the largest medieval cemetery in Hungary situated in the southern part of the Great Hungarian Plain. The total number of individuals found in graves and reduction areas is 3783. The investigated remains derive from the 14-15th centuries AD.

Accepted Okt 28, 2008
*Corresponding author. H-3648, Csernely, Táncsics u. 9., Hungary

Anthropological data

Among 3783 skeletons 1510 belong to the infantia I and II age categories. The number of juvenile individuals is 153, while the number of adult males is 1342, which is almost twice the number of the 719 adult female skeletons. Age at death and sex were determined according to classical methods of physical anthropology (Nemeskéri et al. 1960; Ubelaker 1978).

Radiological examination

On 652 long bones (femur, tibia, fibula, humerus) and 44 innominate bones of 124 adults (79 male and 45 female) two directional plain film radiography was performed for other diagnostical purposes.

Histological examination

Bone pieces were excised from 3 bones in which enostoses were previously detected with radiological examination. The bone pieces (10x5x5 mm) were decalcified in EDTA solution and embedded in paraffin wax. The 5 μm serial sections were stained with Masson's trichrome and sirius supra red dyes. The preparations were examined with plain light and polarized light microscopes.

Results

In six cases (two innominate bones, two fibulas, one femoral neck and head and one tibia) bone islands were detected on radiographic pictures. 0.61% of the long bones, 4.5 % of the innominate bones and 5% of the total 124 individuals have been affected by the alteration.

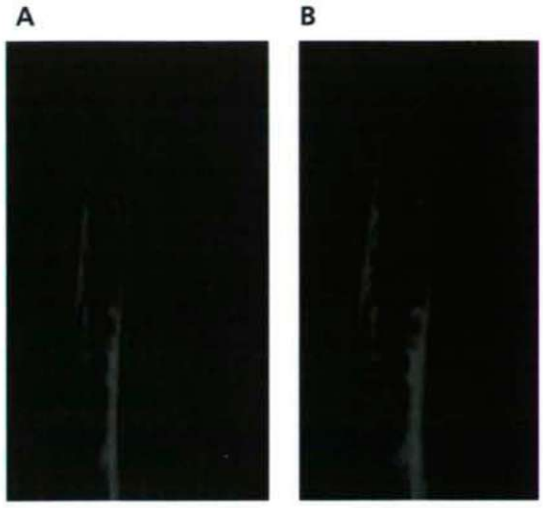

Figure 1. (A) Radiological picture of the enostosis in the fibula of case 1. (B) 3x magnification of the same site.

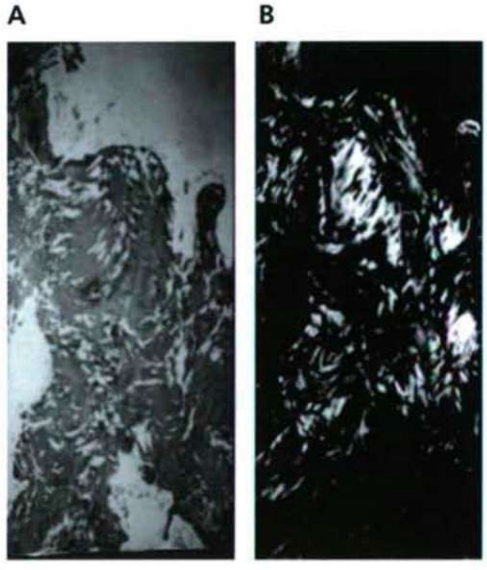

Figure 2. (A) Histological section of the enostosis of case 1: woven bone structures. Masson's trichrome staining , light microscopy, 200x magnification. (B) Histological section of the same site stained with sirius supra red, polarized light microscopy.

Case 1/ grave no. 120, male, aged 21-40 ys. On the diaphysis of the left tibia a dislocated healed fracture was visible. In the proximal metaphysis of the right fibula eight bone islands of 2-4 mm diameters could be seen on the radiograph (Fig. 1A, Fig. 1B). The histological examination reported woven bone structure in the bone island (Fig. 2A, Fig. 2B).

Case 2/ grave no. 1404/05, male, aged 41-60 ys. On the right acetabulum a fracture with 2 mm diastasis was found.

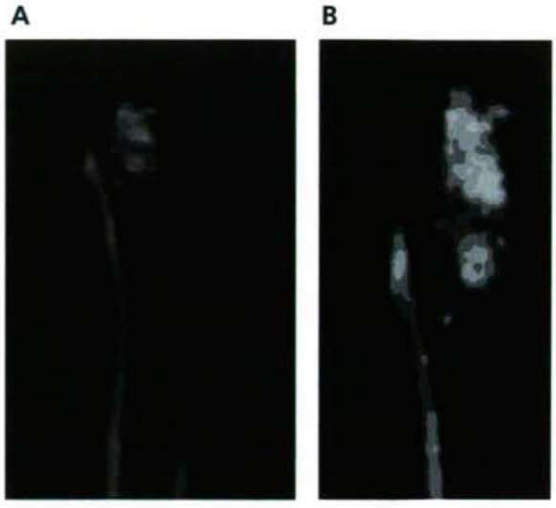

Figure 3. (A) Radiological picture of the giant bone island (22x9 mm) in the fibula of case 6. (B) 3x magnification of the same site.

Both on the acetabulum and on the femoral head signs of osteoarthrosis were seen. In both innonimate bones 4-4 bone islands (2-6 mm in diameter) were detected on the x-ray images.

Case 3/ grave no. 1424, male, aged 41-60 ys. On the posterior surface of proximal metaphysis of the right tibia an osteochondroma of 6x3x3 cm size was found. Within the osteochondroma (exostosis) three bone islands were seen, all oval in shape and 4x3 mm in diameter. On the proximal end of tibia 9 Harris lines were detected. The microscopic examination confirmed the presence of lamellar cortical bone within the cancellous structure of the exostosis.

Case 4/ grave no. 1588, female, aged 41-60 ys. In the right innominate bone seven bone islands were found. Two islands were oval in shape, with diameters of 5x3 mm, while the other five islands were round and 2-3 mm in diameter. In the microscopic picture of the islands typical lamellar cortical bone was seen.

Case 5/ grave no. 1920, male, aged 21-40 ys. Dysplasia coxae congenita and bony ankylosis of the right hip joint was detected. Cervical angle of the right femoral neck was 158 grades, while that of the intact left side was only 130 grades. On the x-ray images within both the head of femur and the innominate bone seven islands were seen, round or oval in shape and 3-4 mm diameter.

Case 6/ grave no. 2586/B, male, aged 21-40 ys. On the diaphysis of right tibia a healed spiral fracture was diagnosed. On the radiographs posttraumatic osteomyelitis could be detected. On the proximal part of the right fibula a 22x9 mm bone island was seen (Fig. 3A, Fig. 3B). Histological examination proved the presence of cortical bone tissue in the structure (Fig. 4).

Figure 4. Histological section of the enostosis of case 6: lamellar cortical bone structures. Sirius supra red staining, polarized light microscopy, 100x magnification.

Discussion

Enostoses (bone islands) are clinically asymptomatic and are often incidental findings on radiographs performed for other diagnostical purposes (Lagier-Nussle 1978; Greenspan et al. 1991). Bone islands exhibit consistent radiographic picture regardless of their location, shape or size. The lesions appear in the spongiosa as round, ovoid or oblong foci of homogenously dense and sclerotic bone tissue. The majority of bone islands (described as "giant islands") range from 1 to 10mm in size. The greatest bone island ever found was located in tibia and 50x50x45mm in size (Smith 1993). The pelvis and the femur are preferred sites of involvement, but the lesion may be found anywhere in the skeleton. This alteration, however, is rarely located in the spine or the ribs (Greenspan 1995). Enostosis is familial is some cases (Forgács 1970). In living patients, enostosis can often be diagnosed after CT, MRI examination or scintigraphy. The histological picture of the lesion is a focus of compact (cortical) bone tissue within the spongious part that consists of mature lamellar trabeculae, while occasionally may contain woven (immature, non-lamellar) bone as well. Mirra et al. (1989) referredt to it as „misplaced hamartous cortical bone", while recent investigations suggest that foci of mature cortical bone within the spongiosa represent areas that failed to resorb during enchondral occification (Greenspan et al. 1991).

Enostoses are only incidentally diagnosed in modern clinical practice. In addition, according to our best knowledge this lesion has only once been described in paleopathological literature. Lagier et al. (1959) found one case in which the caput humeri (1), the caput femoris (2) and distal epiphysis of the same femur (2) contained bone islands. Enostoses cannot be recognized during macroscopic examination, only with radiological imaging techniques. Paleopathological practice, however, has rarely used radiography as part of the routine examination process. In our material we performed radiographic investigation on each bone showing any macroscopic alteration (healed fracture, periostitis, etc.). As a result of this process we could diagnose enostoses and calculate the prevalences in the sample. Due to incidental recognition of the lesion, exact frequency of enostosis is unknown in the sample, just like in any other recent or archeological populations.

Acknowledgement

The project was supported by OTKA project no. TO 32824

References

Forgács S (1970) Familiäre osteopoikylosis.Fortschr Geb Roentgenstr Nuklearmed 112:254-259.

Greenspan A (1995) Bone island (enostosis): current concept – a review. Skeletal Radiol 24:111-115.

Greenspan A, Steiner G, Knutzon R (1991) Bone island (enostosis): clinical significance and radiologic and pathologic correlations. Skeletal Radiol 20:85-93.

Lagier R, Kramar C, Baud CA (1959) Multiple bone islands in a skeleton dating from the neolithic period. Eur J Radiol 9:81-82.

Lagier R, Mbakop A, Bigler A (1984) Osteopolikilosis: a radiological and pathological study. Skeletal Radiol 11:161-168.

Lagier R, Nussle D (1978) Anatomy and radiology of bone island. Fortschr Roentgenstr 128:261-269.

Mirra JM, Picci P, Gold RH (1989) Bone tumors: clinical, radiologic and pathologic correlations. Philadelphia, Lea & Febiger, p. 182.

Nemeskéri J, Harsányi L, Acsády Gy (1960) Methoden zur Diagnose des Lebensalters von Skelettfunden Anthrop Anz 24:70-95.

Smith J (1993) Giant bone island. Radiology 107:35-40.

Ubelaker DH (1978) Human skeletal remains: Explanation, analysis, interpretation. Aldwine, Chicago.

Volume 52(2):333-356, 2008
Acta Biologica Szegediensis
http://www.sci.u-szeged.hu/ABS

DISSERTATION SUMMARIES

DNA Replication across the protein-DNA adduct

Yathish J Achar

Institute of Genetics, Biological Research Center, Szeged, Hungary

In cells, DNA is tightly associated with a variety of proteins that serve both to maintain the structural organization of the genetic material and to coordinate cellular processes including replication, repair, recombination, and transcription. Many endogenous compounds (e.g., metabolites of lipid peroxidation) as well as environmental agents are reactive with both DNA and proteins and thus can produce covalent linkage between these two types of macromolecules.

DNA-protein cross links (DPCs) arise in biological systems as a result of exposure to a variety of chemical and physical agents, many of which are known or suspected carcinogens. These DPCs formed within the cells are usually removed/ cleaved by different cellular mechanisms. The unresolved DPCs can hinder normal functioning of a cell by blocking regular cellular mechanism like DNA replication, transcription and others.

Despite the recognition of the biological significance of DPCs, there are very limited data concerning the repair of these lesions. One possible hypothesis is that the covalent or irreversible bondage of a protein to DNA somehow modifies the whole structure of DNA double helix and hence allowing cell to recognize these DPCs as unnatural nucleotide base pair. . The mechanism how a cell recognizes these DPCs and how these unnatural structures are resolved still remain to be unclear.

Analyses of data generated in prokaryotes revealed the existence of mechanisms of active DPC removal and suggested that more than one repair pathway can be involved in the repair of these lesions. There are couple of possible hypotheses , one being the protein part of the DPCs is to be degraded/ cleaved specifically by a protease, and other Nucleotide excision repair (NER), the repair mechanism in which a damaged base is cleaved and replaces by a regular nucleotide bases. However all the hypotheses lack a proper experimental system. It has been previously reported that DNA replication machinery fails to replicate the DNA in the presence of DPCs revealing the fact of stalling the DNA replication fork at the Site of DPCs. However the exact mechanisms how an ongoing replication fork can bypass these DPCs is largely unknown due to lack of a proper in-vivo or in-vitro experimental system.

In the present study we are developing an in-vitro system to monitor stalling or bypass of DNA replication machinery at the site of DPCs. To accomplish the above task a suicidal DNA substrate is designed to trap a protein irreversibly. DNA binding or DNA modifying proteins can be used to crosslink to the DNA of known sequence. This cross-linked DNA-protein substrate is further purified and can be used as a template for the DNA replication. By using different DNA polymerase including some of the specialized TLS (translesion synthesis) polymerase which specifically replicates damaged DNA; it is possible to check bypass of these DPCs. In future these experiments will also reveal whether a specific polymerase is involved to resolve this kind of naturally occurring cross links.

Baker DJ, Wuenschell G, Xia L, Termini J, Bates SE, Riggs AD, O'Connor TR (2007) Nucleotide excision repair eliminates unique DNA-protein cross-links from mammalian cells. J Biol Chem 282(31):22592-22604.

Barker S, Weinfeld M, Zheng J, Li L, Murray D (2005) Identification of mammalian proteins cross-linked to DNA by ionizing radiation. J Biol Chem 280(40):33826-33838.

Haracska L, Unk I, Johnson RE, Johansson E, Burgers PM, Prakash S, Prakash L (2001) Roles of yeast DNA polymerases δ and ζ and of Rev1 in the bypass of abasic sites. Genes Dev 15(8):945-954.

Nakano T, Morishita S, Terato H, Pack SP, Makino K, Ide H (2007)Repair mechanism of DNA-protein cross-link damage in Escherichia coli. Nucleic Acids Symp Ser (Oxf) 51:213-214.

Supervisor: Lajos Haracska
E-mail: yathish@brc.hu

Data to the analysis of paleopathology of the Medieval Age in the region between the Danube and Tisza rivers (preliminary report)

János Balázs

Department of Anthropology, University of Szeged, Szeged, Hungary

Human paleopathology can be defined as the study of diseases in ancient populations by the examination of human remains (dry skeletons and mummies). However, the anthropological study of diseases in antiquity is very complex and challenging. The interplay of many variables – host resistance, pathogen virulence, cultural practices, ecological settings, malnutrition, crowding – needs to be considered.

The aim is of the investigation is to perform a complete comparative analysis of populations dated to the 11th-17th centuries in the region between the Danube and Tisza rivers based on the presentation and evaluation of the paleopathological alterations.

The following series were included in this study: Nyárlőrinc-Hangár utca, Kalocsa-Szentháromság tér, Kalocsa-Belvárosi Iskola,

Bácsalmás-Mosztonga, Dunapataj-Szent Tamás domb. The samples contain the remains of 756 individuals (163 males, 54 females, 207 undetermined, 332 subadults). This skeletal material is collected at the Department of Anthropology, University of Szeged.

The specimens have been analysed for the determination of the age at death and sex and scored for the measurements. Concerning the pathological conditions, the macro-morphological examination was completed - in some cases - with radiological analyses. In one case the molecular analysis was carried out to estimate the DNA of *Mycobacterium tuberculosis.* (This investigation was made at the München University - Institute of Pathology.)

The following disorders have been identified: traumatic lesions, specific and non-specific infections, haematological anomalies, joint diseases, bone-tumor and tumor-like anomalies, developmental disorders, and enthesopathies.

It is the most important to highlight the cases of skeletal tuberculosis (one case) and –syphilitic lesions (two cases) (Nyárlőrinc-Hangár utca; Pálfi et al. 1997; Balázs et al. 2005), for these diseases were among the most important selective factors in human populations in antiquity. In the sample Dunapataj-Szent Tamás domb, the frequency of the developmental anomalies is very significant by the reason of endogamy (Balázs and Marcsik 2007b).

In the Nyárlőrinc-Hangár series (11th-17th centuries; V. Székely 1987), there was excavated a partly mummified foetus which was buried in a crock at the edge of this cemetery and dated to 19th century on the basis of a copper coin which was put into the crock (Balázs and Bölkei 2007a).

This presentation is only a preliminary result.

Balázs J, Bölkei Z, V. Székely Gy (2005) A Nyárlőrinc-Hangár utcai széria embertani feldolgozásának eredményei, Cumania 21., Kecskemét, 2005., pp. 57-82.
Balázs J, Bölkei Z (2007a) Partly mummified foetus, VI World Congress on Mummy Studies, Teguise (Spain), February 20-24., 2007., p. 277.
Balázs J, Marcsik A (2007b) Paleopatológiai vizsgálatok egy középkori temető embertani anyagában, V. Kárpát-medencei Biológiai Szimpózium, 2007. szeptember 20-22., Konferenciakötet, pp. 331-334.
Pálfi Gy, Panuel M, Molnár E (1997) Paleoradiologic Study of a 17th Century Case of Treponematosis (Nyárlőrinc, Hungary). Acta Biol Szeged. 42:113-122.
V. Székely Gy (1987) Kun eredetű tárgyak és kulturális elemek Nyárlőrinc középkori temetőjében. Kézirat. Kecskemét.

Supervisor: Antónia Marcsik
E-mail: janos.balazs@gmail.com

Functional characterization of the plant SET protein: from phosphatase inhibition to heat stress tolerance

Judit Bíró

Institute of Plant Biology, Biological Research Center, Hungarian Academy of Sciences, Szeged, Hungary

Even small environmental changes can induce expression or repression of hundreds of genes in plants, contributing to their endless adaptation to the changing environment. Regulation of such a synchronized genomic event has to employ chromatin remodelling – a process that involves post-translational modifications of histones. One of the putative proteins involved in the regulation of histone modification patterns is SET. SET, belonging to the NAP/SET family of potential histone chaperones, is a multifunctional protein involved in very diverse cellular processes in mammals.

It was previously shown that human SET inhibits protein phosphatase 2A (PP2A) (Li et al. 1996), a major serine/threonine phosphatase both in plants and animals. It was also demonstrated that SET is associated with transcriptionally active loci in response to heat shock in *Drosophila melanogaster*, and these regions encoding heat shock proteins are marked with phosphorylation of histone H3 at serine 10 (Nowak et al. 2003).

Although the members of the NAP/SET family are well characterized proteins in animals (reviewed in Park and Luger 2006), we have little information on the plant NAP1 (nucleosome assembly protein1)-related proteins. The aim of our studies was hence the characterization of the *Arabidopsis* SET protein.

Our results revealed that the recombinant *Arabidopsis thaliana* SET protein exhibited inhibitory effect on the activity of purified preparations of rabbit PP2A and PP1 (protein phosphatase 1) catalytic subunits against a phospho-histone substrate. In addition, purified SET inhibited the dephosphorylation of histone H3 at serine 10 position by immunoprecipitated *Arabidopsis* PP2A and interacted *in vitro* with purified calf histone H3.

Phosphorylation of serine 10 on histone H3 is coupled with two opposite chromatin states: it is associated with mitotic chromosome condensation, while it occurs also during interphase in correlation with transcriptionally active loci (Johansen and Johansen 2006). Since our results suggest that SET may have a role in the maintaining of this kind of histone modification in plants, we propose a role for SET in transcriptional regulation. The verification of the involvement of the *Arabidopsis* SET in gene expression control, however, needs further investigations.

We also demonstrated that the subcellular localization of SET was influenced by a heat stress treatment at 45°C. In response to heat, SET accumulated in the nucleus, while under standard conditions it is located predominantly in the cytosol. Interestingly, other types of stresses including heat stress at lower temperature (37°C), salt stress, heavy metal stress or genotoxic stress did not cause the nuclear accumulation of SET, suggesting a specific role for SET in certain plant stress responses.

Taken together, the *Arabidopsis* SET protein is a potent inhibitor of animal and plant phosphatases and may have a role in heat shock tolerance as indicated by its altered (nuclear) localization in response to a 1h 45°C treatment. Thus, in the light of our results we can presume that the investigation of SET can be of practical importance, since it might have a role in the stress tolerance of plants. This hypothesis is currently investigated in SET-overexpressing transgenic plants.

Johansen KM, Johansen J (2006) Regulation of chromatin structure by histone H3S10 phosphorylation. Chromosome Res 14(4):393-404.
Li M, Makkinje A, Damuni Z (1996) The myeloid leukemia-associated protein SET is a potent inhibitor of protein phosphatase 2A. J Biol Chem 19:11059-11062.
Nowak SJ, Pai CY, Corces VG (2003) Protein phosphatase 2A activity affects histone H3 phosphorylation and transcription in Drosophila melanogaster. Mol Cell Biol 17:6129-6138.
Park YJ, Luger K (2006) Structure and function of nucleosome assembly proteins. Biochem Cell Biol 4:549-558.

Supervisor: Attila Fehér
E-mail: bzsulesz@gmail.com

Cross-talk between cannabinoid CB_1 and $GABA_B$ receptors in rat brain hippocampus

Resat Cinar[1], Tamas F. Freund[2], Istvan Katona[2], Ken Mackie[3], and Maria Szucs[1]

[1]Institute of Biochemisty, Biological Research Center, Hungarian Academy of Sciences, Szeged, Hungary, [2]Institute of Experimental Medicine, Hungarian Academy of Sciences, Budapest, Hungary, [3]Department of Psychology and Brain Sciences, Indiana University, Bloomington, IN, USA

Cannabinoid CB_1 and the metabotropic $GABA_B$ receptors have been shown to display similar pharmacological effects and co-localization in certain brain regions. Previous studies have reported a functional link between the two systems. As a first step to investigate the underlying molecular mechanism, here we show cross-inhibition of G-protein signaling between $GABA_B$ and CB_1 receptors in rat hippocampal membranes. The CB_1 agonists R-Win55,212-2 displayed high potency and efficacy in stimulating Guanosine-5'-*O*-(3-[^{35}S]thio)triphosphate, [^{35}S]GTPγS binding. Its effect was completely blocked by the specific CB_1 antagonists AM251 suggesting that the signaling was via CB_1 receptors. The $GABA_B$ agonist baclofen and SKF97541 also elevated [^{35}S]GTPγS binding by about 60%, with potency values in the micromolar range. Phaclofen behaved as a low potency antagonist with an an $ED_{50} \approx 1$ mM . However, phaclofen at low doses (1 and 10 nM) slightly but significantly attenuated maximal stimulation of [^{35}S]GTPγS binding by the CB_1 agonist Win55,212-2. The observation that higher concentrations of phaclofen had no such effect rule out the possibility of its direct action on CB_1 receptors. The pharmacologically inactive stereoisomer S-Win55,212-3 had no effect either alone or in combination with phaclofen establishing that the interaction is stereospecific in hippocampus. The specific CB_1 antagonist AM251 at a low dose (1 nM) also inhibited the efficacy of G-protein signaling of the $GABA_B$ receptor agonist SKF97541. Cross-talk of the two receptor systems was not detected in either spinal cord or cerebral cortex membranes. It is suggested that the interaction might occur via an allosteric interaction between a subset of $GABA_B$ and CB_1 receptors in rat hippocampal membranes. Supported by NKTH DNT 08/2004 and OTKA TS 049817 research grants.

Supervisor: Maria Szucs
E-mail: szucsm@brc.hu

Functional analysis of *Drosophila melanogaster* histone H4 specific acetylase complex and its role in regulating chromatin structure

Anita Oriana Ciurciu

Institute of Biochemisty, Biological Research Center, Hungarian Academy of Sciences, Szeged, Hungary

Numerous enzymes and protein complexes are known to bring about changes in the state of chromatin by different mechanisms with resultant effects on gene expression. One class of complexes including the yeast SWI/SNF and a number of others from various organisms, alter the DNA packaging in an ATP-dependent manner. Another class of chromatin structure regulating factors acts by covalently modifying histone proteins. The various modifications include phosphorylation, ubiquitination, ADP-ribosylation, methylation, sumoylation and frequently acetylation, catalyzed by histone acetyltransferases (HATs). In many cases HAT enzymes are components of complexes which also contain among others, ADA-type adaptors.

Recently our laboratory, in parallel with several others, has showed that contrary to the single ADA2 adaptor protein present in *Saccharomyces cerevisiae*, different GCN5-containing HAT complexes of *Drosophila melanogaster* cells contain two related ADA2 proteins encoded by genes referred to as *dAda2a* and *dAda2b*. In several other metazoan organisms, including mouse, human and Arabidopsis, there

Volume 52(2):333-356, 2008
Acta Biologica Szegediensis
http://www.sci.u-szeged.hu/ABS

are also two ADA2-type coactivators. Biochemical separation of ADA2-containing *D. melanogaster* complexes indicated that dADA2a is present in a smaller (0.8 MDa) and dADA2b in a larger (2MDa) complex which corresponds to the Drosophila homologue of yeast SAGA complex. In a number of independent studies it was shown that in the absence of dADA2b or dGCN5, in other words, in the absence of functional SAGA, the acetylation of histone H3K9 and K14 is greatly reduced, while the H4K8 acetylation is not affected.

In this work we provide evidence that the dADA2a protein is a specific component of the smaller *Drosophila* HAT complex which during the course of this work became identified as ATAC. We demonstrate the genetic interaction between *dAda2a* and *dGcn5* genes and show they role in H4 acetylation. Finally, we describe the functional interplay between components of the ATAC complex and ATP-dependent nucleosome remodeling ISWI-containing NURF complex.

We provide several lines of evidence for the functional linkage between dADA2a and dGCN5. We show their physical and genetic interaction by yeast two hybrid assays and by analyzing the phenotype of specific single and double mutants, respectively. The loss of either *dGcn5* or *dAda2a* function results in similar chromosome structural and developmental defects. *dGcn5/dAda2a* double-null mutants or a combination of *dAda2a* and *dGcn5* hypomorph alleles result in a phenotype stronger than that of either of the two mutations alone. The overexpression of dGCN5 protein by the use of an act-GAL4 driver in *dAda2a* mutant background results in a partial rescue. Furthermore, the phenotypic features of *dAda2a* mutants indicate a developmental block at the time of larva-pupa transition similarly as it was shown by others for *dGcn5* mutants. In accord with this, by analyzing the puff formation at sites containing ecdysone induced genes and using RT-PCR and Q-PCR to measure specific mRNA levels we demonstrate that the expression of several ecdysone-induced genes such as BR-C, Eip74 and Eip75 are downregulated in the absence of dADA2a protein.

Immunostaining of *Drosophila* polytene chromosome and Western blot analysis revealed a significantly decreased level of K5 and K12 acetylated histone H4 in *dAda2a* and *dGcn5* mutants, while the acetylation established by dADA2b-containing GCN5 complexes at H3K9 and K14 was unaffected. These results, for the first time in the literature, clearly establish the *D. melanogaster* ATAC as a histone H4-specific HAT complex.

In a set of independent experiments we showed functional interaction between the histone modifying ATAC and the nucleosome remodeling NURF complexe. Using appropriate mutants strains we showed that there is genetic interaction between genes encoding ATAC subunits and the NURF subunit ISWI. In addition, immunostaining of polytene chromosomes with dADA2a-specific Ab revealed that the ADA2a binding to *Iswi* chromosomes was strongly reduced. In agreement with this data, immunoblot analysis and chromosome immunostaining showed a significant decreased of K12 acetylated H4 level of salivary gland polytene chromosomes of *Iswi* and *Nurf301* mutants.

Taken together, these results strongly suggest a functional interaction of nucleosome remodeling and histone acetyltransferase complexes. Our data demonstrate that the function of NURF complex is required for the binding of ATAC to chromatin and for subsequent acetylation of H4K12 residues.

Carré C, Ciurciu A, Komonyi O, Jacquier C, Fagegaltier D, Pidoux J, Tricoire H, Tora L, Boros I, Antoniewski C (2007) The Drosophila NURF remodelling and the ATAC histone acetylase complexes functionally interact and are required for global chromosome organization. EMBO reports. Published online: 14 December 2007

Ciurciu A, Komonyi O, Pankotai T, Boros I (2006) The Drosophila histone acetyltranferase Gcn5 and transcriptional adaptor Ada2a are involved in nucleosomal histone h4 acetylation. Mol Cell Biol (24):9413-9423.

Pankotai T, Komonyi O, Bodai L, Ujfaludi Z, Muratlogu S, Ciurciu A, Tora L, Szabad J, Boros I (2005) The homologous *Drosophila* transcriptional adaptors ADA2a and ADA2b are both required for normal development but have different functions. Mol Cell Biol (18):8215-8227.

Supervisor: Imre Boros
e-mail: canita@brc.hu

Study of *Medicago truncatula* RRK1 receptor-like cytoplasmic kinase interacting proteins

Csilla Fodor-Dunai

Institute of Plant Biology, Biological Research Center, Hungarian Academy of Sciences, Szeged, Hungary

Small GTP-binding proteins of the Rho family play a role as regulators of signal transduction in plants. These proteins called ROP („Rho of plant") participate in key cellular events including the determination of polar growth, vesicular trafficking, stress and hormone responses or cell wall synthesis. ROPs act as molecular switches cycling between a GDP-bound inactive and a GTP-bound active state. In our group an alfalfa receptor-like cytoplasmic kinase, termed RRK1, has been identified by yeast two-hybrid screen as an interacting partner of the active MsROP3 GTPase. RLCKs have no extracellular and/or transmembrane domains and are localized in the cytoplasm. The function of the RLCKs is not well understood; they have hypothetical roles in RLK-dependent signaling. Our finding was among the first indications that Rop GTPases may directly influence kinase activity in plants similarly as in animals.

In order to identify downstream signaling events of RRK1, our group applied the yeast two-hybrid system with a cDNA library made from 4-day-old root nodules on *Medicago truncatula* roots, using RRK1 as bait. Several clones were identified and sequence analyzed. The sequence comparison revealed that one of our clones carries a plant specific guanine nucleotide exchange factor (GEF) domain. Conversion of Rops from the inactive GDP-bound to the active GTP-bound form is catalyzed by GEFs. In *Arabidopsis*, the ROPGEF family has 14 members, which contain a plant-specific central, highly conserved catalytic domain termed PRONE (Plant Specific ROP Nucleotide Exchanger) or formerly DUF315, and variable N-and C terminal regions.

Why is so important to have a kinase that is capable to interact with a ROP GTPase as well as a ROPGEF? GEF proteins have the potential to transfer signals from receptors to ROP GTPases. A huge family of receptor-like kinases (RLKs) has been found in plants but their downstream signaling events are hardly known. Similarly, it is not known what are the upstream signaling steps resulting in ROP activation. What we currently know is that a tomato protein called KPP (kinase partner protein) has been identified as binding partner of the cytosolic domains of the pollen-specific RLKs, LePRK1 and LePRK2. This KPP protein is a homolog of *Arabidopsis* ROPGEF1 and is phosphorylated in vitro by LePRK1. Our results indicate that a further type of kinase (RLCK) might be involved linking ROP- and RLK-mediated signaling pathways.

In order to prove this hypothesis, as a first step, we showed the interaction between the MtGEF and MsROP3 proteins. In our yeast two-hybrid experiments, MtGEF displayed strong interaction with the non-nucleotide bearing wild-type and the constitutive active (CA) mutant of MsROP3. Wild type, CA- and dominant negative (DN) mutants of MBP-fused MsROP3 and His tagged-MtGEF fusion proteins expressed in *E. coli* were used for pull down assay. With this in vitro protein-protein interaction assay we were able to confirm our yeast results. Then the expression level of MtGEF was investigated in different *Medicago truncatula* tissue types by QRT-PCR, but it showed very low expression in almost all tissues therefore a correlation with MsROP3 or RRK1 expression could not be made. Recently, the full length MtGEF cDNA sequence has been amplified by PCR from a *Medicago truncatula* cDNA library and cloned into various expression vectors. In the future we would like to confirm our previous observations with this full length form as well as to further characterize the potential signaling interactions. This will include the determination of GEF activity toward MsROP3 and the RRK1 kinase activity towards MtGEF. We suppose that MtGEF could be an elusive link between RLKs and ROPs in a plant-specific signal transduction mechanism that also includes a ROP-dependent feedback regulation of GEF activity through RRK1.

Berken A, Thomas C, Wittinghofer A (2005) A new family of RhoGEFs activates the Rop molecular switch in plants. Nature 436:1176-1180.
Fehér A, Manuela J, Fodor Cs, Dorjgotov D (2008) Regulation of ROP GTPase signalling at the gene expression level. The Open Plant Science Journal 2008
Gu Y, Li S, Lord E, Yang Z (2006) Members of a novel class of Arabidopsis Rho guanine exchange factors control Rho GTPase-dependent polar growth. Plant Cell18:366-381.
Szűcs A, Dorjgotov D, Ötvös K, Fodor Cs, Domoki M, Györgyey J, Kaló P, Kiss GB, Dudits D, Fehér A (2006) Characterization of three Rop GTPase genes of alfalfa (medicago sativa L). Biochim Biophys Acta 1759:108-115.

Supervisor: Attila Fehér
E-mail: csilla.fodor@gmail.com

Phylogeny of Alloxysta (Hymenoptera, Cynipoidea, Figitidae, Charipinae) species – morphology vs. molecules

Dávid Fülöp

Institute of Genetics, Biological Research Center, Hungarian Academy of Sciences, Szeged, Hungary

Members of the figitid genus Alloxysta (Förster 1869) are parasitoids of hymenopteran natural enemies of economically important aphid species. Therefore these hyperparasitoid species have large impact on the biological control of insect pests. Due to their minute size most of the morphological characters which are widely used in the taxonomy of other cynipoid taxa, are variable and highly reduced. Most of the species are hardly distinguishable morphologically and it is impossible to determine if the variablility is intra- or interspecific. According to some authors there are only a few, very variable and generalist Alloxysta species whereas others suggest that the genus containes much more species which are less variable but more specialized. Current phylogenetic relationships of the genus are based on the same, often questionable morphological characters. So far no studies were carried out using molecular markers determining species limits and resolving the phylogeny of the genus. 20 morphological characters were widely used for Alloxysta species determination. On the basis of three characters: presence of the propodeal carina, pronotal carina, radial cell, the genus might be divided into six species groups. Mapping morphological characters on a molecular-based phylogeny enabled examination of character evolution. In this study, 20 morphological characters from western Palaearctic Alloxysta were mapped on a phylogenetic tree reconstructed from region of the cytochrome-c-oxidase I (COI) and the ribosomal 28S D2 genes analised with parsimony Bayesian, maximum-likelihood and distance based methods. The COI and 28S D2 trees were congruent. The above mentioned morphological characters may have evolved in parallel in different species groups of Alloxysta and, taken alone, may be unsuitable for a subgeneric division of the genus, however, are suitable for species differentiation.

Supervisor: Zsolt Pénzes
E-mail: ocypus@gmail.com

Volume 52(2):333-356, 2008
Acta Biologica Szegediensis
http://www.sci.u-szeged.hu/ABS

The effects of drought on changes in photosynthesis, hormone levels and grain yield in wheat (*Triticum aestivum L.*)

Adrienn Guóth

Department of Plant Biology, University of Szeged, Szeged, Hungary

Wheat is one of the main crops consumed by humans and it is cultivated in different environments. Under the temperate zone early-summer droughts are increasingly frequent and limit grain yield since they coincide with the grain filling period. There are several physiological traits related to water stress, and scientists make considerable effort to find direct correlations between these parameters and grain yield to facilitate the selection of cultivars for drought tolerance.

Photosynthesis is one of the main metabolic processes determining crop production. Chlorophyll fluorescence is a tool for monitoring the function of the photosynthetic apparatus, changes in response to water stress. The effect of drought on photosynthesis has long been a controversial subject and it is still not clear whether chlorophyll a fluorescence parameters are good indicators for drought sensibility (Flexas et al. 2002). The plant hormone abscisic acid (ABA) plays a major role in plant responses to drought stress, facilitating plant survival (Zahng et al. 2006).

A comparison was made between changes of the parameters mentioned above, in seedling stage under osmotic stress and in reproductive growth phase under soil drought in two Hungarian (*Triticum aestivum* L. cv. MV Emese (resistant) and GK Élet (sensitive)) and two internationally known (*Triticum aestivum* L. cv Plainsman (resistant) and Cappelle Desprez (sensitive)) wheat cultivars.

Our object was to compare the effects of osmotic and drought stress to find correlation between these treatments, and to compare the effects of water deficit on different physiological parameters, hormone levels (ABA and cytokine), grain yield and storage protein content in tolerant and sensitive varieties in the grain filling period. The water status parameters, CO_2 assimilation, chlorophyll *a* (chl*a*) fluorescence, pigment content and hormone levels were determined as a function of the development under osmotic stress in seedling stage (from germination to the 21st day after germination) and under water deficit in the grain filling period (from booting stage to the 24th day after anthesis).

Our results suggest that the photosynthetic parameters measured under osmotic stress are not comparable with those measured in flag leaves in the grain filling period. Different genotypes showed unique diversity in changes of these parameters, but common tendencies between the tolerant or sensitive cultivars were not found.

Pre- and post-anthesis soil drought did not result in characteristic modifications in PS II photochemistry of flag leaves in dark and light-adapted leaves, demonstrating that in this experiment these parameters did not correlate with sensitivity. Plants showed early senescence under water deficit. We found that sensitivity of the generative organs could be responsible for the higher decrease in grain yield. Changes of the ABA levels in the kernels showed a differing tendency: sensitive genotypes maintained high hormone levels, which can be unfavourable for grain growth. The different storage protein fractions of the mature grains were not significantly modified by drought, which confirm earlier results (Panozzo et al. 2001), but the gliadin to glutenin ratio increased significantly in one of the tolerant varieties.

Our results indicate that when the sensitivity of a genotype to drought stress are defined whole plants responses have to be taken into consideration. Responses of the vegetative and generative organs can be different and sensitivity of the generative phase and the fertilization process to water deficit may overwrite the efficient acclimation of vegetative organs.

Flexas J, Escalona JM, Evain S, Gulías J, Moya I, Osmond CB, Medrano H (2002) Steady-state chlorophyll fluorescence (Fs) measurements as a tool to follow variations of net CO_2 assimilation and stomatal conductance during water-stress in C_3 plants. Physiol Plant 114:231-240.

Panozzo JF, Eagles HA, Wootton M (2001) Changes in protein composition during grain development in wheat. Aust J Plant Phys 52(4):485-493.

Zhang J, Jia W, Yang J, M Ismail A (2006) Role of ABA in integrating plant responses to drought and salt stress. Field Crosp Res 97:111-119.

Supervisor: László Erdei
E-mail: guotha@bio.u-szeged.hu

Microarray and interaction network based identification of genes involved in germ cell development in *Drosophila melanogaster*

László Henn

Institute of Genetics, Biological Research Center, Hungarian Academy of Sciences, Szeged, Hungary

Embryonic germ cell development of fruit fly *(Drosophila melanogaster)* depends on the germ plasm, the most posterior part of the egg cytoplasm. The germ plasm contains all factors which are necessary to induce germ cell fate. It has a characteristic distribution of proteins and contains a large number of localized RNA species, too (Williamson et al. 1996). Certain gene products being present in germ plasm might play crucial roles in germ cell determination and its subsequent development such as the germ cell migration, the passage through the embryonic midgut, and gonad formation. *Drosophila* is one of the most accepted model organism of germ cell research in the post sequencing era since numerous large Drosophila genomic databases are available for researchers.

We have developed and apply a mircroarray-based method to identfy germ plasm enriched RNA-s. We performed a series of experiments on different microarry platforms to compare the RNA content of numerous germ plasm-less, germ plasm overexpressing and wildtype conditions. Collating our datasets with the list of the known germ plasm enriched trancripts, we found that germ plasm overexpressing vs. wilde type comparison is the most appropriate method to identify new germ plasm enriched transcripts. In such comparisons 380 transcripts showed at least four times increase in germ plasm overexpressing condition. These transcripts were chosen for further analysis to confirm their germ plasm localization by making use of fluorescent RNA in situ hybridization (Lecuyer et al. 2007) on early *Drosophila* embryos. To be able to accomplish such a large number of in situ hybridisations we have developed a suitable PCR based single strand DNA labeling method.

Another approach we used, is a network based identification of novel germ plasm factors. We built up and investigated a germ plasm specific gene interaction network. First, we searched RNA localization databases (BDGP, Fly-FISH) and original publication for genes whose transcripts are exclusively or highly enriched in the germ plasm (Szuperák et al. 2005). This way, 136 as we called "original" germ line specific genes were found. Then we identified their primary genetic and yeast two-hybrid interactors by using the BioGRID database. Based on the GEO database, those primary interactors which are not expressed at early embryonic stages were filtered out. Finally, we constructed a gene interaction network which indicates all known interactions (325) among the original germ line specific factors (136) and primary interactors (325). We assume that the number of interactions of a given gene may mirror its importance in the network. Genes with large number of interactions, also called hubs, can refer to a central role of a given gene that have a good chance to show phenotype when it is mutated. We confirm this hypothesis by RNAi induced phenocopy analysis. We are currently analyzing the germ line specific phenocopies of a representative group of hubs as well as of the low connectivity control genes. The phenocopy of the RNA silencing is followed by the time laps video microscopy which allows distinguishing different type phenocopies: the complete absence or decreased number of germ cells, or its migration defects.

BDGP, Patterns of gene expression in *Drosophila* embryogenesis. http://www.fruitfly.org/cgi-bin/ex/insitu.pl
BioGRID, General repository for Interaction Datasets. http://www.thebiogrid.org/
Fly-FISH, A Database of *Drosophila* embryo mRNA localization patterns. http://fly-fish.ccbr.utoronto.ca/
GEO: Gene Expression Omnibus. http://www.ncbi.nlm.nih.gov/geo/: GEO Accession: GSE3955
Lecuyer E, Krause HM (2007) Global analysis of mRNA localization reveals a prominent role in organizing cellular architecture and function. Cell 131(1):174-184.
Szuperák M, Zvara Á, Erdélyi M (2005) Identification of germ plasm-enriched mRNAs in *Drosophila melanogaster* by the cDNA microarray technique. Gene Expr Patterns 5:717-723.
Williamson A, Lehmann R (1996) Germ cell development in *Drosophila*. Annu Rev Cell Biol 12:365-391.

Supervisor: Miklós Erdélyi
E-mail: henn@brc.hu

Oxidative stress, intrauterine retardation, modes of delivery

Zsuzsanna Hracskó

Department of Biochemistry and Molecular Biology, University of Szeged, Szeged, Hungary

Oxidative stress arises when the balance between oxidants and antioxidants is disturbed. The source of free radicals is the unpaired electron of molecular oxygen, which makes it unstable and electrically charged. In the lack of antioxidant molecules and enzymes, free radicals target lipids, proteins and DNA. Oxidative damage to DNA is a result of interaction of the nucleic acid with hydroxyl radical that generates strand breaks on the DNA. Oxidative stress is a physiological event in the fetal-to-neonatal transition.

The steadily increasing global rate of cesarean sections (CS) has become one of the most debated topics in maternity care. The mode of delivery may have a considerable effect on the state and health of the newborn. CS is a surgical intervention with potential hazards for both mother and child. The opinions of obstetrician-gynecologists regarding normal vaginal delivery (VD) and CS are highly contradictory. The results of previous studies display great differences. We have approached this question from a consideration of oxidative stress and set out to determine a wide range of parameters relating to the oxidative status of neonates born via VD or undergoing CS.

We conclude that the mode of delivery does not have a serious effect on the level of free radical damage if there is no emergency situation. The elective CS does not have an advantage over VD with respect to oxidative stress (Hracsko et al. 2007).

Intrauterine growth retardation (IUGR) is a complication of pregnancy. A newborn with IUGR weighs less than do 90% of all other newborns of the same gestational age. The reported incidence of IUGR ranges between 7 and 10 per cent. This abnormality is associated with increased level of morbidity and mortality, and deformation of the umbilical cord.

The mechanism of development of IUGR has still not been appropriately described, although it is most probably a consequence of an abnormal fetomaternal blood circulation. Accordingly we have carried out examinations on umbilical cord blood and endothelium in order to establish how the antioxidant status of full-term IUGR infants changes and whether the results indicate significant oxidative stress. We compared the antioxidant status and the level of lipid peroxidation (LP) of the umbilical blood in healthy mature neonates and in IUGR neonates. The level of LP was high in the IUGR group while the antioxidant enzyme activities and the levels of antioxidants were significantly

lower in the IUGR group. Damage of proteins and DNA was slightly, but non-significantly higher in the IUGR group. Neonates with IUGR seem to have significant deficiency in antioxidant defense. IUGR is correlated with significant oxidative stress (Hracsko et al 2008).

Nitrogen monoxide (NO) is produced by nitric oxide synthases. The free radical nature of NO and peroxynitrite, renders NO a potent pro-oxidant molecule able to induce oxidative damage and potentially harmful toward cellular targets. Reactive nitrogen species modify amino acid residues, inhibit enzymatic activities, induce lipid peroxidation and deplete cellular antioxidant levels. These features may be associated with the development of different pathologies (Lyall et al. 1996) NO has diverse physiological roles and also known as a vasodilatator.

We investigated the NO_2 and peroxynitrite level and the expression of eNOS by RT-PCR in the umbilical cord of IUGR neonates.

Our results support the hypothesis that increased NO production may be a compensatory response to improve blood flow in the umbilical cord. This increased eNOS expression and hence increased NO production in the fetal-placental vasculature may be an adaptive response to the increased resistance pathological pregnancies.

Hracsko Z, Safar Z, Orvos H, Novak Z, Pal A, Varga IS (2007) Evaluation of oxidative stress markers after vaginal delivery or Caesarean section In Vivo 21(4):703-706.

Hracsko Z, Orvos H, Novak Z, Pal A, Varga IS (2008) Evaluation of oxidative stress markers in neonates with intra-uterine growth retardation Redox Rep 13(1):11-16.

Lyall F, Greer IA, Young A and Myatt L (1996) Nitric oxide concentrations are increased in the feto-placental circulation in intrauterine growth restriction Placenta 17 (2-3):165-168.

Supervisor: Ilona Szőllősi Varga
E-mail: hracsko@bio.u-szeged.hu

Characterization of a family of Arabidopsis receptor-like cytoplasmic kinases (RLCK class VI)

Manuela Jurca, Attila Fehér

Institute of Plant Biology, Biological Research Center, Hungarian Academy of Sciences, Szeged, Hungary

Arabidopsis possess a large family of receptor-like kinases (RLKs) with more than 600 members (Shiu et al. 2004). Approximately 25% of the Arabidopsis RLKs contain only a kinase domain with no apparent signal sequence or transmembrane region and thus were collectively named as receptor like cytoplasmic kinases (RLCKs). Arabidopsis RLCKs can be subdivided into 10 classes with 193 protein coding genes alltogether.

Concerning the function of plant RLCKs, at the present only few members have been characterized and it is very likely that they play major role in the perception and transmission of external signals perceived by RLKs (Zhou et al. 1995; Murase et al. 2004). Moreover, based on our previous investigations and recent literature data, we suppose that kinases belonging to RLCK class VI in Arabidopsis are Rop GTPase targets. Plant specific Rop GTPases are versatile molecular switches in many processes during plant growth, development and responses to the environment and thus a possible implication of RLCKs in these Rop-dependent signal transduction pathways is in discussion.

As part of our investigations related to Rop GTPase-mediated signal transduction in plants, we started to characterize the whole RLCK VI protein family in Arabidopsis. This is underway by studying the genes as well as the encoded proteins. A detailed analysis of the coding sequences and the gene expression pattern of all 14 RLCK_VI members have already been accomplished. Sequence comparison and phylogenetic analysis revealed that gene duplication played a significant role in the formation of this kinase family and allowed the separation of the 14 RCLK VI kinases into two groups with seven members each (A1 to A7 and B1 to B7). It was established that, several members have an N-terminal UspA ("universal stress protein") domain (group B members) or an N-terminal serine –rich region (group A members) (Jurca et al. 2008).

In order to formulate a possible role of AtRLCK_VI kinases, real-time quantitative reverse transcription-polymerase reaction (qRT-PCR) was used to determine relative transcript levels in the various organs (root, rosette leaves, cauline leaves, inflorescence stem, flower buds, open flowers, siliques. exponentially dividing cultured cells) of the Arabidopsis plant as well as under a series of abiotic stress/ hormone (osmotic, sugar, salt stress, oxidative stress, cold and hormone treatment) treatments in seedlings. The obtained data revealed the differentially regulated expression of the genes, which is in agreement with a high variability of sequence elements in their promoter regions. Thus, the encoded kinase proteins may be involved in a wide variety of signal transduction pathways related to plant development and stress responses (Jurca et al. 2008).

After characterizing the expression of the At-RLCK VI genes, it was imperative to study the proteins itself to find a possible function of these cytoplasmic kinases. Our previous data as well as recent publications indicated that some of the RLCK_VI members can interact with Rop GTPases. Therefore we decided to establish an RLCK_VI-to-Rop interaction matrix including 10 members of both families (4 RLCK_VI and one Rop genes could not be cloned due to various reasons) using the yeast two-hybrid system. As controls, RLCK class IV, VII and IX members as well as alfalfa RLCK_VI kinases and Rop GTPases were also involved. In general it could be stated that members of RLCK_VI group A showed interaction with several Rops while that of group B not. The biological role of this interaction needs to be determined. In this direction we further proceed with the in vitro characterization of the activity of these kinases as well as with the produc-

tion of transgenic plants over-expressing or silencing RLCK_VIA genes. The identification of altered phenotypes in these transgenic plants can be very helpful in order to determine the developmental role of RLCK class VI members in Arabidopsis.

Jurca M, Bottka S, Feher A (2008). Characterization of a family of Arabidopsis receptor-like cytoplasmic kinases (RLCK class VI). Plant Cell Reports 27:739-748.
Murase K, Shiba H, Iwano M, Che F, Watanabe M, Isogai A, Takayama S (2004) A membrane-anchored protein kinase involved in Brassica self-incompatibility signaling. Science 303:1516-1519.
Shiu S, Karlowski W, Pan R, Tzeng Y, Mayer K, Li W (2004) Comparative analysis of the receptor-like kinase family in Arabidopsis and rice. Plant Cell 16:1220-1234.
Zhou J, Loh Y, Bresan R, Martin G (1995) The tomato gene Pti1 encodes a serine/threonine kinase that is phosphorylated by Pto and is involved in the hypersensitive response. Cell 83:925-935.

Supervisor: Attila Feher
E-mail: manujurca@yahoo.com

Structural analysis of antimicrobial peptides by molecular dynamics methods

Ádám Kerényi

Institute of Biophysics, Biological Research Center, Hungarian Academy of Sciences, Szeged, Hungary

Cationic antimicrobial peptides (AMPs) play an important role in the innate immune system. There are several experimental methods for investigating the secondary structures of these small molecules but they are not precise enough to provide reliable information. Accordingly, we chose molecular dynamics methods to investigate the structural properties of some AMPs. Three types of peptides were studied: peptides rich in His (alloferon-1 and -2), peptides rich in Trp and Arg (indolicidin and tritrpticin) and cyclic peptides containing a disulfide bridge (bactenecin and tigerinin-1).

Alloferon-1 and -2 isolated from insects are rich in His and they possess antiviral and antitumor activities with immunomodulatory effect (Chernysh 2002). The secondary structure of alloferons has not been examined yet. Indolicidin and tritrpticin are peptides containing aromatic residues isolated from bovine neutrophils (Selsted 1992; Lawyer 1996). They possess broad spectrum of antibacterial, antifungal and hemolytic activities. Both indolicidin and tritrpticin are known to be flexible in aqueous solution and adopt either helical (poly-proline II helix) or turn structures in membrane mimic environment. Bactenecin and tigerinin-1 are cyclic peptides with serious antimicrobial activity (Romeo 1988; Sai 2001). Bactenecin was isolated from bovine neutrophils and tigerinin-1 was isolated from the skin of Rana tigerina. Each of them tends to adopt β-turn conformation. Because of the controversial assumptions and the lack of reasonable information about the secondary structures of these AMPs our goal was to perform conformational analysis of these peptides.

To explore the conformational spaces of molecules simulated annealing calculations were performed using implicit solvent model. For peptides containing Pro residues, torsional restraints were applied to keep the Xxx-Pro peptide bonds either in *cis* or *trans* configurations. The evolving secondary structures and the intramolecular interactions were examined.

For indolicidin and tritrpticin, it was observed that the *cis-trans* isomerisation plays a key role in the distribution of secondary structural elements (Kerényi 2007). For *trans* isomers, mainly type I and III β-turns were identified. Nevetheless, 3_{10}- and poly-proline II helical segments also appeared along the sequence of peptides possessing *trans* Xxx-Pro peptide bonds. In *cis* isomers, type VI β-turns were observed in specific tetrapeptide units. The stabilizing intramolecular interactions were in good agreement with the structural data: the observed H-bonds play a role in the stabilization of type I and III β-turns, as well as of 3_{10}-helical segments, while the proline-aromatic interactions participate in the stabilization of type VI β-turns. In alloferons, type I, II, II' and III β-turns were the most frequent structural elements. These secondary structures were also stabilized by backbone H-bonds. In the cyclic peptides (bactenecin and tigerinin-1), type I and III β-turns could be found in major population. In the *cis* isomers of tigerinin-1, type VI β-turns were also identified. In every peptide examined, minor populations of backbone-sidechain and sidechain-sidechain H-bonds were also found.

The results obtained from modelling the secondary structures and stabilizing intramolecular interactions were coherent and the conclusions derived from these calculations coincided with the data published so far.

Chernysh S, Kim SI, Bekker G, Pleskach VA, Filatova NA, Anikin VB, Platonov VG, Bulet P (2002) Antiviral and antitumor peptides from insects. Proc Nat Acad Sci USA 99(20):12628-12632.
Kerényi Á, Rákhely G, Leitgeb B (2007) Peptides 2006. In Proceedings of the 29th European Peptide Symposium., eds. Rolka K, Rekowski P, Silberring J), Kenes International, pp. 222.
Lawyer C, Pai S, Watabe M, Borgia P, Mashimo T, Eagleton L, Watabe, K (1996) Antimicrobial activity of a 13 amino acid tryptophan-rich peptide derived from a putative porcine precursor protein of a novel family of antibacterial peptides. FEBS Lett 390:95-98.
Romeo D, Skerlavaj B, Bolognesi M, Gennaro R (1988) Structure and bactericidal activity of an antibiotic dodecapeptide purified from bovine neutrophils. J Biol Chem 263:9573-9575.
Sai KP, Jaganadham MV, Vairamani M, Raju NP, Devi AS, Nagaraj R, Sitaram N (2001) Tigerinins: novel antimicrobial peptides from the Indian frog Rana tigerina. J Biol Chem 276:2701-2707.
Selsted ME, Novotny MJ, Morris WL, Tang YQ, Smith W, Cullor JS (1992) Indolicidin, a novel bactericidal tridecapeptide amide from neutrophils. J Biol Chem 267:4292-4295.

Supervisors: Balázs Leitgeb, Gábor Rákhely
E-mail: kerenyi@brc.hu

Volume 52(2):333-356, 2008
Acta Biologica Szegediensis
http://www.sci.u-szeged.hu/ABS

Regulation of hox genes in the cyanobacterium *Synechocystis* PCC 6806

Eva Kiss

Department of Plant Biology, Biological Research Center, Hungarian Academy of Sciences, Szeged, Hungary

Hydrogenases are widespread amongst prokaryotes, and they play a central role in microbial energy metabolism. The hydrogenase of the cyanobacterium *Synechocystis* PCC 6803, which is a unicellular oxygenic photoautotroph cyanobacterium, is a NiFe-type bidirectional enzyme, that can reversibly oxidize hydrogen (Houchins 1984). However, its physiological role has not been clarified.

Throughout the present investigation, we studied the regulation of the hox genes encoding the bidirectional enzyme on the transcript level by quantitative RT PCR, which was carried out as described elsewhere (Kós PB et al. 2008).

The bidirectional hydrogenase is an oxygen sensitive enzyme (Eisbrenner 1981). Oxygen may affect not only the enzyme activity, but also the expression of the hox genes. In order to verify this hypothesis we studied the effect of anaerobiosis on the hox transcript levels. Lowering the oxygen content of the media below 1μM caused induction of the hox genes.

One hypothesis about the function of the bidirectional hydrogenase is that it plays a role in adapting to new environmental conditions, predominantly adjusting to changes in the intensity and/or spectral quality of light (Appel et al. 2000). According to this idea, it is probable, that the hydrogenase is regulated by photosynthetic electron transport, in particular, by the redox poise of one of the electron carriers of the electron transport chain. We tested if this plausible regulation occurs at the transcript level. Obstruction of the linear electron transport by inhibitors during anaerobic treatment did not alter the induction pattern of hox genes. However, blocking the cyclic electron transport increased the level of the first two genes in the operon, while the last three genes were slightly repressed. These data indicate the existence of a transcriptional regulatory mechanism connected to the cyclic electron transport.

The hydrogenase of *Synechocystis* 6803 is encoded by the hoxEFUYH gene cluster (Bothe H. et al.1986) which can be transcribed as a single operon (Appel et al. 2005; Oliveira et al. 2005). During anaerobic induction the intensity of the accumulation of the first two genes in the operon (hoxE, and hoxF) differs from the last three genes (hoxU, hoxY and hoxH), implying that there is an additional transcriptional regulatory mechanism acting on the hox operon, which results in an alteration between the transcript levels of the genes within the operon. We supported this assumption by Northern blot analysis.

It has been shown recently that the transcription factor LexA binds to the untranslated region of the hox operon, and suggested to act as a positive regulator of hox gene expression (Appel et al. 2005; Oliveira et al. 2005). During our experiments we monitored the lexA transcript level in parallel with the hox mRNA level. In most of the cases we could not find correlation between the transcript levels of the hox operon, and its putative transcriptional regulator. Furthermore, we frequently observed that changes in their expression levels were opposite to one another. This result shows that lexA is unlikely to act as a direct transcriptional regulator of hox gene expression. Our data is also in agreement with the recent identification of another transcriptional regulator which is also proposed to bind the hox promoter region (Oliveira et al. 2007).

Appel J, Phunpruch S, Steinmüller K, Schulz R (2000) The bidirectional hydrogenase of *Synechocystis* sp. PCC 6803 works as an electron valve during photosynthesis. Arch Microbiol 173(5-6):333-338.

Eisbrenner G, Roos P, Bothe H (1981) The number of hydrogenases in cyanobacteria J Gen Microbiol 125:383-390.

Gutekunst K, Phunpruch S, Schwarz C, Schuchardt S, Schulz-Friedrich R, Appel J (2005) LexA regulates the bidirectional hydrogenase in the cyanobacterium *Synechocystis* sp. PCC 6803 as a transcription activator. Mol Microbiol 58(3):810-823.

Houchins JP (1984) The physiology and biochemistry of hydrogen metabolism in cyanobacteria. Biochim Biophys Acta 768:227-255.

Kós PB, Deák Zs, Cheregi O, Vass I (2008) Differential regulation of psbA and psbD gene expression, and the role of the different D1 protein copies in the cyanobacterium *Thermosynechococcus elongatus* BP-1. Biochim Biophys Acta 1777(1):74-83.

Oliveira P, Lindblad P (2005) LexA, a transcription regulator binding in the promoter region of the bidirectional hydrogenase in the cyanobacterium *Synechocystis* sp. PCC 6803. FEMS Microbiol Lett 251:59-66.

Oliveira P, Lindblad P (2007) An AbrB-Like Protein Regulates the Expression of the Bidirectional Hydrogenase in *Synechocystis* sp. Strain PCC 6803. J Bacteriol 190(3):1011-1019.

Papen H, Kentemich T, Schmulling T, Bothe H (1986) Hydrogenase activities in cyanobacteria. Biochim 68:121-132.

Supervisor: Imre Vass
E-mail: evakiss@brc.hu

The role of nitric oxide (NO), as signalling molecule in root development

Zsuzsanna Kolbert

Department of Plant Biology, University of Szeged, Szeged, Hungary

In this work the effects of osmotic stress and exogenous auxin (indole-3-butyric acid, IBA) on root morphology and nitric oxide (NO) generation in roots were compared in pea plants. Five-day old plants were treated with 0, 10^{-3}, 10^{-4}, 10^{-5}, 10^{-6}, 10^{-7}, 10^{-8} or 10^{-9} M IBA or with polyethylene glycol (PEG 6000) at concentrations that determined 0, 50, 100, 200 or 400 mOsm in the medium, during 5 days. NO generation was examined by *in situ* and *in vivo* fluorescence method, using a NO-specific dye, 4,5-diaminofluorescein diacetate (DAF-2DA).

Increasing concentrations of PEG as well as IBA resulted in shortening of primary root (PR), enhancement of lateral root (LR) number and significant increase of NO generation. Time-dependence investigations revealed that in the case of IBA treatments, the LR number increased in parallel with an intensified NO generation, while elongation of PR was not followed by changes in NO levels. Under osmotic stress, the time curve of NO development was distinct compared to that of IBA-treated roots, since significantly, the appearance of lateral initials was preceded by a transient burst of NO. This early phase of NO generation under osmotic stress was clearly distinguishable from that which accompanied LR initiation. It is concluded that osmotic stress and the presence of exogenous auxin resulted in partly similar root architecture but different time courses of NO synthesis. We suppose that the early phase of NO generation may fulfill a role in the osmotic stress-induced signalization process leading to the modification of root morphology (Kolbert et al. 2008a).

As we already know, NO functions in variable physiological and developmental processes in plants (Bartha et al. 2005; Kolbert et al. 2005) however, the source of this signaling molecule in the diverse plant responses is not well understood. Therefore in our further work we provide genetic and pharmacological evidence that the production of NO is associated with the nitrate reductase (NR) enzyme during IBA-induced lateral root development and under osmotic stress conditions (PEG treatments) in *Arabidopsis thaliana* L. NO production was detected in the NR-deficient *nia1, nia2* and *Atnoa1* (former *Atnos1*) mutants of *Arabidopsis thaliana.* As inhibitor for nitric oxide synthase (NOS) N^G–monomethyl-L-arginine (L-NMMA) was applied. Our data clearly show that IBA has increased LR frequency in the wild-type plant and the LR initials emitted intensive NO-dependent fluorescence of the triazol product of NO and DAF-2DA. The presence of increased level of NO was restricted only to the LR initials in contrast to PR sections where it remained at the control level. 200 and 400 mOsm PEG treatments also increased NO fluorescence in roots of *Arabidopsis*. The role of NR in IBA or PEG-induced NO formation in the wild type was shown by the zero effects of the NOS inhibitor L-NMMA. In cases of both treatments the NO synthesis could be inhibited by tungstate treatment, wich is a specific inhibitor of NR enzyme. The mutants had different NO levels in their control state (*i.e.* without IBA or PEG treatment), as *nia1, nia2* showed lower NO fluorescence than *Atnoa1* or the wild type plant. Finally it was clearly demonstrated that IBA as well as PEG induced NO generation in both the wild type and *Atnoa1* plants, but it totally failed in the NR-deficient mutant. It is concluded that the IBA or osmotic stress-induced NO production is nitrate reductase-associated during lateral root development in *Arabidopsis thaliana (*Kolbert et al. 2008b).

Bartha B, Kolbert Zs, Erdei L (2005) Nitric oxide production induced by heavy metals in Brassica juncea L. Czern. And Pisum sativum L. Acta Biol Szeged 49(1-2-:9-12.

Kolbert Zs, Bartha B, Erdei L (2005) Generation of nitric oxide in roots of Pisum sativum, Triticum aestivum and Petroselinum crispum plants osmotic and drought stress. Acta Biol Szeged 49(1-2):13-16.

Kolbert Zs, Bartha B, Erdei L(2008) Exogenous auxin-induced NO synthesis is nitrate reductase-associated in Arabidopsis thaliana root primordia- Journal of Plant Physiology doi:10.1016/j.jplph.2007.07.019 (in press).

Kolbert Zs, Bartha B, Erdei L (2008) Osmotic stress- and indole-3-butyric acid -induced NO generations are partially distinct processes in root growth and development in Pisum sativum L.- Physiologia Plantarum doi: 10.1111/j.1399-3054.2008.01056.x (in press).

Supervisor: László Erdei
E-mail: kolzsu@bio.u-szeged.hu

Comparative anthropological analysis of non-Hungarian skeletal populations from the 16-17th centuries

Gabriella Lovász

Department of Anthropology, University of Szeged, Szeged, Hungary

The period of the 16th to the 17th centuries was the age of the Turkish occupation of Hungary. Therefore many Hungarians from the southern region of the country escaped to the north, which was not invaded. On the basis of the archaeological and historical data, it is known that appreciable mass of southern Slav populations immigrated from the Balkan-peninsula and settled down mainly to this deserted, empty, southern countryside (Wicker 2006).

The subject of this research is the comparative anthropological examination of these non-Hungarian skeletal populations from the 16-17th centuries. The project has two aims: 1) to describe these populations from an anthropological point of view using osteological age and sex determination, metrical analyses and pathological investigations; 2) to find out the relationship among these non-Hungarian groups and the late medieval Hungarian populations, as well as the origin of the immigrated populations.

The material of this survey is the skeletal population of 6 burial sites (ca. 900 skeletons), which the archaeologists suggest belonged to this immigrated community: Győr-Gabonavásártér, Bácsalmás-Óalmás, Madaras-Bajmoki út, Katymár-Téglagyár, Csávoly-Határ út, Zombor-Repülőtér, (Zombor-Bükkszállás).

To determine the sex and age of death we have used common anthropological methods. The Martin and Saller's (1957) method was applied for measuring the skeletons, and the obtained data have been statistically evaluated with cluster analyses (R Development Core Team 2006). Southern Slav and Romanian series were also involved in the comparison. Paleopathological examinations have been carried out using macromorphological methods, though in certain cases radiographic, histological and molecular biological analyses have been applied as well.

After determination of sex and age, we could establish that in each examined populations the sex ratio was 50% : 50% except Győr-Gabonavásártér series, where the male:female ratio is 70% : 30% – this result might be due to the uncompleted excavation. It is also interesting that in the Bácsalmás-Óalmás series the percentage of infants is high compared to other series, which is due to the well-preserved skeletons and the precise excavation methods.

Many of the skeletons showed different forms of paleopathological lesions, the most common disorders being joint diseases and minor developmental anomalies. According to the prevalence of traumas, the analysed populations could be classified into two groups: a quiet agro-pastoralist population and another group with a more violent lifestyle. Infectious bony lesions were also frequent in each series, many of these cases possibly due to TB-infection (Lovász et al. 2007a). In addition, in the Bácsalmás-Óalmás series 6 cases of scurvy (proved by the histological analyses) were found, a disease rarely described in paleopathological literature (Lovász et al. 2007b). The large number of pathological alterations might indicate a poor state of health in each examined populations.

The results of the statistical analyses indicated that the foreign populations of this study were separated from the late medieval Hungarian series in a distinct group. The comparison of the examined series with the Southern Slav and Romanian data showed that only the southern Bosnian Raška Gora series revealed a close relationship with the foreign ethnic groups in Hungary.

Lovász G, Molnár E, Marcsik A (2007a) Tuberkulózisra utaló elváltozások megjelenése két késő középkori temető embertani anyagában. V. Kárpát-medencei Biológiai Szimpozium, Budapest. Előadáskötet: 165-174.
Lovász G, Molnár E, Gödde J, Schultz M, Marcsik A (2007b) Skeletal manifestations of scurvy in a medieval anthropological series from Hungary. 7. Kongress der GFA, Freiburg. Abstracts.
Martin R, Saller, K (1957) Lehrbuch der Anthropologie. Gustav Fischer Verlag, 3. Aufl, Stuttgart.
R Development Core Team (2006) R: A language and environment for statistical computing. R Foundation for Statistical Computing, Vienna, Austria. URL http://www.R-project.org.
Wicker E (2006) Rácok és vlahok a török hódoltság kori Észak-Bácskában. PhD dissertation. ELTE BTK.

Supervisor: Erika Molnár
E-mail: lovaszg@bio.u-szeged.hu

Applications of protein and small molecule microarrays

Eszter Molnár

Laboratory of Functional Genomics, Biological Research Center, Hungarian Academy of Sciences, Szeged, Hungary

While DNA microarrays measure changes at the transcription level, protein microarrays can provide information on the protein expression in a parallel way (Tao et al. 2007). Several disease-specific genes and their protein products are overexpressed reflecting the specific genotype of the disease. The direct inhibition of such proteins and the relevant signaling pathways could provide novel opportunities for targeted therapy. Small molecule microarrays (small molecule library printed with high density on a modified glass surface) can be used to screen potential inhibitors of these proteins (Darvas et al. 2004; Walsh et al. 2004).

Protein microarrays manufactured up to date are focused on a specific field (apoptosis, cell cycle, cancer etc.) of the proteome. We tested two different commercially available microarrays for our protein expression studies. We applied the Panorama Ab Microarray Cell Signaling Kit (Sigma-Aldrich) to compare protein extracts from *cerebellum* and *hippocampus* of fat-1 transgenic and wild type (control) mice. The Apoptosis Antibody Microarray (Full Moon BioSystems) was used to investigate the effects of the Ac-177 anticancer compound (from the immunomodulatory drug chemical library of Avidin Ltd.) on apoptosis-related protein expression/phosphorylation.

Small molecule microarrays with 8800 compounds of diverse structures in duplicates were applied for high-throughput screening of protein-ligand interaction studies. A purified serine protease was fluorescently labeled with Cy5 dye and incubated on the microarray. The binding intensity data of each spot representing each compound on the array were determined. To identify its potential inhibitors (molecules which bind to the active site) we incubated the labeled protease with its known substrate on the microarray. Competition for binding between the substrate and the spotted compounds resulted a decreased fluorescence intensity when compared to the substrate-free experiment.

This work was supported by the following grants: Ányos Jedlik „AVINOMID" (NKTH) and GVOP-3.3.1-0168/3.0.

Darvas F, Dormán G, Krajcsi P, Puskás LG, Kovári Z, Lőrincz Z, Urge L (2004) Recent advances in chemical genomics. Curr Med Chem 11(23):3119-3145.
Tao SC, Chen CS, Zhu H (2007) Applications of protein microarray technology. Comb Chem High Throughput Screen 10(8):706-718.
Walsh DP, Chang YT (2004) Recent advances in small molecule microarrays: applications and technology. Comb Chem High Throughput Screen 7(6):557-564.

Supervisor: László G. Puskás
E-mail: molnareszter1@gmail.com

Volume 52(2):333-356, 2008
Acta Biologica Szegediensis
http://www.sci.u-szeged.hu/ABS

The *lemming* gene encodes the Apc11 subunit of the anaphase-promoting complex in *Drosophila melanogaster*

Olga Nagy

Institute of Biochemistry, Biological Research Center, Hungarian Academy of Sciences, Szeged, Hungary

The ubiquitin-mediated proteolysis of regulatory proteins plays an essential role in regulating the eukaryotic cell cycle. A multi-subunit complex called the anaphase-promoting complex/cyclosome or APC/C plays a key role in this process as an ubiquitin-protein ligase. By targeting mitotic regulatory proteins for degradation, it regulates chromosome segregation and exit from mitosis. The APC/C contains at least 11 subunits, most of which are evolutionarily conserved from yeasts to humans (Castro et al. 2005). The role of most of the subunits within the APC/C complex is still poorly understood.

We have isolated and characterized hypomorph and null alleles of the *lemming* (*lmg*) gene. They show different pupal and pharate-adult lethal phenotypes. Larval neuroblasts from *lmg* mutants show mitotic defects including high mitotic index, chromosome overcondensation, metaphase-like arrest and frequent aneuploid and polyploid cells. Beside the mitotic phenotype, we observed elevated level of apoptosis in *lmg* mutant neuroblasts. Immunostaining of *lmg* mutants shows abnormal cyclin A and cyclin B accumulation in the metaphase arrested mitotic cells.

The *lmg* gene was cloned by plasmid rescue. The predicted coding region consists of 255 nucleotides, and encodes a small, 10 kDa polypeptide containing a RING-finger motif. The Lmg protein shows more than 50% sequence identity and more than 80% sequence homology with the Apc11 subunits of the budding yeast and human APC/C.

Yeast two hybrid experiments revealed that the Lmg protein specifically interacts with a protein identified as the *Drosophila* orthologue of the Apc2/Mr subunit of the yeast and human APC/C (Kashevsky et al. 2002). This interaction was underlined by the synergistic genetic interaction between hypomorph alleles of *lmg* and *mr*.

When introduced and expressed in budding yeast cells, the *lmg* gene was able to fully complement the proliferation defect of yeast temperature sensitive *APC11-myc9* mutant. This result demonstrates that the *lmg* gene product from the fruit fly can functionally replace the yeast APC11 protein.

These phenotypic and functional assays indicate that the *lmg* gene encodes the Apc11 orthologue of the *Drosophila* APC/C. Our work represents the first genetic study of this subunit of the APC/C in a multicellular organism.

Castro A, Bernis C, Vigneron S, Labbé JC, Lorca T (2005) The anaphase-promoting complex: a key factor in the regulation of cell cycle. Oncogene 13;24(3):314-325.

Kashevsky H, Wallace JA, Reed BH, Lai C, Hayashi-Hagihara A, Orr-Weaver TL (2002). The anaphase promoting complex/cyclosome is required during development for modified cell cycles. Proc Natl Acad Sci U S A 99:11217-11222.

Supervisor: Péter Deák
E-mail: nagyo@brc.hu

Network evolution and related models in biology

Sergiu Netotea

Bioinformatics Group, Biological Research Center, Hungarian Academy of Sciences, Szeged, Hungary

Every complex natural system is characterized by several things: redundancy - that ensures information has several good options for circulating across a system, decoupling - the capacity to separate into functional parts that can work even if they are separated, modularity – the property of subparts to work independently and have specific functions, and feedback control – a basic mechanism that allows a system to observe its fitness, making it able to adapt to external or internal pressures. We are investigating how can the properties of general complex systems be measured in evolving networks, and what are the similarities and differences to naturally occurring networks.

Many biological networks evolve using a tradeoff between two basic properties: efficiency, which deals with the capacity of using resources to the maximum extent, and robustness, that deals with resistance to various external pressures. A conceptually simple model of evolution is explained, the outcome of it is however surprising: highly evolved networks have some properties far from many naturally occurring networks.

Simulations of network evolution were done using both a distributed evolutionary algorithm and a random rewiring of the links without the possibility to backtrack in the case of finding a better fitted network, storing the network structures. The efficiency was expressed as computing the number and length of shortest paths, and the robustness by evaluating the efficiency cost of attacking the most central nodes. We used both directed and undirected networks. The resulted over-all topology is showing a highly connected central core surrounded by a dense periphery connected only to the core. Many biological networks have scaled node distributions; this implies that their evolution is never completed, or that it acts modular, in subparts of the network. Several examples are discussed.

The network of protein folding pathways is a particularly interesting one in terms of evolutionary fitness. The number of possible folding states a protein can have during its folding process is huge but the protein is folding extremely quickly, and this is an unsolved problem of today science. Groups of proteins form complexes that generally interact weakly but sometimes the bond can have high specificity. These complexes together can establish a strong structure, but to attain it they need to go through a network of states in a similar manner to protein folding. We are investigating ways to model this in terms of network evolution.

Also not every evolved system is suitable to be expressed as a proper network, but the evolutionary mechanism remains the same. We investigate the fitness of different populations of bacteria forming fractal shaped colonies using an agent based model that simulate the behavior of individual bacteria and the diffusion and sensing of different substances across the medium.

Ágoston V, Csermely P, Pongor S (2005) Multiple weak hits confuse complex systems: a transcriptional regulatory network as an example. Phys Rev E Stat Nonlin Soft Matter Phys 71(5 Pt 1): p.051909.

Ágoston V, Cemazar M, Kaján L, Pongor S (2005) Graph-representation of oxidative folding pathways. BMC Bioinformatics 6(1):19.

Alon U, Surette MG, Barkai N, Leibler S (1999) Robustness in bacterial chemotaxis. Nature 397(6715):168-171.

Csermely P, Ágoston V, Pongor S (2005) The efficiency of multi-target drugs: the network approach might help drug design. Trends Pharmacol Sci 26(4):178-182.

Guarnaccia C, Raman B, Zahariev S, Simoncsits A, Pongor S (2004) DNA-mediated assembly of weakly interacting DNA-binding protein subunits: in vitro recruitment of phage 434 repressor and yeast GCN4,DNA-binding domains. Nucleic Acids Research 32(17):4992-5002.

Netotea S, Pongor S (2006) Evolution of robust and efficient system topologies. International Conference on Immunogenomics and Immunomics, Budapest, Hungary, October 8-12, 2006. Cell Immunol 244(2):80-83.

Supervisor: Sándor Pongor
E-mail: sergiun@brc.hu

Axonal and dendritic effects of neurogliaform cells in rat and human neocortex

Szabolcs Oláh

Department of Physiology, Anatomy and Neuroscience, University of Szeged, Szeged, Hungary

Neurogliaform cells have a unique position among cortical interneurons (Kawaguchi 1995) because they can elicit combined GABAA and GABAB receptor-mediated inhibition on pyramidal cells (Tamas et al. 2003). Moreover, they establish electrical synapses with each other and with other interneuron types (Price et al. 2005; Simon et al. 2005).

We measured the pre- and postsynaptic effects of neurogliaform cells applying simultaneous whole-cell recordings in layers I-IV of rat somatosensory cortex and in human association cortex *in vitro*.

Apart from the GABAA receptor mediated component in postsynaptic responses, single action potentials in neurogliaform cells elicited GABAB receptor mediated responses in neurogliaform, regular spiking and fast spiking interneurons in rat cerebral cortex.

Neurogliaform cells recorded in human cortical brain slices evoked GABAA and GABAB receptor mediated slow inhibition in various types of inteneurons and one of them established heterologous electrical coupling. These are the first multiple patch clamp recordings which analyse the functions of neuorgliaform cells in human cortex (Oláh et al. 2007).

These cells can effectively recruit GABAB receptors not only on classical postsynaptic compartments like dendritic spines and shafts but on presynaptic axon terminals as well. This presynaptic inhibitory effect can reduce synaptic transmission and this is reflected in the altered paired pulse ratios and reduced amplitudes of the evoked postsynaptic potentials. In one case we show phamacological dissection of this presynaptic modulation by applying GABAB receptor antagonist.

Our results highlight the peculiar role of neurogliaform cells in cortical circuits and extend their contributions to slow inhibition in cortex.

Kawaguchi Y (1995) Physiological subgroups of nonpyramidal cells with specific morphological characteristics in layer II/III of rat frontal cortex. J Neurosci 15:2638-2655.

Oláh S, Komlósi G, Szabadics J, Varga C, Tóth É, Barzó P, Tamás G (2007) Output of neurogliaform cells to various neuron types in the human and rat cerebral cortex. Frontiers in neuronal circuits 1:1-7.

Price CJ, Cauli B, Kovacs ER, Kulik A, Lambolez B, Shigemoto R, Capogna M (2005) Neurogliaform neurons form a novel inhibitory network in the hippocampal CA1 area. J Neurosci 25:6775-6786.

Simon A, Olah S, Molnar G, Szabadics J, Tamas G (2005) Gap-junctional coupling between neurogliaform cells and various interneuron types in the neocortex. J Neurosci 25:6278-6285.

Tamas G, Lorincz A, Simon A, Szabadics J (2003) Identified sources and targets of slow inhibition in the neocortex. Science 299:1902-1905.

Supervisor: Gábor Tamás
E-mail: szolah@bio.u-szeged.hu

Volume 52(2):333-356, 2008
Acta Biologica Szegediensis
http://www.sci.u-szeged.hu/ABS

The molecular mechanism of entrainment of the plant circadian clock by light

Andrea Palágyi

Institute of Plant Biology, Biological Research Center, Hungarian Academy of Sciences, Szeged, Hungary

At the core of the eukaryotic circadian network, clock genes/proteins form multiple transcriptional/translational negative feed-back loops and generate a basic ~24h oscillation, which provides daily regulation for a wide range of processes. This temporal organization enhances the fitness of the organism only if it corresponds to the natural day/night cycles. Light is the most effective signal in synchronizing the oscillator to environmental cycles. Light signals mediated by photoreceptors are forwarded to the oscillator and cause an acute change in the level/activity of certain clock components that eventually results in a phase shift of the oscillation (Devlin and Kay 2001). Our aim is to reveal the molecular details of this process (also called entrainment or resetting) in *Arabidopsis thaliana*.

The plant circadian oscillator is supposed to consist of three inter-locked feedback loops Locke et al. 2006). In the first loop the morning-expressed CIRCADIAN CLOCK ASSOCIATED 1 (CCA1)/LATE ELONGATED HYPOCOTYL (LHY) transcription factors inhibit the expression of the TIMING OF CAB EXPRESSION 1 (TOC1) gene; conversely, the evening-expressed TOC1 positively regulates the transcription of CCA1/LHY. In the second loop GIGANTEA (GI) induces TOC1 expression during the afternoon/evening, while TOC1 represses GI during the night. Recent data suggested the operation of a third loop, where CCA1/LHY up-regulate the PSEUDO RESPONSE REGULATOR 7/9 (PRR7/9) genes (homologs of TOC1) in the morning and PRR7/9 proteins down-regulate CCA1/LHY expression during the day. In Arabidopsis, CCA1/LHY, GI and PRR9 may represent the primary targets of resetting light signals, merely based on the fact that these clock genes are acutely light-inducible. However, the role of their light induction in phase resetting has not been tested directly.

The primary elements of the plant light input pathway are the red/far-red light absorbing phytochromes (PHYA, B, D, E) and blue light absorbing cryptochromes (CRY1,2; Devlin and Kay 2000). However, the molecular links between phytochrome signalling and the core clock components are still missing.

In the first set of experiments we studied the function of the red/far-red absorbing phytochrome B (PHYB) photoreceptor in the resetting process. Our data show that the *phyb-9* mutation affects different parameters (phase and/or period) of rhythmic expression of components of the multi-loop circadian oscillator in Arabidopsis. This could be explained by decoupling of the different loops of the oscillator in *phyb-9*. However, we showed that genetic manipulation of a single loop has the same effect on the other loops in wild type and *phyb-9*, which indicates that absence of PHYB does not separate the individual loops. Rather, our data suggest the existence of tissue-specific clocks, which are regulated by PHYB in different ways.

The circadian oscillator responds with characteristic phase shifts to short light pulses. In the second set of experiments we investigated the effect of light induction of certain clock components on the magnitude of such phase shifts. Our data showed that the pattern of light induction of a single clock component does not correspond directly to particular phase responses, but high level of CCA1 and GI induction coincides with strong phase delays, while high level of GI and PRR9 induction coincides with strong phase advances. Phase response curves in single clock mutants indicate that among the light inducible clock components, CCA1, LHY and GI are negative elements of resetting during the subjective night, but PRR9 is a positive element of resetting during the subjective day.

Devlin PF, Kay SA (2001) Circadian photoperception. Annu Rev Physiol. 63:677-94.
Locke JC, Kozma-Bognár L, Gould PD, Fehér B, Kevei E, Nagy F, Turner MS, Hall A, Millar AJ (2006) Experimental validation of a predicted feedback loop in the multi-oscillator clock of Arabidopsis thaliana. Mol Syst Biol 2:59
Devlin PF, Kay SA (2000) Cryptochromes are required for phytochrome signaling to the circadian clock but not for rhythmicity. Plant Cell 12:2499-2510.

Supervisor: Laszlo Kozma-Bognar
E-mail: palagyi@brc.hu

Study of the genetic relationships of oribatid mites (Acari, Oribatida) using nucleotide sequences

István Prazsák, Péter Maróy

Department of Genetics, University of Szeged, Szeged, Hungary

Oribatid mites play important role worldwide in soil life, due to their high abundance and soil dwelling lifestyle. They are the most species rich order in the subclassis of Acari. Members of different groups of oribatid mites show very different and peculiar morphological appearance, however they belong to single taxonomical unit. There are almost 10 000 described species on the world, from which 523 species are reported in the area of Hungary to date. The species living in Hungary represent 5 major taxonomical units, divided in 77 families and 191 genera. The system of oribatid mites based on morphological features.

In order to study genetic relationships at large and small scale taxonomical levels we chose molecular markers. We used the 160 base pair long part of the 28S D3 nuclear ribosomal DNA coding domain and the 680 base pair long partial sequence of mitochondrial cytochrome-oxydase I (Cox1) subunit. 96 species were collected and determined from different localities of Hungary. 36 species, representing the main

Volume 52(2):333-356, 2008
Acta Biologica Szegediensis
http://www.sci.u-szeged.hu/ABS

taxonomical groups were selected, and used for the molecular studies. All species used were documented with light and scanning electron microscope images. Distance and likelihood based methods were used in combination with our own and GenBank sequences to determine the genetic similarity between oribatid mites at family level.

Our results suggest that the similarity of 28S ribosomal DNA sequences support the monophyly of lower, but not higher oribatid groups. Cytochrome-oxidase (Cox1) sequences are known to be useful at taxonomical level of genera. We introduced Cox1 sequence in the identification of larva stages.

Supervisor: Péter Maróy
E-mail: prazsi@bio.u-szeged.hu

Kynurenines: neuroactive compounds in the central nervous system: An *in vitro* study

Éva Rózsa

Department of Physiology, Anatomy and Neuroscience, University of Szeged, Szeged, Hungary

Kynurenic acid (KYNA) is a neuroprotective endogenous tryptophan metabolite produced by astrocytes and neurons via the kynurenine pathway in both humans and rodents. At non-physiological concentrations, KYNA is an excitatory amino acid receptor antagonist that can partially act at both the α-amino-3-hydroxy-5-methylisoxazole-4-propionic acid and N-methyl-D-aspartate subunits of the glutamate receptors (Stone 1993).

In the brain, KYNA is synthesized in astrocytes from its bioprecursor L-kynurenine (KYN) and is then rapidly released into the extracellular compartment. Previous studies have indicated that rat cortical slices have also the ability to synthesize KYNA from exogenously added KYN (Turski et al. 1989). The synthesis of KYNA from KYN is catalysed by kynurenine aminotransferase I and II (KAT I and II) (Schwarcz et al. 2002).

The use of KYNA as a neuroprotective agent is rather restricted, however, because KYNA has only a very limited ability to cross the blood–brain barrier (Fukui et al. 1991). In contrast, KYN and different synthetic KYNA derivatives cross this barrier more readily (Giles et al. 2003).

In the course of the experiments on rat brain slices, the Schaffer collaterals were stimulated and field excitatory postsynaptic potentials (fEPSPs) were recorded in the pyramidal layer of the hippocampal CA1 region. To test the effects of KYNA, we used an *in vitro* pentylenetetrazole (PTZ) model. PTZ, a chemical convulsant frequently utilized in the study of seizures (Yudkoff et al. 2006), exerts its effects by binding to the picrotoxin binding site of the post-synaptic GABA-A receptor (Macdonald et al. 1977). PTZ administered *in vitro* at 1mM induced a considerable increase in the amplitude of the fEPSPs recorded from the hippocampal CA1 region. When applied locally in an extremely high concentration (20 mM), PTZ resulted in characteristic wavelets. However, KYNA administration not only decreased the amplitude of the hippocampal CA1 responses evoked by Schaffer collateral stimulation, but also afforded protection from the PTZ-induced response enhancement.

The KYNA precursor KYN also blocked the development of the PTZ-induced high increase in amplitude. To prove that the KYN→KYNA conversion did take place in our experiments and that it was KYNA which afforded the protection against the effects of PTZ, we applied *N*-omega-nitro-l-arginine, an inhibitor of KAT I and II (Rozsa et al. 2008).

SZR-72, a synthetic kynurenic acid derivative, applied *in vitro*, prooved to be also effective in preventing the high increase in fEPSP amplitudes, generated by PTZ.

These findings show that treatment with KYN, or the synthetic kynurenic acid derivative, SZR-72, even at very low concentration, has an effect on enhanced neural excitability and thus support the hypothesis that manipulations of the kynurenine pathway might be a rewarding target in different neuronal disorders affected by neuronal hyperexcitation.

Additionally we have shown, that KYNA in submicromolar concentration range has a positive neuromodulatory effect. In nM concentrations, kynurenic acid does not give rise to inhibition, but in fact facilitates the field excitatory postsynaptic potentials, recorded from the hippocampal CA1 region (Rozsa et al. 2008).

Fukui S, Schwarcz R, Rapoport SI, Takada Y, Smith QR (1991) Blood-brain barrier transport of kynurenines: implications for brain synthesis and metabolism. J Neurochem 56:2007-2017.

Giles GI, Collins CA, Stone TW, Jacob C (2003) Electrochemical and *in vitro* evaluation of the redox properties of kynurenine species, Biochem Biophy Res Commun 300:719-724.

Luchowski P, Kocki T, Urbanska EM (2001) N(G)-nitro-l-arginine and its methyl ester inhibit brain synthesis of kynurenic acid possibly via nitric oxide-independent mechanism, Polish J Pharmacol 53:597-604.

Macdonald RL, Barker JL (1977) Penicillin and pentylenetetrazol selectively antagonize GABA-mediated postsynaptic inhibition of cultured mammalian neurons, Neurology 27:337-1337.

Rozsa E, Robotka H, Nagy D, Farkas T, Sas K, Vecsei L, Toldi J (2008) The pentylenetetrazole-induced activity in the hippocampus can be inhibited by the conversion of l-kynurenine to kynurenic acid: An *in vitro* study, Brain Res Bull (in press)

Rozsa E, Robtoka H, Vecsei L, Toldi J (2008) The Janus-face kynurenic acid, J Neur. Transm (in press)

Schwarcz R, Pellicciari R (2002) Manipulation of brain kynurenines: glial targets, neuronal effects, and clinical opportunities, J Pharmacol Exp Therap 303:1-10.
Stone TW (1993) Neuropharmacology of quinolinic and kynurenic acids. Pharmacol Rev 45:309-379.
Turski WA, Gramsbergen JB, Traitler H, Schwarcz R (1989) Rat brain slices produce and liberate kynurenic acid upon exposure to l-kynurenine. J Neurochem 52:1629-1636.
Yudkoff M, Daikhin Y, Nissim I, Horyn O, Luhovyy B, Lazarow A, Nissim I (2006) Short-term fasting, seizure control and brain amino acid metabolism, Neurochem Int 48:650-656.

Supervisor: József Toldi
E-mail: evicime@gmail.com

Examination of the hydrogen-metabolism in *Methylococcus capsulatus* (Bath)

Zsolt Sáfár

Department of Biotechnology, University of Szeged, Szeged, Hungary

Methylococcus capsulatus (Bath) is a Gram-negative, methylotrophic bacterium, which oxidizes methane to carbon dioxide for energy generation. The enzyme complexes methane monooxygenases (MMOs) oxidize methane to methanol and co-oxidize a wide variety of aliphatic, aromatic and halogenated hydrocarbons, therefore they are extremely versatile enzymes for biocatalysis and bioremediation. The in vivo electron donor of the MMOs is NADH, which must be regenerated. Since biodegradation processes using MMO are co-oxidation processes, alternative ways of supplying reducing power are needed. Possible candidate could be H_2 for NADH + H^+ generation.

Hydrogenases are metalloenzymes catalyzing the reversible oxidation of H_2. *M. capsulatus* (Bath) contains a soluble (Hox) hydrogenase - which is able to reduce NAD^+ using H_2 - , and a membrane-bound nickel-iron Hup hydrogenase - which plays an important role in the recycling of hydrogen, and maybe donates the electrons to the quinone pool. Another enzyme – nitrogenase - produces H_2 as a byproduct under nitrogen fixing condition.

Δ*hupSL* and Δ*hoxH* deletion mutants were generated (Csáki et al. 2001). H_2-driven MMO activities of these mutants and wild type were measured to obtain information about the *in vivo* function of the hydrogenases (Hanczár et al. 2002). The deletion mutants revealed unexpected behavior: the Δ*hupSL* mutant did not show H_2-driven MMO activity, while the Δ*hoxH* mutant showed. The Hup hydrogenase - which is unable to reduce NAD^+ directly - is required for the H_2-driven activity of MMO. To understand the role of Hup hydrogenase in H_2-metabolism the first step is to find all genes coding for proteins, which has any affect on Hup hydrogenase activity.

Several Hup^- phenotype mutants were isolated from a *M. capsulatus* random mutant library, which was generated by transposon mutagenesis. The transposon was found in a structural gene (*hupL*), in an accessory gene (*hupD*) of Hup hydrogenase, and in other genes: TonB-dependent receptor-like putative protein coding gene (*tonB*) and conserved hypothetical protein for NADH ubiquinone/plastoquinone complex coding gene (*nupX*).

The *in vivo* H_2 production capacities of the wild type and the mutant strains were compared. The Hup hydrogenase of the wild type consumed a lot of H_2 from the gas phase, while the mutants had lower H_2 consumption activity both under nitrogen fixing and nitrogenase repressed conditions. Hup hydrogenase structural proteins were detected both in wild type, $HupD^-$, $TonB^-$ and $NupX^-$ transposon mutants with HupL antibody by Western Blot assay, in contrast to the Δ*hupSL* deletion and $HulpL^-$ transposon mutants.

The results show the presence of the matured Hup hydrogenase in $TonB^-$ and $NupX^-$ transposon mutants, but hydrogen-metabolism of these mutants is damaged, therefore they have Hup^- phenotype. According to the *in silico* analysis and global protein alignment the proteins of the *nupX* containing operon are similar to the NuoM, NuoL and NuoN proteins of the NUO (NADH ubiquinon-plastoquinon oxydoreductase) complex. In our hypothesis the proteins of the examined nuo-like operon maybe play a role in the energy conversion of the bacterium, while the examined TonB-dependent receptor-like putative protein perhaps takes part in the mechanism of TonB-catalyzed iron transport through the bacterial cell envelope, indirectly contributing to the assembly of the membrane-bound nickel-iron Hup hydrogenase.

To determine the role of the mutant genes further investigations are needed.

Csáki R, Hanczár T, Bodrossy L, Murrell JC, Kovács KL (2001) Molecular characterization of structural genes coding for a membrane bound hydrogenase in *Methylococcus capsulatus* (Bath). FEMS Microbiol Lett 205:203-207.
Hanczár T, Csáki R, Bodrossy L, Murrell JC, Kovács KL (2002) Detection and localization of two hydrogenases in *Methylococcus capsulatus* (Bath) and their potential role in methane metabolism. Arch Microbiol 177:167-172.

Supervisor: Kornél L. Kovács
E-mail: safarzs@brc.hu

Volume 52(2):333-356, 2008
Acta Biologica Szegediensis
http://www.sci.u-szeged.hu/ABS

Macro-organization and structural flexibility of the light-harvesting system of diatoms (Bacillariophyceae) and their significance in the photosynthetic light energy utilisation

Milán Szabó

Institute of Plant Biology, Biological Research Center, Hungarian Academy of Sciences, Szeged, Hungary

Among the phytoplankton species of marine and freshwater communities, diatoms play a dominant role in the biogeochemical cycles of carbon, nitrogen, phosphorus and silicon with a strong impact on the global climate. Since diatoms experience randomly fluctuating light intensities and large scale temperature changes, they have developed various mechanisms of photoprotection.

In higher plants, it has been established that the photosystems (PSs) with their peripheral chlorophyll *a/b* light-harvesting antenna complexes (LHCs) form supercomplexes. The PSII-LHCII and PSI-LHCI supercomplexes are laterally segregated in the granal and stromal thylakoid membranes, respectively (cf. e.g. Mustárdy and Garab 2003). It has also been shown that LHCII and PSII-LHCII are assembled into macrodomains with long-range chiral order, which possess remarkable structural flexibility and by this means the structural flexibility of the macroassemblies plays an important role in the regulation of the light energy conversion (Garab 1996).

Diatoms contain specialized peripheral light-harvesting antennas, the fucoxanthin-chlorophyll *a/c* proteins (FCPs), instead of LHCs. FCPs are also intrinsic light-harvesting complexes but their carotenoid is the fucoxanthin and contains chlorophyll *c* as accessory pigment. Compared to higher plants, our knowledge concerning the arrangement and the supramolecular organization of the antenna complexes in the thylakoid membranes is quite rudimentary, and much less is known about their possible role in different regulatory processes.

The major aim of our studies was to characterize the (macro-)organization of the complexes in *Phaeodactylum tricornutum* and *Cyclotella meneghiniana* cells, as well as on isolated thylakoid membranes and FCPs. By using circular dichroism (CD) spectroscopy, we found that the spectra of the whole cells were dominated by an intense band at (+)698 nm, with typical psi-type features (psi, polymerization or salt-induced). This band, which appeared to be associated with the multilamellar membrane architecture, was sensitive to the light intensity during growth, to the osmotic pressure of the medium and to heat. We also found that it was capable of undergoing reversible changes upon illumination with actinic light. In isolated thylakoid membranes, the psi-type CD band, which was lost during the isolation procedure, could be partially restored by addition of Mg^{2+} ions; the same treatment was also important for optimizing the quantum yield of PSII and the non-photochemical quenching of chlorophyll *a* (Szabó et al. 2008). With a refined isolation method, we were able to isolate the oligomeric form of FCP, which represented the native form of the antenna system in thylakoid membranes of diatoms (Lepetit et al. 2007). We also gained information on the orientation and local environment of a special fucoxanthin pigment molecule of the FCP, which exhibited an extremely strong electrochromic response and intense linear dichroism (LD) signal at around 550 nm, most probably given rise by strong fucoxanthin/chlorophyll *c* interaction.

In summary, our data have shown the presence of highly flexible macroassemblies of the light-harvesting system in diatoms, which also appears to participate in different regulatory processes of the photosynthetic light energy conversion.

Garab G (1996) Linear and Circular Dichroism. In Amesz J and Hoff AJ, eds., Biophysical Techniques in Photosynthesis, Advances in Photosynthesis, Vol. 3. Kluwer Academic Publishers, Dordrecht/Boston/London, pp. 11-40.

Lepetit B, Volke D, Szabó M, Hoffmann R, Garab G, Wilhelm C, and Goss R (2007) Spectroscopic and molecular characterization of the oligomeric antenna of the diatom *Phaeodactylum tricornutum*. Biochemistry 46:9813-9822 .

Mustárdy L and Garab G (2003) Granum revisited. A three-dimensional model - where things fall into place. Trends Plant Sci 8:117-122.

Szabó M, Lepetit B, Goss R, Wilhelm C, Mustárdy L and Garab G (2008) Structurally flexible macro-organization of the pigment–protein complexes of the diatom *Phaeodactylum tricornutum*. Photosynth Res 95:237-245.

Supervisor: Győző Garab
E-mail: szabom@brc.hu

Characterization of beta-glucosidase enzymes and their coding genes from the fungal class Zygomycetes

Miklós Takó

Department of Microbiology, University of Szeged, Szeged, Hungary

The genus *Rhizomucor* (Zygomycetes, Mucorales) comprises two well-established thermophilic species, *R. pusillus* and *R. miehei* (Vágvölgyi et al. 1999). Both of them are well known from biotechnological applications in consequence of their effective extracellular enzymes, e.g. proteases and lipases (Rao et al. 1998). Beta-glucosidases play important roles in biology, including the degradation of cellulose biomass by fungi and bacteria, degradation of glycolipids in mammalian lysosomes, and the cleavage of glycosylated flavonoids in plants (Bhatia et al. 2002).

Filamentous fungi are known to be good producers of beta-glucosidases and several fungal glucosidases have been isolated and analyzed. Unfortunately, Zygomycetes are poorly characterized from this aspect. In the frame of a recent study, beta-glucosidase activity of

several Zygomycetes fungi was tested in solid-state fermentation assays. Some *R. miehei* strains showed intensive extracellular enzyme activity. The aim of our present study is the identification and molecular and biochemical characterization of a beta-glucosidase enzyme and its coding gene (*bgl*) from *R. miehei*.

Degenerated beta-glucosidase-specific primer pairs were designed to conserved regions of fungal glycoside hydrolase family 3 genes and a 493 bps long fragment was amplified by PCR from the genomic DNA of the *R. miehei*. The sequence of the amplicon was determined; it showed high homology with the C-terminal domains of the beta-glucosidases belonging to the family 3. Based on this sequence, specific primers were designed for inverse PCR. The original fragment has been lengthened to a 4063 bps long sequence which contained the 2826 bps long beta-glucosidase gene encoding a protein with a length of 743 amino acids. *Rhizomucor bgl* showed the highest homology with the beta-glucosidases of *Phanerochaete chrysosporium*, *Trichoderma reesei* and *Piromyces* sp. strain E2.

For gene expression studies two transformation vectors were constructed: the plasmid pTM1 contained *bgl* under the control of the regulator sequences of the related *Mucor circinelloides gpd1* gene, while the plasmid pTM4 harboured the promoter region of the *bgl* fused with a green fluorescent protein gene. In the lack of an efficient transformation system in *R. miehei*, genetic transformations were started in a heterologous system: PEG-mediated protoplast transformations were performed in an uracile auxotrophic *M. circinelloides* strain. Induction of the *bgl* promoter by different substrates was studied in the *M. circinelloides* transformants harbouring the pTM4 plasmid. Strong fluorescence was observed only in the transformants growing on cellobiose containing medium. Analysis of the transformants containing pTM1 is in progress.

For production of the extracellular beta-glucosidase enzyme in high amount, *R. miehei* was grown on wheat bran medium for six days at 40°C. The enzyme was purified from the crude extract to homogeneity by ammonium sulphate fractionation and two-step chromatographic separation through Sephadex G100 and G200 columns was performed. The molecular mass of the purified enzyme was determined by SDS-polyacrylamide gel electrophoresis. The optimum temperature and pH for the action of the enzyme were at 60°C and 4.0 to 5.0, respectively; the beta-glucosidase proved to be highly stable at temperatures up to 50°C but it almost lost its activity at temperatures above 70°C. The enzyme was fairly stable at pH 4.0 to 6.0 and 20% of the activity remained after incubation at pH 3.0.

Bhatia Y, Mishra S, Bisaria VS (2002) Microbial ß-glucosidases: Cloning, Properties, and Applications. Crit Rev Biotechnol 22:375-407.
Rao MB, Tanksale AM, Ghatge MS, Deshpande VV (1998) Molecular and biotechnological aspects of microbial proteases. Microbiol Mol Biol Rev 62:597-635.
Vágvölgyi Cs, Vastag M, Ács K, Papp T (1999) *Rhizomucor tauricus*: a questionable species of the genus. Mycol Res 103:1318-1322.

Supervisor: Csaba Vágvölgyi
E-mail: tako78@bio.u-szeged.hu

Map based cloning of leaf developmental abnormality in *Medicago sativa* and comparison of the rDNA (NOR) regions in *Medicago truncatula* and *Medicago sativa*

Hilda Tiricz

Institute of Genetics, Biological Research Center, Hungarian Academy of Sciences, Szeged, Hungary

A *Medicago sativa* mutation called sticky leaf (*stl*), which appears in the nature occasionally was reported previously (Stanford 1959) and used as a morphological marker in cross-fertilizations. The *stl* mutant is characterized by the adhesion of the adaxial sides of adjacent leaflets in the same leaf, as well as adhesion of opposite halves of the same leaflet. The inheritance of the mutant in tetraploid populations suggested that the *stl* character is determined by a single recessive gene (Stanford 1965). This was confirmed later in a diploid F2 segregating population originating from a cross between *M. sativa* ssp. *quasifalcata* and *M. sativa* ssp. *coerulea* (Endre G. PhD thesis 1997). Genetic mapping of this trait in this population placed the *Stl* gene on Linkage Group six (LG6) in the close vicinity of the rRNA coding region (NOR). In the closely related model legume *M. truncatula* that shows very high overall macrosynteny with *M. sativa* the position of NOR region is different, it is located on LG5.

Our aim is to identify the mutant gene which is responsible for the *stl* phenotype in *M. sativa* with the help of the available genomic information of the model *M. truncatula*. For this the localization of the ortholog *Stl* gene in *M. truncatula* is needed, therefore we compare the NOR and its flanking regions in these *Medicago* species. To explore this syntenic relationship we used three approaches. One of these was to map the molecular markers linked to the *M. sativa stl* trait on the *M. truncatula* linkage map. The second direction was to search for and use structural genomic information of *M. truncatula* sequenced BAC clones carrying rDNA sequences. We have identified the repeat unit sequences and looked for discrete sequences for mapping on *M. sativa*. As a third approach we have screened a *M. truncatula Tnt1* insertional mutant plant collection for leaf phenotypes similar to *stl*.

Molecular markers Q5C and P16C closely linked to *stl* phenotype on the *M. sativa* map were used to identify *M. truncatula* BAC clones. Some have already been mapped in *M. truncatula*, but their position was neither on LG5 near NOR region nor on LG6 in syntenic position of *stl* in *M. sativa*. We have subcloned and sequenced other BACs with unknown location but only intergenic repetitive sequences were identified not suitable for syntenic mapping purposes.

Following the second approach with the help of BAC sequences we determined the rDNA units (the 18S-5.8S-25S rRNA coding + IGS sequences) in *M. truncatula*. The thorough analyses of these BACs identified only one putative other coding sequence but so far mapping efforts failed in *M. sativa*.

Volume 52(2):333-356, 2008
Acta Biologica Szegediensis
http://www.sci.u-szeged.hu/ABS

In the meantime a publication reported about positioning *M. truncatula* FUT2 (α-1.3-fucosyltransferase) genes by FISH method on five chromosomes (LG1,4,5,7,8), one of them inserted in the NOR region. Based on this information we checked if FUT2 gene was present also in *M. sativa* NOR region or not. Southern blot experiments suggested that FUT2 gene has lower copy number in the *M. sativa* genome and no position inside the rDNA region was detected. This further suggests a low synteny between these regions in the two *Medicago* species.

Insertional mutagenesis technology is important tool for isolation of new genes by phenotypes (forward genetics) or study their function (reverse genetics). We have found a number of plants with leaf phenotype similar to *stl* among *M. truncatula* insertional mutants carrying tobacco *Tnt1* retrotransposons. Sequence of *Tnt1* flanking regions of these mutant lines were determined by AFLP-PCR method. These sequences have been analyzed by their potential coding function as well as by their map position. Possible candidates were identified based on location (Mt LG5, LG6 or unknown) and are subject for further studies.

d'Erfurth I, Cosson V, Eschstruth A, Lucas H, Kondorosi A and Ratet P (2003) Efficient transposition of the Tnt1 tobacco retrotransposon in the model legume Medicago truncatula. Plant J 34:95-106.
Stanford H (1959) The Use of Chromosome Deficient Plants in Cytogenetic Analyses of Alfalfa. Agron J 51:470-472.
Stanford H (1965) Inheritance of Sticky Leaf Character in Alfalfa. Crop Sci 5:281.

Supervisor: Gabriella Endre
E-mail: tiriczh@brc.hu

Typing of bacterial symbionts of entomopathogenic nematodes, and their potenital use as biocontrol agents

Tímea Tóth

Research and Extension Centre for Fruit Growing, Újfehértó, Hungary

The extensively used biocontrol organisms, entomopathogenic nematodes belong to the *Heterorhabditis* and *Steinernema* genus are symbiotically associated with *Photorhabdus* and *Xenorhabdus* bacteria. The bacterial partners have an outstanding role in the life-cycle of their nematode hosts: they produce wide range of toxins, hydrolitic exoenzymes and antibacterial compounds that are responsible for the death and bioconversion of the infected insect larvae and prevent other soil organisms from degradating the insect cadavers. The bacterial partners highly determine the effectiveness of the symbiotic complex against different insects, therefore bacteria have an interests from the viewpoint of biocontrol practice. The aim of this study was to survey the diversity of the Hungarian *Photorhabdus* isolates, and to obtain comprehensive view about their potential use as industrial entomotoxin and antimicrobial compound producers.

Photorhabdus strains from entomopathogenic nematodes isolated from Hungarian soils (Tóth 2006) were characterized by morphological, physiological and genetic properties to survey the diversity of bacterial symbionts of *Heterorhabditis* species of commercial importance. Entomopathogenic bacteria (EPB) were isolated from 245 entomopathogenic nematode strains originated from different part of Hungary. There were 156 *Photorhabdus* and 77 *Xenorhabdus* from the successfully cultured 233 EPB isolates. 65 *Photorhabdus* isolates representing the whole collection from the point of view of geographical and nematode host distribution were analysed. First stage bacteria cells selected on NBTA indicator plates were used to determine the morphological traits and to perform physiological tests using Biolog GN microplates and API20E strips. Cytotoxic and antibacterial properties of cell-free culture broth were measured against *Drosophila melanogaster* S2 and *Spodoptera frugiperda* Sf9 cell lines or *Stpahylococcus aureus* and *Bacillus subtilis* bacteria, respectively. Morphologically and physiologically homogenous groups of *Photorhabdus* isolates were characterized by partial sequencing of 16S rRNA and *gyr*B subunit gene.

High physiological and morphological diversity were proved among the *Photorhabdus* isolates, and all of physiological and morphological bacteria types could be isolated both from *Heterorhabditis megidis* and *H. downesi*. A number of bacteria isolates were shown only moderate 16S rRNA gene sequence similarities with type strains of all described *Photorhabdus* species/subspecies. Using *gyrB* sequences to the phylogenetic analysis, these isolates were proved to be part of the species *Photorhabdus temperata*, with clear separation from both palearctic and American strains (phylogenetic distances are 93.1% and 92.1%, respectively). The physiological and carbon source utilization characters supported the phylogenetic position of these strains, therefore a new subspecies, *Photorhabdus temperata* subsp. *cinerea* (Tóth and Lakatos 2008).

The 39% and 13% of all studied isolates were uneffective against *S. aureus* and *B. subtilis*, respectively, while 26% and 7% were much more effective, than 100 ppm streptomycine, which was the control. About 10% of the studied isolates do not produce effective ingredients against *S. aureus* and *B. subtilis* bacteria, while 10% of them were highly effective against both bacteria.

59% and 8% of isolates had no cytotoxic effect on S2 and Sf9 cells, while 3% and 21% were highly toxic to dipteran and lepidopteran cells. There was not any *Photorhabdus* isolates, of which fermentation liquid was toxic to both cell types.

Tóth T (2006) Collection of entomopathogenic nematodes for biological control of insect pests. J Fruit Ornam Plant Res 14:225-230.
Tóth T, Lakatos T (2008) A new subspecies of *Photorhabdus temperata*, isolated from *Heterorhabditis* nematodes: *Photorhabdus temperata* subsp. *cinerea* subsp. nov. Int J Syst Evol Microbiol (in press)

Supervisor:
E-mail: timi42@gmail.com

Volume 52(2):333-356, 2008
Acta Biologica Szegediensis
http://www.sci.u-szeged.hu/ABS

Engineering plant abiotic stress tolerance by the overexpression of aldo/keto reductases

Zoltán Turóczy

Institute of Plant Biology, Biological Research Center, Hungarian Academy of Sciences, Szeged, Hungary

Due to the sessile life style, plants are continuously exposed to a wide range of biotic and abiotic stress factors. This stress exposure severly affects their bioproductivity by causing the rapid and excessive accumulation of reactive oxygen species (ROS). ROS production in the vicinity of biomembranes containing polyunsaturated fatty acids can lead to lipid peroxidation and generate chemically reactive cleavage products, largely represented by aldehydes. Plant aldo/keto reductases (AKRs), among other enzymes, have been shown to be effective in the detoxification of lipid peroxidation-derived reactive aldehydes (Oberschall et al. 2000; Hideg et al. 2003).

In the present work we characterize a novel rice (*Oryza sativa*) AKR protein (OsAKR1) and investigate the transcriptomic changes in the gene expression profile of additional two AKR genes (*OsAKR2, OsAKR3*) in response to different stress treatments. A wide range of stress factors (abscisic acid, hydrogen-peroxide, mannitol etc.) was shown to trigger the expression of these AKR genes in rice cell suspensions, resulting in several folds of increased transcript levels. The most effective inducers were the ABA and hydrogen-peroxide, and *OsAKR1* gene turned out to be the most stress responsive. Stimulated by these results we investigated further the properties of the encoded protein by the *OsAKR1* gene, by cloning the full-length *OsAKR1* cDNA into recombinant protein expression construct, and purifying the glutathione-S-transferase (GST)-OsAKR1 fusion protein. Results of subsequent assays revealed that the GST-OsAKR1 recombinant protein exhibited a high, NADPH-dependent catalitic activity to metabolize toxic aldehydes (methylglyoxal, phenylglyoxal, glyoxal). Since cytotoxic reactive aldehydes can produce significant damages in the plant cells, the function of OsAKR1 protein to metabolize some of these harmful products was very promising. We also showed through *in vivo* experiments, that overproduction of this enzyme in *E. coli*, increased the tolerance of bacterial cells against high concentration (2mM) of methylglyoxal. The stress induced transcription of this AKR gene, as well as the data obtained from its biochemical characterization, supported its possible involvement in the abiotic stress induced reactive carbonyl detoxification pathways.

Till now there are several approaches to increase stress tolerance by manipulating the expression of endogenous, stress-related genes. Strategies targeting transcription factor expression have been shown to be effective, but on the other hand, stress tolerance can also be achieved by changing the expression of a single gene (Zhu 2001). Following the latter approach, we overexpressed the *OsAKR1* gene in tobacco (*Nicotiana tabacum*) and verified the effects of a single gene overexpression on the stress tolerance of the transgenic plants. We found, that the transgenic lines overproducing the OsAKR1 protein, accumulated significantly lower reactive aldehydes in response to the methylviologen (MV) treatment than the wild type. MV is a strong oxidative stress inducing herbicide, linked to ROS production and consequently to the formation of toxic aldehyde degradation products. In addition, the overexpressing lines reserved their photosynthetic functions more efficiently after heat treatments then the wild type. Therefore we suggest, that overexpression of a single gene (*OsAKR1*) and the accumulation of OsAKR1 protein is mainly beneficial in the detoxification processes against the reactive aldehydes generated at increased levels under stress conditions in the transgenic plants.

Hideg É, Nagy T, Oberschall A, Dudits D, Vass I (2003) Detoxification function of aldose/aldehyde reductase during drought and ultraviolet-B (280-320 nm) stresses. Plant Cell & Environment 26:513-522.

Oberschall A, Deák M, Török K, Sass L, Vass I, Kovács I, Fehér A, Dudits D, Horváth GV (2000) A novel aldose/aldehyde reductase protects transgenic plants against lipid peroxidation under chemical and drought stress. The Plant Journal 24:437-446.

Zhu JK (2001) Plant salt tolerance. Trends Plant Sci 6:66-71.

Supervisor: Gábor V. Horváth
E-mail: placebo_tz@yahoo.com

Toxicogenomics screening of small molecules using high-density nanocapillary QRT-PCR technique

Laura Vass

Laboratory of Functional Genomics, Biological Research Centre, Hungarian Academy of Sciences, Szeged, Hungary

Toxicogenomics combines studies of genomics, cell and tissue-wide protein expression and metabonomics to understand the role of gene-environment interactions in healthy and diseased samples. Predictive toxicogenomics is the acquisition of advanced knowledge of the safety profile of a compound using genomic biomarkers (Fielden et al. 2006). By clustering analysis of the gene expression profiles over selected biomarkers induced by the lead molecules and relevant derivatives, the medicinal chemist can deduce the relationship between structural modifications and changes in the toxicity profile (structure-toxicity relationship). Involvement of well-characterized reference compounds can be of help in this profiling, for instance defining the specific tissue or organ toxicity.

Using in-house validated chemical reactions that are suitable for parallel synthesis and a collection of multifunctional „drug-like" scaffolds, a dedicated discovery screening library of 10,000 compounds has been enumerated by a cascading diversity building approach (www.amriglobal.com). Based on the cytotoxicity measured in MRC-5 human fibroblast assay, further on HepG2 human hepatocarcinoma assay and the interpolated IC_{50} values, 668 compounds were selected aiming for maximal diversity of scaffolds.

These selected 668 small, drug-like compounds of unknown effects and other, toxic compounds of known and of yet unknown effects and pharmaceutical active entities were screened for their gene expression profiles *in vitro*, over 56 selected biomarkers (toxicology, transporters). Our objective was to see to what extent the highly similar chemical structures induce similarities in their hepatotoxic fingerprints and to test the analytical performance of the nanocapillary QRT-PCR technique and its general applicability for the field of toxicogenomics.

Preliminary tests have been performed with our inhouse ToxicoScreen DNA-microarrays (Vass et al. 2006) and with the traditional QRT-PCR technique, following which we shifted to the OpenArray nanocapillary quantitative real-time PCR-technology (Morrison et al. 2006; Avidin Ltd.-BioTrove Inc.) that has meanwhile appeared on the market. This later technology merges the high-throughput of DNA-microarrays with the sound characteristics of QRT-PCR.

By the combination of a relatively large combinatorial chemical library and a relatively small set of selected toxicological biomarkers, we intended to avoid the two culprits of toxicogenomics: 'the curse of dimensionality' (too many genes), and 'the curse of dataset sparsity' (too few samples). The generally accepted, however rarely adapted sample-per-feature ratio for robust clustering performance is at least 5 to 10.

Based on the scaffold structure or the characteristic residues, we assigned the tested chemicals into subgroups. Different clustering methods were applied, based on results from unsupervised hiearchical clustering we performed supervised, K-means clustering. Our objective was to see wether the correlation between gene expression fingerprint and structure of the compound inducing it can be detected and to what extent can this correlation be rooted back to the scaffolds.

This work was supported by the following grants: Oszkár Asboth „XTTP" (NKTH), GVOP-3.1.1.-0280/3.0

Fielden MR, Kolaja KL (2006) The state-of-the-art in predictive toxicogenomics. Curr Opin Drug Discov Devel 9(1):84-91.

Morrison T, Hurley J, Garcia J, Yoder K, Katz A, Roberts D, Cho J, Kanigan T, Ilyin SE, Horowitz D, Dixon JM, Brenan CJ (2006) Nanoliter high throughput quantitative PCR. Nucleic Acids Res 34(18):e123.

Vass L, Kis Z, Fehér LZ, Zvara Á, Lőrincz Zs, Borbola I, Cseh S, Kulin S, Ürge L, Dormán Gy, Puskás LG (2006) Medium-throughput microarray-based approach for toxicogenomics profiling of small molecules. QSAR Comb Sci 25 (11):1039-1046.

Supervisor: László G. Puskás
E-mail: vass.laura@gmail.com

Tools for improving stress adaptation in cereals

Zoltán Zombori

Institute of Plant Biology, Biological Research Center, Hungarian Academy of Sciences, Szeged, Hungary

Abiotic stresses are very important factors that reduce crop productivity. Plant root is the primary organ for uptake of water and nutrients, therefore it plays important role in tolerance to stresses like drought or salinity. Plants developing stronger and deeper roots suffer less from water deficit. The aim of our work was to improve the stress-tolerance in cereals using transcriptome analysis of rice cultivars under drought stress conditions, and stress-induced and root-specific promoters.

Genes facilitating development of efficient root system can increase the survival of the plant. Fusions of drought stress-related root-specific promoters to these genes may provide environment friendly and efficient solution to improve roots of crop plants under stress conditions.

Based on published data two candidate promoters were selected: the rice *CatB* and the *RSOsPR10* promoters. The *CatB* promoter is known to be root-specific (Iwamoto et al. 2004), the expression of the *RSOsPR10* mRNA is high in salt and drought stress conditions in root (Hashimoto et al. 2004). Both promoters have stress-related transcription factor binding sites and (MYB, WRKY, DREB, LTRE) in their sequence. The 1.6 kb CatB promoter and the 2 kb of the 5` flanking region of the *RSOsPR10* were cloned, and fused to reporter genes. The constructs were transformed into rice calli and tobacco leaves.

On the regenerated T_0 rice plants, salt stress was performed that revealed the *RSOsPR10* promoter directing root-specific and stress-induced expression pattern of GFP reporter. CatB::GUS transformed T_0 and T_1 tobacco plants showed root and vascular bundle-specific GUS expression, and induction under salt stress.

The changes of the rice root transcriptome under stress conditions and its alterations during a daytime period were investigated in a greenhouse experiment including three cultivars growing in a sand-perlite soil mixture. The stressed plants were irrigated with 20% of water for one month, causing drought-stress condition. The samples were collected three times in a day from each genotype both from drought stressed and control.

To follow the transcriptional changes, root samples from the most tolerant genotype were hybridized with rice oligonucleotide DNA chip. 3200 of the genes represented on the chip gave signal in all of the hybridizations, and 11.6% were up-regulated, and 6.7% were down-regulated in the adaptive cultivar.

Based on the expression profiles of genes during the day under drought-stress, eight clusters were built, and functional categorization was done based on the known or putative function of the encoded proteins, following the classification established by Yang et al. (2004).

Comparing the ratios of the gene-classes between the induced and repressed genes four groups showed significant difference in favor of the up-regulated genes. The ratio of the genes encoding proteins involved in metabolism, signal transduction and cell growth was higher among the induced genes.

To validate the results of the chip-hybridization, and to find stress-induced and root-specific genes, quantitative real-time PCR experiments were performed. Seven genes were tested, and the chip-hybridization results were confirmed for four of them: an *ABA/WDS induced* gene, a *LEA group 3*, a putative *LEA*, and a gene with unknown function. Furthermore, these genes` expression levels were determined in the shoot samples in all of the three genotypes. The alterations of the expression patterns reflected the differences in the stress-tolerance of the three cultivars. However all of them showed higher induction in roots than in shoots, the *LEA group 3* gene appeared to be the most stress-inducible and root-specific, becoming a candidate to develop expression cassettes including this gene.

Hashimoto M, Kisseleva L, Sawa S, Furukawa T, Komatsu S, Koshiba T (2004) A novel rice PR10 protein, RSOsPR10, specifically induced in roots by biotic and abiotic stresses, possibly via the jasmonic acid signaling pathway. Plant Cell Physiol 45:550-559.

Iwamoto M, Higo H, Higo K (2004) Strong expression of the rice catalase gene *CatB* promoter in protoplasts and roots of both a monocot and dicots. Plant Physiology and Biochemistry 42:241-249.

Yang L, Zheng B, Mao C, Qi X, Liu F, Wu P (2004) Analysis of transcripts that are differentially expressed in three sectors of the rice root system under water deficit. Mol Gen Genomics 272:433-442.

Supervisor: János Györgyey
E-mail: zzoli@brc.hu

The study of the Nimrod protein and gene cluster in *Drosophila melanogaster*

János Zsámboki

Institute of Genetics, Biological Research Center, Hungarian Academy of Sciences, Szeged, Hungary

Every multicellular organism has to maintain its homeostasis in masses of invading microbes in its environment. The innate immunity constitutes the first line of defence against this challenge. As the defence mechanism of *Drosophila melanogaster* consists of innate immune processes only, lacking an adaptive immune system, it can be characterised as a less complex homologue of its mammalian counterpart, making the fruit fly a valuable model organism for studying innate immune responses.

The circulating blood cells of the fruit fly are key effectors of its immune defence. These hemocytes can be divided into three characteristic types. In wild type third instar larvae 97% of all circulating hemocytes are plasmatocytes, but even though it is the most abundant cell type in circulation, previously it could only be characterised based on its phagocytic capacity.

Our group identified the first plasmatocyte-specific immunological marker. After screening thousands of candidate hibridoma clones, we found two specific monoclonal antibodies, recognising different epitopes on the same molecule. We purified the antigenic protein, and analysed it with MALDI-TOF. A protein was identified with characteristic domain structure, containing a signal peptide, a CCxGY motif, EGF repeats, one transmembrane and an intracellular domain.

We have shown that the protein functions as a putative phagocytosis receptor of the plasmatocytes. As this protein helps the major sentinel cells catching bacteria we decided to name it after the big hunter Nimrod (*nimC1*; Kurucz et al. 2007b). The RNAi induced loss of function *nimC1* mutant plasmatocytes phagocytose *S. aureus* bacteria at significantly lower levels than the wild type, but *E. coli* phagocytic capacity was not compromised. On the other hand ectopic expression of the *nimC1* gene in S2 *Drosophila* cell line significantly enhanced the phagocytic capacity of cultured cells.

As it seemed that NimC1 is not the only phagocytosis receptor in *Drosophila*, we did in silico analysis searching for similar proteins in the fruit fly genome. Nimrod belongs to the superfamily of EGF repeat containing proteins, from which only 12 contain the characteristic CCxGY motif. In these proteins one or more EGF domains can be found, which fit a specific, more stringent consensus sequence, which we named NIM repeat. Nine of these genes, including *nimC1* can be found in a genomic region spanning 88 kilobase on the second chromosome. (Kurucz et al. 2007a; Somogyi et al.)

To prove, that these predicted genes are really transcribed, and to characterise their expression pattern we performed reverse transcription polymerase chain reactions using samples from whole third instar larvae, isolated hemocytes in wild type and hemocyte overproducing *l(3)mbn-1* mutant, and wild type adults.

All of the predicted genes were transcribed in every studied condition; the only exception was *nimA* which did not show any transcription activity in hemocytes.

In order to study the expression pattern of the *nimC1* homologues in more detail, we intend to produce new specific antibodies recognising the NimC1 homologue proteins. In order to acquire suitable amount of isolated protein for immunization, we have cloned the non-homologues regions of four different *nim* genes into prokaryotic expression vectors containing a HIS affinity tag, allowing isolation of the produced protein. In order to allow possible post-translational modifications of the expressed proteins, two of them are already cloned into affinity tagged eukaryotic expression vectors.

Kurucz É, Márkus R, Zsámboki J, Folkl-Medzihradszky K, Darula Zs, Vilmos P, Udvardy A, Krausz I, Lukacsovich T, Gateff E, Zettervall C-J, Hultmark D, Andó I (2007a): Nimrod, a putative phagocytosis receptor with EGF repeats in *Drosophila melanogaster*. Curr Biol 17:1-6.

Kurucz É, Váczi B, Márkus R, Laurinyecz B, Vilmos P, Zsámboki J, Csorba K, Gateff E, Hultmark D, Ando I (2007b) Definition of Drosophila hemocyte subsets by cell-type specific antigens. Acta Biol Hung 58:95-111.

Somogyi K, Sipos B, Pénzes Zs, Kurucz É, Zsámboki J, Hultmark D, Andó I. Evolution of genes and repeats in the Nimrod superfamily. (Submitted manuscript).

Supervisors: István Andó, Éva Kurucz
E-mail: legyezorobot@yahoo.com

Instructions to Authors

Submission of manuscripts

Submission of a manuscript to Acta Biologica Szegediensis automatically involves the assurance that it has not been published and will not be published elsewhere in the same form. Manuscripts should be written in English. Since poorly-written material will not be considered for publication, authors are encouraged to have their manuscripts corrected for language and usage by a trusted expert.

There are no explicit length limitations: a normal research article will occupy 4-6 printed pages; reviews might be considerably longer. Authors should submit three sets of the complete manuscript and illustrations, together with a computer disk containing an electronic version of their manuscript. The elctronic file is considered the final material. Both Macintosh and PC versions will be accepted. The disk should be labeled with the date, the first author's name, the file name of the manuscript and the software, disk format and hardware used. Acta Biologica Szegediensis will not return copies of submitted manuscripts and figures. Requests to return original figures will be honored as a courtesy, but cannot be guaranteed. If instructions are not followed, authors will be asked to retype their manuscripts.

Manuscript format

Only good-quality laser printouts will be accepted. All pages should be printed with full double spacing, 2.5 cm margins, and a nonjustified right margin. A standard 12 point typeface (e.g. Times, Helvetica or Courier) should be used throughout the manuscript, with symbol font for Greek letters. Boldface, italics or underlined text should not be used anywhere in the manuscript. Footnotes are not permitted. Each page should be numbered at the bottom as follows:

Page 1. Title page: Complete title, first name, middle initial, last name of each author; where the work was done (authors' initials in parentheses if necessary); mailing address, phone, fax, and e-mail of the corresponding author; a running title of no more than 48 characters and spaces.

Page 2. Abstract: no more than 200 words, followed by 4-6 key words.

Beginning on page 3: Introduction, Materials and Methods, Results, Discussion, Acknowledgments, References, Figure Legends, Tables. Each section should be begun on a new page.

The manufacturer's name and location should be given in parentheses for reagents and instruments. Sources for all antibodies and nucleotide sequences should be indicated. Customary abbreviations in common use need not be defined in the text (e.g. DNA or ATP). Other abbreviations should be defined the first time that they are used. Quantitative results must be presented as graphs or tables and supported by appropriate experimental design and statistical tests. Only SI units may be used. For studies that involve animals or human subjects, the institutional, national or international guidelines that were followed should be indicated.

References

Only work that has been published or is in the press may be referred to. Personal communications should be acknowledged in the text and accompanied by written permission. In the text, references should be cited by name and year, e.g. Bloom (1983) or (Schwarz-Sommer et al. 1990) or (Maxam and Gilbert 1977). In the References, references should be listed alphabetically by first authors (including all co-authors) and chronologically for a given author (beginning with the most recent date of publication). Where the same author has more than one publication in a year, lower case letters should be used (e.g. 1999a, 1999b, etc.). Periods should not be used after authors' initials or abbreviated journal titles (e.g. Acta Biologica Szegediensis should be cited as Acta Biol Szeged). Inclusive page numbers should be used. Examples:

Bloom FE (1983) The endorphins: a growing family of pharmacologically pertinent peptides. Annu Rev Pharmacol Toxicol 23:151-170.

Coons AH (1978) Fluorescent antibody methods. In Danielli JF, ed., General Cytochemical Methods. Academic Press, New York, 399-422.

Maxam AM, Gilbert WA (1977) A new method for sequencing DNA. Proc Natl Acad Sci USA 74:560-564.

Monod J, Changeux J-P, Jacob F (1963) Allosteric proteins and cellular control systems. J Mol Biol 6:306-329.

Schwarz-Sommer Z, Huijser P, Nacken W, Saedler H, Sommer H (1990) Genetic control of flower development by homeotic genes in Antirrhinum majus. Science 250:931-936.

Illustrations

Three complete sets, including a high-quality "original" for publication, must be submitted with the manuscript. The back of each figure or composite plate should be labeled in soft lead pencil, indicating the orientation, the figure number, and the first author's name. The back of the best set should be marked "use for reproduction" or "original". Authors are encouraged to submit digital images of photographs, line drawings or graphs for printing. Most major image editing and drawing/illustrator computer software files (both Macintosh and PC) in TIFF or EPS formats are acceptable. It is particularly important that adequate resolution (at least 300 dpi, preferably 600 dpi) is used in making the original image.

Figure legends

Figures should be numbered consecutively with Arabic numerals. Material in the text should not be duplicated and methods should not be described. The size of scale bars should be indicated when appropriate. The first figure in the text should be referred to as Fig. 1, and so on.

Tables

Tables should be numbered consecutively with Arabic numerals. A brief title should be included above the table. Each table should be printed double spaced, without vertical or horizontal lines, and on a separate sheet. Material in text should not be duplicated and methods should not be described. The first table in the text should be referred to as Table 1, and so on.